DEFINING AND CHARACTERISING AN ENDOTHELIAL MICROVESICLE SIGNATURE FOR IMPROVED DETECTION OF CARDIOVASCULAR DISEASE RISK IN SYSTEMIC LUPUS ERYTHEMATOSUS

NICOLA EDWARDS

A thesis submitted in partial fulfilment of the requirements of Manchester Metropolitan University for the degree of Doctor of Philosophy

Department of Life Sciences

Faculty of Science and Engineering

2019

Acknowledgements

I would first like to express my sincere gratitude to Dr Fiona Wilkinson and Professor Yvonne Alexander for their continual guidance, support and direction throughout the course of this project. It has been inspirational to work under two strong female leaders and I will remember and implement everything they have taught me. Many thanks also to Dr Alex Langford-Smith for his advice, teaching and technical assistance, particularly when developing new techniques and building my confidence. Further thanks to all my friends and colleagues, who have helped me to keep smiling!

I would like to acknowledge the clinical team at the University of Manchester/Manchester Royal Infirmary, the nurses and all of the volunteers who participated in these studies, as without them, this work would not have been possible. Particular thanks go to Professor Ian Bruce, Dr Eoghan McCarthy, Dr Ben Parker, Dr John Reynolds and Dr Michelle Barraclough for their enthusiasm and clinical guidance. It has been a pleasure collaborating with the team and I hope to continue building the relationship into the future.

I am incredibly grateful and blessed to have such a supportive family, whose unfailing love and encouragement have enabled me to keep going when times were tough. To my parents, Jutta and Mark, and my sister, Hannah, who have always believed I could do it, and to my family in Germany, whose support I feel from across the sea. Finally, I would like to dedicate this thesis to my husband, Ryan, whose unending patience and understanding has carried me throughout.

List of Figures

List of Tables

List of Abbreviations

±SD	± Standard Deviation
±SEM	± Standard Error Mean
ACR	American College of Rheumatology
AGE	Advanced Glycation End-product
AMOTL2	Angiomotin-Like Protein 2
ANOVA	One-Way Analysis of Variance
BB515	Brilliant™ Blue 515
BCA	Bicinchroninic Acid
BECN1	Beclin 1
BILAG	British Isles Lupus Assessment Group
BLyS	B Lymphocyte Stimulator
BMI	Body Mass Index
BMP	Bone Morphogenetic Protein
BP (Systolic)	Blood Pressure (Systolic)
C (3)	Complement component (3)
CD (144)	Cluster of Differentiation (144)
CDK	Cyclin Dependent Kinase
cDNA	Complementary DNA
CVD	Cardiovascular Disease
DMEM	Dulbecco's Modified Eagle's Media

dsDNA	Double Stranded Deoxyribonucleic Acid
DMSO	Dimethyl Sulphoxide
ECAR	Extracellular Acidification Rate
E. Coli	Escherichia Coli
ECV	Extracellular Vesicle
EGFR	Epidermal Growth Factor Receptor
ELISA	Enzyme-Linked Immunosorbent Assay
EMV	Endothelial Microvesicle
ESR	Erythrocyte Sedimentation Rate
FCCP	Carbonyl Cyanide-4-Phenylhydrazone
FCS	Foetal Calf Serum
FLT4	Fms Related Tyrosine Kinase 4
FMD	Flow Mediated Dilatation
FSMC	Fatigue Scale for Motor and Cognitive Functions
GFP	Green Fluorescent Protein
GO	Gene Ontology
GP	General Practitioner
HDL	High Density Lipoproteins
HEK	Human Embryonic Kidney
HIF1α	Hypoxia Inducible Factor-1α
hsCRP	High Sensitivity C-Reactive Protein
HUVEC	Human Umbilical Vein Endothelial Cell
ICAM-1	Intercellular Adhesion Molecule-1

IFN (-α)	Interferon (-α)
Ig (G)	Immunoglobulin (G)
IGF1	Insulin-Like Growth Factor 1
IL (-6)	Interleukin (-6)
LDL	Low Density Lipoproteins
LupusQoL	Lupus Quality of Life
MAP	Mean Arterial Pressure
MBL2	Mannose Binding Lectin 2
MCP-1	Monocyte Chemoattractant Protein-1
miRNA	Micro-Ribonucleic Acid
MMP	Matrix Metalloproteinase
mRNA	Messenger Ribonucleic Acid
NCBI	National Centre for Biotechnology
NET	Neutrophil Extracellular Trap
NICE	National Institute for Health and Care Excellence
NLRP3	NACHT, LRR and PYD Domains-Containing Protein 3
NO	Nitric Oxide
OCR	Oxygen Consumption Rate
PBS	Phosphate Buffered Saline
PDGFRα	Platelet Derived Growth Factor Receptorα
PEI	Polyethylenimine
PMV	Platelet Microvesicle
PRCP	Lysosomal Pro-X Carboxypeptidase

PS	Phosphatidylserine
PTGS2	Cyclooxygenase 2
PWV	Pulse Wave Velocity
qPCR	Quantitative Polymerase Chain Reaction
RISC	RNA Induced Silencing Complex
ROCK1	Rho-Associated Protein Kinase 1
ROS	Reactive Oxygen Species
RT	Room Temperature
RUNX2	Runt-Related Transcription Factor 2
SLE	Systemic Lupus Erythematosus
SLEDAI	Systemic Lupus Erythematosus Disease Activity Index
SOC	Super Optimal Broth
SOCS1	Suppressor of Cytokine Signalling 1
SORT1	Sortilin 1
TBE	Tris-Borate-Ethylenediaminetetra-Acetic Acid
TE	Tris- Ethylenediaminetetra-Acetic Acid
Th (1)	Helper T Cell (1)
TNFα	Tumour Necrosis Factorα
Treg	Regulatory T Cell
VCAM-1	Vascular Cell Adhesion Molecule-1
VEGF	Vascular Endothelial Growth Factor
VLDL	Very Low Density Lipoprotein
VSMC	Vascular Smooth Muscle Cell

List of Publications

Original Research

- Langford-Smith AWW, Hasan A, Weston R, **Edwards N**, Jones AM, Boulton AJM, Bowling FL, Rashid ST, Wilkinson FL, Alexander MY. Diabetic endothelial colony forming cells have the potential for restoration with glycomimetics. Scientific Reports. 2019; 9(1):2309. doi: 10.1038/s41598-019-38921-z.

- **Edwards N**, Langford-Smith AWW, Parker BJ, Bruce IN, Reynolds JA, Alexander MY, McCarthy EM, Wilkinson FL. QRISK3 improves detection of cardiovascular disease risk in patients with systemic lupus erythematosus. Lupus Science & Medicine 2018;5:e000272. doi:10.1136/lupus-2018-000272.

Review Article

- **Edwards N**, Langford-Smith AWW, Wilkinson FL, Alexander MY. Endothelial Progenitor Cells: New Targets for Therapeutics for Inflammatory Conditions With High Cardiovascular Risk. Frontiers in Medicine. 2018; 5:200. doi:10.3389/fmed.2018.00200.

Published Conference Abstracts

- **Edwards N,** Langford-Smith AW, Tandel S, *et al.* P-03-001 Improving patient stratification in systemic lupus erythematosus using endothelial microvesicles as novel biomarkers of cardiovascular risk. FEBS Open Bio. 2019;9(S1):1-431.
- **Edwards N**, Langford-Smith AWW, Floren M, *et al.* P33 Mitochondrial Hyperactivity, Impaired Matrix Adhesion and Functional Activity in Endothelial Colony Forming Cells Isolated from Patients with Diabetic Foot Ulcers. Cardiovasc Drugs Ther. 2019; 33: 261.

- **Edwards N**, Langford-Smith A, Parker B, et al. 147 QRISK3 improves identification of endothelial dysfunction and cardiovascular disease risk in patients with systemic lupus erythematosus. Heart. 2018; 104:A106.
- **Payton N,** Langford-Smith A, Weston R, et al. PoB-14 Mitochondrial Hyperactivity, Impaired Matrix Adhesion and Functional Activity in Endothelial Colony Forming Cells Isolated from Patients with Diabetic Foot Ulcers. J Vasc Res. 2017;54(suppl 1):1-80.

List of Scientific Meetings Attended

2019

1. 19th FEBS Young Scientist Forum and 44th FEBS Congress, Poland. Oral and poster presentation. Awarded full sponsorship by the Biochemical Society.
2. British Society for Cardiovascular Research spring meeting, Manchester.
3. European Society for Microcirculation-European Vascular Biology Organisation joint summer meeting, The Netherlands. Poster presentation. Awarded travel grant by Manchester Metropolitan University.

2018

1. Northern Vascular Biology Forum, Bradford. First place oral presentation prize.
2. Manchester Metropolitan University Science and Engineering Symposium. Oral and poster presentation. Awarded oral presentation prize.
3. British Society for Cardiovascular Research autumn meeting, Sheffield. First place poster presentation prize.
4. European Society for Microcirculation-European Vascular Biology Organisation summer school, Germany. Poster presentation. Awarded travel grant by the Biochemical Society.
5. British Society for Cardiovascular Research spring meeting, Manchester. Poster presentation.

2017

1. Northern Vascular Biology Forum, Liverpool. Poster presentation.
2. 19th Imperial College London Symposium, London. Oral presentation.

3. Manchester Metropolitan University Science and Engineering Symposium. Oral and poster presentation. Awarded oral presentation prize.
4. British Society for Cardiovascular Research spring meeting, Manchester.
5. European Society for Microcirculation-European Vascular Biology Organisation joint summer meeting, Switzerland. Poster presentation.

2016

1. Mercia Stem Cell Alliance annual meeting, Manchester. Awarded poster presentation prize.
2. Northern Vascular Biology Forum, Hull.
3. 18th Imperial College London Symposium, London.

Abstract

Systemic lupus erythematosus (SLE) is associated with increased risk of cardiovascular disease; up to 50-fold in young women. Cardiovascular risk algorithms do not take SLE into account, nor are there biomarkers available to stratify patient risk. This project aimed to consider the role of endothelial microvesicles (EMVs) as biomarkers of cardiovascular risk and also as effectors through their miRNA content.

To do so, EMVs were isolated and quantified from patient plasma by flow cytometry, before being correlated with QRISK cardiovascular risk scores and patient data. Key miRNAs were identified by data mining, and their abundance was determined in the vesicular fraction of patient plasma by quantitative PCR (qPCR). Thus an SLE miRNA panel was characterised. Finally, the effects of miRNA overexpression in endothelial cells were probed by developing miRNA constructs and lentiviral vectors through Gateway® cloning prior to functional tests.

This revealed that patients with SLE demonstrated elevated QRISK3 scores, as well as markers of inflammation and cardiovascular risk, compared to controls. They were also found to have increased numbers of EMVs, which were further associated with cardiovascular risk. Five miRNAs were chosen to be studied and lentiviral vectors were successfully generated to model their overexpression. Of these, miR-126-3p was elevated in patients with an SLE flare, where it was associated with musculoskeletal symptoms, and caused a glycolytic shift when overexpressed in endothelial cells; miR-3148 was also elevated in SLE. MiR-93-5p, miR-320a and miR-30d-5p were reduced in SLE, but their overexpression resulted in impaired angiogenic tube formation *in vitro,* and they were associated with measures of fatigue in patients.

This project supports the use of EMVs as biomarkers of cardiovascular risk in SLE, where they reflect disease activity and cardiovascular involvement. The identification of a miRNA panel further refines patient stratification and allows future identification of functional mechanisms and novel therapeutic targets.

Chapter 1

Introduction

1.1. Cardiovascular Disease

1.1.1. The Societal Impact of Cardiovascular Disease

According to the British Heart Foundation, approximately 7 million people in the UK are currently living with cardiovascular disease (CVD). Within the UK, CVD accounts for 25% of all deaths, meaning around 420 people die from this disease each day(1). Furthermore, CVD is the greatest cause of death globally. However, this is unequally distributed such that over 75% of these global deaths occur in countries of low or middle income(2); Manchester carries the highest rate of premature deaths due to CVD in the UK (140.7 deaths/100,000 population; Figure 1.1), which is substantially higher than more affluent areas(1). This is likely due to a number of lifestyle factors including diet, exercise and smoking – on average, 19.3% of Greater Manchester residents smoke compared to 17.2% across England and 16.2% in the more affluent South East(3) – as well as the level of governmental support and socioeconomic factors. Indeed, the prevalence of CVD places a huge burden on the economy, with UK healthcare costs of £9 billion per year. Furthermore, CVD greatly impacts quality of life, thus when disability and other costs are taken into account, this figure is estimated to rise to £19 billion per year(1).

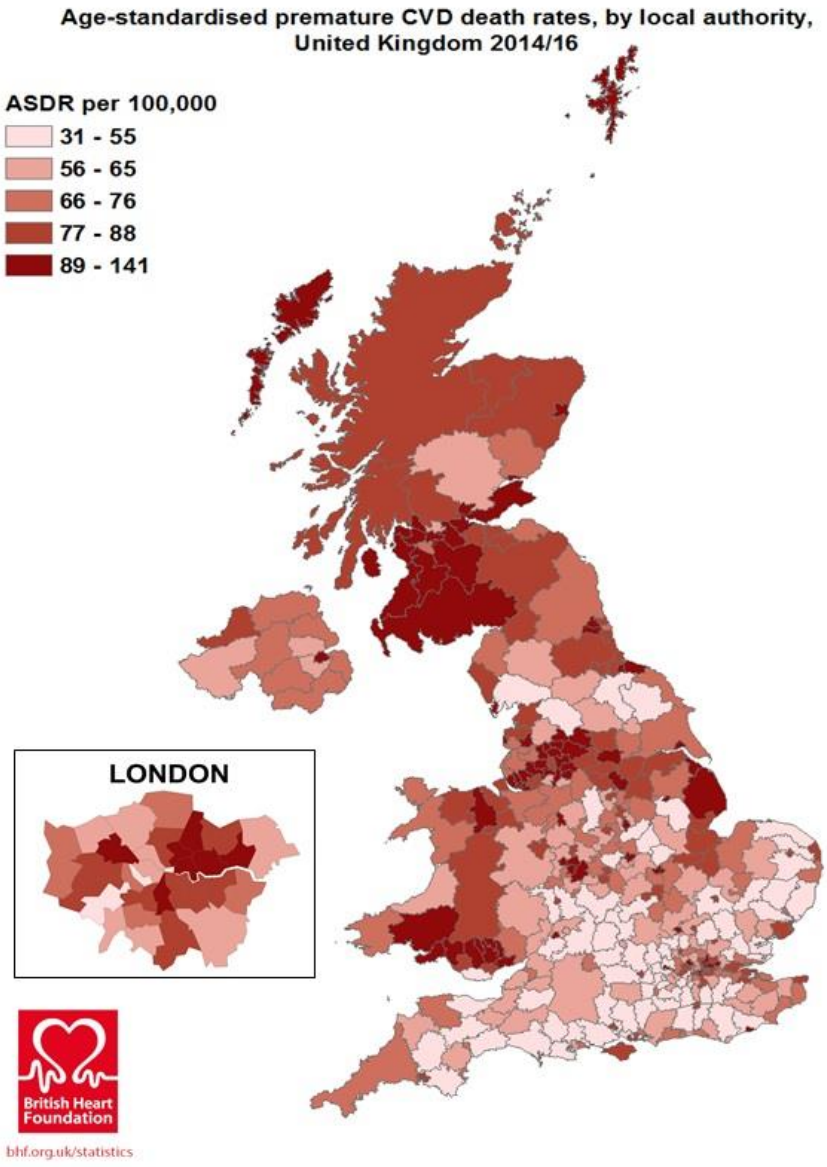

Figure 1.1: Premature mortality from CVD in the UK. *This heatmap shows premature death rates grouped by local authority. 'Premature' defined as <75 years. Image courtesy of British Heart Foundation (BHF/University of Birmingham calculated rates in partnership with UK statistical agencies: ONS/NRS/NISRA (2014-16 data).*

1.1.2. The Clinical Problem of CVD and its Co-Morbidities

'Cardiovascular disease' is an umbrella term, encompassing a number of disorders of the heart and blood vessels. Examples of cardiac presentations include coronary heart disease, congestive heart failure, rheumatic and congenital heart disease, while vascular diseases range from stroke and cerebrovascular disease to peripheral arterial disease, as well as deep vein thrombosis and pulmonary embolism. Hypertension may also be considered a CVD. Although CVDs cover a spectrum of conditions, they often share similar risk factors or pathologies. A common link is that of damage and inflammation, whether limited to a certain vascular bed or spread throughout the circulatory system. Development of atherosclerosis or changes in blood clotting can also both predispose to acute events such as myocardial infarction or stroke, and can propagate chronic CVDs. Generally, common CVDs are associated with the same risk factors of poor diet/obesity, sedentary lifestyle, smoking and drinking excessive amounts of alcohol. Others, such as rheumatic heart disease and vasculitis, are related to the presence or history of other diseases. Further information can be found on the respective websites of the British Heart Foundation (https://www.bhf.org.uk/) and the World Health Organisation (https://www.who.int/cardiovascular_diseases/en/).

Within this text, the use of 'CVD' will refer to conditions of the cardiovascular system involving damage, inflammation and increased risk of acute events. Although CVDs are characterised by multiple functional and physiological changes throughout the vasculature, this text will focus on dysfunction within the endothelial layer, the mechanisms of which will be further discussed.

1.1.3. The Vascular Endothelium in CVD

The structure of an artery is trilaminar, being composed of, in order of lumen outwards, a tunica intima, tunica media and an adventitia. The tunica intima comprises a monolayer of endothelial cells atop a collagen-rich basement membrane, the contents of which are produced by the smooth muscle cells of the tunica media layer below(4). Thus, the endothelial cells are in direct contact with the blood and exert critical functions at the

interface between blood and vasculature, such as prevention of inappropriate coagulation through surface molecules or modulation of vascular tone e.g. via release of nitric oxide (NO). It is therefore unsurprising that dysfunction of the vascular endothelium could support development of cardiovascular disease(5).

1.1.3.1. Endothelial Activation and Dysfunction

Endothelial dysfunction is typically characterised by reduced activity or production of NO by the endothelial cells, for instance due to oxidative stress, resulting in impaired vascular reactivity(6). The reduction in vasodilation can be detected non-invasively by flow mediated dilatation (FMD), a widely used method to measure endothelial dysfunction in the clinic, particularly in patients with rheumatological disorders(7). Endothelial dysfunction is often the first indication of future atherosclerotic changes, the development of which may then lead to cardiovascular disease(7-9).

The formation of an atherosclerotic plaque is depicted in figure 1.2. Briefly, low density lipoproteins (LDL) are deposited into the intimal layer, over time forming fatty streaks along the vessel wall. Monocytes are recruited from the blood into the intima, where they differentiate into macrophages and, further, foam cells via uptake of the oxidised LDL. The subsequent release of reactive oxygen species (ROS), growth factors and inflammatory cytokines, such as tumour necrosis factor-α (TNFα) and interferons, causes the proliferation of vascular smooth muscle cells (VSMCs), which then increase production of extracellular matrix(7-9). The result is a fibrous cap covering a necrotic core rich in lipids and cellular debris, accompanied by inflammation and calcification. If this is left to continue, extensive matrix remodelling and further infiltration by inflammatory cells decreases plaque stability and can result in rupture or erosion. The plaque contents are extremely thrombogenic, inciting thrombus formation, vessel occlusion and clinical symptoms of CVD(8, 9).

The terms ‘endothelial dysfunction’ and ‘endothelial activation’ are sometimes, incorrectly, used interchangeably. However, they are fundamentally linked in the process of

atherosclerosis and so both may be used in this text, depending on the angle of investigation. While endothelial dysfunction describes abnormalities of vascular tone prior to atherogenesis, endothelial activation refers to the expression of cell-surface adhesion molecules, which are responsible for leukocyte recruitment and downstream propagation of inflammation(6, 9). It may be said that, in the process of atherogenesis, activation occurs before dysfunction and this has been indicated in figure 1.2. Yet it is also understood that NO suppresses endothelial activation, reinforcing the intricate relationships that hold endothelial homeostasis in balance(6, 10, 11).

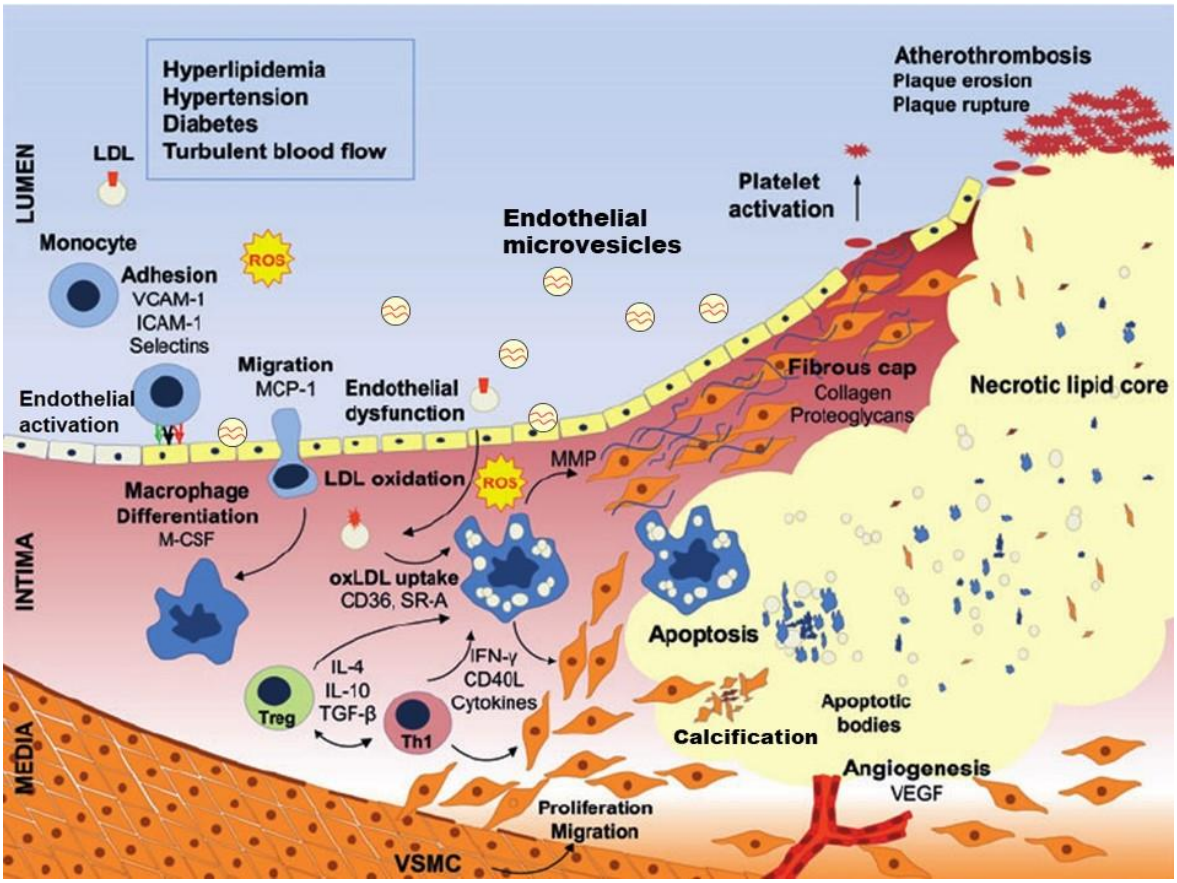

Figure 1.2: Pathological mechanisms in atherogenesis. *Long term exposure to cardiovascular risk factors leads to intimal LDL retention and oxidation. Upregulated expression of adhesion molecules supports recruitment and transmigration of leukocytes such as monocytes and T cells. Monocytes mature into macrophages within the intima, where they ingest oxidised LDL (oxLDL), becoming foam cells. Release of inflammatory factors such as cytokines, matrix metalloproteinases (MMPs) and reactive oxygen species by leukocytes contributes to development of highly inflammatory environment. Endothelial microvesicles are further released from the endothelium into the circulation. This environment stimulates vascular smooth muscle cell (VSMC) proliferation, migration and production of extracellular matrix, which forms a fibrous cap. VSMCs can also undergo calcification, reducing arterial elasticity. Cellular apoptosis causes build-up of a necrotic, lipid-rich core underneath the cap. Extensive matrix remodelling (such as through MMPs) and increased angiogenesis stimulated by hypoxia threaten plaque stability and can result in rupture, triggering activation of platelets and formation of a thrombus. IFN-γ, interferon-gamma; IL, interleukin; MCP-1, monocyte chemoattractant protein; M-CSF, macrophage colony-stimulating factor; SR-A, scavenger receptor A; TGF-β, transforming growth factor-beta; Th1, T helper cell type 1; Treg, T regulatory cell; VEGF, vascular endothelial growth factor. Adapted from Wilck and Ludwig (2014).*

1.1.3.2. Risk Factors for Endothelial Dysfunction and CVD

Atherosclerosis is more likely to develop in 'atheroprone' regions such as arterial bifurcations and branches. This is due to a region-specific change in blood flow from pulsatile and unidirectional to oscillatory or turbulent(12). This difference in shear stress triggers alternative signalling pathways by the endothelial cells and a phenotypic switch that increases permeability and monocyte attachment, as is elegantly reviewed by Zhou *et al.* (2014). Indeed, endothelial cells at these regions undergo endothelial to mesenchymal transition, which is associated with vascular fibrosis and atherogenesis(13). Furthermore, changes in shear stress are associated with alterations in the endothelial glycocalyx, resulting in impaired mechanosensing and signal transduction(14). Therefore the endothelium at atheroprone sites is more susceptible to infiltration by lipids and

leukocytes, and phenotypic changes linked to development of atherosclerosis(12). Accordingly, changes in shear stress can predict plaque development(15, 16). Perturbations in blood pressure can further increase stress and predispose to vascular remodelling and endothelial dysfunction, which, as has been discussed, then results in reduced vascular reactivity and propagation of hypertension. Thus hypertension is often noted as a risk marker for CVD, and is a primary treatment target(4, 12).

Other common risk markers pertain to diet and associated obesity. The role of lipids, particularly LDL cholesterol, is described in the previous section and is well documented, with implications in foam cell accumulation, vascular smooth muscle proliferation and inflammation, especially when oxidised(17-19). While LDL is associated with atherogenesis, high density lipoproteins (HDL) show the inverse relationship(20). The mechanisms underpinning this are still under investigation, however HDL appears to have a crucial role in removal of excess cholesterol, as well as anti-oxidant, anti-inflammatory and endothelial-protective functions(21-24). As such, HDL:LDL ratios may be used diagnostically to predict cardiovascular risk and therapeutic interventions aimed at restoring lipid balance, such as statins, are often prescribed to high risk individuals(20, 24). Circulating triglyceride levels may additionally be utilised in cardiovascular risk prediction as they appear to follow a positive correlation; whether this is a causal relationship or triglyceride levels solely reflect LDL status has historically been debated(25). Nevertheless, recent studies of individuals with genetic variations affecting triglycerides, including lipoprotein lipase, have begun to yield fascinating causal links between triglycerides and CVD(26, 27).

Hyperglycaemia and associated insulin resistance is another major risk factor for CVD; elevated fasting glucose level is linked to increased risk of death, including from CVD(28). Hyperglycaemia affects the endothelium through formation of advanced glycation end products (AGEs), which bind to endothelial receptors and support dysfunction via induction of oxidative stress and reduced NO production(29, 30). Consequently, patients with diabetes develop accelerated atherosclerosis and impaired vasodilator function(30, 31).

A third aspect of diet that increases cardiovascular risk is salt intake. Excessive salt intake is linked to hypertension, which then predisposes to endothelial dysfunction, as discussed above and is therefore a relatively simple target for preventative therapy(32, 33). Sodium

chloride may also directly affect the endothelium, independently of hypertension, through ROS production and impaired vasodilation(33, 34).

In contrast, a non-modifiable risk factor for CVD is age, which is arguably the strongest predictor of cardiovascular health. As we age, the vasculature undergoes a series of changes that render it more susceptible to damage and dysfunction. Arteries lose elasticity and vasoreactivity through a combination of hypertrophy, extracellular matrix deposition and NO reduction(35, 36); they also may become subject to eutrophic remodelling, supporting the development of hypertension(37). Furthermore, the aged endothelium shows compromised barrier function and increased cytokine production, boosting the inflammatory environment; the combination of inflammation, endothelial dysfunction and vascular stiffening hastens atherogenesis(36, 38, 39).

A final risk factor for atherosclerosis is the presence and extent of inflammation; elevated risk of CVD has been well documented in autoimmune conditions characterised by chronic inflammation, which is associated with endothelial dysfunction. Large quantities of inflammatory cytokines such as TNFα are present in the circulation of these patients(8, 40). TNFα reduces NO bioavailability as well as stimulating production of further inflammatory mediators(40, 41), the result of which is an activated endothelium expressing chemotactic and adhesion molecules, and increased atherosclerosis(8, 42). The role of infiltrating leukocytes in atherosclerosis is introduced in section 1.1.3.1., and can be altered by the specific cell subtypes present. For example, helper Th1 and Th17 T cells have been linked to deleterious effects on the vasculature whereas regulatory (Treg) T cells appear to be protective(43, 44). These cells often demonstrate a 'skew' in autoimmune inflammatory conditions, with pro-inflammatory subsets playing a greater role(44-46). Furthermore, increased numbers of patrolling monocyte subsets are also found in these conditions, predisposing to development of subclinical atherosclerosis(47, 48). The connections between inflammation and CVD have also opened the door to new biomarkers to quantify cardiovascular risk, such as high-sensitivity C-reactive protein (hsCRP), an acute phase protein released under inflammatory conditions(49). By improving understanding and knowledge of the processes underlying endothelial dysfunction and atherosclerosis in conditions with high risk of CVD, novel biomarkers and therapeutic targets can be identified and strategies developed to reduce patient mortality and improve quality of life. One such

inflammatory disorder that carries a high cardiovascular risk is systemic lupus erythematosus (SLE), which is an excellent disease model to study endothelial damage and vascular aging and is discussed further below.

1.2. Systemic Lupus Erythematosus

1.2. The Impact of SLE

SLE is an autoimmune condition characterised by autoantibody production, immune complex deposition and disseminated inflammation. Patients are predominantly female and the disease is more prevalent in those with African or Asian heritage(50-52). Incidence and prevalence varies across the globe(51), although UK figures estimated a prevalence of 97.04/100,000 in 2012(50). SLE is a complex disease with individual variations and a significant delay in diagnosis. A 2014 LUPUS UK study involving 2527 participants found that 72.7% of patients struggled to carry out daily activities and only 15% were in full time employment, highlighting the impact of this condition on quality of life(52).

1.2.1.1. The Symptoms of SLE are Heterogeneous and Patient-Specific

The same LUPUS UK study stated that 53.8% of patients frequently suffered between 6-10 different physical symptoms, highlighting the heterogeneity and systemic nature of the disease. The most common symptoms were weakness, fatigue and joint swelling, with 50%+ also experiencing poor circulation, back pain and flu-like symptoms/night sweats(52). Another UK study described musculoskeletal, mucocutaneous and psychological symptoms, as well as fatigue, as most commonly recorded prior to diagnosis (arthritis/arthralgia, rash and depression respectively). The mean age at diagnosis in this study was found to be 49.4 years, with a mean wait time of 26.4 months following first musculoskeletal symptoms, although this increased to 6.4 years in some patients(53). The range of assorted and nonspecific symptoms most likely contribute to longer waiting times,

and establish the necessity of tailored treatment dependent on the particular constellation of symptoms within an individual (Figure 1.3).

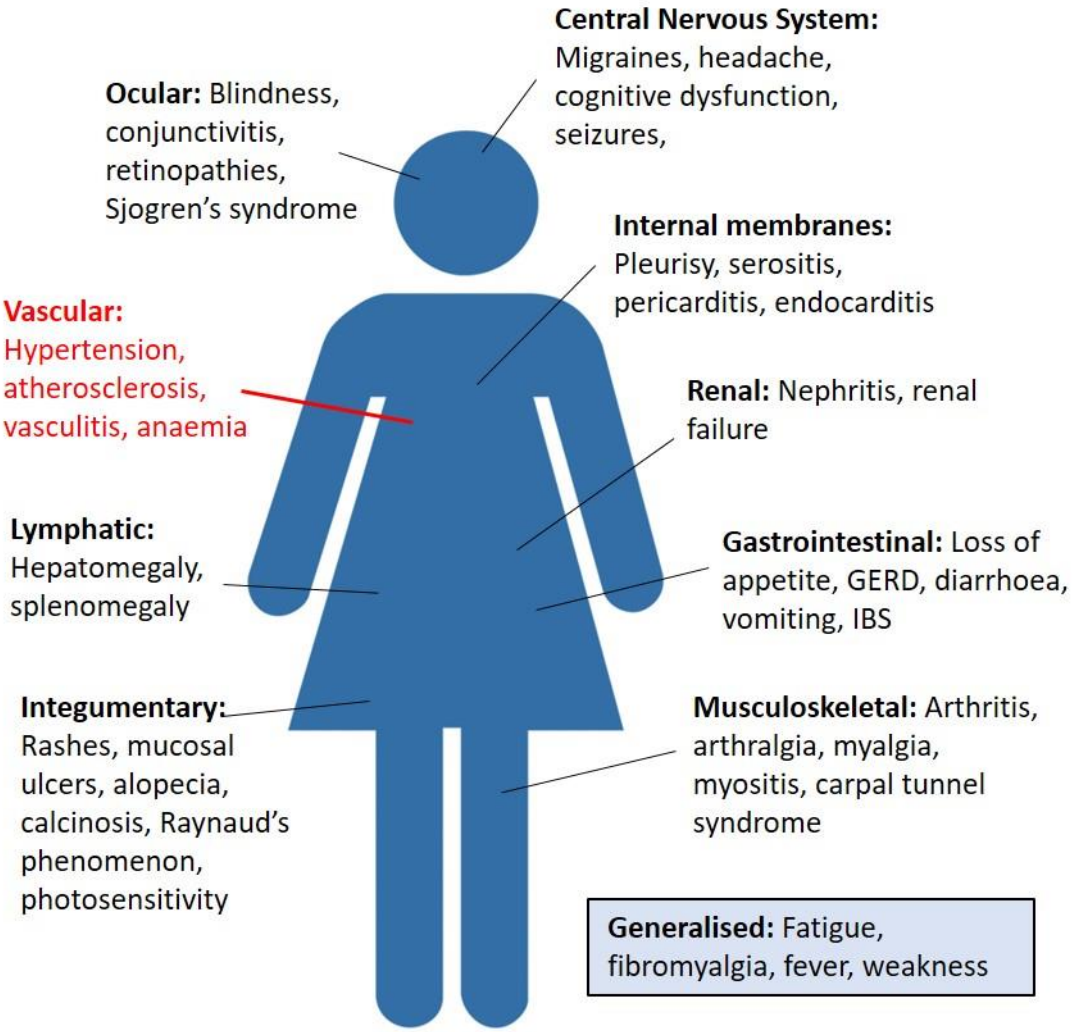

Figure 1.3: SLE affects multiple organ systems. *Due to the presence of antinuclear antibodies and deposition of immune complexes, virtually any organ system can be affected by SLE, producing a wide range of symptoms.*

1.2.1.2. Autoimmunity in SLE

Autoantibodies are a hallmark of SLE and contribute to immune complex deposition and activation of the immune response. Immunoglobulin G (IgG) is the predominant isotype of autoantibody, and is commonly reactive against the patients' own double stranded DNA (dsDNA) but may also target complement factors, endothelial cells, histones, nucleosomal material and ribosomal P protein. The autoantibody profile of a patient is often used diagnostically to confirm disease but also contributes to the disease through formation of immune complexes. Tissue damage causes further release of DNA and associated factors, thus restarting the cycle(54, 55).

Autoantibodies can propagate SLE in a number of ways. For example, anti-dsDNA antibodies activate the NLRP3 inflammasome in monocytes and macrophages, increasing the production of inflammatory cytokines such as interleukin-1 (IL-1)(56). The formation of immune complexes containing autoantibodies is a key process in the pathology of SLE; these complexes are deposited, and become lodged, within capillaries and other tissues where they cause damage and occlusion. Furthermore, the complexed antibodies are able to activate complement, and recruit and activate leukocytes, particularly neutrophils, while offering additional antigens for recognition by immune cells(57).

Although IgG isotypes may be elevated in SLE, other antibody classes are reduced, such as IgM(55, 58). Depleted levels of IgM are associated with presence of autoimmunity and inflammation, although autoreactive IgM are also observed(58). In particular, IgM antibodies targeting phosphorylcholine promote polarisation of anti-inflammatory Treg cells(59), and confer athero- and renal protection(60, 61).

1.2.1.3. The Inflammatory Environment of SLE

As described in section 1.2.1.2, propagation of tissue damage releases further autoantigens such as dsDNA. Interestingly, patients with SLE demonstrate inadequate clearance of apoptotic debris, which is related to reduced activity of DNase(62, 63). Complement factors also play a role in this process through coating of apoptotic material to facilitate removal;

polymorphisms or deficiency in early complement components such as C1q and C4 predisposes to loss of immune tolerance and development of SLE(62). Additionally, patients with SLE may show hypocomplementaemia as complement factors, especially C3 and C4, continue to be sequestered by immune complexes(64).

Activation of neutrophils by complexed antibodies and complement stimulates formation of neutrophil extracellular traps (NETs), fibrous networks containing nuclear and granular factors as well as pro-inflammatory proteins and complement factors(65, 66). Inflammasome activation and prolonged display of autoantigens strongly links NETs to autoimmunity and vasculitis; autoantigens trapped within the NETs can also undergo post-translational modifications that render them more immunogenic, such as citrullinated histones(65). As well as this, reduced DNase activity in SLE impairs NET removal, supporting chronic inflammation, particularly when NET clearance is impaired in germinal centres and thus exposing autoantigens to autoreactive B cells(65, 66). Indeed, activation of neutrophils in SLE induces a shift from immune complex phagocytosis to inflammatory NET formation(67), one of a number of suspected impairments in SLE neutrophils. As well NET overproduction and reduced degradation, neutrophils of patients with SLE have been found to have impaired phagocytosis combined with increased aggregation and production of inflammatory mediators(68). In this way, immunogenic material including oxidised mitochondrial DNA may be extruded from the neutrophil and proceed to activate further leukocytes such as dendritic cells(69).

The activated dendritic cells then release large amounts of interferon-α (IFNα), which play a major role in SLE pathogenesis and as such, will be revisited in later chapters(69, 70). IFNα is greatly immunostimulatory, skewing T cell development in favour of Th1 rather than Treg pathways, enhancing inflammasomal activity and mobilising BLyS for B cell differentiation (70). Dendritic cells activated by autogenic immune complexes also directly promote expansion of autoreactive B cells alongside failed induction of regulatory B cell phenotypes (71, 72). A similar pattern is present in T cell subsets, in that T cells of patients with SLE show a skew in favour of inflammatory Th17 cells and away from Treg cells, thus losing self-tolerance(73, 74).

The inflammatory environment of SLE is complex, featuring many interwoven pathways that culminate in a cycle of autoreactivity. This chronic inflammation then opens the door to tissue damage, resulting in symptomatic disease.

1.2.2. Cardiovascular Disease in SLE

Cardiovascular disease is a leading cause of mortality and morbidity in SLE(75, 76); risk of experiencing a major cardiovascular event is significantly higher, up to fifty times in some SLE populations(77, 78). Patients with SLE develop subclinical atherosclerosis and plaque development that takes an accelerated course compared to a healthy population(79, 80). However, endothelial dysfunction is also present in SLE without previous cardiovascular history and thus presents an interesting area of study(81, 82).

There are numerous factors that could explain the increased cardiovascular risk in SLE, and the inflammatory environment plays a large role. For example, type 1 interferons such as IFNα are associated with endothelial dysfunction and plaque development in murine SLE models(83). *In vitro* studies have found that IFNα produces an endothelial 'interferon signature' of induced genes comparable to those observed in SLE(84), and suppresses production of endothelial NO synthase, promoting endothelial dysfunction(85). Moreover, within patient populations, type 1 IFNs correlate with endothelial dysfunction and vascular calcification(86). Type 1 interferons may also support increased lipid uptake and foam cell formation, furthering atherogenesis(87).

Other SLE-related cytokines, including B lymphocyte stimulator (BLyS) and TNFα, may contribute to atherogenesis. Indeed, patients with genetically high levels of BLyS show accelerated plaque formation and arterial wall thickening(88), while elevated levels of TNFα have been linked to endothelial dysfunction and premature atherosclerosis in SLE(89, 90). This is unsurprising as TNFα has already been implicated in atherosclerosis in other diseases and models(40, 42, 91). BLyS and TNFα will be used to generate *in vitro* models of SLE in this study and will be described further in chapter 3.

On the other hand, IgM antibodies may offer a protective role in SLE, as introduced earlier. These antibodies may recognise components of atherosclerotic plaques such as oxidised lipids, reducing incidence and risk of cardiovascular events(92, 93). Antibody subtyping shows potential for future biomarker development in SLE; IgG antibodies targeting cardiolipin, HDL and paraoxonase 1 have already been suggested alongside atheroprotective IgM(93-95).

The cellular aspects of inflammation in SLE additionally contribute to atherogenesis. One study found a specific neutrophil subset in patients, which carried an atherogenic gene signature and was associated with vascular inflammation as well as atherosclerosis(96). Further research described endothelial dysfunction induced by MMPs associated with NETs, which would establish chronic subclinical atherogenesis in SLE(97). Similarly, monocyte subsets have been linked to subclinical atherosclerosis in SLE(98), alongside distinct SLE-specific gene profiles in differentiation of monocytes to macrophages(99).

Finally, non-traditional risk factors and pathological mechanisms remain to be elucidated. Other circulating elements that could contribute to atherosclerosis in SLE include transformed, pro-inflammatory HDL, elevated homocysteine and presence of adipokines(100). Vitamin D status is another area for further study, as deficiency is linked to endothelial dysfunction in both mouse and patient studies(101, 102). Furthermore, treatment options for SLE should also be taken into account – corticosteroid use is associated with atherosclerosis in SLE, whereas hydroxychloroquine shows atheroprotective properties(100, 103, 104).

1.2.3. Improvements are Needed in SLE Diagnostics

1.2.3.1. Diagnosis of SLE

A diagnosis of SLE may be complicated by the remittent nature of the disease and the high variability between patients. The diagnostic criteria published by the American College of Rheumatology (ACR; Table 1.1) are among the most common methods used for SLE diagnosis with specificity and sensitivity of 95% and 85% respectively, provided the patient fulfils four of the criteria, indicating SLE(105). The criteria, as published in 1997, detailed 10

identified symptoms spanning a variety of organs, as well as the presence of anti-nuclear antibodies at a titre of ≥1:160 (106, 107). These criteria were then further developed in 2012 by the Systemic Lupus International Collaborating Clinics (SLICC) group, producing an alternative 'SLICC' diagnostic tool, featuring seventeen variables (Table 1.2). This was intended to clarify potentially overlapping symptoms such as 'malar rash' and 'photosensitivity', further define organ involvement, and increase both specificity and sensitivity(106). Both methods may be used in the clinic to ensure definitive diagnosis; the current use of two similar techniques highlights the need for a further updated method merging and corroborating the complementary criteria, which is a current global research objective(108).

Feature	Details
Malar Rash	Fixed erythema, flat or raised, over the malar eminences, tending to spare the nasolabial folds
Discoid Rash	Erythematous raised patches with adherent keratotic scaling and follicular plugging; atrophic scarring may occur in older lesions
Photosensitivity	Skin rash in response to sun exposure
Oral Ulcers	Painless oral or nasopharyngeal ulceration
Arthritis	Nonerosive arthritis of 2 or more peripheral joints, associated with tenderness, swelling or effusion
Serositis	Pleuritis or pericarditis
Renal Disorder	Persistent proteinuria >0.5g/day or 3+ on dipstick, or cellular casts present
Neurologic Disorder	Seizures or psychosis
Haematologic Disorder	Haemolytic anaemia with reticulocytosis, leukopenia <4000/mm^3 on ≥2 occasions, lymphopenia <1500/mm^3 on ≥2 occasions or thrombocytopenia <100,000/mm^3 in the absence of offending drugs
Immunologic Disorder	Anti-DNA, anti-Sm or positive finding of antiphospholipid antibodies based on i) abnormal serum level of IgG or IgM antibodies ii) positive test result for lupus anticoagulant or iii) false positive serologic test for syphilis known to be positive for min. 6 months
Antinuclear Antibody	Abnormal titre by immunofluorescence or equivalent assay at any point in time and in the absence of drugs

Table 1.1: Diagnostic criteria for SLE, as specified by the American College of Rheumatology 1997 revised ACR criteria*(109, 110). SLE confirmed by positive presence of ≥4 criteria in the absence of other causes.*

Feature	Details
Clinical: Acute Cutaneous Lupus	Lupus malar rash, bullous lupus, toxic epidermal necrolysis variant, maculopapular lupus rash, photosensitivity or subacute cutaneous lupus
Clinical: Chronic Cutaneous Lupus	Classic discoid rash, hypertrophic lupus, lupus panniculitis, mucosal lupus, lupus erythematosus tumidus, chilblains lupus, discoid lupus/lichen planus overlap
Clinical: Oral Ulcers	Palate, buccal, tongue or nasal in the absence of other causes
Clinical: Nonscarring Alopecia	Diffuse thinning or hair fragility
Clinical: Synovitis	Involvement of ≥2 joints, characterised by swelling or effusion, or tenderness and ≥30 minutes morning stiffness
Clinical: Serositis	Pleuritis or pericarditis
Clinical: Renal	Persistent proteinuria >0.5g/day or red blood cell casts
Clinical: Neurologic	Seizures, psychosis, mononeuritis multiplex, myelitis, peripheral/cranial neuropathy or acute confusional state
Clinical: Haemolytic Anaemia	Haemolytic anaemia with reticulocytosis, leukopenia <4000/mm^3 on ≥2 occasions, lymphopenia <1000/mm^3 on ≥2 occasions or thrombocytopenia <100,000/mm^3 in the absence of offending drugs
Clinical: Leukopenia or Lymphopenia	<4000/mm^3 at least once or <1000/mm^3 at least once
Clinical: Thrombocytopenia	<100,000/mm^3 at least once
Immunological: ANA	Above laboratory reference range
Immunological: Anti-dsDNA	Above laboratory reference range, or twice above if using ELISA
Immunological: Anti-Sm	
Immunological: Anti-phospholipid Antibody	Lupus anticoagulant, false positive RPR, medium-high titre anticardiolipin or anti-β_2 glycoprotein I
Immunological: Low Complement	Low C3, C4 or CH50
Immunological: Direct Coombs Test	In the absence of haemolytic anaemia

Table 1.2: Diagnostic criteria for SLE, as specified by the Systemic Lupus International Collaborating Clinics 2012 report(106). *SLE confirmed by positive presence of ≥4 criteria, including both clinical and immunological or a combination of ANA/ anti-dsDNA antibodies and biopsy-proven lupus nephritis. Criteria must be found in the absence of any other causes.*

Further tools exist to determine patients experiencing a disease flare, thus supporting clinical decisions regarding treatment plans. The British Isles Lupus Assessment Group (BILAG) is a popular method due to its sensitive and comprehensive review of multiple organ systems, and its emphasis on the intention to treat. The system comprises an assessment of eight organ systems, with a score assigned to each based on symptomatic activity over the previous four weeks. The appearance of a new active or intermediate symptom in at least one organ system then indicates flared disease(111-113). Other methods include the Systemic Lupus Erythematosus Disease Activity Index, a global evaluation of disease activity in nine organ systems over the previous ten days(112). Both methods have comparable sensitivity however BILAG is considered most representative of disease activity over time(113).

1.2.3.2. Diagnosis of Cardiovascular Risk

1.2.3.2.1. Cardiovascular Risk Algorithms are Used Worldwide

A number of diagnostic tools have been developed for evaluation of cardiovascular risk, supporting identification of high risk patients who would benefit from clinical intervention. Screening algorithms, such as the Framingham risk calculator, predict cardiovascular risk based on factors such as age, blood pressure and cholesterol levels, although age consistently produces the dominant effect. Nevertheless, risk estimation appears to vary between algorithms(114).

The Framingham risk score was derived from a large-scale study spanning thousands of American citizens and is now a widely used risk tool across the globe. However, it has also been considered less representative of varied populations, overestimating risk in multi-ethnic communities(115, 116). Other algorithms such as Systematic COronary Risk Evaluation (SCORE), which stratifies risk groups across Europe, have been considered more representative of a wider population(116), although they may feature fewer variables.

1.2.3.2.2. The Use of QRISK Algorithms in Cardiovascular Risk Stratification

In light of the growing cultural diversity in the United Kingdom, a new CVD risk score targeted for the modern UK population was developed in 2007. QRISK was shaped using health records for approximately 7% of the population, supporting validation of cardiovascular risk factors and development of a risk equation using the Cox proportional hazards model. This algorithm aimed to provide a more extensive review of risk factors, with improved discrimination for a diverse population compared to Framingham(117).

As knowledge grew, this was further updated in 2008, producing QRISK2, with the inclusion of additional risk factors, self-assigned ethnicity and inter-relationships between factors, which is updated yearly(118, 119). The QRISK2 algorithm proved superior to the Framingham risk score, estimating risk with greater accuracy and avoiding the overestimation within the mixed population(120); it is now the CVD risk tool recommended by the National Institute for Health and Care Excellence (NICE) for clinical use in the UK, with a score of ≥10% indicating high risk(121).

However, NICE also recognised the increased cardiovascular risk in SLE and associated medications, such as corticosteroids, advising that risk may be underestimated in this population(122). Risk underestimation in patients was also observed when using Framingham, indicating the need for an SLE-inclusive score(123), such as that suggested by Fava *et al*.(124) and will be an area of investigation in this study.

1.2.3.2.3. Identification of Cardiovascular Risk in SLE

In 2017, an updated QRISK3 algorithm was produced to address the issues of inclusivity. It did this by incorporating a number of additional risk factors, including both SLE and corticosteroid prescription (Table 1.3). As with previous algorithms, a 10% likelihood of experiencing a major cardiovascular event over the proceeding 10 year period was deemed 'high risk'.

When Hippisley-Cox *et al*. validated and compared this to QRISK2, they found an improvement in accuracy of risk evaluation(119, 124) although this has not yet been

independently evaluated, particularly within a cohort of patients with SLE. Our interest in developing the QRISK3 algorithm extends to a current biomarker of interest, namely endothelial microvesicles, which show promise as a marker of endothelial damage. Accurate identification of patients with high cardiovascular risk would enable early provision of treatment and monitoring, potentially preventing premature mortality and improving quality of life.

Framingham Risk Score	QRISK2	QRISK3
Age (30-79 years)	Age (25-84 years)	Age (25-84 years)
Sex	Sex	Sex
Smoking status	Ethnicity	Ethnicity
Total cholesterol	UK postcode	UK postcode
HDL cholesterol	Smoking status	Smoking status
Systolic blood pressure	Diabetes status	Diabetes status
Blood pressure medication	Angina or heart attack in a 1st degree relative <60	Angina or heart attack in a 1st degree relative <60
	Chronic kidney disease (stage 4-5)	Chronic kidney disease (**stage 3-5**)
	Atrial fibrillation	Atrial fibrillation
	Blood pressure medication	Blood pressure medication
	Rheumatoid arthritis	**Migraines**
	Cholesterol/HDL ratio	Rheumatoid arthritis
	Systolic blood pressure	**Systemic Lupus Erythematosus**
	Body mass index (height, weight)	**Severe mental illness**
		Atypical antipsychotic medication
		Regular steroid medication
		Erectile dysfunction
		Cholesterol/HDL ratio
		Systolic blood pressure
		Standard deviation of min. 2 most recent systolic blood pressure readings (mmHg
		Body mass index (height, weight)

Table 1.3: A comparison of cardiovascular risk algorithms available in the UK. *The updated QRISK3 algorithm includes novel risk factors relevant to patients with SLE, such as SLE and steroid medication. Additional risk factors highlighted in bold. Severe mental illness is inclusive of schizophrenia, bipolar disorder and moderate-severe depression.*

1.3. Endothelial Microvesicles as Biomarkers and Effectors of Endothelial Dysfunction

1.3.1. Endothelial Microvesicles

Endothelial microvesicles (EMVs) are anucleoid, membrane-bound cell fragments 100-1000nm in size, characterised by a phospholipid bilayer studded with phosphatidylserine (PS). EMVs are released in response to diverse stimuli, including shear and oxidative stress, and have been found to transport bioactive proteins, lipids, mRNAs and microRNAs (miRNAs) to recipient cells. In this way, they have been considered as future biomarkers, as well as effectors of disease and repair processes (125-127).

1.3.1.1. Identification of EMVs

The presence of extracellular vesicles (ECVs) in plasma and blood products was first communicated by Peter Wolf in 1967, who referred to them as 'platelet dust'(128). Since then, ECVs have been scrutinised and found to be quite the opposite of the 'cell debris' they were first thought of; ECVs have been shown to mediate endocrine and paracrine effects(125, 127). ECVs were subsequently classified according to size and cellular origin. Current understanding is that there are three distinct groups of vesicles present in the extracellular space, with specific characteristics and mechanisms of formation. Of these, microvesicles are defined by their size, release pathway and unique surface markers obtained from the membrane of the donor cell, which can be determined using labelled antibodies and flow cytometry (figure 1.4). Surface markers may also be used to distinguish

between the varied microvesicle populations present in blood, such as those of endothelial origin (EMVs) compared to platelet-derived microvesicles (PMVs)(126, 129).Nomenclature may also vary, such that microvesicles may also be referred to as microparticles.

	Exosomes	Microvesicles	Apoptotic Bodies
Size	20-120nm	100-1000nm	0.5-2μm, potentially up to 5μm
Density	1.13-1.19g/ml	1.04-1.07g/ml	1.16-1.28g/ml
Characteristics	Cup-shaped morphology	Heterogenous	Heterogenous
Formation	Released extracellularly from multivesicular bodies in endolysosomal pathway	Blebbing from membrane following cell activation	Blebbing from membrane during apoptosis
Pathways Involved	Endosomal sorting complex, tetraspannins, ceramide	Calcium signalling, ROCK1 activation	Apoptotic pathways
Membrane Properties	Impermeable, PI-ve	Impermeable, PI -ve	Permeable, PI +ve
Markers	CD81, CD63, integrins, actin, clathrin, tetraspannins, alix	CD40, cell-specific markers, annexin V+ve	Caspase 3, histone proteins, annexin V +ve
Known Composition	Proteins, lipids, nuclear components, RNA, ncRNA, MHC	Proteins, lipids, cell organelles, RNA, ncRNA	Proteins, cell organelles, DNA, RNA, ncRNA

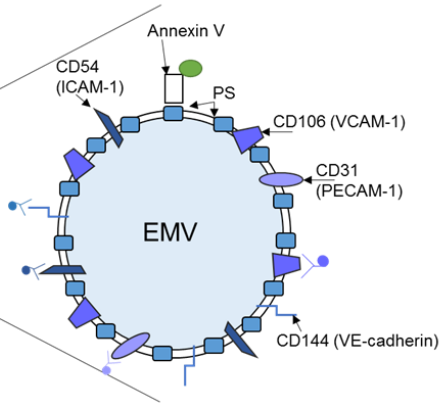

Figure 1.4: The characteristics and phenotypic distinctions of EMVs. *Endothelial microvesicles are characterised by a number of phenotypic features including specific surface markers representative of the endothelial lineage, which are often upregulated following cell activation e.g. ICAM-1, CD144, CD31. These can be detected using labelled antibodies; the presence of phosphatidylserine (PS) within the membrane can also be detected by labelling annexin V. Adapted from Yin et al. (2015).*

1.3.1.2. EMV Release and Uptake

EMVs are released by blebbing from the cell membrane following cellular activation, a process that occurs seconds after activation and cytoskeletal disruption(130). This results in downstream calcium signalling and ROCK1 activation, which leads to translocation of phosphatidylserine, a cytoplasmic aminophospholipid, to the cell membrane(125). Recognition of phosphatidylserine by recipient cells appears crucial in phagocytosis of

extracellular vesicles, although transfer of contents can also be enabled by receptor-mediated, clathrin-independent endocytosis and pinocytosis(126, 131-133). Despite this, microvesicular uptake appears dependent on a number of variables such as membrane composition, and both intracellular and extracellular conditions. Donor and target cells can also be of different lineages (Figure 1.5)(133, 134).

The first evidence of this uptake was presented by Scholz *et al*. in 2002(135) whereas the first evidence of miRNA transfer, albeit in exosomes, was published by Valadi *et al.* in 2007 followed by microvesicular miRNA transfer by Yuan *et al*. in 2009(136, 137). The possibility of transfer of material using MVs provides new therapeutic options and potential for delivery of drugs(126, 127, 129, 133). Once released, MVs are cleared fairly rapidly, most likely by hepatic or phagocytic mechanisms; monocellular culture means they are quite stable *in vitro*, supporting the development of cellular models for further study(129).

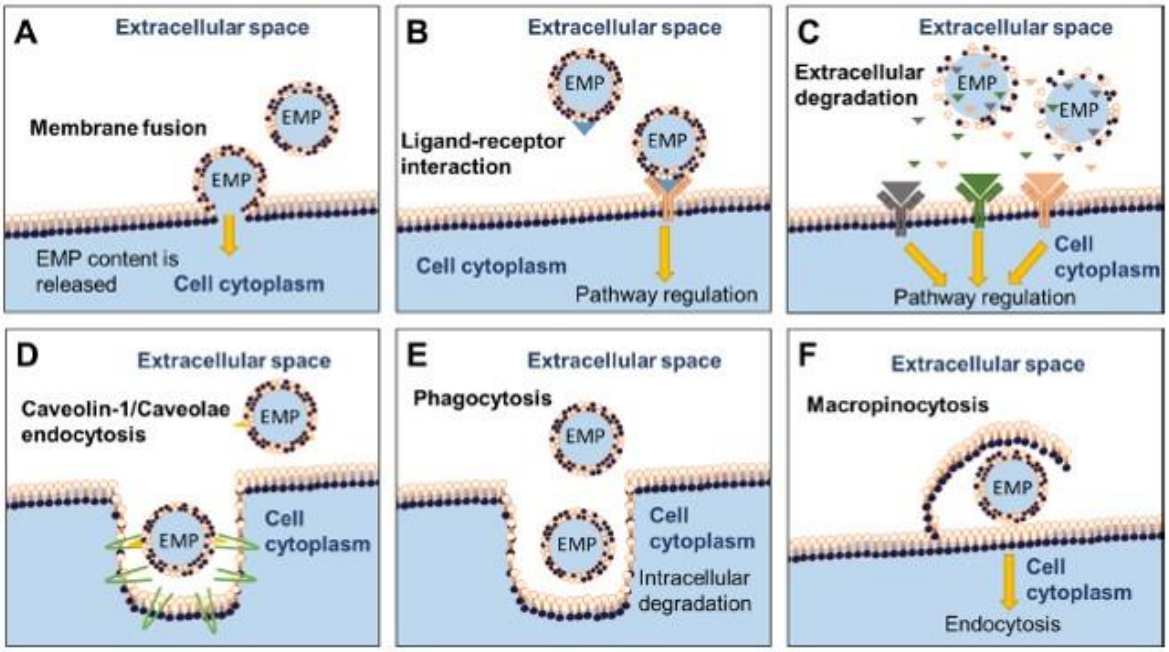

Figure 1.5: Proposed mechanisms of EMV uptake. *Uptake appears to be dependent on the environment and interacting cells, with potential mechanisms including A: membrane fusion, B: ligand-receptor interactions, C: extracellular degradation, D: caveolin-dependent endocytosis, E: phagocytosis and F: micropinocytosis. EMVs are referred to here as EMPs (endothelial microparticles). Figure courtesy of Dr Daniel Moreno Martinez(138).*

1.3.2. EMV Content: miRNA

As described previously, EMVs transport bioactive contents through the circulation, and can transfer these to recipient cells(125). EMV contents include miRNAs, which offer potential for further cardiovascular biomarker studies and patient stratification(139), as well as elucidation of pathways by which EMV content may affect endothelial function in SLE.

1.3.2.1. MiRNA Structure and Function

Small RNAs are found across eukaryotic organisms and are defined by a size of 20-30 nucleotides. Of this family, miRNAs are a dominant class, comprising 18-22 nucleotides(140, 141).

Transcription of miRNA genes by RNA polymerase II results in a long transcript with miRNA sequences found within a hairpin structure; the initial products are primary miRs (pri-miRs), which are then processed into pre-miRs by RNAse III protein Drosha prior to nuclear export. Once within the cytoplasm, another RNAse III protein, Dicer, further processes the pre-miRs into mature and functional miRNA. In most cases, these miRNAs proceed to bind to 3'UTR sites of target mRNA and regulate their expression (figure 1.6)(140, 141). They do this by two modes of action; miRNAs can integrate into a ribonucleoprotein RNA-induced silencing complex (RISC) which then either silences gene expression by e.g. endonucleolytic cleavage of mRNA or blocks translation through recruitment of repressors(142).

The miRNA gene family is extremely abundant and as such, has complex nomenclature and relationships. It is relatively common to find similar miRNA loci that are products of gene duplication, and therefore mature miRNAs with identical sequences within the first 2-7 nucleotides (the miRNA 'seed') are considered part of the same family. miRNAs can also share a common origin and so belong to an evolutionary superfamily but demonstrate single nucleotide differences within the miRNA seed sequence. Nomenclature may also be inconsistent, with miRNAs referred to according to phenotype, e.g. let-7, or numerically by order of discovery. Furthermore, miRNA 'sisters' may be differentiated by the suffix a and

b, while the directionality of the miRNA transcription from the loci is also described e.g. miR-30d-5p(140, 143).

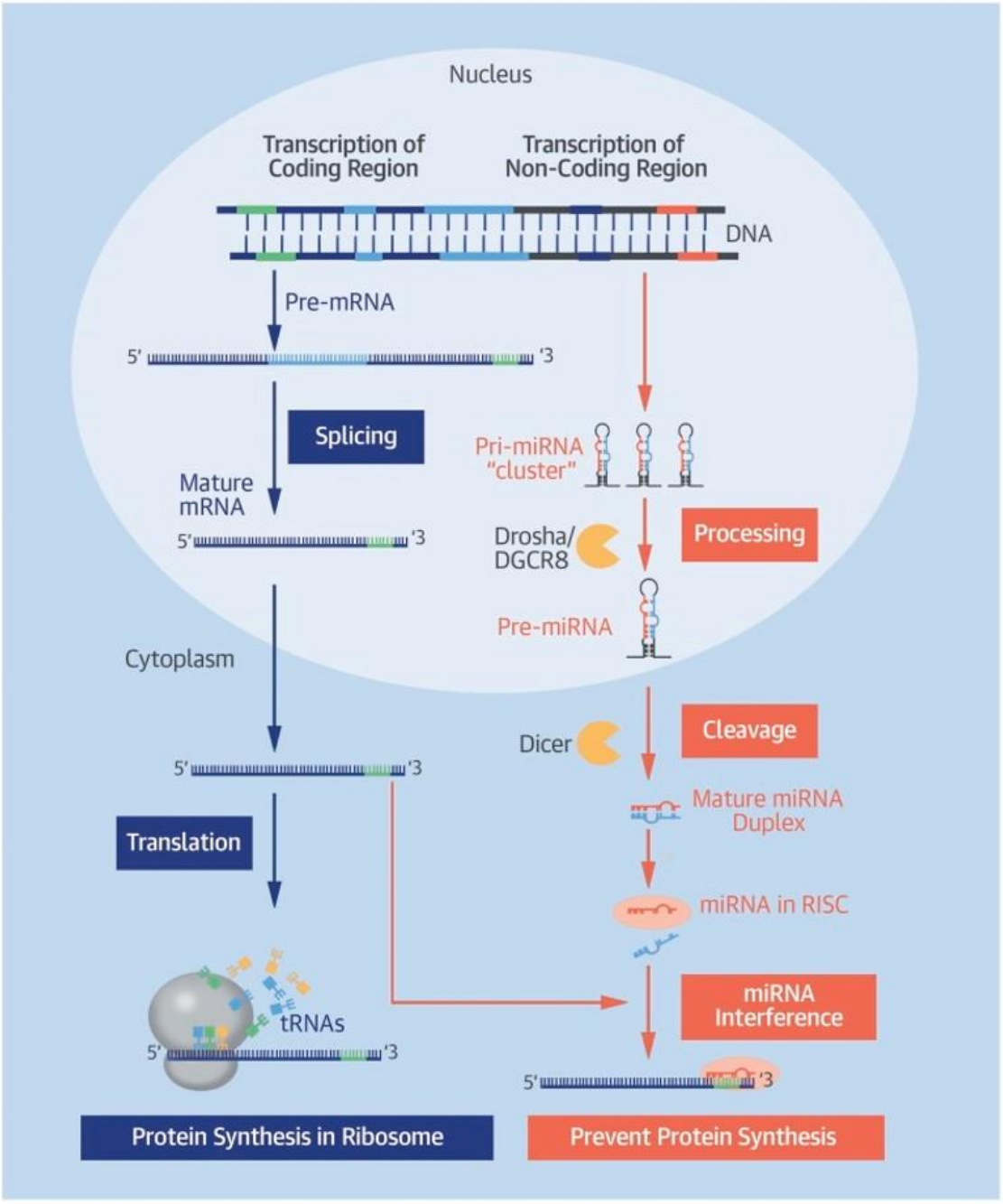

Figure 1.6: MiRNA formation and action in relation to mRNA. *miRNAs are processed in the nucleus before final cleavage in the cytoplasm, producing mature miRNA. Once mature, the miRNA can interact with target mRNA to prevent protein synthesis. Figure by Barwari et al. (2016).*

1.3.2.2. MiRNAs in CVD

Disease-specific miRNAs show great promise for both mechanistic and biomarker studies. As yet, a clear picture of the role of miRNAs in cardiovascular health has not been determined however numerous studies have suggested roles for individual miRNAs associated with various cardiovascular morbidities. The sheer quantity of identified human miRNAs makes a full description of their potential actions beyond the scope of this work, although summaries of possible cardiovascular interactions have been elegantly reviewed elsewhere(141, 144).

As mentioned, miRNAs can post-transcriptionally alter gene expression, most commonly preventing translation of target mRNAs. The mRNA targets differ between miRNAs; one of the most extensively studied miRNAs in cardiovascular research is miR-145, which appears to be pro-atherosclerotic, through phenotypic switching and fate determination of VSMCs (145-147). MiR-21 also acts on VSMCs, and by doing so can influence the stability of atherosclerotic plaques, but has historically been studied for its role in fibrosis and cardiac function(144, 148, 149). In this way, miRNAs can have unique roles that interrelate and create a dynamic environment during vascular health and disease.

The associations between certain miRNAs and disease states supports the development of miRNA 'signatures' as biomarkers of disease activity. For example, miR-126-3p (and miR-145-3p) has been recommended as a biomarker of acute myocardial infarction(150), while miR-93 has been suggested for use in stroke diagnosis, as well as coronary artery disease(151, 152). Thus the quantification of individual miRNAs packaged into EMVs shows great potential in the fields of diagnostics and precision medicine(153) and will be investigated in this study within the context of SLE.

1.3.3. EMVs as Biomarkers of Cardiovascular Risk

By providing a 'snapshot' of valuable information regarding the state of the endothelium, EMVs have been suggested for future use as biomarkers in cardiovascular disease. Indeed, increased levels are associated with unstable, asymptomatic carotid plaque formation,

coronary endothelial dysfunction and increased risk of a major cardiovascular event (125, 154-156).

EMVs and their contents may also be utilised in other conditions, such as SLE. Our group has previously shown that circulating EMVs are elevated in patients with SLE compared to controls, and not only were associated with endothelial dysfunction, but also could be reduced by immunosuppressive therapy, implying a connection between EMVs and inflammation(157-159). Suggested effects of microvesicles in SLE include stimulation of NETosis, immune complex formation and ROS production(160-163); a number of studies have also performed high throughput screening of miRNAs isolated from blood, although the primary focus is often on lupus nephritis or mononuclear cells(164-167). Characterising EMV function in SLE within the context of cardiovascular involvement is a relatively novel area; and should provide crucial knowledge to the field of diagnostics and treatment of SLE through innovative biomarker development and identification of future targets for therapy.

1.4. Hypothesis, Aims and Objectives

1.4.1. Study Summary and Rationale

Incidence of cardiovascular disease is increased in SLE, meaning young patients are at risk of endothelial damage, subclinical atherosclerosis and premature death. It is therefore critical that this risk is recognised.

1.4.2. Hypothesis

We hypothesise that endothelial damage may be assessed through the identity and quantification of EMVs as novel biomarkers, and *in vitro* models using endothelial cells may be used to interrogate the mechanisms by which the endothelium becomes damaged in SLE.

The overarching aim of this study is to establish whether EMVs can be added to the armament of risk factors used for identifying patients with SLE at elevated risk of future cardiovascular events.

1.4.3. Aims and Objectives

The specific aims and objectives of this project are thus:

AIM 1: To identify novel biomarkers for cardiovascular risk in SLE.

- Objective 1. Clinical cardiovascular risk algorithms will be compared in relation to markers of inflammation and cardiovascular health in a cohort of patients with SLE using SPSS statistical software.
- Objective 2. EMV levels in the SLE cohort will be quantified using flow cytometry to establish whether correlations might exist with clinical data.

AIM 2: To determine a vesicular miRNA signature in patient plasma.

- Objective 1. Data mining will be used to screen miRNAs of interest, which will be quantified in patient plasma by quantitative PCR and correlated with clinical data.
- Objective 2. Predicted miRNA targets will be identified by gene ontology analysis.

AIM 3: To elucidate functional effects of SLE-related miRNAs in endothelial cells.

- Objective 1. An *in vitro* model of miRNA overexpression will be generated using a lentiviral vector transfer strategy.
- Objective 2. The effects of miRNA overexpression on endothelial cell function will be probed using migration, angiogenesis and cellular respiration assays.

Chapter 2

Materials and Methods

2.1. Mammalian Cell Culture

Cell culture plates, flasks and plasticware were obtained from ThermoFisher Scientific. To ensure sterility, cells were handled within a class II safety cabinet and relevant equipment treated with 70% v/v industrial methylated spirits (Fisher).

2.1.1. Culture and Passage of Human Umbilical Vein Endothelial Cells (HUVECs)

Early passage HUVECs from pooled donors were sourced from Caltag Medsystems and revived in complete endothelial cell growth medium MV2, with supplied supplements (Promocell) and 1% v/v penicillin/streptomycin mix at 10,000U/ml each (Lonza).

0.1% w/v bovine skin gelatine (Sigma) diluted in phosphate-buffered saline without Ca^{2+} or Mg^{2+} (PBS; Lonza) was used to coat culture vessels by incubating for 30 minutes prior to removal and washing with PBS. Individual vials of cells were seeded into 25cm^2 flasks, where they were incubated at 37°C, 5% CO_2 until confluence and for routine maintenance, passaged 1:3 into 75cm^2 flasks, twice weekly using 200mg/L trypsin (Lonza) as a dissociation reagent (2ml per 25cm^2). Cells were cryopreserved in 10% dimethyl sulphoxide (DMSO; Sigma), 40% foetal calf serum (FCS), 50% media and chilled for 24 hours in a Nalgene® Mr Frosty freezing container at -80°C prior to storage in liquid nitrogen. To enable revival, cryopreserved cells were thawed at 37°C for <5 minutes before seeding into pre-warmed media (25cm^2). Media was discarded and fresh added at 24 hours, to ensure removal of remaining DMSO.

2.1.2. Culture and Passage of Human Embryonic Kidney 293T Cells

HEK293T cells (ATCC® CRL-3216™) at early passage were revived and cultured in Dulbecco's Modified Eagle's Media (DMEM; Lonza) with supplementation as specified below. Revived cells were transferred directly to 75cm^2 flasks and incubated as in 2.1.1. Cells were passaged once confluent (2-3 times weekly), at a ratio of 1:6 using 200mg/L trypsin as before, and cryopreserved as in 2.1.1.

DMEM Media Composition

DMEM (Lonza)

10% FCS (ThermoFisher Scientific)

1% L-glutamine (Corning)

1% Penicillin/streptomycin mix (Lonza)

2.2. Cellular Function Tests

2.2.1. Cell Treatment: Cytokines

10ng/ml TNFα and BLyS (Peprotech) were used to treat cells and simulate the inflammatory environment present in patients with SLE, as these cytokines are commonly associated with the disease, as discussed in chapter 1.

2.2.2. Cell Viability: Alamar Blue Assay

Cells were cultured in clear 96 well microplates at 1x10^4 cells per well in 100µl media. 10ul alamarBlue reagent (Invitrogen) was added and plates incubated for 24 hours. Absorbance was then read at 570/600 and fluorescence at 530/590 using a Synergy™ HT Microplate Reader (BioTek).

2.2.3. Scratch Migration Assay

Cells were plated at $1x10^5$ cells per well and cultured to confluence in 12 well culture plates. A P200 pipette tip was used to draw a vertical line through each well, creating a cell-free scratch area. Media was then removed and cells washed with PBS twice to remove non-adherent cells. Media was replaced and images were taken at x4 magnification on a Zeiss Primovert inverted microscope with Axiocam 105 colour camera at 0, 5 and 24 hours. Images were then analysed using ImageJ software.

2.2.4. Angiogenic Tube Formation Assay

Prior to performing this assay, Matrigel® Matrix (Corning) was refrigerated on ice overnight to thaw slowly, alongside pipette tips and a clear 96 well microplate. On the day of the assay, 30µl of Matrigel® was used to coat the microplate wells, which were then incubated for 30 minutes at 37°C in order to set. Next, cells were plated on top of the matrix at $9x10^3$ per well in 50µl media. Images were taken at x10 magnification using the Zeiss microscope at 5 and 24 hours. Images were analysed manually, using ImageJ software and the flowchart below (figure 2.1).

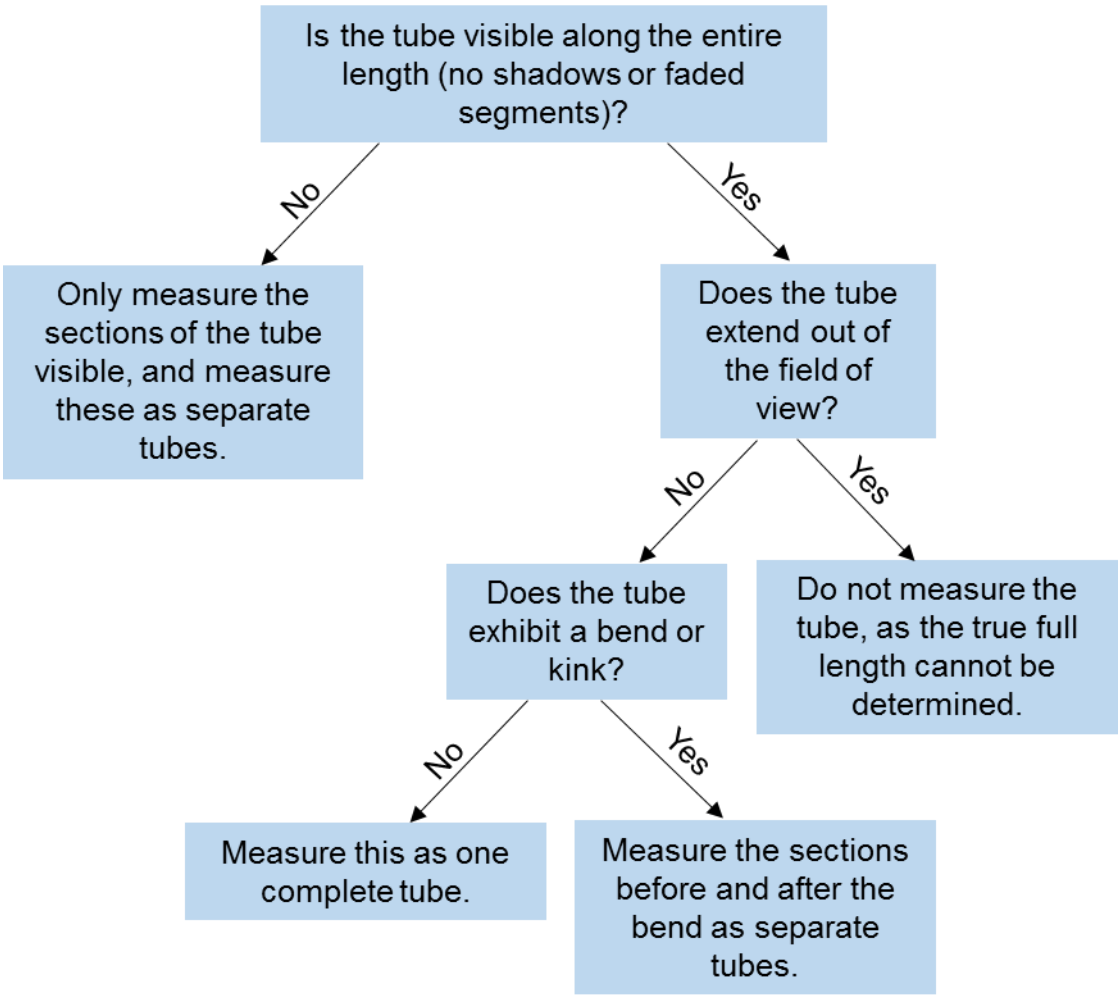

Figure 2.1: Flowchart for tube recognition in manual angiogenesis analysis.

2.2.5. Seahorse Mitochondrial Bioanalysis

Seahorse bioanalysis allows interrogation of oxygen consumption rate (OCR) and extracellular acidification rate (ECAR), providing data on mitochondrial and glycolytic respiration. To do this, compounds are sequentially added to cells, which inhibit or boost certain respiratory pathways. In this work, oligomycin, carbonyl cyanide-4-phenylhydrazone (FCCP) and rotenone/antimycin A were injected to target the respiratory aspects as depicted in figure 2.2 (168).

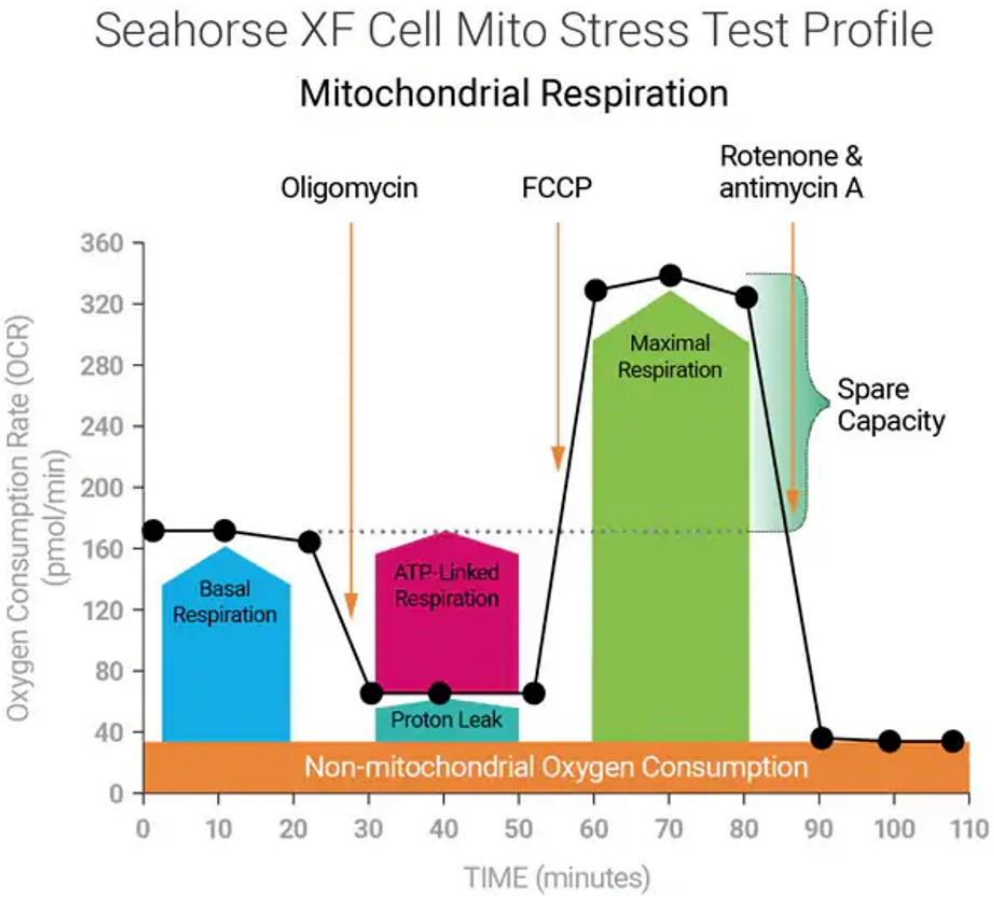

Figure 2.2. Seahorse cell mito stress test profile. *When performing a cell mito stress test, oligomycin is injected first to inhibit ATP synthase, reducing mitochondrial respiratory ability. FCCP is next added to disrupt the proton gradient and alter mitochondrial membrane potential, increasing OCR to maximum. The final addition is a mix of rotenone and antimycin A, which inhibit complexes i and iii of the mitochondrial electron transport chain, stopping all mitochondrial respiration. Figure courtesy of Agilent Technologies.*

Cells were plated at $8x10^3$ cells per well into a Seahorse XF96 Cell Culture Microplate and cultured overnight under standard conditions (section 2.1.1). On the day of the assay, a Seahorse XFe96 FluxPak was hydrated in Seahorse XF calibrant solution for 1 hour and cell media was changed to Seahorse XF base media supplemented with 1mM pyruvate, 2mM glutamine and 10mM glucose (all Sigma) at pH 7.4 for 45-60 minutes. Mitochondrial function was then assessed using a Seahorse XFp Cell Mito Stress Test kit, in accordance with kit protocol. Seahorse reagents were acquired from Agilent Technologies. Consistent cell plating was confirmed by Pierce™ BCA assay (ThermoFisher Scientific).

2.3. EMV Isolation and Quantification

2.3.1. EMV Isolation

Whole blood samples were centrifuged at 1,500g for 10 minutes at 4°C and the plasma removed. Plasma was then centrifuged at 20,000g for 10 minutes at 4°C and the supernatant harvested, and stored at -80°C prior to analysis by flow cytometry or use in experiments. When isolating EMVs released from cells in culture, the media was removed and centrifuged at 1,500g for 10 minutes at 4°C. The supernatant was harvested and stored as above.

Exosome-free media was prepared using media with 2% exosome-depleted FCS. The FCS was prepared by ultracentrifugation at 100,000g for 18 hours using an OptimaTM XE ultracentrifuge (Beckman Coulter). The exosome-rich pellet was discarded and supernatant used in the media.

2.3.2. EMV quantification

Optimisation of settings on FACSVerse (BD) was undertaken prior to flow cytometric analysis. Polystyrene beads of known size (Spherotech) were used to identify and gate areas expected to yield microvesicles (figures 2.3 and 2.4).

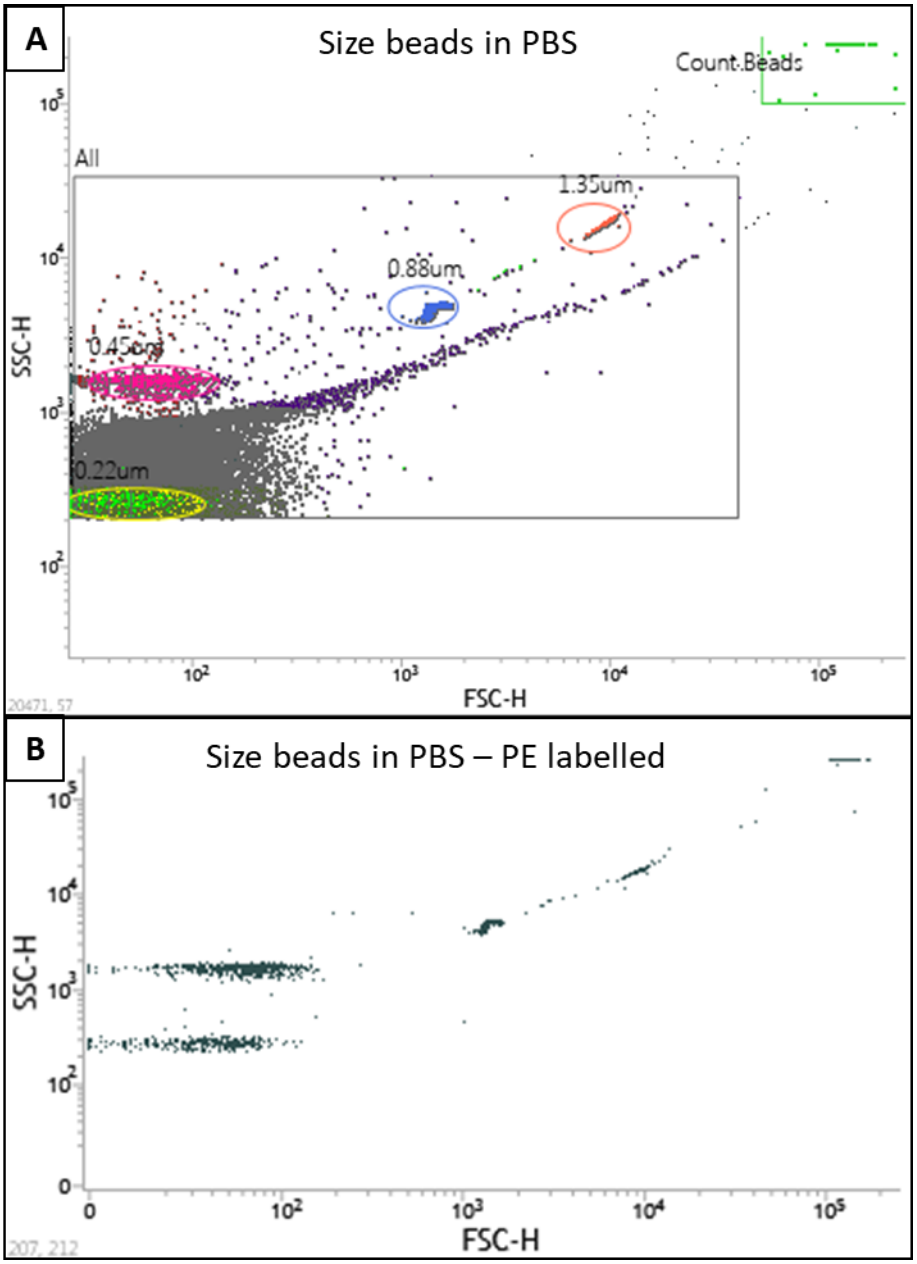

Figure 2.3: ***Vesicle positioning using beads of known size.*** *A and B: The use of phycoerythrin (PE)-labelled beads allows identification of the areas in which MVs would expect to be visualised, supporting the determination of gates prior to flow cytometric analysis.*

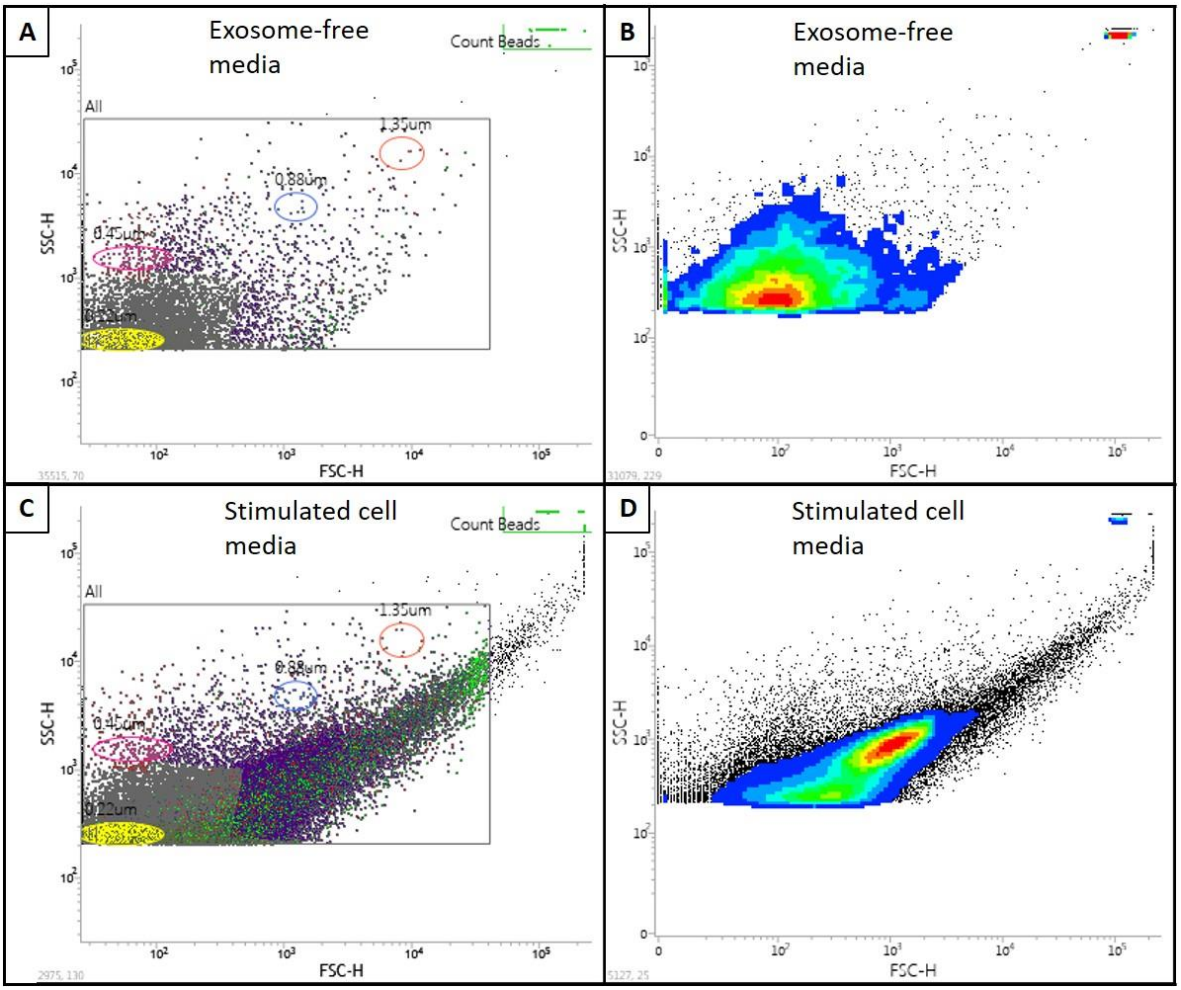

Figure 2.4: Establishment of gates to characterise MV populations. *MVs isolated from exosome-free media following cell treatment with TNFα exhibited a characteristic tail appearance under flow cytometry (A), compared to fresh exosome-free media (C). There was also high particulate density in regions corresponding to larger vesicle size (D), which was not present in media only (B). Gating was conducted to maximise capture of tail areas with highest particulate density.*

Flow cytometry was then performed to quantify MV numbers present in human plasma and to characterise their cellular origin, such that EMVs may be identified. Patient plasma was isolated as described in 2.3.1 and 20µl added to a flow tube. Tube contents were made up to 200µl with 1µl each of CD31 antibody labelled with BD Horizon Brilliant™ Blue 515, CD144 and CD42b antibodies, 5µl count beads (Beckman Coulter; Table 2.1) and 172µl 0.22µm-filtered PBS. Following this, tubes were kept on ice in the dark for 30 minutes before flow cytometric analysis.

Antibody	Company
BB515 Mouse Anti-Human CD31	BD Biosciences
PE Mouse anti-Human CD144	BD Biosciences
APC Mouse Anti-Human CD42b	BD Biosciences

Table 2.1: Antibodies used for flow cytometry.

2.4. MiRNA Analysis

2.4.1. MiRNA Selection

A literature search of PubMed and Google Scholar was performed on publications up to October 2017 using keywords 'miR' and 'SLE', 'systemic lupus erythematosus', 'cardiovascular', 'endothelial', 'microvesicles', 'microparticles' or 'extracellular vesicles'. Results of miRNA sequencing, microarray and qPCR analysis of adult cell-free plasma and EMVs were noted, whilst experiments using other cell types, such as lymphocytes and renal cells, were excluded. Only primary research papers were used; review articles were utilised solely as reference guides.

A shortlist of potential miRNAs of interest was produced based on extent of current knowledge, notes found in relevant papers, unpublished preliminary data previously generated by our group pertaining to miRNA expression in a cellular model of SLE, and data

from DAVID(169, 170) and TargetScan(171) regarding potential implicated molecular pathways. 7 miRNAs of interest were chosen based on this method and located across 14 research papers; let-7a was also included for analysis as a 'housekeeper', as it has often been suggested by other researchers, albeit in oncogenic settings, and is frequently reported in numerous tissue types, including endothelial cells, in publication and on ExoCarta/Vesiclepedia miRNA databases(172-176).

2.4.2. MiRNA Isolation and Amplification

Prior to miRNA isolation, plasma and media samples, which had previously been processed as in 2.3.1., were centrifuged at 100,000xg for 1 hour at 4°C to extract the vesicular fraction. MiRNA was isolated using a miRNeasy micro kit (Qiagen), from 1ml plasma or following kit instructions regarding starting amount of cellular material. To amplify transcripts for quantification, reverse transcription was performed using miRCURY LNA reverse transcription kit (Qiagen) following the manufacturer's instructions. Incubation cycles were performed on an Agilent Sure Cycler 8800 Thermocycler, as below, and cDNA stored at -20°C.

Incubation Protocol

42°C – 60 mins

95°C – 5 mins

Chill on ice

2.4.3. MiRNA Quantification

MiRNA abundance was analysed by qPCR using the cDNA generated as in 2.4.2. This was achieved using miRCURY LNA miRNA PCR assays (Qiagen) with primer sequences below (table 2.2).

Primer	Sequence
hsa-let7a-5p	5'UGAGGUAGUAGGUUGUAUAGUU
hsa-miR-126-3p	5'UCGUACCGUGAGUAAUAAUGCG
hsa-miR-93-5p	5'CAAAGUGCUGUUCGUGCAGGUAG
hsa-miR-3148	5'UGGAAAAAACUGGUGUGUGCUU
hsa-miR-320a	5'AAAAGCUGGGUUGAGAGGGCGA
hsa-miR-30d-5p	5'UGUAAACAUCCCCGACUGGAAG
hsa-miR-15b-5p	5'UAGCAGCACAUCAUGGUUUACA
hsa-miR-20a-5p	5'UAAAGUGCUUAUAGUGCAGGUAG

Table 2.2: LNA miRNA PCR assay primers used in quantification of miRNAs.

Kit instructions were followed, using the 60x dilution for plasma and cellular analysis, and 10x dilution for vesicles generated in *vitro.* 7µl mastermix (composition below) was added to wells of a 0.2ml semi-skirted 96-well plate (Starlab) before inclusion of 3µl cDNA in each well. A qPCR reaction was then performed in a 2-step program on an Applied Biosystems Step One Plus Real Time Thermocycler using the protocol below.

<u>Mastermix composition (per well)</u>

5µl 2x miRCURY SYBR green master mix (Qiagen)

1µl PCR primer mix

1µl RNase-free water

<u>Cycling protocol</u>

95°C – 2 mins

95°C – 10 secs

56°C – 1 min

*40 cycles

2.4.4. MiRNA Predicted Target Identification

Predicted targets of the miRNAs of interest were recorded from DIANA microT v5(177) and matched with results obtained from the Gene Ontology (GO) Consortium(178, 179) regarding genes implicated in 'endothelial cell activation', 'blood microparticles', 'IFNα signalling', 'SLE', 'cellular respiration', 'ossification' and 'bone mineralisation'. Cytoscape(180) was then used to identify crucial proteins and pathways targeted, highlighting key nodes associated with each miRNA. Finally, the data were ranked according to DIANA miTG prediction score and Cytoscape degree ranking.

2.5. DNA and Analysis using Electrophoresis

Agarose gels were made to appropriate concentration e.g. 1.5% by diluting ultra-pure agarose (Invitrogen) in 1xTBE buffer (ThermoFisher Scientific), boiling to dissolve crystals, then addition of Midori green at 0.01% (5µl in 50ml [Nippon Genetics Europe]). The solution was poured into a gel cast system with the addition of a comb to form the wells and was left to set for 30 minutes at room temperature. 5µl NEB loading dye was added to samples prior to loading into the gel, alongside 10µl of 1kb ladder (New England Biolabs) and electrophoresis was conducted at 120V for 30 minutes.

2.6. Generation of *In Vitro* MiRNA Overexpression Models

2.6.1. General Bacterial Methods

2.6.1.1. Preparation of Bacterial Broth and Agar

Lennox Lysogeny Broth (LB) broth and agar mixes (both Sigma) were prepared in deionised water, in accordance with the manufacturer's protocol. Both were autoclaved for 15 minutes at 121°C; once cooled, the appropriate antibiotic was added to the agar, which

was poured over a flame into petri dishes. Antibiotic was mixed into aliquots of bacterial broth immediately before use.

2.6.1.2. Preparation of Antibiotics

100mg/ml stock solutions of kanamycin and ampicillin (both Sigma) were aseptically prepared in deionised water, within a laminar flow cabinet. Final working concentrations of 50µg/ml and 100 µg/ml were used for kanamycin and ampicillin respectively. Antibiotics were stored at -20°C.

2.6.1.3. Preparation of Glycerol Stocks

Following overnight culture of bacterial colonies in 5ml LB broth, 1ml of culture was removed and mixed with 1ml glycerol (Fisher Scientific). Glycerol stocks were then stored in cryovials at -80°C.

2.6.1.4. Bacterial Strains and Transformation

DH5α competent *E.Coli* cells were used to generate entry clones whereas One Shot™ Stbl3™ competent *E.coli* cells (both Invitrogen) were used in the generation of expression clones prior to lentivirus production. To transform cells, 1µl DNA was added to individual vials of bacterial cells, which were then chilled for 30 minutes on ice. Next, they received a heat shock for 45 seconds at 42°C, followed by a further incubation on ice for 2 minutes. Finally, 450µl of room temperature (RT) super optimal broth (SOC media) was added and vials shaken horizontally at 37°C for 1 hour at 200rpm, prior to plating.

2.6.2. Generation of MiRNA Overexpression Plasmid Constructs by Gateway® Cloning

Gateway® Cloning technology was first developed by Invitrogen to simplify cloning workflows by minimising the use of restriction enzymes and subcloning, while maintaining high recombination efficiency(181). Precise recombination is mediated by the inclusion of *att* sites, which only recognise specific enzymes and recombine with their paired *att* site; in this way, nucleotides are neither gained nor lost and DNA can only be inserted monodirectionally (figure 2.5). The inclusion of Gateway cassettes containing antibiotic resistance and the toxic *ccdB* gene allow further confirmation of correct recombination(182, 183). This technique was utilised to generate plasmids throughout this study.

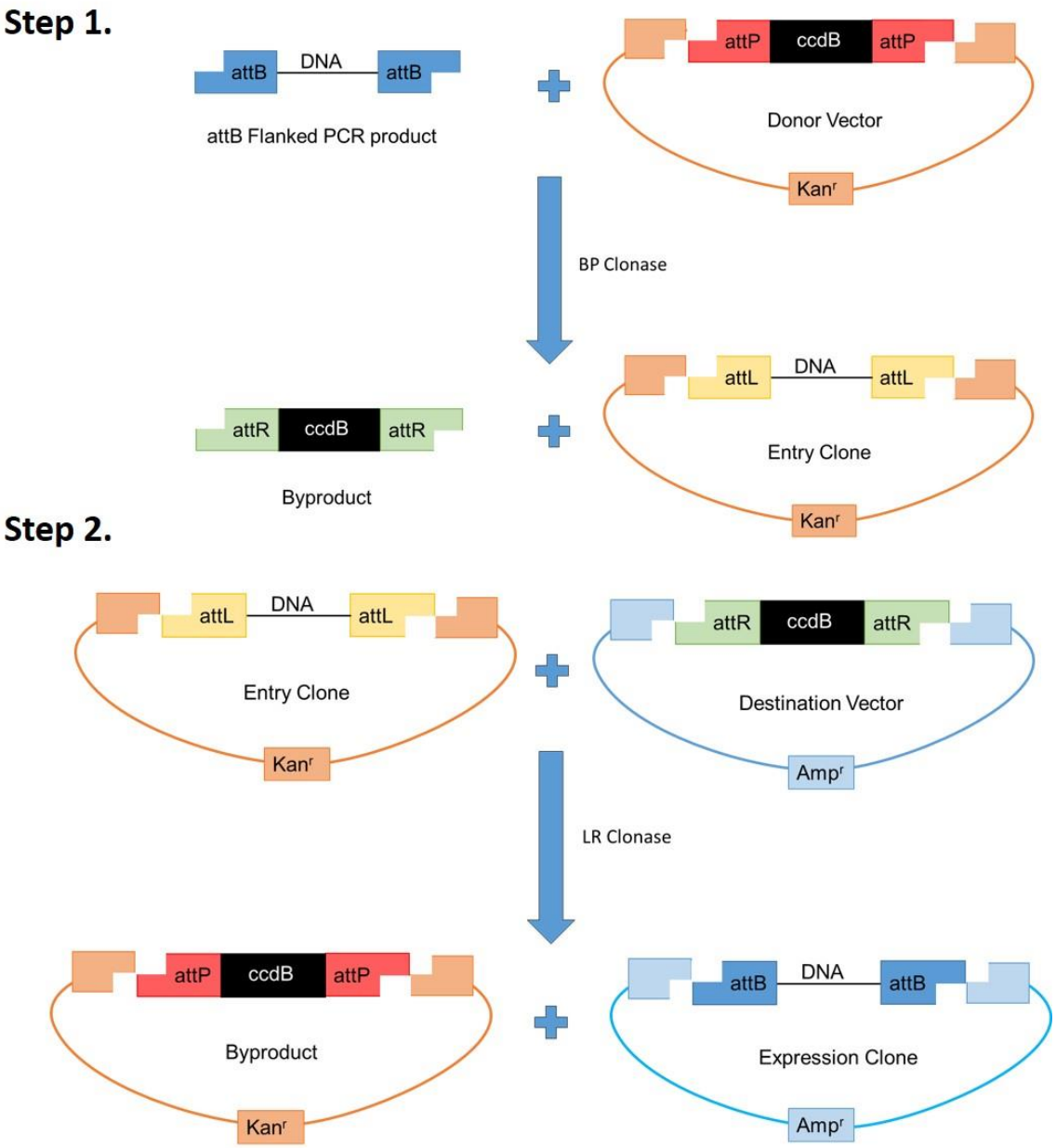

Figure 2.5: Gateway® Cloning workflow. *During step 1, the attB-flanked gene or PCR product is combined with a donor vector containing the toxic ccdB gene and expressing kanamycin resistance, using BP clonase enzyme. This yields a recombined entry clone with the DNA flanked by attL sites and a by-product that is toxic to cells. The entry clone is then recombined with a destination vector expressing ampicillin resistance using LR clonase. The final result is an expression clone containing both the attB-flanked DNA and ampicillin resistance.*

2.6.2.1. Design of MiRNA Constructs

MiRNA sequences were identified using the online National Centre for Biotechnology (NCBI) database. Constructs were supplied by Life Technologies, and were designed to include flanking sequences for *att*B1 and *att*B2, as well as for restriction enzymes Hpa1 and Xho1 to support recombination and ligation (figure 2.6 and table 2.3).

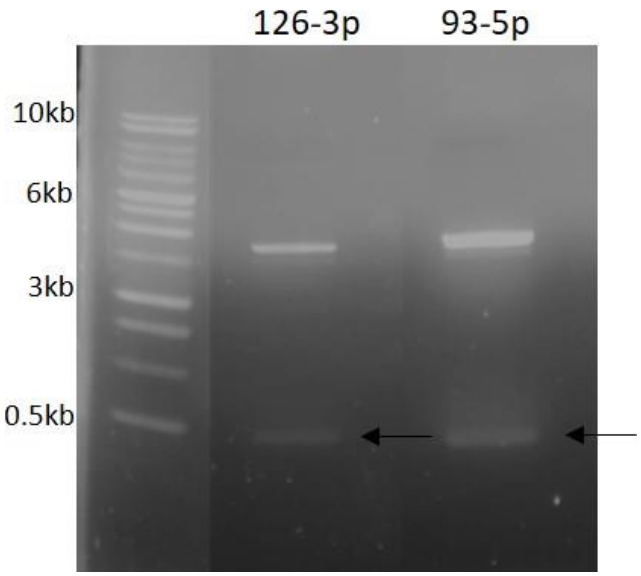

Figure 2.6: Representative DNA gel of miRNA constructs*. Prior to cloning, purchased miRNA constructs were analysed by gel electrophoresis on a 1.5% agarose gel, conducted at 120V for 30 minutes. Constructs were digested with restriction enzyme Hpa and Xho1, yielding bands at 400-500bp, corresponding with the designed construct, and remaining bands corresponding with the carrier plasmid. 1kb ladder ranging from 0.5-10kb.*

DNA	Sequence
hsa-miR-126-3p	TCGCAGGTTGCCCGGAGCCTCATATCAGCCAAGAAG GCAGAAGTGCCCCGTCCCGGGGTCCTGTCTGCATCC AGCGCAGCATTCTGGAAGACGCCACGCCTCCGCTGG CGACGGGACATTATTACTTTTGGTACGCGCTGTGAC ACTTCAAACTCGTACCGTGAGTAATAATGCGCCGTC CACGGCACCGCATCGAAAACGCCGCTGAGACCTCAG CCTTGACCTCCCTCAGCGTGGCCGGGACCCTGAGCC TCTGCGCAGAGCCACCCGCCCCGACGTACTTAGGCG
hsa-miR-93-5p	TCAACCTTCACTGAGAGGGTGGTTGGGGTCTGTTTC ACTCCATGTGTCCTAGATCCTGTGCTACAGACCTTCC TTTCTGTCCTCCCGTCTTGGACCTCAGTCCTGGGGGC TCCAAAGTGCTGTTCGTGCAGGTAGTGTGATTACCC AACCTACTGCTGAGCTAGCACTTCCCGAGCCCCCGG GACACGTTCTCTCTGCCAATTGTCTTCTTGGCTGAGC TCCCCAAGCTCCATCTGTCATGCTGGGGAGCCCAGT GGCGTTCAAAAGGGTCTGGTCTCCCTCCTCGAGG
hsa-miR-3148	TCTCTTCCCACAGGAAGGCAATGTGTGGAATGGAGA AGGCTGCTTCAGCAACATCCTCTCCCATGCACCTTAA ACGTCTCTTTCTTTCTCAGCTCCTTTCTGGAGTTAAG ATGGAAAAAACTGGTGTGTGCTTATTGATGTAGCCA ACAAGCATACATCAGTTTTTTCCAACTTAACTCCAGT ATTTTCCCCAATTCATCCTGAAATTGCTGCCCTATCC ATTCTCCCTCCTACACAGCCAAGATTCTTAAAAAACC AATCCAAATTTGCAGAATCTCCG
hsa-miR-320a	TCGGCGGAAGTCTGCGTGGCAGGGCCTGGGCGCCG CCATCTTGGCGCGGGGCGGAAGTGACGTTAGGGGG GCGGGACTGGGCCACAGTATTTATCAGGCGGCGCTT CGCTCCCCTCCGCCTTCTCTTCCCGGTTCTTCCCGGA GTCGGGAAAAGCTGGGTTGAGAGGGCGAAAAAGGA TGAGGTGACTGGTCTGGGCTACGCTATGCTGCGGCG CTCGGGGGTCTTGGCCTCCGGGCGGTGGCGTGGAG GCGCCAAGATCAGGGTCCCGGGTTTTGTCGGCCACC TCGAGG
hsa-miR-30d	TCTATTGTTCAGCACTAGAAATTATATAAATTATTAG CTGAAGATGATGACTGGCAACATTTATGTCTGTTCC TCCTCTTAAATTTCTTGTTCAGAAAGTCTGTTGTTGT AAACATCCCCGACTGGAAGCTGTAAGACACAGCTAA GCTTTCAGTCAGATGTTTGCTGCTACCGGCTATTCAC AGACATCCTCTTGATATAATTCTGTCCCGGAGTGGA GTTGAGGAGGCTATAAAATGTGTGGGAAAACCTCAG AAATCTTTAGCTGCATTCTCGAGG
*att*B1	CAAGTTTGTACAAAAAAGCAGGCT
*att*B2	ACCCAGCTTTCTTGTACAAAGTGGT
Hpa1	GTTAAC
Xho1	CTCGAG

Table 2.3: Sequences used to generate miRNA constructs.

2.6.2.2. Generation of Entry Clones

The amounts of DNA construct and plasmid pDONR221 (Invitrogen; figure 2.7) to be used were calculated using the equation (50 x no. base pairs) x 600 x (1/10^6) = ng. 10ng/µl miRNA construct was added to 150ng/µl pDONR221 vector and TE buffer (ThermoFisher Scientific), pH 8.0 used to yield an 8µl mixture. BP Clonase II enzyme (Invitrogen) was briefly thawed and vortexed, before 2µl was incorporated into the mixture. The reactions were then incubated at 25°C for 18 hours. Following this, 1µl proteinase K (Sigma) was added to terminate the reactions, which were incubated for 10 minutes at 37°C. 1µl of the BP recombination reactions were then used to transform DH5α competent *E.Coli* cells as described in 2.6.1.4. 20µl and 100µl aliquots were plated onto pre-warmed selective plates (kanamycin inoculated), which were incubated overnight at 37°C.

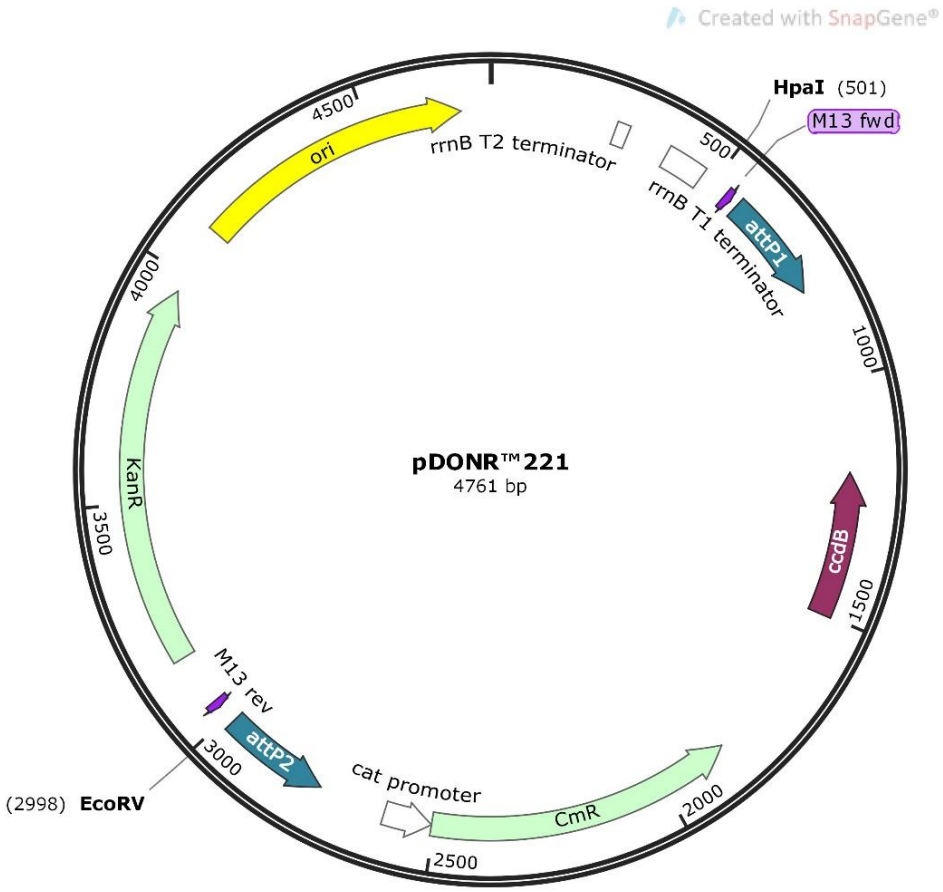

Figure 2.7: Sequence map of pDONR221 vector. *Note the presence of attP sites and associated restriction enzyme sites. Other restriction enzyme sites have been hidden in order to simplify the image.*

Individual colonies were subsequently selected and cultured in LB broth with kanamycin, overnight at 37°C on a shaker at 200rpm. Following this, entry clone DNA was extracted from 4ml of liquid culture using a QiaPrep Spin Miniprep kit (Qiagen) and quantified by NanoDrop. Glycerol stocks were generated from the remaining 1ml. To confirm DNA integrity of entry clones, 800ng DNA was diluted to 25µl in dH_2O. 3µl Cutsmart buffer and 1µl each Hpa1 and ECORV restriction enzymes (all New England Biolabs) were added, and the solution was incubated for 2 hours at 37°C. Gel electrophoresis was then performed using a 1% agarose gel, as described 2.5. To improve band visualisation, gels were incubated in 1xTAE buffer containing SYBR™ Gold (Invitrogen) at 0.1µl/ml for 15-30 minutes before viewing under an LED transilluminator (Biorad).

2.6.2.3. Generation of Expression Clones

Upon confirmation of correct bands, 50-150ng entry clones were added to 150ng/µl destination vector, a pLL3.7 lentiviral backbone (Addgene), and TE buffer pH 8.0 used to achieve an 8µl solution. LR clonase II enzyme (Invitrogen) was thawed as recommended by the manufacturer and 2µl added to each sample before incubation for 18 hours at 25°C. As before, the reaction was terminated with 1µl proteinase K and an incubation for 10 minutes at 37°C. The same transformation protocol was used to transform One Shot™ Stbl3™ competent *E.coli* cells, which were plated on pre-warmed selective agar plates with incorporated ampicillin. Colonies were selected and cultured, DNA extracted as before and further glycerol stocks were made. Expression clones (Figure 2.8) were digested using 1µl each HPa1 and Xho1 (NEB), and correct banding was checked by gel electrophoresis before confirmation by sequencing, described in 2.6.2.4. PLL3.7 plasmids without miRNA constructs added (empty pLL3.7 as in figure 2.8 section a.) were used to generate controls.

A.

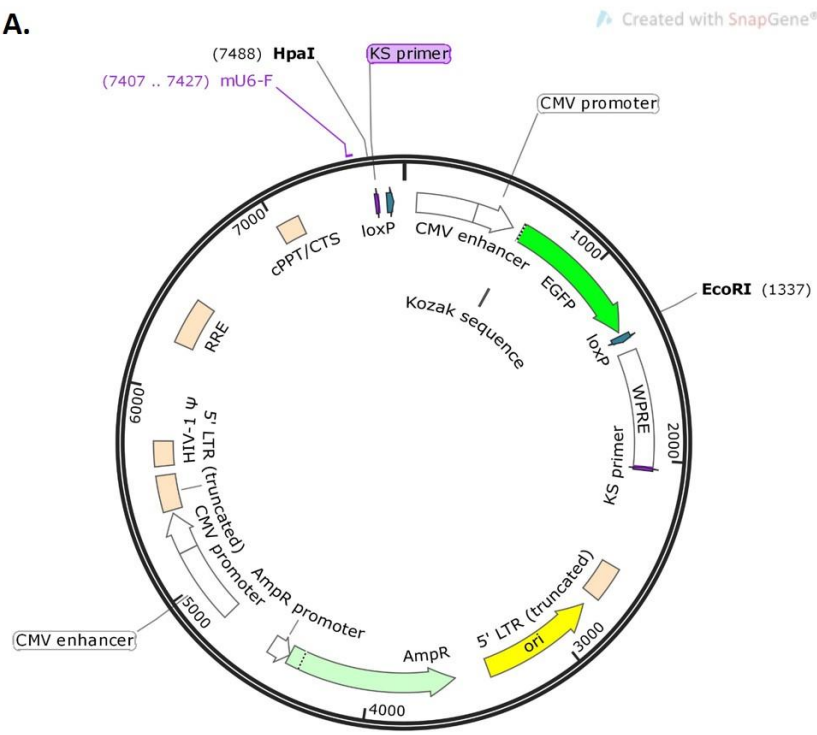

pLL3.7
7647bp

B.

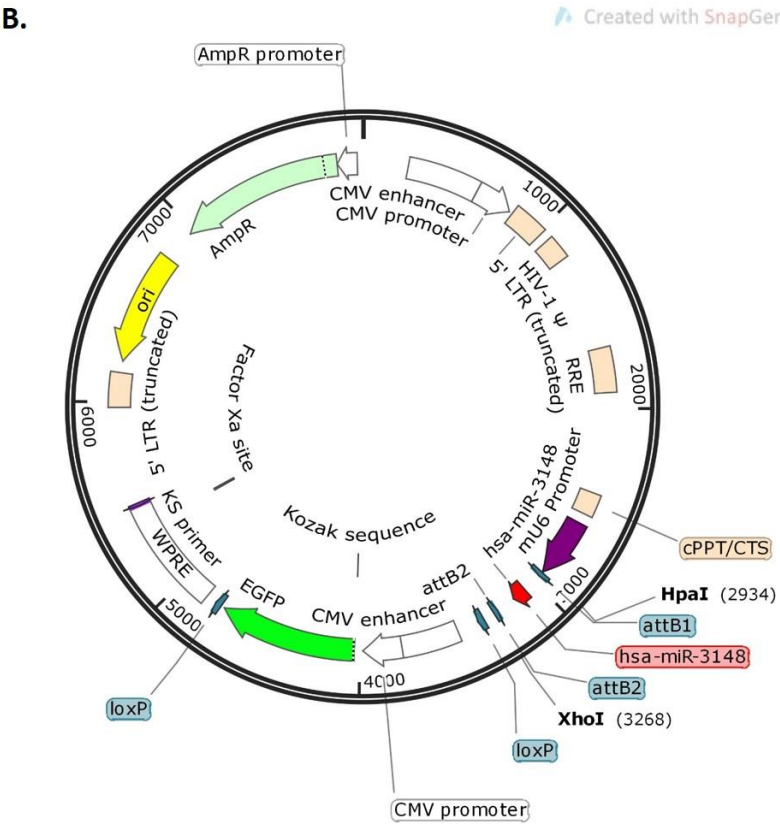

pLL3.7 miR-3148
7968bp

Figure 2.8: Plasmid maps for pLL3.7 vector and miR-3148 expression clone. *Image A depicts the pLL3.7 vector utilised in the LR reaction of Gateway® cloning and in control lentiviral vectors whereas image B shows the expression clone generated by the recombination of pLL3.7 and the miR-3148 construct. Note the inclusion of GFP in the vector to mediate fluorescence, and the attB sites flanking the construct.*

2.6.2.4. Sequencing of Expression Clones

Expression clones were prepared for sequencing by adding 1µl of 4pm/µl mU6 primer (Addgene) to 300ng DNA in a 10µl H_20 solution. The primer sequence was as follows: 5'AGGAAACTCACCCTAACTGTAAAG.

Sequencing was performed at the Manchester Regenerative Medicine Network, University of Manchester. Thanks to Dr Fraser Combe for coordinating this collaboration.

2.6.3. Generation and Use of Lentiviral Vectors to Transduce Endothelial Cells

Three plasmids were used to generate virions prior to HUVEC transduction: the pMD.G2 plasmid (Addgene) encoded the vesicular stomatitis virus glycoprotein (VSV-G) envelope, the pCMV--dR8.91 plasmid encoded the human immunodeficiency virus *gag/pol/rev* genes and the previously generated expression clone contained the miRNA overexpression construct. The two former plasmids enabled the packaging of the expression clone into lentiviral particles (figure 2.9). The pCMV--dR8.91 plasmid was kindly donated by Prof. Tristan McKay at Manchester Metropolitan University.

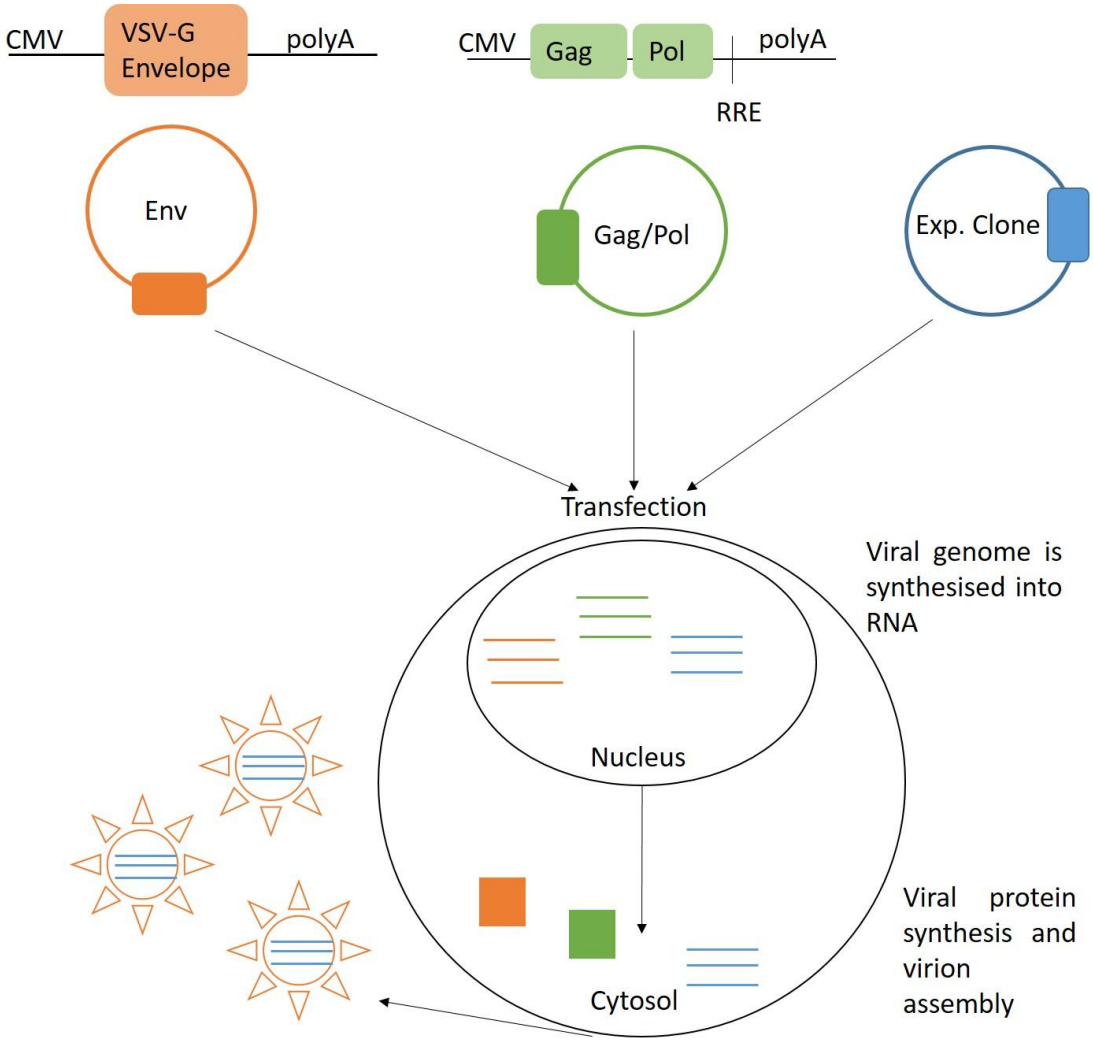

Figure 2.9: Generation and packaging of lentiviral particles. *HEK293T cells are transfected with plasmids encoding viral envelope and assembly proteins alongside expression clones. Assembly of viral proteins is completed in the cytosol, before virions are released, containing the DNA provided by the expression clone.*

2.6.3.1. Generation of Lentiviral Vectors

7500ng expression clone DNA was added to 5000ng pMD2.G and 10,000ng PCMV plasmids, before 150mM NaCl (Fisher) was incorporated to yield a 1ml solution. 7mM Polyethylenimine (PEI) reagent (Polysciences) was prepared by diluting PEI stock in 150mM NaCl and incubated for 10 minutes at RT. DNA-PEI complexes were then generated by adding the PEI reagent to DNA in a dropwise manner, followed by gentle mixing and another incubation for 10 minutes at RT. Finally, the resulting mixture was added dropwise to HEK293T cells, which had been seeded previously into 6 well plates and cultured to 60-70% confluency. Media was discarded and replaced after 4 hours and again at 24 hours. Virions in cell-free supernatant were harvested at 48 and 72 hours by centrifugation at 1000g for 10 minutes at 4°C, and aliquots were stored at -80°C.

2.6.3.2. Transduction using Lentivirus

Lentiviral aliquots were thawed on ice prior to filtration through a 0.22µm filter. In order to ascertain viral volume required for efficient transduction, a series of volumes were added dropwise to HUVECs at 60-70% confluency. Media was replaced at 4 hours and green fluorescent protein (GFP) expression analysed at 48 hours using a Leica CTR 6000 live cell imaging microscope at x10 magnification. Comparison of the number of GFP-expressing cells compared to non-expressors was performed using ImageJ, and the production of a GFP expression gradient indicated that 500µl should be used for each well of a 6 well plate in order to obtain 80% transduction efficiency (figure 2.10). For further experiments, HUVECs were transduced at passage 3 and GFP expression was tested and confirmed up to passage 7. Lentivirus generated with empty pLL3.7 plasmid was used as a control in functional experiments.

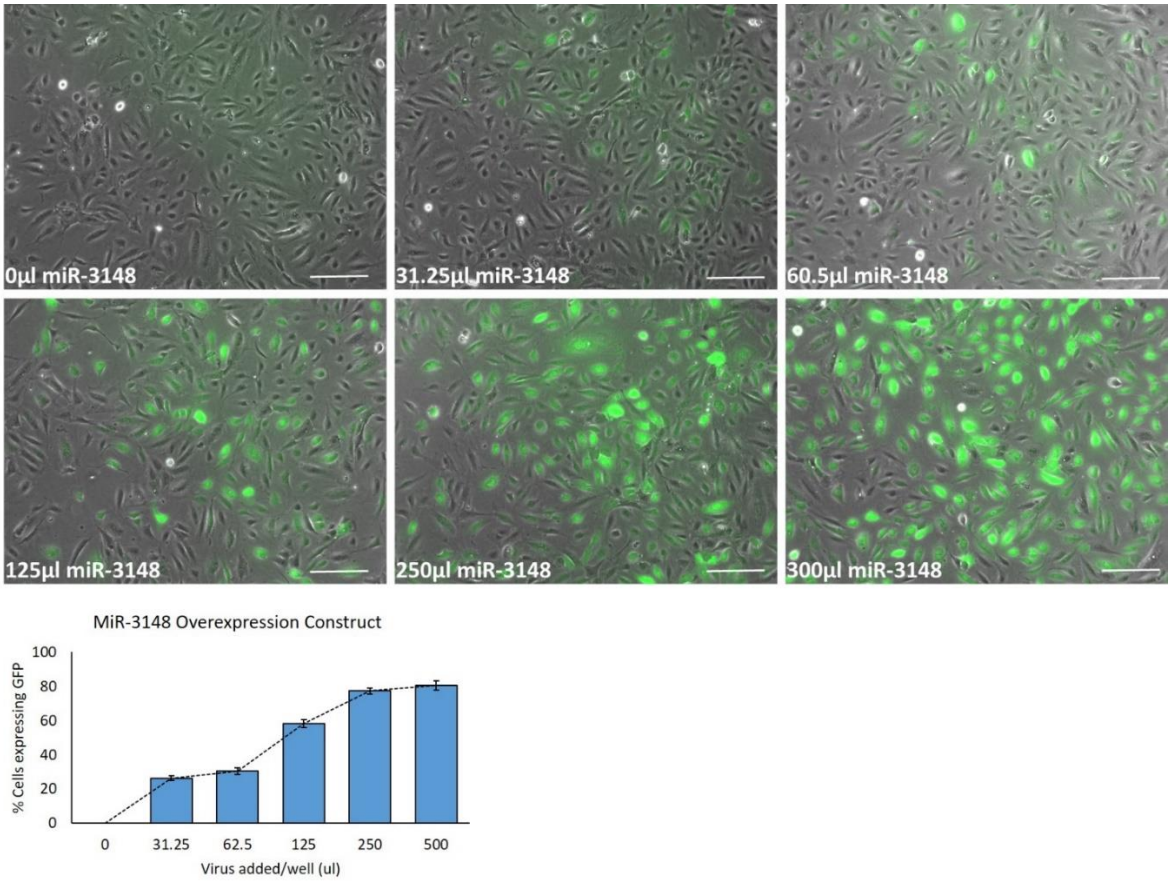

Figure 2.10: Transduction efficiency of miR-3148 construct. *HUVECs at p4 were transduced with differing concentrations of lentiviral vectors containing miR-3148 overexpression constructs. Images were taken after 48 hours and the ratio of cells expressing GFP was calculated manually, producing a titration curve that indicated 500µl lentivirus yielded 80.6% efficiency. This was repeated with 5 other miRNA constructs. Experiments were performed in triplicate, with error bars denoting SEM. Scale bar=200µm.*

2.6.3.3. Confirmation of MiRNA Overexpression by QPCR

Following transduction of HUVECs with lentiviral vectors, intracellular abundance of miRNA was quantified to confirm successful upregulation of each miRNA (figure 2.11). Transduction with miR-126-3p, miR-320a and miR-30d-5p constructs increased abundance 2 – 4.5-fold compared to HUVECs transduced with the empty pLL3.7 plasmid. Transduction with the miR-93-5p construct resulted in greatly increased abundance, albeit with very

large error bars ranging from 4-23-fold; the n=2 prevents determination of whether this is a true finding or if the larger value was the result of an error. Only miR-3148 abundance did not change following transduction, which may be due to the low abundance and difficulty in detecting this miRNA from *in vitro* samples.

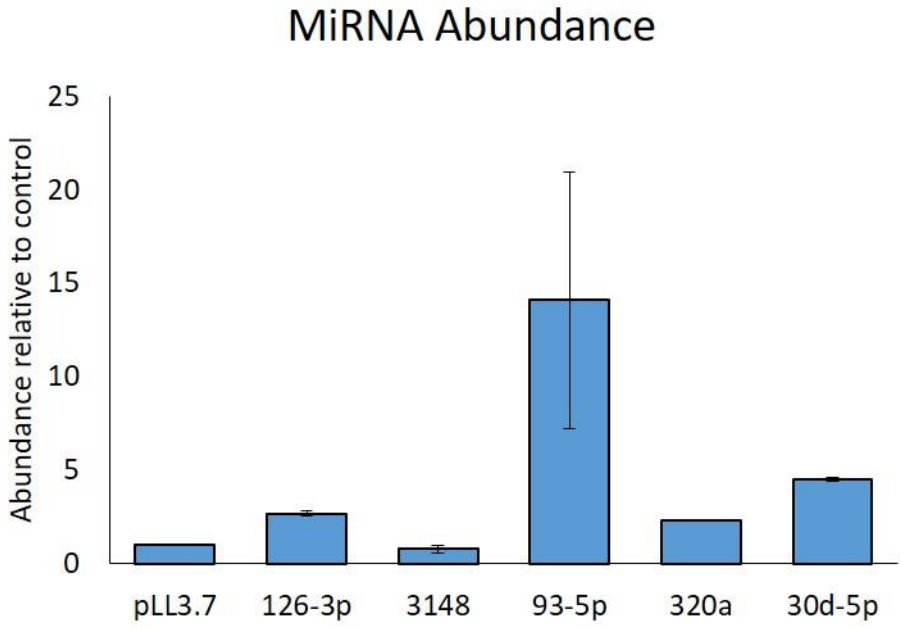

Figure 2.11: MiRNA abundance following transduction with lentiviral vectors. *HUVECs were transduced with 500µl of miRNA-containing lentiviral vectors at passage 3, and cultured to passage 4 before miRNA was extracted. Abundance of key miRNAs were quantified by qPCR to confirm successful overexpression. Data shown represent abundance following transduction relative to control cells transduced with empty pLL3.7 plasmid. Error bars represent SEM. N=2 in independent experiments with technical duplicates.*

2.7. Patient Studies

Controls and patients with SLE were identified and recruited by clinical collaborators at the Kellgren Centre for Rheumatology, Manchester Royal Infirmary. Patients were identified according to the 1997 ACR criteria(109), with exclusion criteria consisting of current infection, pregnancy and prior history of a cardiovascular event. Full ethical approval was granted (Studies; 11/NW/0090 and 13/NW/0564) and informed written consent was obtained from all participants. Fasting blood samples were collected in sodium citrate tubes following peripheral venepuncture by the clinical research team.

The clinical research team also conducted physiological and clinical laboratory tests. A full assessment of disease activity, incorporating BILAG and ACR scores, was performed and blood samples were analysed for glucose levels, lipid profiling, erythrocyte sedimentation rate (ESR), complement levels and autoantibody titres. Circulating markers of inflammation and vascular health were assessed by ELISA kits (R&D Systems), according to manufacturer's instructions(158). These were conducted in a Manchester University NHS Foundation Trust clinical laboratory.

Further information regarding n numbers and tests used are located in individual chapters.

2.7.1. Risk Score Calculation

Cardiovascular risk scores were computed using online calculators indicated below. Following QRISK guidelines(119), in the instance of missing data, variables were left blank during calculation, although Framingham calculation was not possible for patients with missing measurements. A score of ≥10% indicated high cardiovascular risk, in accordance with the National Institute for Health and Care Excellence (NICE) guidelines(121).
Online calculation tools available at:

Framingham: *https://www.framinghamheartstudy.org/fhs-risk-functions/cardiovascular-disease-10-year-risk/*

QRISK2: *https://qrisk.org/2017/*

QRISK3: *https://qrisk.org/three/*

2.7.2. Fatigue and Quality of Life Calculations

The Fatigue Scale for Motor and Cognitive Functions (FSMC)(184) was utilised to assess fatigue levels, taking into account measures of both motor fatigue and cognition (table 2.4). Data pertaining to fatigue and cognitive measures were collected by Dr Michelle Barraclough and team.

Cognitive Functions	Motor Functions
1. When I concentrate for a long time, I get exhausted sooner than other people of my age.	**1.** When I am experiencing episodes of exhaustion, my movements become noticeably clumsier and less coordinated.
2. When I am experiencing episodes of exhaustion, I am incapable of making decisions.	**2.** Because of my episodes of exhaustion, I now need more frequent and/or longer rests during physical activity than I used to.
3. Because of my episodes of exhaustion, I now find it more difficult to learn new things than I used to.	**3.** When faced with stressful situations, I now find that I get physically exhausted quicker than I used to.
4. The demands of my work exhaust me mentally more quickly than they used to.	**4.** Because of my episodes of exhaustion, I now have considerably less social contact than I used to.
5. My powers of concentration decrease considerably when I'm under stress.	**5.** I feel the episodes of exhaustion particularly strongly in my muscles.
6. My thinking gets increasingly slow when it is hot.	**6.** I no longer have the stamina for long periods of physical activity that I used to have.
7. Because of my episodes of exhaustion, I now feel less like doing things which require concentration.	**7.** When I am experiencing episodes of exhaustion, I am less motivated than others to start activities that involve physical effort.
8. When I am experiencing episodes of exhaustion, certain words simply escape me.	**8.** When I am experiencing an episode of exhaustion, my movements become noticeably slower.
9. When I am experiencing episodes of exhaustion, I lose concentration considerably quicker than I used to.	**9.** When an episode of exhaustion comes on, I am simply no longer able to react quickly.
10. During episodes of exhaustion, I am noticeably more forgetful.	**10.** When it is hot, my main feeling is one of extreme physical weakness and lack of energy.

Table 2.4: Fatigue Scale for Motor and Cognitive Functions. *The scale comprises two subsets of statements relating to cognitive and motor functions. Participants are required to rate their agreement with each statement on a 5 point Likert scale from 'does not apply at all' (1 point) to 'applies completely' (5 points). Scores can then be counted, with a score of ≥43 indicating mild, ≥53 moderate and ≥63 severe fatigue(184).*

Patients with SLE underwent further investigation, completing a Quality of Life assessment (LupusQoL). This test was developed from patient interviews and psychometric tests, resulting in a comprehensive questionnaire featuring 34 items upon a Likert scale and lower total scores reflecting reduced quality of life(185).

2.8. Statistical analysis

Statistical analysis was performed using IBM® SPSS® Statistics 25 and normality assessed by Kolmogorov Smirnov test; data were then analysed by parametric or non-parametric tests with comparison correction, as appropriate. Mean, standard deviation and standard error were calculated from a minimum of three data points in individual experiments, and a p value of ≤0.05 was considered significant. Asterisks used denote: * p≤0.05, ** p≤0.01 and *** p≤0.001.

Chapter 3

The Use of Diagnostic Algorithms and Novel Biomarkers in Identification of Patients with SLE at High Cardiovascular Risk

3.1. Study Introduction

As discussed in the introductory chapter, improved detection of patients at high cardiovascular risk may prevent premature mortality by providing early indication for increased patient monitoring, evaluation of lifestyle and prescription of relevant treatment. Online risk calculators are available free of charge to assist with risk identification, while potential clinical biomarkers such as EMVs may shed light on the extent of vascular involvement.

This study recruited a cohort of 138 participants, consisting of 109 patients with SLE and 29 controls, before online Framingham, QRISK2 and QRISK3 calculators were used to predict cardiovascular risk, which was analysed in relation to numerous clinical measurements. The overall aim was to assess the use of novel and longstanding diagnostic tools, as well as potential biomarkers, for cardiovascular risk identification in patients with SLE. The objectives of this study were as follows:

- Determine the number of patients with SLE and controls identified as having high cardiovascular risk using QRISK and Framingham algorithms.
- Identify differences in traditional cardiovascular risk factors between low and high risk groups.
- Analyse differences in clinical and circulating markers of inflammation, dyslipidaemia and vascular health between patients and controls, and low and high risk groups.
- Consider the use of EMVs as biomarkers of cardiovascular risk through associations with disease, vascular health and QRISK algorithms.

3.2. Chapter Methodology

Cardiovascular risk scores were calculated as described in 2.7.1. Participants aged below minimum values for QRISK (25yrs; patients n=13, controls n=2) and Framingham (30yrs; patients n=23, controls n= 11) were entered as 25 or 30 years old respectively.

QRISK3 risk factors, as well as clinical disease measurements and current prescription data, were recorded for all patients at the time of entry into the study. Additional measurements were taken from a subset of patients (n=58), such as EMVs, cardiovascular evaluations e.g. aortic pulse wave velocity (PWV), and circulating factors e.g. cytokines. EMVs were quantified as described in 2.3; other measurements were collected by clinical research collaborators, as discussed in 2.7.

3.3. Results

3.3.1. Demographics

No significant differences were detected between controls and patients with SLE when comparing basic demographic measures (table 3.1). These included traditional cardiovascular risk factors such as blood pressure, cholesterol, smoking status and diagnosis of diabetes.

Variable	Controls (n=29)	SLE (n=109)	p Values
Age (years), mean ± SD	36.66 ± 12.95	40.75 ± 12.69	0.063
Female	29 (100%)	105 (96.33%)	1.000
Caucasian	23 (79.31%)	80 (73.39%)	0.634
BP Systolic (mm Hg)	119.0 (111.75, 130.5) *n=28*	124.0 (114.75, 133.25) *n=97*	0.251
HDL-Cholesterol (mmol/l)	1.7 (1.5, 2.0) *n=25*	1.6 (1.2, 1.9) *n=97*	0.097
Non-HDL Cholesterol (mmol/l)	2.6 (2.3, 3.2) *n=25*	2.8 (2.4, 3.3)*n=97*	0.374
Current Smoker	4 (13.79%)	24 (22.02%)	0.439
Type 2 Diabetes	0 (0%)	6 (5.50%)	1.000

Table 3.1: Demographic measures of controls and patients with SLE. *Data represented as number (%) or median (lower and upper quartiles) unless otherwise indicated. Comparisons analysed by Mann-Whitney U and Fisher's exact tests.*

3.3.2. QRISK3 Identifies More Patients at High Cardiovascular Risk Compared to Previous Algorithms

QRISK2 score was significantly greater in the SLE population (p=0.001), with an average score of 1.8% for patients compared to 0.3% for controls (table 3.2). While the average control score remained unchanged when using the QRISK3 algorithm, patients exhibited a significant increase (p<0.001) up to 5.0%, which was, again, elevated compared to controls (p<0.001). A similar trend was observed using the Framingham algorithm, where patients possessed greater average risk scores than controls (2.2% vs 1.2%, p=0.013), which were still significantly lower than those calculated by QRISK3 (p<0.001).

8 (7%) patients with SLE were determined to possess high cardiovascular risk (>10%) when using the QRISK2 algorithm and 5 (4.6%) when using Framingham. In contrast, QRISK3 identified 29 (27%) patients at high risk, almost quadruple the number (p<0.001) compared to both QRISK2 and Framingham.

Therefore, 21 patients were newly identified as high risk by the QRISK3 algorithm – these will now be referred to as the 'missed' patients due to their lack of recognition by the current QRISK2 calculator. Additionally, the missed group rose to 24 patients when comparing QRISK3 to Framingham; this may be of relevance to healthcare organisations outside the UK that are still using Framingham, however ensuing sections of this chapter will compare QRISK2 and 3 only.

QRISK3 scores were also calculated without inclusion of SLE as a factor, to determine the impact of this additional variable in assessment of risk. This reduced the average patient score to 1.9% and identified 3 missed patients (not identified by QRISK2). No differences between QRISK2/3 or Framingham were observed in the control groups, and no missed controls were identified by QRISK3.

	Controls (n=29)	SLE (n=109)	Control v SLE (p Values)
QRISK2 Score (%)	0.3 (0.2, 1.9)	1.8 (0.6, 3.9)	**p=0.001**
QRISK3 Score (%)	0.3 (0.1, 1.7)	5.0 (3.0, 10.7)	**p<0.001**
QRISK2 v 3 Score (p Values)	p=0.676	**p<0.001**	-
Number of High QRISK2 (n)	1 (3.45%)	8 (7.34%)	p=0.458
Number of High QRISK3 (n)	1 (3.45%)	29 (26.61%)	**p=0.009**
Number of High QRISK2 v 3 (p Value)	p=1.000	**p<0.001**	-
Missed Patients (n)	0 (0%)	21 (19.27%)	**p=0.007**

Table 3.2: Calculation of cardiovascular risk using QRISK algorithms. *High risk is indicated by a score of ≥10%. Missed patients denoted as those identified as high risk by QRISK3 but low risk by QRISK2. Data represented as number (%) or median (lower and upper quartiles). Data analysed by Mann-Whitney U and Fisher's exact tests.*

3.3.2.1. Missed Patients: Differences in QRISK Factors and Medications

High risk patients missed by QRISK2 were found to have significantly higher BMI compared to both controls (p=0.003) and to patients identified as low risk by both algorithms (p=0.026; table 3.3). The missed group also presented with elevated systolic blood pressure (both p<0.10) and were more likely to be experiencing chronic kidney disease (both p<0.05). The missed patients additionally demonstrated significantly reduced levels of HDL cholesterol compared to controls (p=0.037) and diagnosis of type 2 diabetes was more prevalent than in the low risk group (p=0.008).

Furthermore, a greater proportion of missed patients were prescribed anti-hypertensive and/or oral corticosteroid treatments compared to controls and low risk patients (all p<0.001); indeed 100% of missed patients were receiving steroid therapy.

Variable	Controls (n=29)	Missed Patients (n=21)	p Value	Low Risk Patients (n=80)	Missed Patients (n=21)	p Value
Age (years), mean ± SD	36.66 ± 12.95	42.16 ± 12.36	0.130	38.02 ± 10.68	42.16 ± 12.36	0.155
Female	29 (100%)	19 (90.48%)	0.420	78 (97.50%)	19 (90.48%)	0.507
Ethnicity: Caucasian	23 (79.31%)	13 (61.90%)	0.213	58 (72.50%)	13 (61.90%)	0.292
BMI (kg/m^2)	22.6 (21.3, 25.3)	31.8 (24.3, 37.0)	**0.003**	25.3 (22.2, 28.4)	31.8 (24.3, 37.0)	**0.026**
BP Systolic (mm Hg)	119.0 (111.75, 130.5) *n=28*	141.0 (131.0, 160.5) *n=14*	**0.006**	122.0 (110.5, 128.0) *n=75*	141.0 (131.0, 160.5) *n=14*	**<0.001**
HDL Cholesterol (mmol/l)	1.7 (1.5, 2.0) *n=25*	1.5 (1.3, 1.8)	**0.037**	1.7 (1.2, 2.0) *n=71*	1.5 (1.3, 1.8)	0.222
Non-HDL Cholesterol (mmol/l)	2.6 (2.3, 3.2) *n=25*	3.2 (2.5, 3.6)	0.115	2.7 (2.2, 3.2) *n=71*	3.2 (2.5, 3.6)	0.053
Type 2 Diabetes	0 (0%)	3 (14.29%)	1.000	0 (0%)	3 (14.29%)	**0.008**
Rheumatoid Arthritis	0 (0%)	0 (0%)	1.000	5 (6.25%)	0 (0%)	0.312
Chronic Kidney Disease (Stage 3-5)	0 (0%)	5 (23.81%)	**0.010**	3 (3.75%)	5 (23.81%)	**0.021**
Migraines	3 (10.34%)	1 (4.76%)	0.630	8 (10%)	1 (4.76%)	0.681
Severe Mental Illness	2 (6.90%)	2 (9.52%)	1.000	3 (3.75%)	2 (9.52%)	0.277
Current Smoker	4 (13.79%)	6 (28.57%)	0.286	15 (18.75%)	6 (28.57%)	0.368
Anti-Hypertensive	3 (10.34%)	15 (71.43%)	**<0.001**	13 (16.25%)	15 (71.43%)	**<0.001**
Current Oral Corticostero-ids	0 (0%)	21 (100%)	**<0.001**	46 (57.50%)	21 (100%)	**<0.001**

Table 3.3: Baseline cardiovascular measures of controls, low risk and missed patients, as required by the QRISK3 algorithm. *Variables shown as requested by the QRISK3 algorithm; severe mental illness inclusive of depression, schizophrenia and bipolar disorder. Data represented as number (%) or median (lower and upper quartiles). Comparisons analysed by Mann-Whitney U and Fisher's exact test as appropriate.*

3.3.2.2. Missed patients: Differences in SLE Factors

Additional, SLE-specific measures were available in a reduced cohort of patients (n=71). When comparing these measures, fewer missed patients presented with arthritis than low risk patients (p=0.047) yet more were experiencing renal disease at the time of measurement (p=0.038; table 3.4). This figure differs from that of the chronic kidney disease used in QRISK calculation due to the use of the ACR criteria for SLE disease activity. Missed patients were additionally found to have significantly higher levels of anti-cardiolipin antibodies compared to low risk patients (p=0.027), despite no significant alterations in other autoantibody titres. Current steroid prescription was also elevated in the missed group (p<0.001), although average dose was unaltered.

Variable	Low Risk SLE n=50	Missed SLE n=21	p Value
Disease Duration (years)	13.0 (8.0, 19.0)	12.0 (6.7, 15.0)	0.326
ACR Criteria: Malar Rash	35 (70%)	14 (66.67%)	0.785
ACR Criteria: Discoid Rash	25 (50%)	6 (28.57%)	0.120
ACR Criteria: Photosensitivity	34 (68%)	14 (66.67%)	1.000
ACR Criteria: Oral Ulcers	36 (72%)	14 (66.67%)	0.777
ACR Criteria: Serositis	15 (30%)	6 (28.57%)	1.000
ACR Criteria: Arthritis	44 (88%)	14 (66.67%)	**0.047**
ACR Criteria: Renal Disorder	19 (38%)	14 (66.67%)	**0.038**
ACR Criteria: Neurologic Disorder	4 (8%)	2 (9.52%)	1.000
ACR Criteria: Haematologic Disorder	30 (60%)	11 (52.38%)	0.605
ACR Criteria: Immunologic Disorder	39 (78%)	14 (66.67%)	0.375
ACR Criteria: ANA-Positive*	46 (94%)	18 (85.71%)	0.352
Anti-dsDNA Antibodies*	15 (30%)	9 (42.86%)	0.429
Anti-Cardiolipin Antibodies*	4 (8%)	7 (33.33%)	**0.027**
Low C3 + Low C4 Levels*	5 (10%)	2 (9.52%)	1.000
Current Oral Corticosteroids	19 (38%)	21 (100%)	**<0.001**
Prednisolone Dose (mg/day)	7.5 (5.0, 11.3)	10 (5.5, 15.0)	0.304
Current Immunosuppressive Use	29 (58%)	13 (61.90%)	0.582
Current Antimalarial Use	36 (72%)	17 (80.95%)	0.556
BILAG-2004	1.5 (0.25, 6.75) *n=50*	5.5 (0.0, 9.3) *n=8*	0.542
SLEDAI-2K	2.5 (0.25, 4.0) *n=50*	3.0 (2.0, 4.5) *n=50*	0.444

Table 3.4: Clinical and immunological measures of low risk and missed patients at point of entry into the study. ** Indicated by laboratory reference range. Data represented as number (%) or median (lower and upper quartiles). Comparisons were analysed by Mann-Whitney U and Fisher's exact tests.*

3.3.3. Inflammation and Vascular Dysfunction are Increased in Patients with SLE

Results from extensive clinical and laboratory tests in a cohort of 60 patients confirmed increased levels of inflammation and dyslipidaemia compared to controls (n=29, table 3.5). Clinical indicators of inflammation, ESR and CRP were elevated in patients with SLE (both $p<0.02$), as were vascular cell adhesion molecule 1 (VCAM1), monocyte chemoattractant protein-1 (MCP1), IL6 and BLyS (all $p<0.03$). Conversely, lymphocytes were found in reduced numbers in patients ($p=0.001$), while haemoglobin and glucose levels were also diminished (both $p<0.01$). However, levels of triglycerides in the blood were increased in patients compared to controls ($p=0.019$).

Variable	Controls	SLE	p Value
ESR (mm/hr)	6 (2, 8) *n=25*	12 (6, 25) *n=59*	**0.013**
hsCRP (ng/ml)	0.86 (0.41, 1.20) *n=27*	1.22 (0.62, 4.76) *n=57*	**0.006**
VCAM-1 (ng/ml)	333.93 (312.37, 385.17) *n=29*	436.41 (355.02, 530.28) *n=58*	**<0.001**
MCP-1 (pg/ml)	138.87 (106.41, 187.53) *n=27*	188.36 (112.65, 305.38) *n=57*	**0.029**
IL-6 (pg/ml)	0.50 0.50, 1.29) *n=27*	1.75 (0.51, 5.39) *n=57*	**0.001**
BLyS (ng/ml)	0.34 (0.28, 0.39) *n=27*	0.50 (0.35, 0.66) *n=57*	**<0.001**
Triglycerides (mg/dl)	0.70 (0.60, 0.80) *n=25*	0.90 (0.60, 1.45) *n=55*	**0.019**
Lymphocytes (x10^3/µl)	1.73 (1.41, 1.87) *n=25*	1.25 (0.97, 1.61) *n=59*	**0.001**
Haemoglobin (g/l)	132 (125, 140) *n=25*	124 (113, 133) *n=59*	**0.006**
Glucose (mmol/l)	4.90 (4.50, 5.10) *n=26*	4.50 (4.30, 4.70) *n=57*	**0.004**

Table 3.5: Differences in clinical markers of inflammation and vascular health between patients and controls. *N numbers provided for each variable due to cases of unobtainable data within groups. Variables shown chosen due to p values <0.05. Data represented as median (lower and upper quartiles). Comparisons were analysed by Mann-Whitney U test.*

This patient cohort could be further subdivided into patients experiencing stable or exacerbated (flare) disease at time of measurement, as identified by BILAG score(112). Flare patients were prescribed higher doses of prednisolone and were more likely to be on a regimen of immunosuppressives and/or antimalarials (all $p<0.05$; table 3.6). No differences were observed in any other demographic or QRISK measurements e.g. ACR criteria, blood pressure, such that QRISK3 scores were not significantly different (p=0.222)

Variable	Flare n=25	Stable n=35	p Value
BILAG-2004	7 (6, 12)	1 (0, 1)	**<0.001**
SLEDAI-2K	6 (4, 8)	2 (0, 2)	**<0.001**
Prednisolone Dose (mg/day)	10.00 (6.25, 20.00)	5.00 (5.00, 7.50)	**0.005**
Current Immunosuppressive Use	20 (80%)	14 (40%)	**0.003**
Current Antimalarial Use	21 (84%)	20 (57.14%)	**0.047**

Table 3.6: Immunological demographics of flare and stable patients. *All other demographic measurements p>0.05. Data represented as number (%) or median (lower and upper quartiles). Comparisons were analysed by Mann-Whitney U and Fisher's exact tests.*

Within this cohort, flare patients were found to have significantly higher triglyceride levels than stable patients (p=0.045, table 3.7). Furthermore, platelet count was increased (p=0.014) alongside reduced haemoglobin levels (p=0.030), although there were no significant differences in incidence of haematological disorders as characterised by ACR criteria (p>0.05).

Variable	Flare	Stable	p Value
Triglycerides (mg/dl)	1.30 (0.70, 1.98) *n=24*	0.80 (0.60, 1.15) *n=31*	**0.045**
Platelets (x10^3/µl)	259 (223, 355) *n=25*	217.00 (181.50, 285.75) *n=34*	**0.014**
Haemoglobin (g/l)	118 (109, 126) *n=34*	127.50 (118.50, 135.75) *n=34*	**0.030**

Table 3.7: Differences in blood components between flare and stable patients. *N numbers provided for each variable due to cases of unobtainable data within groups. All other variables p>0.05. Data represented as median (lower and upper quartiles). Comparisons were analysed by Mann-Whitney U test.*

3.3.3.1. Inflammation and Vascular Health in Missed Patients

Detailed laboratory results were available for a subset of low risk and missed patients, and demonstrated striking differences in markers of inflammation and vascular function. Once more, triglyceride levels showed significant variation, with higher levels in missed patients (p=0.017, table 3.8); mean arterial pressure (MAP) was also substantially increased (p<0.001). Moreover, CRP was elevated (p<0.001), whereas circulating IgM levels were reduced in the missed group (p=0.004).

Variable	Low Risk	Missed	p Value
hsCRP (ng/ml)	0.89 (0.54, 3.01) *n=47*	6.30 (4.47, 8.18) *n=8*	**<0.001**
IgM (g/l)	1.10 (0.79, 1.48) *n=49*	0.49 (0.48, 0.62) *n=8*	**0.004**
Triglycerides (mg/dl)	0.80 (0.60, 1.25) *n=45*	1.45 (1.05, 2.53) *n=8*	**0.017**
MAP (mmHg)	92 (83, 96) *n=49*	112 (100, 121) *n=7*	**<0.001**

Table 3.8: Differences in clinical inflammatory and cardiovascular markers between low risk and missed patients. *N numbers provided for each variable due to cases of unobtainable data within groups. All other variables p>0.05. Data represented as median (lower and upper quartiles). Comparisons were analysed by Mann-Whitney U test.*

3.3.4. Endothelial Microvesicles are Increased in SLE and are Associated with Inflammation, Dyslipidaemia and Vascular Dysfunction

Numbers of circulating EMVs were enumerated within the reduced cohort described in 3.3.3 and demonstrated significant differences according to disease, with numbers increased in patients compared to controls (p=0.001; figure 3.1). Furthermore, EMV number demonstrated a disease-dependent increase, with presence of a disease flare associated with increased EMV abundance compared to controls (p=0.004); abundance was also increased in stable disease (p=0.047)

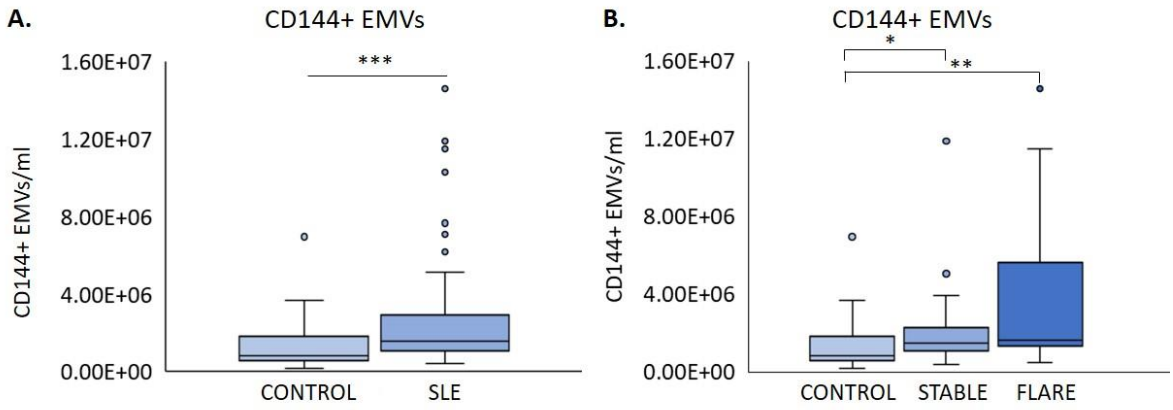

Figure 3.1: EMV abundance in SLE. *Number of CD144^{+} microvesicles per ml of plasma were measured by flow cytometry in controls vs patients with SLE (A) and in controls vs stable vs flare patients (B). Data analysed by Mann-Whitney U (control vs SLE) and Kruskal-Wallis tests (controls vs stable vs flare). Asterisks used denote: * p≤0.05, ** p≤0.01 and *** p≤0.001. N=89; controls n=29, SLE n=60, stable n=35, flare n=25.*

Within the cohort of patients with SLE, EMV number correlated positively with ESR (p<0.001; table 3.9) and elevated EMVs were associated with a number of markers of vascular health and dyslipidaemia, including blood pressure, triglycerides and MAP (all p<0.02). Furthermore, greater EMV numbers were associated with patient use of a number

of medications, namely immunosuppressives, antimalarials, steroids and the contraceptive pill (all p≤0.03). None of these associations were apparent in the control group.

Variable	Spearman rho	p Value
Haemoglobin	-0.457	**<0.001**
Triglycerides	0.573	**<0.001**
Glucose	-0.264	**0.047**
ESR	0.513	**<0.001**
VCAM1	0.271	**0.039**
MCP1	0.426	**0.001**
hsCRP	0.356	**0.006**
IL6	0.418	**0.001**
IgG	0.380	**0.003**
Systolic BP	0.324	**0.013**
MAP	0.371	**0.004**
Anti-nuclear Antibodies	-	**0.018**
Current Contraceptive Pill Use	-	**0.018**
Current Immunosuppressive Use	-	**0.013**
Current Antimalarial Use	-	**0.007**
Current Steroid Use		**0.026**

Table 3.9: Correlations between EMV number and demographics, measures of inflammation and cardiovascular health in patients with SLE. *N=60, all patients (no controls). Associations made using Spearman's Rank Correlation Coefficient and Mann-Whitney U test.*

3.3.5. Endothelial Microvesicles Correlate with QRISK3 Score

EMVs were additionally connected to the cardiovascular risk algorithms, correlating positively with QRISK3 score across the whole cohort (controls and patients; rho:0.322, p=0.002) but demonstrating no such association with QRISK2 (rho:0.096, p=0.376). This correlation was also apparent in the missed group of patients, which demonstrated significantly higher EMV numbers than the low risk group (p=0.019; figure 3.2).

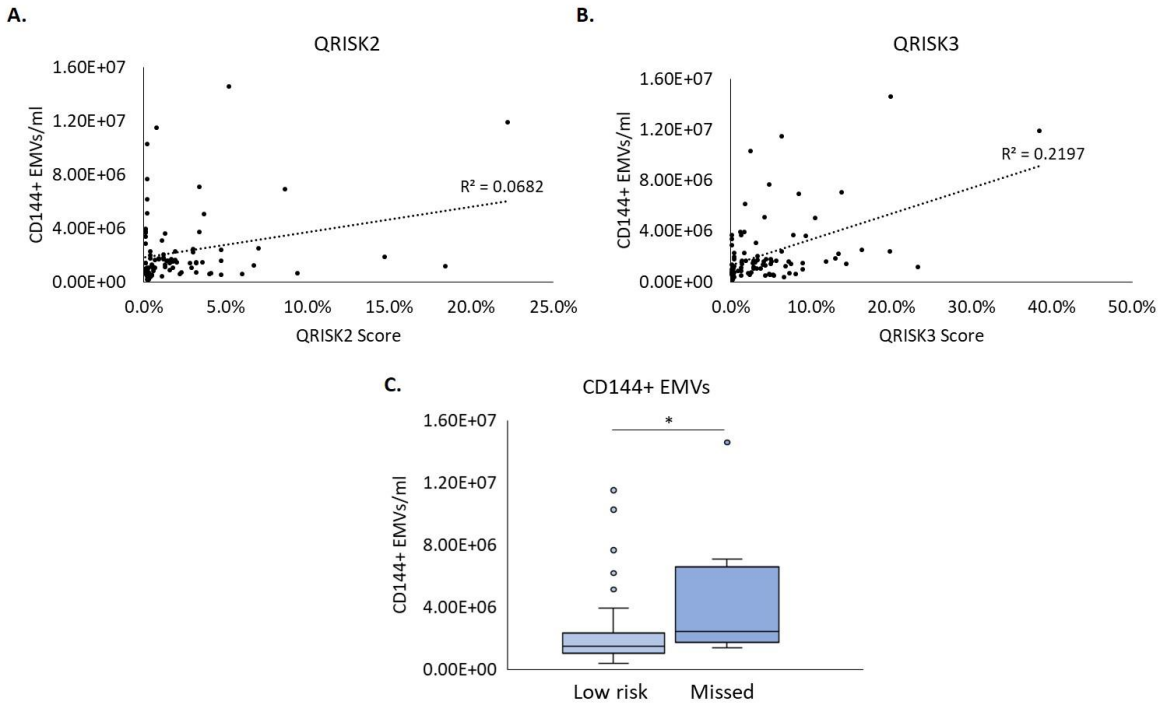

Figure 3.2: Correlations between EMVs and risk scores, and EMV abundance in missed patients. *EMV number was correlated with QRISK2 (A) and QRISK3 scores (B) using Spearman's Rank Correlation Coefficient; n=89 (patients and controls). Number of CD144⁺ EMVs per ml of plasma was quantified in patients with low risk and with missed high risk when using QRISK3 (C), with statistical analysis using Mann-Whitney U test; low risk n=50, missed n=8. * denotes p≤0.05.*

3.4. Chapter Discussion

3.4.1. The Use of QRISK3 Identifies an Unmet Clinical Need

This research highlights the need for accurate diagnosis of cardiovascular risk in patients with SLE, who experience underlying inflammation, dyslipidaemia and vascular involvement, and development of novel biomarkers to improve diagnosis and monitor treatment strategies. QRISK2 has been established as the algorithm of choice for UK doctors evaluating cardiovascular risk(118), while the Framingham risk score is extensively used outside the UK(116). The results in section 3.3.2 demonstrate the relative inaccuracy of both these measures when compared to the newly developed QRISK3 algorithm, which identified almost four times as many high risk patients as QRISK2 and almost 6 times as many as Framingham. The accuracy of Framingham scores have been questioned previously, particularly in females and multi-ethnic communities(115, 186), as the original model was based on a homogenous subset of middle-aged white participants(187). However, the discrepancies between QRISK3 and its predecessor are interesting, arising from a combination of additional factors; the removal of SLE as a risk factor still resulted in identification of three missed patients.

The identification of a cohort of missed patients is likely to have a resounding effect on patient care; indeed, the GPs of all missed patients identified in this study have been contacted to review treatment and monitoring of these individuals. In terms of traditional cardiovascular risk factors, the missed patients showed higher BMI and systolic blood pressure than both controls and low risk patients. Despite this, more of the missed group were regularly taking anti-hypertensive drugs, implying that the high cardiovascular risk was perhaps maintained during standard treatment. Additionally, all missed patients were prescribed oral corticosteroids, most likely due to dysregulated SLE symptoms. Long-term and, more strongly, current administration of corticosteroids have been associated with atherosclerosis development, particularly in SLE, in a dose-dependent manner(188-190). Previous data from our group demonstrated that use of the corticosteroid dexamethasone enhanced the osteogenic differentiation of vascular pericytes and downregulated genes associated with inhibition of mineralisation, highlighting the need for caution in considering the long-term consequences of prolonged glucocorticoid therapy on vascular

calcification(191). Furthermore, prednisolone use by patients with SLE has been linked to hypercholesterolemia(192), foreshadowing the patterns of dyslipidaemia presented by this study.

3.4.2. Inflammatory Markers Produce a Complex Picture of Endothelial Dysfunction in SLE

Lipid levels have been a predominant risk factor throughout this chapter, with missed patients demonstrating reduced HDL and increased triglyceride levels. Triglycerides were elevated in patients compared to controls, in concordance with disease activity, potentially indicating increased abundance of atherogenic lipoproteins such as VLDL(193, 194). Moreover, increased platelet counts were prominent in flare patients. This is important as increased platelet activation can support IFN production and endothelial dysfunction(195), as well as atherogenesis and plaque progression(196, 197). Anti-cardiolipin antibodies also interact with platelets, amplifying activation and complement deposition, activating the classical complement pathway and increasing the risk of thrombosis(198, 199). Although anti-dsDNA antibodies were consistent across low and missed groups, anti-cardiolipin antibodies were more prevalent in missed patients, which are further associated with endothelial dysfunction and thrombosis(94, 200). Thus, it becomes clear that patients with SLE at high risk or with high disease activity are subject to a pro-atherogenic internal environment, with dyslipidaemia, elevated blood pressure and pro-thrombotic circulating factors.

However, this is further augmented by the dysregulated inflammatory response experienced by the patients in this study. CRP and ESR were both raised in patients, and CRP in missed patients, consistent with increased disease activity and inflammation(201, 202); both have previously been implicated in atherosclerosis and vascular damage, for example through reductions in NO bioavailability(49, 203, 204). As well as acute phase proteins, a number of cytokines such as BLyS, IL6 and MCP-1 were found at increased levels in SLE, all of which have previously been suggested as biomarkers for disease activity(205-207) and may contribute to CVD, as depicted in figure 3.3.

Of note are the increased levels of VCAM-1, which have been linked to cardiovascular mortality and atherosclerosis in SLE(208), as well as the wider population(209). VCAM-1 is an adhesion molecule expressed on endothelial cells following activation by, for example, inflammatory cytokines, dysregulated lipid levels and oxidative stress, particularly during pro-thrombotic conditions, and supports leukocyte trafficking along the vascular wall(209, 210). Nonetheless, lymphocyte count was reduced in SLE, which is common in this condition, and has been associated with disease activity, likely due to deficient regulatory T cells(211). It has also been linked to carotid intima-medial thickening in patients with juvenile onset SLE(212) but a role in adults has yet to be disclosed. The reasoning behind lymphopenia in SLE is remains to be determined, although immunosuppressive drugs prescribed to patients(211) and autoantibodies targeting lymphocytes have been implicated(213). Haemoglobin was also reduced in SLE, consistent with disease activity, yet anaemia was not indicated nor were ACR-defined haematological conditions. Anaemia is often observed in patients with SLE, and is not uncommon in females, where it may be due to menorrhagia, sustained inflammation, anaemia of chronic disease, or erythropoietin deficiency as a result of renal involvement or autoantibodies(214, 215).

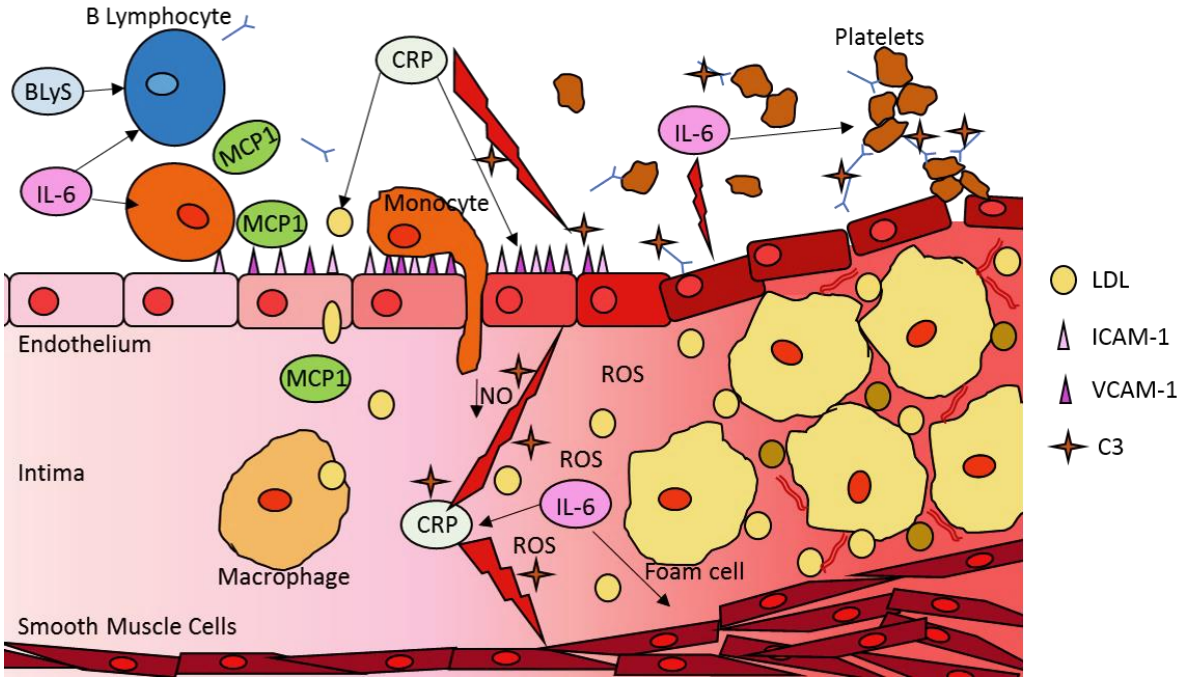

Figure 3.3: Interplay between cytokines and acute phase proteins in SLE-related endothelial dysfunction. *This schematic diagram introduces some of the numerous interactions between inflammatory mediators during atherogenesis in SLE. CRP facilitates opsonisation of LDL and smooth muscle cell activation, as well as endothelial dysfunction via upregulation of adhesion molecules, production of ROS, activation of complement cascade and downregulation of NO. IL-6 reinforces this by increasing CRP levels. It also activates B cells, endothelial cells and platelets, and promotes monocytic chemotaxis and smooth muscle cell proliferation. VCAM-1 and MCP1 further promote monocyte infiltration prior to macrophage and foam cell differentiation while BLyS stimulates B cells and supports production of autoantibodies.*

While the involvement of autoantibodies in SLE pathogenesis and inflammation has been discussed, potential protective roles for self-directed antibodies may also be considered. This study found significantly reduced levels of IgM in missed patients; research by Jost *et al.* highlights the involvement of antinuclear IgM antibodies in SLE disease activity but suggests augmented IgM-IgG class-switching and concedes a potential protective role of IgM(216). This is particularly prominent in vascular health, as diminished levels of IgM antibodies targeting phosphorylcholine, malondialdehyde and apolipoprotein antigens have been linked to increased risk of atherosclerotic plaque formation in SLE(217-219).

3.4.3. The Impact of Medication: A Causal or Coincidental Link with Endothelial Microvesicle Release?

Many correlations and associations between prescribed medications and markers of inflammation and vascular health became apparent during this study, making it difficult to judge whether the links were causal or coincidental. One interesting observation was between high EMV number and use of the contraceptive pill. Numerous clinicians hesitate to prescribe combined oral contraceptives to patients with SLE due to ongoing beliefs that they may exacerbate disease symptoms; this is largely being disproven, yet results of

animal studies and investigations into oestrogenic interactions with the immune system suggests a more complex picture(220). It has been suggested that prolonged use of oral contraceptives may support development of SLE(221), while oestrogen has been found to upregulate BLyS expression in a murine SLE model(222). Furthermore, oestrogen application appears to regulate the expression of a number of miRNAs, including miR-126(223), which will be discussed in chapter 4, and prolonged use may promote endothelial dysfunction and early atherogenic changes(224). Therefore, more research into the effects of oral contraceptives on endothelial activation and cardiovascular risk may be prudent.

The final medications to be discussed in this chapter are the immunosuppressives and anti-malarials. Both were more prevalent in flare patients and linked to elevated EMVs, which is perhaps unsurprising as these patients experienced higher levels of inflammation and vascular risk. Mycophenolate mofetil and hydroxychloroquine, by far the most commonly prescribed immunosuppressive and anti-malarial drugs in this patient population respectively, have previously been independently shown to protect against endothelial dysfunction(103, 225) and atherosclerosis(226, 227) in murine SLE models. Thus, additional avenues of future research are identified, exploring the relationships between commonly prescribed medication and endothelial health in SLE.

3.4.4. Endothelial Microvesicles as Potential Biomarkers of Cardiovascular Risk

Thus far, many of the variables described could be considered future biomarkers for cardiovascular risk in patients with SLE due to their prominence in active disease and in missed high risk patients. However, it may be argued that EMVs may be more representative of underlying endothelial dysfunction due to their direct release from the endothelium itself in response to activation. Indeed, previous work by our group has demonstrated that increased EMVs are associated with unstable asymptomatic plaque formation in carotid artery disease(154) and reduced endothelial function in SLE(157), linking this to dysregulated inflammation(158). The current study supports the use of EMVs as novel biomarkers by confirming a significant increase in SLE, with correlations to more typical cardiovascular signals including blood pressure, triglycerides and pulse wave

velocity. Furthermore, elevated EMVs were concurrent with QRISK3 score, reinforcing the use of both measures as indicators of cardiovascular risk.

3.5. Chapter Summary

The use of the QRISK3 algorithm identified significantly more patients with high cardiovascular risk than either the current QRISK2 model or another popular algorithm, the Framingham score. These previously missed patients differed from low risk patients and controls in a number of cardiovascular risk factors e.g. blood pressure, BMI. Laboratory tests confirmed increased levels of inflammation and dyslipidaemia in patients with SLE compared to controls, which were further elevated in patients experiencing a disease flare or in missed high risk patients. Finally, EMV levels were significantly increased in patients with SLE, correlating with markers of inflammation, dyslipidaemia and vascular dysfunction. They also correlated with QRISK3 score, and were significantly elevated in missed patients.

The significance of the raised EMV levels in SLE will be addressed in the next chapter.

Chapter 4

Dissecting Endothelial Microvesicle Content for the Analysis of Vesicular MiRNA Abundance in Patients with SLE

4.1. Study Introduction

As indicated in chapter 3, EMVs of patients with SLE are associated with cardiovascular risk alongside other elements of inflammation and disease activity. Identification of vesicular components demonstrating biological activity will enhance current understanding of the mechanisms underpinning endothelial dysfunction in SLE, as well as potentially provide novel targets for biomarker studies and therapeutic interventions. Due to their critical role in post-transcriptional gene regulation and their uptake within EMVs, this study focused on miRNAs in SLE, with the following aim: to establish the expression profile of circulating and vesicular miRNAs in patients with SLE and identify predicted targets of interest.

This aim was addressed using the following objectives:

- Establish a shortlist of miRNAs to screen by data mining.
- Assess miRNA abundance in an *in vitro* model of the SLE endothelium.
- Determine levels of miRNA abundance in the vesicular fraction of plasma from patients and controls.
- Correlate miRNA abundance with clinical markers of inflammation and cardiovascular risk.
- Identify and rank key predicted binding targets using gene ontology.

4.2. Chapter Methodology

Firstly, key miRNAs were identified by extensive data mining and shortlisting, dependent on a number of factors such as available data and novelty. To model the inflammatory environment surrounding the vascular endothelium in SLE, HUVECs at passage 4-6 were then treated for 24 hours with either 10ng/ml TNFα, BLyS or both. EMVs were obtained from the media, as described in 2.3.1, and miRNA extracted as in 2.4.2; intracellular miRNA was also extracted. Next, key miRNAs were quantified in order to provide insight into miRNA trafficking during inflammation.

In order to ascertain whether the results noted during the *in vitro* testing correlated with *in vivo* observations, the vesicular fraction of 1ml plasma was isolated and miRNA quantified. 14 control and 26 patients with SLE (15 with stable and 11 with flared disease) were included in this study, with recruitment as defined in 2.7. Inclusion was dependent on plasma stores remaining from the analysis described in chapter 3. Following qPCR, associations between miRNA expression levels and clinical data were probed, as in chapter 3. Full miRNA protocols are located in section 2.4. Finally, predicted targets were determined using the gene ontology techniques described in 2.4.4, excluding 'cellular respiration', which was performed in later chapters. The workflow for this body of research is depicted in figure 4.1.

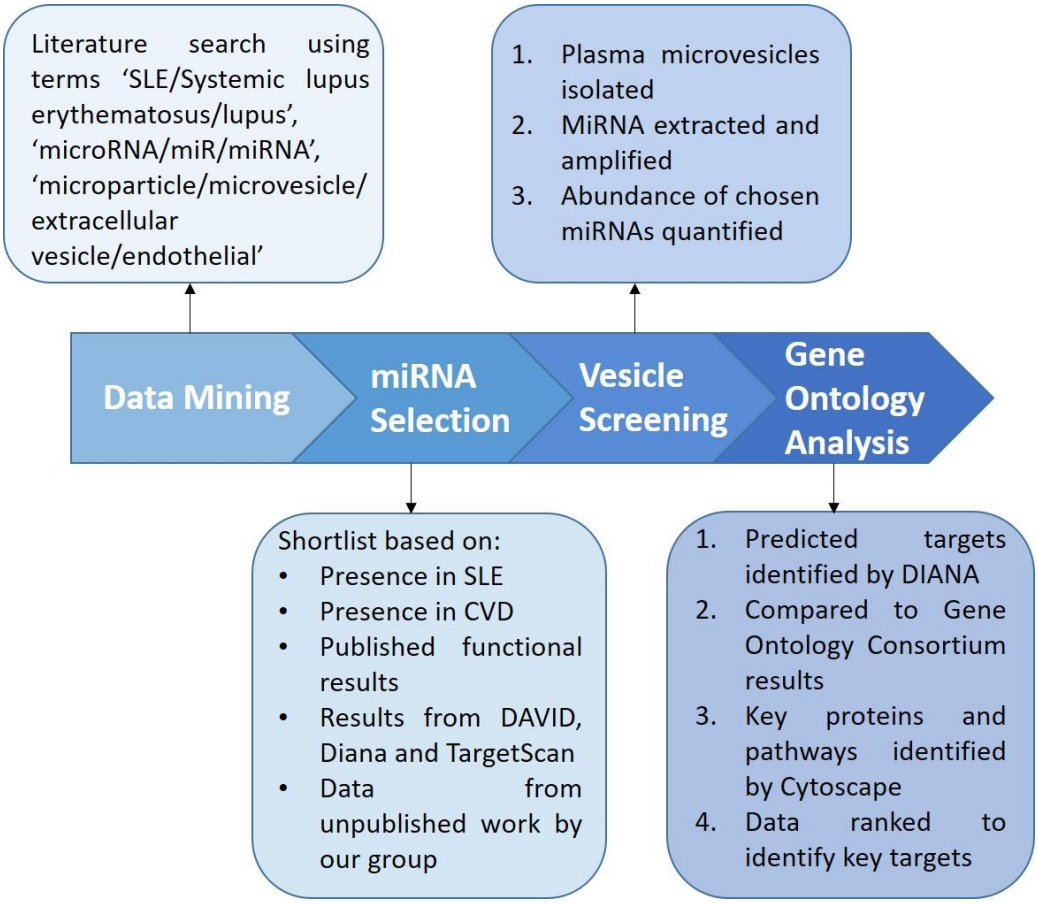

Figure 4.1: Workflow for elucidation of miRNA contents and predicted targets in microvesicles of patients with SLE.

4.3. Results

4.3.1. MiRNA Abundance within HUVECs and EMVs Released after Treatment with TNFα and BLyS

Cytokine treatment was used to determine miRNA abundance in a model of the inflamed endothelium. HUVECs were treated with either TNFα, BLyS or an equal mix of both, and the amounts of target miRNAs within the cells and in vesicles extracted from the media were quantified. The data shown in figure 4.2 represent miR-320a abundance as other vesicular miRNAs were unable to be quantified and thus, could not be compared to cellular abundance.

Interestingly, when HUVECs were treated with inflammatory cytokines, miR-320a abundance decreased, most significantly following TNFα treatment (p=0.010). A similar trend was apparent with BLyS (p=0.020) and mixed treatments (p=0.015), although an n=2 for these samples prevented statistical analysis. The opposite effect was observed in the microvesicles produced, which yielded increased miR-320a abundance in response to TNFα (p=0.026) but no change in response to BLyS (p=0.150) or mixed treatment (p=1.000).

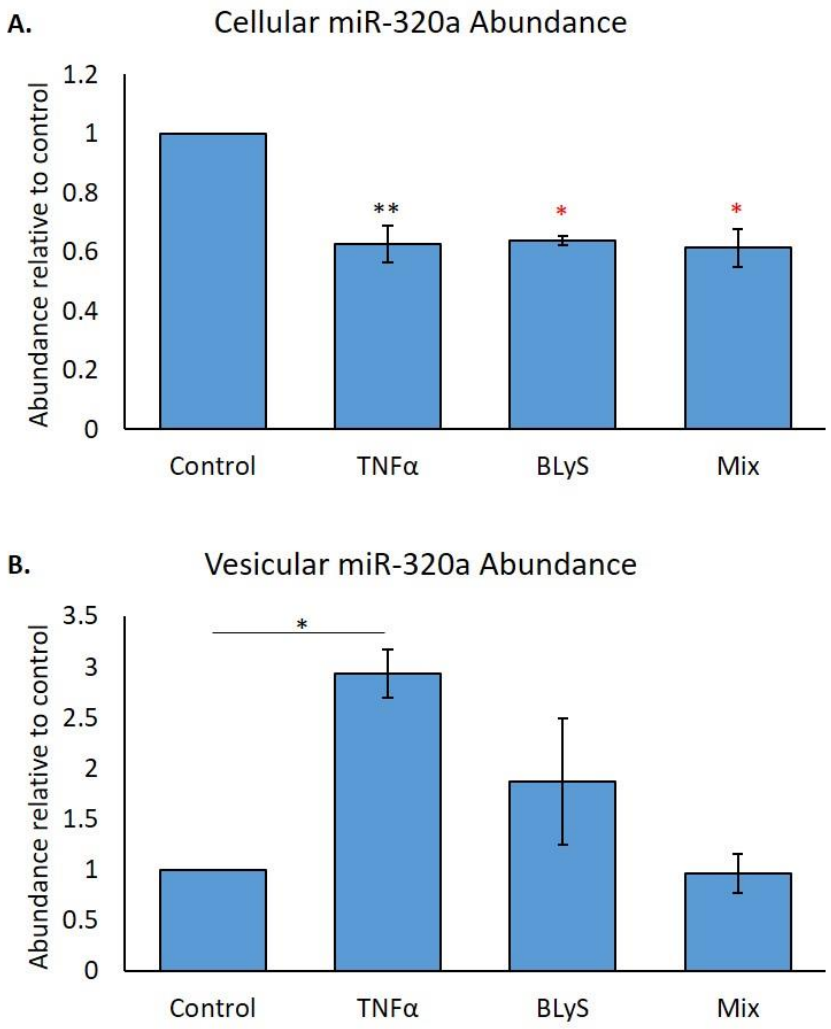

Figure 4.2: Endothelial miR-320a abundance following cytokine treatment. *Confluent HUVECs were treated for 24 hours at p4-6 with 10ng/ml TNF-α, BLyS or a mix of both, before vesicular and intracellular miR-320a was quantified. N=3 in control and TNF-a treated cells, and n=2 in BLyS and mixed treatment cells. Statistical analyses performed using one-way ANOVA with Tukey post-hoc test. Asterisks used denote: * p≤0.05 and ** p≤0.01.*

4.3.2. Demographic Details of Patients used in this Study

Plasma samples from this subset (n=40) of the original cohort of participants (n=138) introduced in chapter 3 were utilised in this study. Demographic measures were generally similar between controls and patients with SLE, although the control group were younger in age; 36.50 (± 13.61) for controls vs 42.58 (± 10.11) of patients with SLE (p=0.023; table 4.1). However, there was substantial variation in age across both groups, therefore it was deemed acceptable to continue the study. The SLE group also demonstrated higher QRISK3 scores (p<0.001), which is consistent with the results of chapter 3. There were no significant differences in demographic measures when the patient group was further subdivided into those experiencing flared and stable disease.

Variable	Controls (n=14)	SLE (n=26)	p Values
Age (years), mean ± SD	36.50 ± 13.61	42.58 ± 10.11	**0.023**
Female	14 (100%)	25 (96.15%)	1.000
Caucasian	11 (78.57%)	17 (65.38%)	0.484
BP Systolic (mm Hg)	120.0 (115.0, 130.0) *n=13*	126.0 (122.0, 137.0) *n=25*	0.199
HDL-Cholesterol (mmol/l)	1.6 (1.5, 2.0)	1.7 (1.2, 2.0) *n=25*	0.613
Non-HDL Cholesterol (mmol/l)	2.7 (2.5, 3.4)	2.8 (2.5, 3.2) *n=25*	0.897
Current Smoker	1 (7.14%)	2 (7.69%)	1.000
Type 2 Diabetes	0 (0%)	0 (0%)	1.000
QRISK3 Score (%)	0.3 (0.1, 0.4)	5.4 (3.4, 8.9)	**<0.001**
High QRISK3	0 (0%)	6 (23.08%)	0.074
	Flare (n=11)	**Stable (n=15)**	**p Values**
Age (years), mean ± SD	43.09 ± 7.90	42.20 ± 11.45	0.721
Female	11 (100%)	14 (93.33%)	1.000
Caucasian	7 (63.64%)	10 (66.67%)	1.000
BP Systolic (mm Hg)	128.0 (121.5, 137.0)	124.5 (122.3, 132.5) *n=14*	0.536
HDL-Cholesterol (mmol/l)	1.5 (1.0, 1.9)	1.8 (1.4, 2.1) *n=14*	0.120
Non-HDL Cholesterol (mmol/l)	3.1 (2.6, 4.0)	2.6 (2.3, 3.1) *n=14*	0.403
Current Smoker	0 (0%)	2 (13.33%)	0.492
Type 2 Diabetes	0 (0%)	0 (0%)	1.000
QRISK3 Score (%)	6.3 (4.7, 9.8)	5.0 (2.3, 8.4)	0.281
High QRISK3	3 (27.27%)	3 (20.00%)	1.000

Table 4.1: Demographic measures of controls and patients with SLE included in miRNA cohort. *Data represented as number (%) or median (lower and upper quartiles). P values calculated by Mann-Whitney U test or Fisher's exact test, as appropriate.*

4.3.3. Vesicular MiRNA Abundance is Altered in SLE

Seven miRNAs of interest were investigated, firstly by general abundance within the vesicular fraction of plasma (table 4.2). These miRNAs had been selected through data mining, which is further examined in discussion section of this chapter. Levels of both miR-126-3p and miR-3148 appeared to be increased in the plasma of patients with SLE compared to controls (2.29-fold and 6.31-fold respectively).

MiRNA	Control	SLE	SLE Fold Control
MiR-126-3p	2.5E-09	5.8E-09	2.29
MiR-3148	1.1E-12	6.6E-12	6.31
MiR-93-5p	3.6E-09	2.9E-09	0.81
MiR-320a	2.6E-09	3.4E-09	1.34
MiR-30d-5p	1.7E-09	1.8E-09	1.04
MiR-15b-5p	2.3E-09	3.8E-09	1.66
MiR-20a-5p	9.4E-09	1.3E-08	1.37

Table 4.2: Plasma abundance of vesicular miRNAs. *Abundance presented as calculated by $2^{-\Delta\Delta Ct}$ method following QPCR. Control n=14, SLE n=26.*

Chapter 3 described elevated numbers of EMVs in the circulation of the patient group, therefore let-7a was chosen to act as a 'housekeeper' to normalise levels of miRNA abundance. Levels of let-7a showed a trend towards an increase in patients compared to controls, although this was not significant (p=0.154; figure 4.3). Likewise, let-7a abundance was not significantly increased in patients experiencing flared (p=0.064) or stable (p=1.000) disease compared to controls, nor compared to each other (p=0.145).

There were no differences in let-7a abundance per microvesicle in patients vs controls (p=0.900) nor when comparing any other group (controls vs stable p=1.000, control vs flare p=0.935, stable vs flare p=0.346). Thus, it was decided to present the miRNA abundance data in 3 formats, including relative to let-7a, to provide the most in depth analysis.

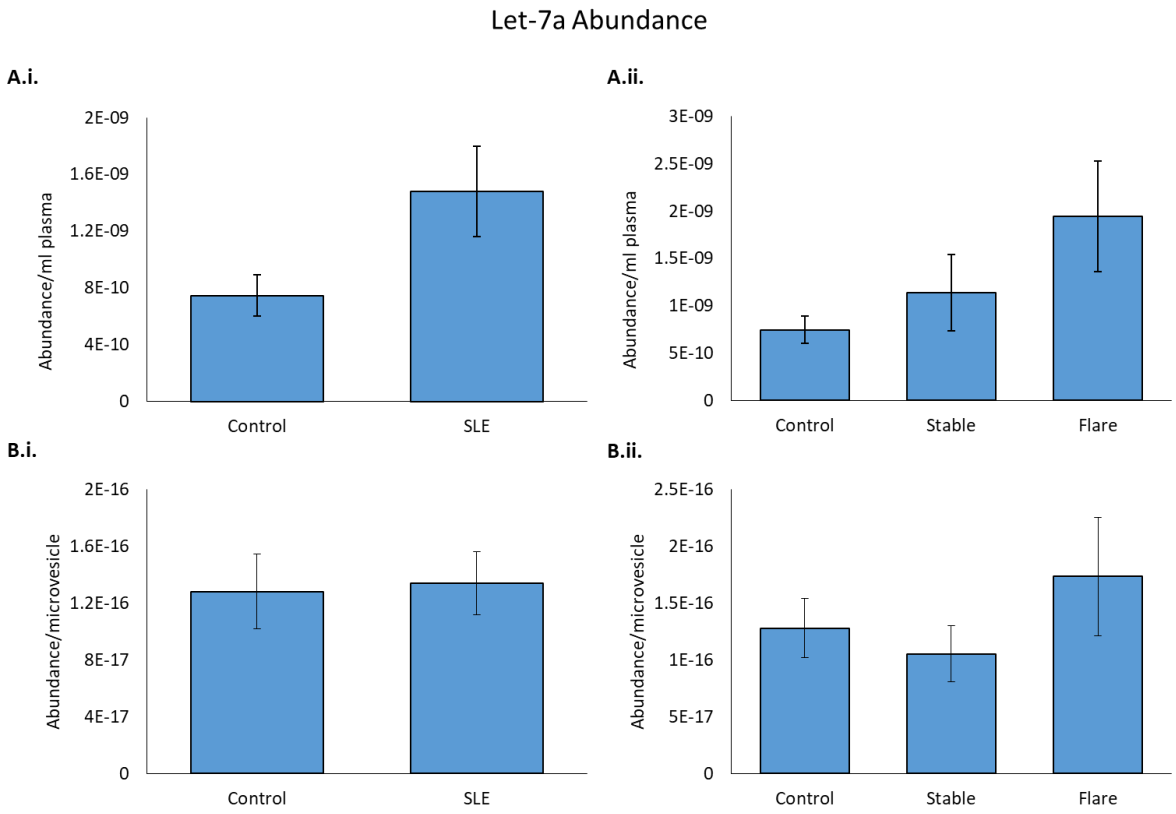

Figure 4.3: Abundance of let-7a in plasma samples. *Abundance of let-7a was quantified in 1ml of plasma and analysed per ml (A) and per microvesicle (B). Comparisons between controls and all patients assessed by Mann-Whitney U test, and between controls and disease activity (stable and flare) by Kruskal-Wallis test. Error bars represent SEM. Control n=14, SLE n=26, stable n=15, flare n=11.*

4.3.4. Identifying an SLE MiRNA Signature: Increased MiRNA Abundance

4.3.4.1. MiR-126-3p is Associated with SLE Disease Flares

A trend towards increased abundance of miR-126-3p was observed in patients compared to controls, significantly so with patients experiencing flared disease (figure 4.4). This was the case when analysing abundance per ml of plasma (p=0.001), relative to let-7a (p=0.024) and per microvesicle (p=0.009). Abundance was also consistently higher in patients with flared compared to stable disease (p=0.002, p=0.0.19 and p=0.001 respectively). There were no differences in stable patients compared to controls (p=1.000 for all measures), nor in SLE vs controls, despite the apparent trend (p=0.059, p=0.190 and p=0.254).

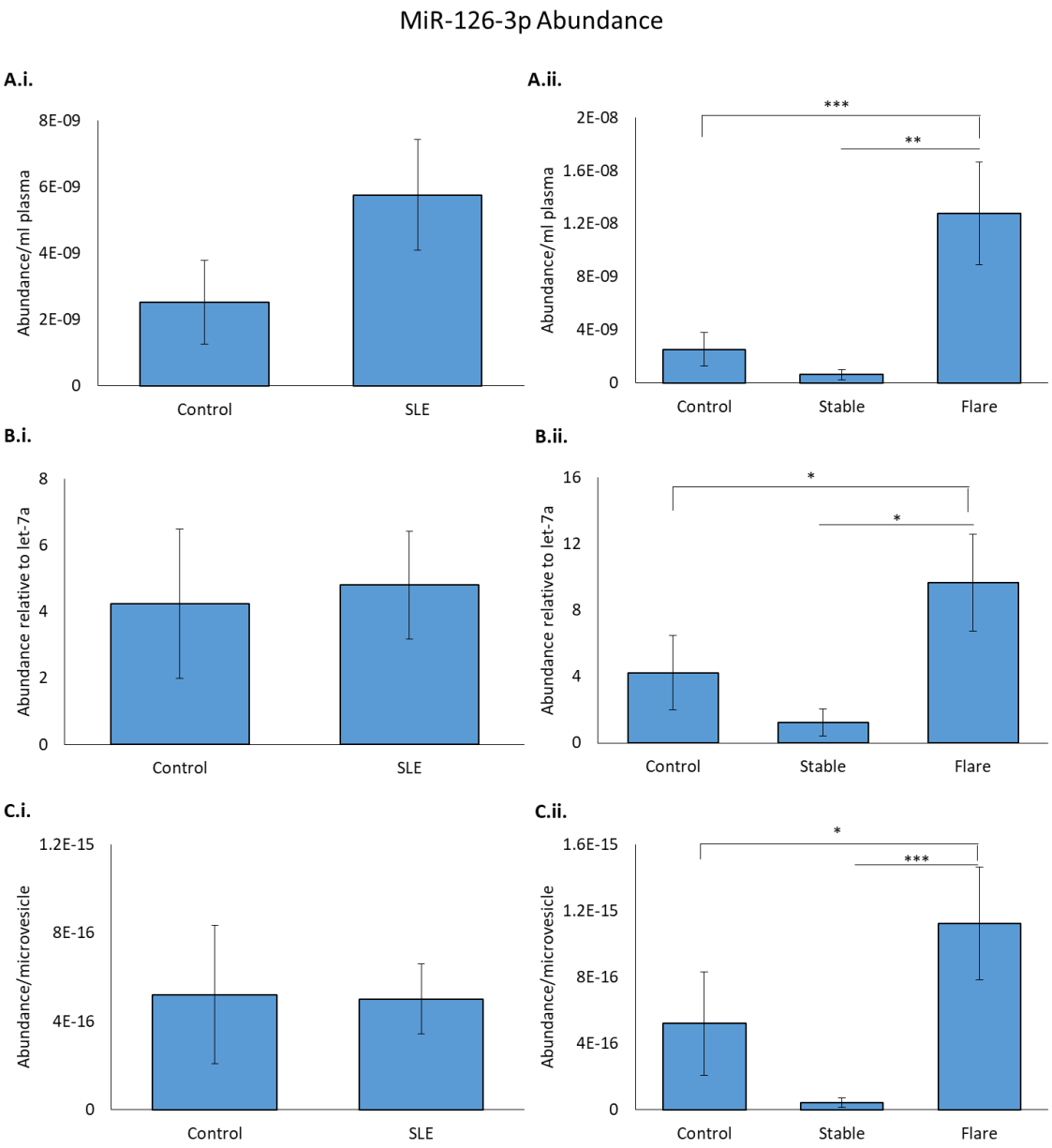

Figure 4.4: MiR-126-3p abundance in plasma vesicular fractions. *Abundance of miR-126-3p was measured in participants by qPCR and compared against volume of plasma (A), relative let-7a abundance (B) and per microvesicle (C). Comparisons between controls and all patients assessed by Mann-Whitney U test, and between controls and disease activity (stable and flare) by Kruskal-Wallis test. Error bars represent SEM. Control n=14, SLE n=26, stable n=15, flare n=11. Asterisks used denote: * p≤0.05, ** p≤0.01 and *** p≤0.001.*

When miR-126-3p abundance was correlated with clinical data (table 4.3), increased levels correlated positively with QRISK2 and 3 scores ($p<0.05$), as well as EMV number ($p<0.01$). Increased abundance also correlated with increased age ($p<0.04$), cholesterol/HDL ratio ($p<0.05$), adiponectin ($p=0.025$) and BLyS levels ($p=0.024$), although a negative correlation was observed with haemoglobin ($p=0.020$). Furthermore, increased miR-126-3p abundance was associated with anti-hypertensive ($p<0.05$) and statin use ($p=0.047$). In the patient cohort only, miR-126-3p correlated negatively with both IgM ($p=0.001$) and anticardiolipin IgM antibodies ($p=0.039$), and was associated with renal disorder ($p<0.040$) and immunosuppressive use ($p<0.05$).

Variable		Abundance/ml plasma	Abundance relative to Let-7a	Abundance/MV
QRISK2 Score		0.403 **p=0.010**	0.327 **p=0.040**	0.342 **p=0.031**
QRISK3 Score		0.518 **p=0.001**	0.474 **p=0.002**	0.415 **p=0.008**
CD144^{+} EMVs		0.521 **p=0.001**	0.445 **p=0.004**	0.315 **p=0.048**
Age		0.343 **p=0.030**	0.271 p=0.090	**0.331** **p=0.037**
Haemoglobin		-0.367 **p=0.020**	-0.206 p=0.201	-0.299 p=0.061
Total Cholesterol/HDL Ratio		0.527 **p=0.007**	0.406 **p=0.044**	0.092 p=0.576
Adiponectin		0.201 p=0.215	0.355 **p=0.025**	0.288 p=0.071
IgM (SLE)		-0.603 **p=0.001**	-0.622 **p=0.001**	-0.627 **p=0.001**
Anticardiolipin IgM (SLE)		-0.269 p=0.194	-0.171 p=0.413	-0.415 **p=0.039**
BLyS		0.356 **p=0.024**	0.299 p=0.061	0.298 p=0.062
Renal Disorder (SLE)	Present *(n=9)* Absent	$8.8\times10^{-9} \pm 1.0\times10^{-8}$ $4.2\times10^{-9} \pm 7.0\times10^{-9}$ **p=0.034**	9.6 ± 11.8 2.3 ± 3.6 **p=0.009**	$5.7\times10^{-16} \pm 6.3\times10^{-16}$ $4.6\times10^{-16} \pm 8.9\times10^{-16}$ p=0.087
Anti hyper-tensive Use	Present *(n=10)* Absent	$1.0\times10^{-8} \pm 9.2\times10^{-9}$ $2.7\times10^{-9} \pm 5.7\times10^{-9}$ **p=0.001**	10.0 ± 10.9 2.8 ± 6.3 **p=0.001**	$9.9\times10^{-16} \pm 1.1\times10^{-15}$ $3.5\times10^{-16} \pm 8.3\times10^{-16}$ **p=0.002**
Statin Use	Present *(n=5)* Absent	$6.1\times10^{-9} \pm 4.3\times10^{-9}$ $4.4\times10^{-9} \pm 7.9\times10^{-9}$ p=0.279	7.5 ± 4.1 4.2 ± 8.9 **p=0.047**	$1.1\times10^{-15} \pm 1.4\times10^{-15}$ $4.3\times10^{-16} \pm 8.5\times10^{-16}$ p=0.261
Immuno suppressa-nt Use (SLE)	Present *(n=18)* Absent	$8.3\times10^{-9} \pm 9.4\times10^{-9}$ $1.0\times10^{-9} \pm 2.9\times10^{-9}$ **p=0.047**	6.8 ± 9.4 1.0 ± 2.7 **p=0.035**	$7.0\times10^{-16} \pm 9.0\times10^{-16}$ $6.4\times10^{-17} \pm 1.6\times10^{-16}$ p=0.082

Table 4.3: Associations between miR-126-3p abundance and clinical data. *Renal disorder characterised by ACR criteria. Upper section presents Spearman's rho correlation coefficients; lower section presents mean expression (± standard deviation) with statistical analysis using Mann-Whitney U test. Comparisons made across whole cohort unless otherwise stated. Control n=14, SLE n=26.*

An investigation into the targets of miR-126-3p yielded a predicted binding score of 0.999 (maximum 1) for epidermal growth factor receptor (EGFR), the highest score with this miRNA (table 4.4). This was listed under 'ossification' by the GO consortium and yielded the largest node degree on Cytoscape, indicating its importance in a variety of processes other than osteogenesis. Other highly likely targets included vascular endothelial growth factor receptor 3 kinase (FLT4), cyclooxygenase 2 (PTGS2) and platelet derived growth factor receptor-α (PDGFRA), which are implicated in vascular function and SLE-related inflammation.

Gene ID	GO Consortium Area	Cytoscape Rank/Node Degree	DIANA miTG Score
EGFR	Ossification	1/974	0.999
CD44	SLE	N/A	0.960
FLT4	Angiogenesis	931/12	0.959
DICER1	Angiogenesis	180/97	0.941
CREB1	SLE	N/A	0.935
CSF1	Ossification	96/51	0.922
SMAD4	EC activation	2/230	0.900
MS4A1	SLE	N/A	0.898
PTGS2	SLE	N/A	0.894
PDGFRA	Angiogenesis	302/56	0.892

Table 4.4: Highest ranking predicted targets of miR-126-3p. *Data ranked by DIANA miTG score of predicted binding, supported by cytoscape ranking and node degree (corresponding with number of networks and connections to other cellular pathways).*

4.3.4.2. MiR-3148 is Increased in SLE and has Predicted Ossification Targets

Although miR-3148 was detected at lower levels than the other miRNAs, expression per ml of plasma was significantly elevated in patients with SLE (p=0.009; figure 4.5). This was also significant in stable disease compared to controls (p=0.012) and demonstrated a trend in flared disease (p=0.094); there was no difference between flared and stable disease (p=1.000). Similarly, trends towards increased abundance in SLE were apparent but not significant when analysing levels relative to let-7a (p=0.162) and per microvesicle (p=0.279). Nor were there any differences according to disease activity when relative to let-7a (control vs stable p=0.214, control vs flare p=1.000, flare vs stable p=0.698) or per microvesicle (control vs stable p=0.725, control vs flare and flare vs stable both p=1.000).

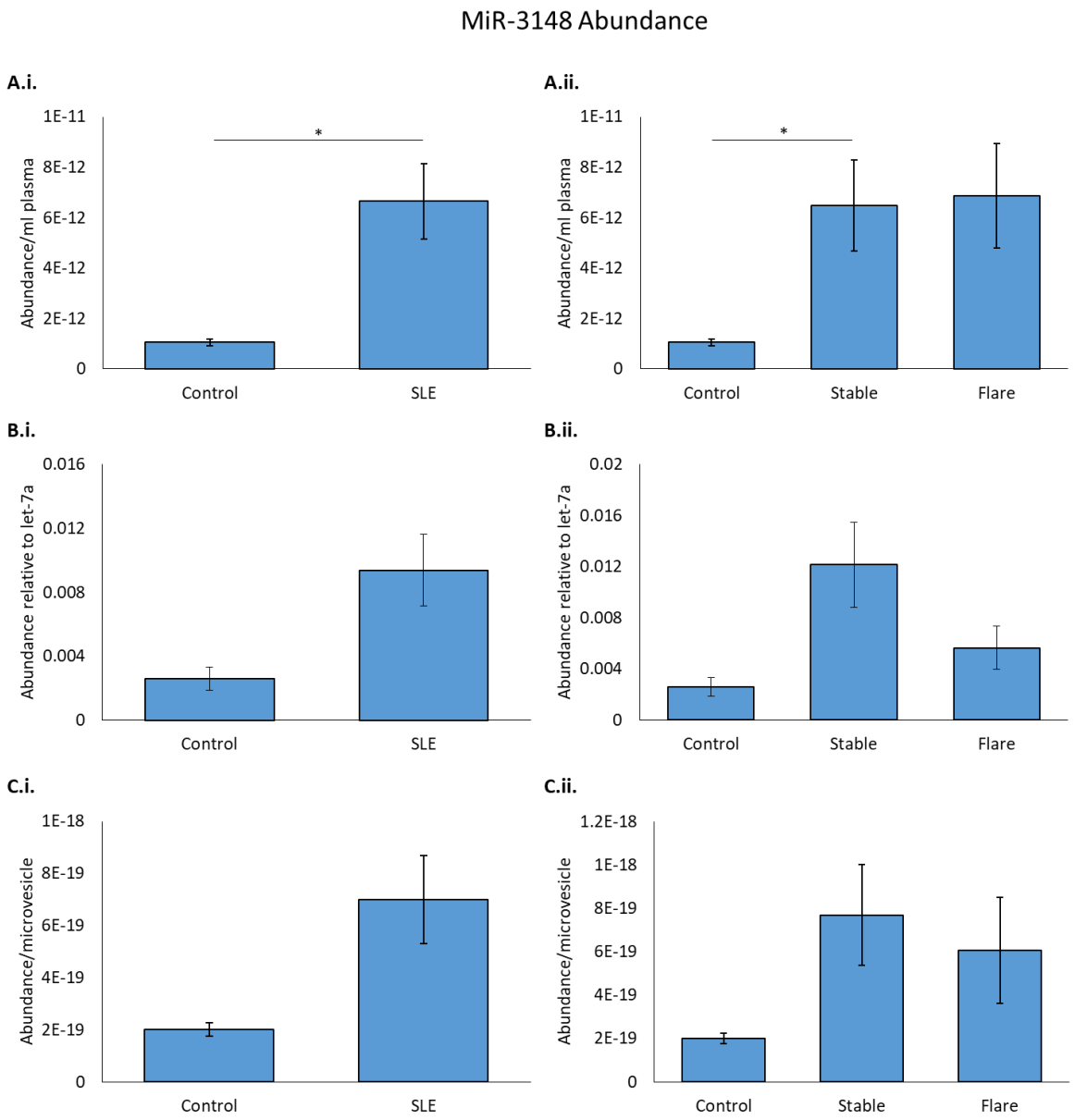

Figure 4.5: MiR-3148 abundance in plasma vesicular fractions. *Abundance of miR-3148 was measured in participants by qPCR and compared against volume of plasma (A), relative let-7a abundance (B) and per microvesicle (C). Comparisons between controls and all patients assessed by Mann-Whitney U test, and between controls and disease activity (stable and flare) by Kruskal-Wallis test. Error bars represent SEM. Control n=14, SLE n=26, stable n=15, flare n=11. * denotes p≤0.05.*

Elevated miR-3148 abundance per ml of plasma was associated with increased QRISK3 score and EMV number ($p<0.03$; table 4.5), whereas abundance per microvesicle correlated negatively with PMVs ($p=0.024$). Abundance also correlated negatively with glucose ($p<0.04$) and positively with MCP-1 ($p=0.035$). Furthermore, it was associated with ACR count ($p=0.047$), anticardiolipin antibodies ($p=0.018$) and serositis ($p<0.01$) in patients with SLE.

Variable		Abundance/ml plasma	Abundance relative to Let-7a	Abundance/MV
QRISK3		0.448 **p=0.004**	0.293 p=0.067	0.220 p=0.172
CD144$^+$ EMVs		0.356 **p=0.024**	0.106 p=0.515	-0.125 p=0.442
CD42b$^+$ PMVs		0.204 p=0.207	-0.017 p=0.916	-0.356 **p=0.024**
Glucose		-0.348 **p=0.030**	-0.342 **p=0.033**	-0.346 **p=0.031**
ACR Count (SLE)		0.393 **p=0.047**	0.167 p=0.414	0.278 p=0.169
Anticardiolipin antibodies (SLE)		-0.282 p=0.172	-0.020 p=0.923	-0.470 **p=0.018**
MCP1		0.333 **p=0.035**	0.283 p=0.076	0.208 p=0.198
Serositis	Present *(n=7)* Absent	$3.1\times10^{-9} \pm 4.7\times10^{-9}$ $2.8\times10^{-9} \pm 2.8\times10^{-9}$ **p=0.003**	3.2 ± 3.3 2.2 ± 1.5 **p=0.001**	$1.7\times10^{-18} \pm 1.1\times10^{-18}$ $3.8\times10^{-19} \pm 5.1\times10^{-19}$ **p=0.009**

Table 4.5: Associations between miR-3148 abundance and clinical data. *Serositis characterised by ACR criteria. Upper section presents Spearman's rho correlation coefficients; lower section presents mean expression (± standard deviation) with statistical analysis using Mann-Whitney U test. Comparisons made across whole cohort unless otherwise stated. Control n=14, SLE n=26.*

One possible target of miR-3148, insulin-like growth factor 1 (IGF1) yielded the maximum possible binding score of 1.000, indicating certain binding (table 4.6); this was associated with ossification, as was RUNX2 (0.999).

Gene ID	GO Consortium Area	Cytoscape Rank/Node Degree	DIANA miTG Score
IGF1	Ossification	158/26	1.000
RHOA	Angiogenesis	199/88	0.999
SATB2	Ossification	118/40	0.999
RUNX2	Ossification	150/27	0.999
BCHE	Blood Microparticles	866/14	0.998
PTPRB	Angiogenesis	457/34	0.996
PDPK1	Angiogenesis	267/63	0.992
INTU	Ossification	178/21	0.991
MBL2	SLE	Na	0.991
MEIS1	Angiogenesis	737/18	0.990

Table 4.6: Highest ranking predicted targets of miR-3148. *Data ranked by DIANA miTG score of predicted binding, supported by cytoscape ranking and node degree (corresponding with number of networks and connections to other cellular pathways).*

4.3.5. Identifying an SLE MiRNA Signature: Decreased MiRNA Abundance

4.3.5.1. Mir-93-5p Abundance is Significantly Reduced in SLE

While abundance of miR-93-5p per ml of plasma appeared to be reduced in patients compared to controls (p=0.130), it was significantly so when relative to let-7a (p=0.018) and per microvesicle (p=0.015; figure 4.6). Indeed, while no differences were observed in miRNA abundance per ml of plasma (controls vs stable p=0.275, controls vs flare and flare vs stable both p=1.000), abundance relative to let-7a was significantly decreased in patients experiencing a disease flare compared to controls (p=0.043). There were no differences in flare vs stable patients (p=1.000) nor in stable patients vs controls, despite an apparent trend towards a reduction (p=0.270). Conversely, miR-93-5p abundance per microvesicle was significantly reduced in stable patients compared to controls (p=0.049) but not in flare patients vs controls (p=0.288) nor in flare vs stable patients (p=1.000).

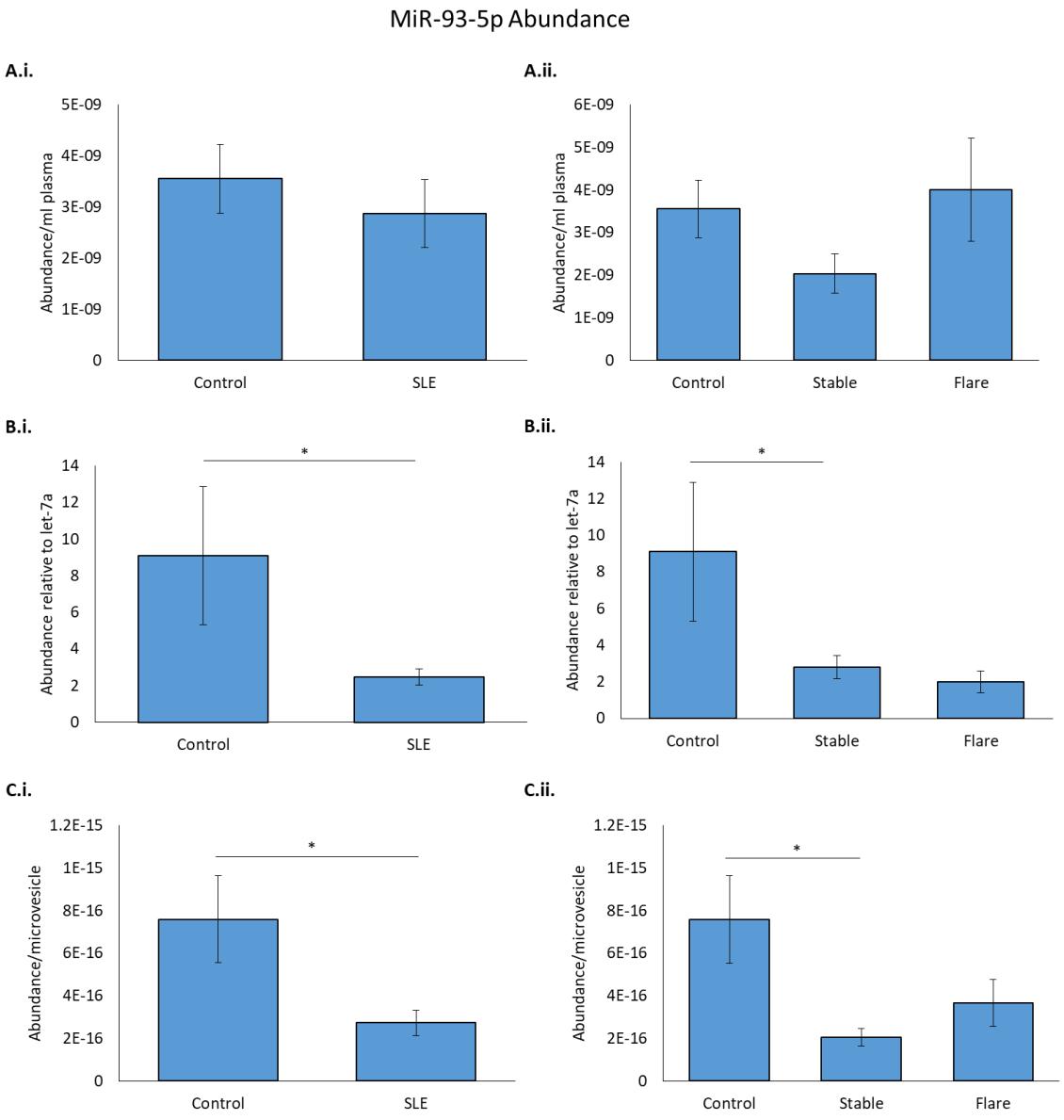

Figure 4.6: MiR-93-5p abundance in plasma vesicular fractions. *Abundance of miR-93-5p was measured in participants by qPCR and compared against volume of plasma (A), relative let-7a abundance (B) and per microvesicle (C). Comparisons between controls and all patients assessed by Mann-Whitney U test, and between controls and disease activity (stable and flare) by Kruskal-Wallis test. Error bars represent SEM. Control n=14, SLE n=26, stable n=15, flare n=11. * denotes p≤0.05.*

Across the whole cohort, abundance of miR-93-5p correlated negatively with both EMVs and PMVs ($p<0.04$), as well as MCP-1 ($p<0.05$) and positively with glucose ($p<0.02$; table 4.7). Moreover, within the patient population, it was associated with neutrophil number, IgM and the presence of haematological disorders ($p<0.05$).

Variable		Abundance/ml plasma	Abundance relative to Let-7a	Abundance/MV
$CD144^+$ EMVs		-0.215 p=0.183	-0.422 **p=0.007**	-0.604 **p<0.001**
$CD42b^+$ PMVs		-0.086 p=0.596	-0.344 **p=0.030**	-0.611 **p<0.001**
Neutrophils (SLE)		-0.377 p=0.058	0.075 p=0.715	-0.391 **p=0.048**
MCP1		-0.314 **p=0.049**	-0.181 p=0.265	-0.346 **p=0.029**
IgM (SLE)		0.036 p=0.863	0.430 **p=0.028**	0.074 p=0.721
Glucose		0.410 **p=0.010**	0.379 **p=0.017**	0.302 p=0.062
Haematol -ogic Disorder (SLE)	Present *(n=12)* Absent	$3.4x10^{-9} \pm 4.1x10^{-9}$ $2.4x10^{-9} \pm 2.6x10^{-9}$ p=1.000	1.3 ± 0.9 3.5 ± 2.4 **p=0.003**	$2.4x10^{-16} \pm 2.6x10^{16}$ $3.1x10^{-16} \pm 3.3x10^{-16}$ p=0.681

Table 4.7: Associations between miR-93-5p abundance and clinical data. *Haematologic disorder characterised by ACR criteria. Upper section presents Spearman's rho correlation coefficients; lower section presents mean expression (± standard deviation) with statistical analysis using Mann-Whitney U test. Comparisons made across whole cohort unless otherwise stated. Control n=14, SLE n=26.*

Sortilin 1 (SORT1) was the highest ranking potential target of miR-93-5p, with a predicted binding score of 0.962 (table 4.8). While the GO consortium identified SORT1 as implicated in ossification, many high-ranking targets were involved in angiogenesis, such as hypoxia inducible factor 1-α (HIF1A; 0.940), STAT3 (0.914) and matrix metalloproteinase 2 (MMP2; 0.901).

Gene ID	GO Consortium Area	Cytoscape Rank/Node Degree	DIANA miTG Score
SORT1	Ossification	28/147	0.962
RASSF2	Ossification	76/65	0.962
HIF1A	Angiogenesis	52/256	0.940
PIAS2	Ossification	35/125	0.927
STAT3	Angiogenesis	36/326	0.914
EPHB4	Angiogenesis	856/14	0.910
GAB1	Angiogenesis	34/331	0.904
MMP2	Angiogenesis	552/27	0.901
HSPA8	Blood Microparticles	78/167	0.882
CNOT7	IFNA Signalling	32/45	0.860

***Table 4.8: Highest ranking predicted targets of miR-93-5p**. Data ranked by DIANA miTG score of predicted binding, supported by cytoscape ranking and node degree (corresponding with number of networks and connections to other cellular pathways).*

4.3.5.2. MiR-320a is Reduced in SLE and May Target Pathways Involved in Angiogenesis and Ossification

Abundance of miR-320a per ml of plasma (p=0.856) and relative to let-7a (p=0.154) revealed contrasting trends, with no clear pattern detected until analysis of abundance per microvesicle, which was significantly reduced in patients compared to controls (p=0.045; figure 4.7). No other differences were detected, in either abundance per ml (all p=1.000), relative to let-7a (controls vs flare p=0.110, controls vs stable p=1.000, flare vs stable p=0.328) or per microvesicle (controls vs flare p=0.364, controls vs stable p=0.180, flare vs stable p=1.000).

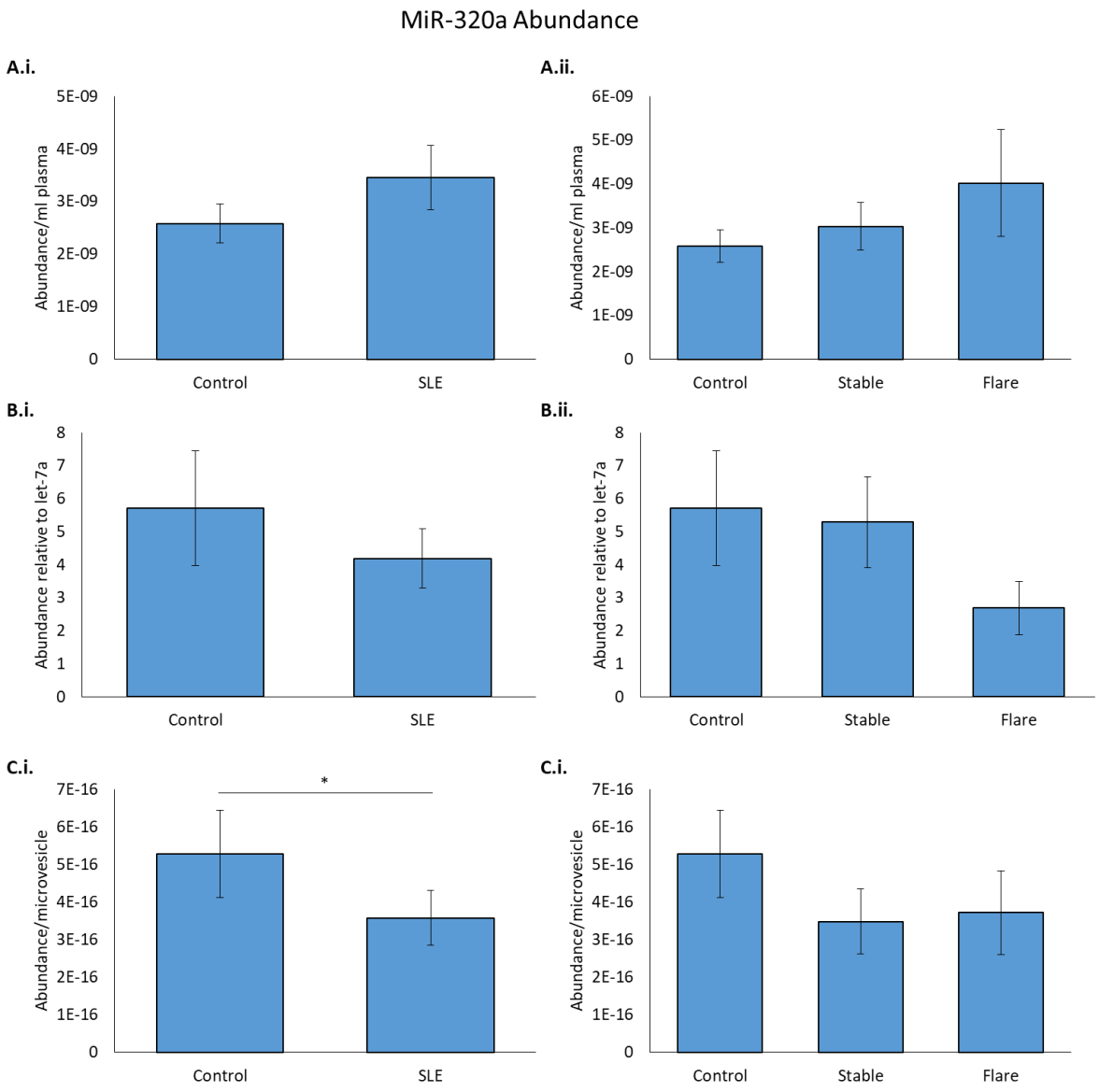

Figure 4.7: MiR-320a abundance in plasma vesicular fractions. *Abundance of miR-320a was measured in participants by qPCR and compared against volume of plasma (A), relative let-7a abundance (B) and per microvesicle (C). Comparisons between controls and all patients assessed by Mann-Whitney U test, and between controls and disease activity (stable and flare) by Kruskal-Wallis test. Error bars represent SEM. Control n=14, SLE n=26, stable n=15, flare n=11. * denotes p≤0.05.*

While miR-320a abundance correlated with fewer clinical measures than the other miRNAs (table 4.9), it did demonstrate negative correlations with both EMVs and PMVs across the whole cohort of participants ($p<0.05$), whereas in patients, it was associated with anticardiolipin antibodies and a diagnosis of fibromyalgia alongside SLE ($p<0.05$).

Variable		Abundance/ml plasma	Abundance relative to Let-7a	Abundance/MV
$CD144^+$ EMVs		-0.034 p=0.837	-0.322 **p=0.043**	-0.593 **p<0.001**
$CD42b^+$ PMVs		0.052 p=0.749	-0.245 p=0.127	-0.680 **p<0.001**
Anticardiolipin antibodies (SLE)		-0.143 p=0.495	0.286 p=0.165	-0.409 **p=0.042**
Fibromyalgia (SLE)	Present *(n=5)* Absent	$5.1x10^{-9} \pm 4.2x10^{-9}$ $2.4x10^{-9} \pm 1.6x10^{-9}$ p=0.235	1.5 ± 2.0 6.9 ± 1.5 p=0.297	$7.1x10^{-16} \pm 5.4x10^{-16}$ $3.7x10^{-16} \pm 2.4x10^{-16}$ **p=0.036**

Table 4.9: Associations between miR-320a abundance and clinical data. *Upper section presents Spearman's rho correlation coefficients; lower section presents mean expression (± standard deviation) with statistical analysis using Mann-Whitney U test. Comparisons made across whole cohort unless otherwise stated. Control n=14, SLE n=26.*

The highest ranking predicted targets often fell within the fields of 'angiogenesis' and 'ossification' and many were associated with smaller nodes, as ranked by Cytoscape (table 4.10). The highest predicted targets were matrix metalloproteinase 16 (MMP16; 0.991), cyclin-dependent kinase 6 (CDK6; 0.990) and bone morphogenic protein receptor type 1α (BMPR1A); these are all implicated in ossification, as is RUNX2, which had an miTG score of 0.940.

Gene ID	GO Consortium Area	Cytoscape Rank/Node Degree	DIANA miTG Score
MMP16	Ossification	420/0	0.991
CDK6	Ossification	22/170	0.990
BMPR1A	Ossification	102/48	0.987
IRF6	IFNA signalling	83/5	0.975
HOXA5	Angiogenesis	1080/9	0.974
MAP3K7	Angiogenesis	337/50	0.973
NFATC3	Angiogenesis	1240/6	0.970
NR3C1	SLE	na	0.967
PRCP	Angiogenesis	1327/5	0.964
SASH1	Angiogenesis	1493/4	0.959

Table 4.10: Highest ranking predicted targets of miR-320a*. Data ranked by DIANA miTG score of predicted binding, supported by cytoscape ranking and node degree (corresponding with number of networks and connections to other cellular pathways).*

4.3.5.3. MiR-30d-5p is Reduced in SLE and Associated with Markers of Inflammation and Dyslipidaemia

The final miRNA to be analysed was miR-30d-5p (figure 4.8). Abundance of this miRNA demonstrated no differences when analysed per ml of plasma (controls vs SLE p=0.769, controls vs stable p=0.275, controls vs flare and flare vs stable both p=1.000). However, when abundance was analysed relative to let-7a and per microvesicle, it was significantly reduced in patients with SLE compared to controls (p=0.025 and p=0.029 respectively). When analysed relative to let-7a, abundance was further reduced in flare patients compared to controls (p=0.043) but not in stable patients (p=0.270) nor in flare vs stable patients (p=1.000). This was reversed when analysed per microvesicle, such that abundance was lowest in stable patients compared to controls (p=0.049) but no differences were apparent in controls vs flare (p=0.288) or flare vs stable (p=1.000).

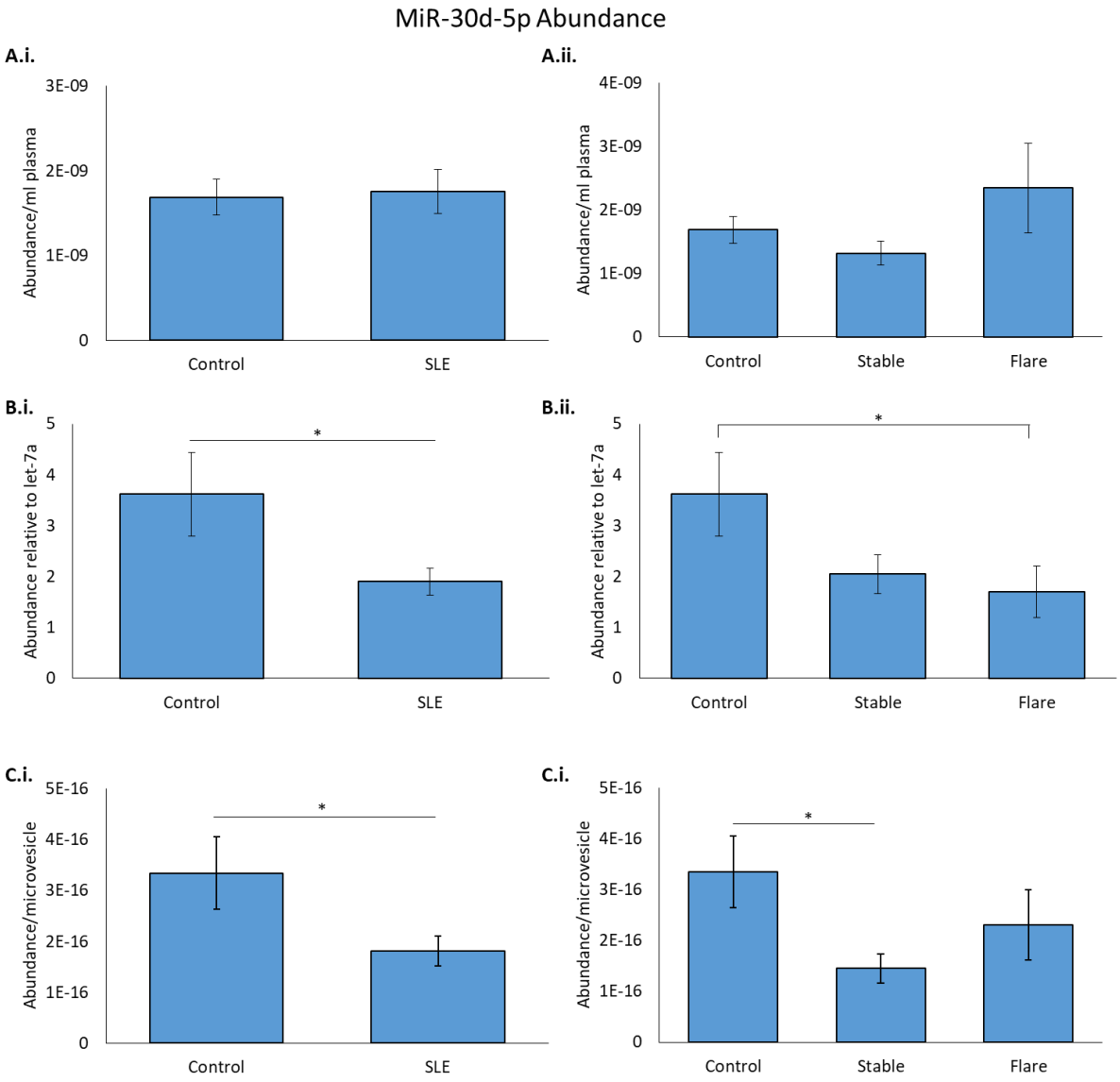

Figure 4.8: MiR-30d-5p abundance in plasma vesicular fractions. *Abundance of miR-30d-5p was measured in participants by qPCR and compared against volume of plasma (A), relative let-7a abundance (B) and per microvesicle (C). Comparisons between controls and all patients assessed by Mann-Whitney U test, and between controls and disease activity (stable and flare) by Kruskal-Wallis test. Error bars represent SEM. Control n=14, SLE n=26, stable n=15, flare n=11. * denotes p≤0.05.*

MiR-30d-5p abundance correlated with a number of clinical markers such as cholesterols and both EMVs and PMVs ($p<0.05$; table 4.11). Within the patient cohort, abundance correlated negatively with white blood cell and neutrophil numbers ($p<0.03$), as well as

anticardiolipin IgM molecules (p=0.008). Furthermore, abundance was associated with photosensitivity and haematological disorders (p<0.030).

Variable		Abundance/ml plasma	Abundance relative to Let-7a	Abundance/MV
$CD144^+$ EMVs		-0.034 p=0.837	-0.407 **p=0.009**	-0.646 **p<0.001**
$CD42b^+$ PMVs		0.062 p=0.702	-0.325 **p=0.041**	-0.752 **p<0.001**
Symptom Years (SLE)		0.169 p=0.420	0.443 **p=0.027**	0.482 **p=0.015**
Total Cholesterol/HDL Ratio		-0.036 p=0.828	-0.247 p=0.129	-0.319 **p=0.048**
Non-HDL Cholesterol		-0.176 p=0.284	-0.141 p=0.391	-0.325 **p=0.044**
Haemoglobin		-0.021 p=0.897	0.431 **p=0.006**	0.206 p=0.202
White Blood Cells (SLE)		-0.291 p=0.149	0.115 p=0.577	-0.430 **p=0.028**
Neutrophils (SLE)		-0.497 **p=0.010**	0.190 p=0.351	-0.460 **p=0.018**
Anticardiolipin IgM (SLE)		-0.356 p=0.081	0.280 p=0.176	-0.521 **p=0.008**
Photo-sensitivity (SLE)	Present *(n=21)* Absent	$2.0x10^{-9} \pm 1.3x10^{-9}$ $8.5x10^{-10} \pm 7.1x10^{-10}$ p=0.057	1.8 ± 1.0 2.5 ± 2.2 p=0.659	$2.1x10^{-16} \pm 1.5x10^{-16}$ $8.6x10^{-17} \pm 8.6x10^{-17}$ **p=0.029**
Haemato-logic Disorder (SLE)	Present *(n=12)* Absent	$2.1x10^{-9} \pm 1.6x10^{-9}$ $1.4x10^{-9} \pm 9.5x10^{-19}$ p=0.274	1.3 ± 1.0 2.4 ± 1.4 **p=0.006**	$2.0x10^{-16} \pm 1.6x10^{-16}$ $1.8x10^{-16} \pm 1.4x10^{-16}$ p=0.797

Table 4.11: Associations between miR-30d-5p abundance and clinical data. *Photosensitivity and haematology disorder characterised by ACR criteria. Upper section presents Spearman's rho correlation coefficients; lower section presents mean expression (± standard deviation) with statistical analysis using Mann-Whitney U test. Comparisons made across whole cohort unless otherwise stated. Control n=14, SLE n=26.*

The highest ranked predicted targets were associated with a range of GO consortium areas, but three demonstrated the highest predicted binding score of 1 (table 4.12). These were beclin 1 (BECN1), SNAI1/snail and suppressor of cytokine signalling 1 (SOCS1). Cytoscape data were unavailable for SOCS1, however, both BECN1 and SNAI1 showed large nodes of 350 and 177 degrees respectively. Other predicted targets included RUNX2 (0.998) and angiomotin-like protein 2 (AMOTL2; 0.997).

Gene ID	GO Consortium Area	Cytoscape Rank/Node Degree	DIANA miTG Score
BECN1	Angiogenesis	29/350	1.000
SNAI1	Ossification	20/177	1.000
SOCS1	SLE	na	1.000
RUNX2	Ossification	150/27	0.998
AMOTL2	Angiogenesis	99/160	0.997
ACTC1	Blood Microparticles	473/31	0.996
EFNA	Angiogenesis	847/14	0.994
KLF10	Ossification	196/17	0.991
SH2B3	Angiogenesis	973/11	0.990
HDAC5	Angiogenesis	365/45	0.988

Table 4.12: Highest ranking predicted targets of miR-30d-5p*. Data ranked by DIANA miTG score of predicted binding, supported by cytoscape ranking and node degree (corresponding with number of networks and connections to other cellular pathways).*

4.3.6. Additional MiRNA Analysis

A further two miRNAs were tested, namely miR-15b-5p and miR-20a-5p. They both demonstrated similar patterns of increase in SLE, particularly in disease flares, but no statistical significance between when analysing abundance levels per ml of plasma (p=0.644 and p=0.747 respectively; figure 4.9). This was mirrored in abundance relative to let-7a and per microvesicle, which demonstrated the same weak trends without significance for both miR-15b-5p (p=0.266 and p=0.604) and miR-20a-5p (p=0.424 and p=0.361). Similarly, no significant differences were apparent when comparing patients with

stable and flared disease across any measure (p>0.05; data not shown). Thus it was decided to discontinue further work with these miRNAs, instead focussing on those with stronger relationships to SLE. As such, gene ontology analysis was not carried out.

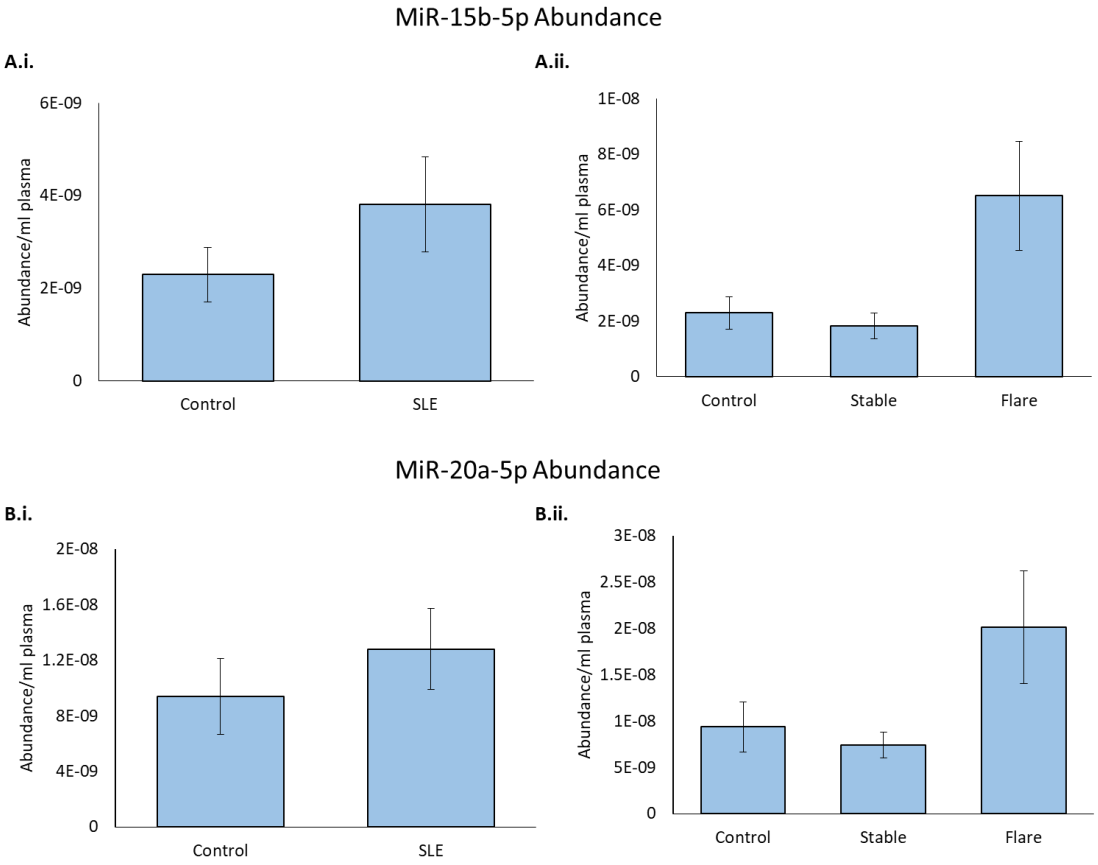

Figure 4.9: MiR-15b-5p and miR-20a-5p abundance in plasma vesicular fractions. *Abundance of miR-15b-5p (A) and miR-20a-5p (B)was measured in participants by qPCR and compared against volume of plasma. Comparisons between controls and all patients assessed by Mann-Whitney U test, and between controls and disease activity (stable and flare) by Kruskal-Wallis test. Error bars represent SEM. Control n=14, SLE n=26, stable n=15, flare n=11.*

4.4. Chapter Discussion

4.4.1. Rationale for MiRNA Selection

The presence of miRNA within extracellular vesicles has been previously documented, suggesting a mode of action by which vesicles may interact with and affect the function of the endothelium(125, 136, 137). This study interrogated the expression of seven miRNAs associated with microvesicles in the circulation of patients with SLE, all of which were carefully selected in order to build a panel of both disease-relevant and interesting targets. MiR-126-3p was the first to be chosen as it is implicated in both SLE and CVD; a number of papers have documented increased levels in SLE and other autoimmune diseases(228, 229), while Jansen *et al*. found it predicted a reduced risk of a major adverse cardiovascular event in patients with coronary artery disease(230), and described its role in endothelial repair(231). These studies affirm that it has been isolated from EMVs both *in vivo* and *in vitro*, and furthermore, previous unpublished work by our group found increased levels following BLyS stimulation in an *in vitro* endothelial model. MiR-126-3p was therefore included to validate and build on previous research using this patient cohort.

In contrast, miR-93-5p was chosen as a novel, less well understood miRNA. It had previously been isolated from plasma and it was suggested to be an independent predictor of stroke and coronary artery disease(151, 152), yet little was known about its activity in SLE. Thus, it presented an opportunity for novel data combining cardiovascular effects in SLE.

Even less was known about miR-3148 at the time of experimentation, although earlier unpublished data by our group observed its presence within EMVs and positive effects on vascular calcification. It was included in this study to advance the knowledge base and investigate its effects upon the endothelium. MiR-3148 has also been associated with toll like receptor expression in SLE, albeit in peripheral blood mononuclear cells(232).

MiR-30d-5p was likewise associated with calcification(233), as well as heart failure(234), but its endothelial effects have not, to our knowledge, been described. More had been documented regarding miR-320a in CVD, including endothelial interactions and presence in EMVs (235, 236), although the data centred around chest pain and acute cardiovascular

events(237, 238). Consequently, miR-30d-5p and miR-320a were both chosen in order to characterise this expression profile and fill the knowledge gaps.

MiR-15b-5p showed promise in the selection stage, as an upregulation in plasma from patients with SLE had previously been detected(239), and a potential pathway of angiogenic repression suggested(240, 241), thus inviting the elucidation of the molecular mechanisms underpinning its endothelial effects in SLE. MiR-20a-5p was also selected, as an unpublished preliminary screen had associated it with vascular calcification, a pathology of interest in our group and also prevalent in SLE(242).However, neither of these miRNAs yielded significant data in this study but could be addressed using different models in the future.

4.4.2. The Use of an *In Vitro* Model for Studying MiRNA Abundance

Prior to quantification in patient plasma, miRNA abundance was measured following cytokine treatment of endothelial cells *in vitro*. This was intended to model the inflammatory environment of SLE, and to confirm miRNA presence in EMVs and compare this to intracellular abundance. The low levels of the miRNAs selected prevented full quantification of all except one – miR-320a. Following treatment with TNFα, abundance of miR-320a in endothelial cells decreased significantly, mirroring the situation in patients with SLE described in this chapter. In this way, the inflammatory model appeared to reflect the situation *in vivo*. However, an interesting point was the increase in vesicular miR-320a abundance following the same treatment, potentially indicating a deliberate shuttling of this miRNA into the vesicles for their release. It is unclear whether this is a protective mechanism to rid the cell of a potentially harmful overload or if the miRNA-loaded vesicles serve another purpose, perhaps affecting another cell type; while functional analysis, as in the following chapters, may provide an indication of function, further investigation is needed to define the role of miR-320a in disease, and whether cellular models can accurately reflect patient studies. Nevertheless, this preliminary test confirmed the release of miR-320a in EMVs following inflammatory treatment, supporting progression to *in vivo* studies.

When conducting the *in vitro* experiments, miRNA abundance was analysed relative to control cells, and it was clear that the vesicles isolated would be of endothelial origin as only endothelial cells had been included. This was not the case with the patient studies, as while abundance per ml was the simplest form of analysis, it did not reflect the increase in EMVs detected in the patient group. Accordingly, a housekeeping miRNA was considered, as is often the case in standard qPCR(243). Let-7a was selected for this study as its suitability as a reference gene has been previously considered by other groups (172, 173, 175, 176), however the trend in let-7a abundance in this study did not appear to be constant across participants. Nevertheless, the pattern was not significantly different; it may have been reflective of disease activity or another mechanism not studied here, so analysis relative to let-7a was continued, also to control for small differences in miRNA extracted. There remains a lack of consensus regarding housekeeping genes in miRNA analysis and the validity of using any one gene is questioned by the constantly evolving field(174); let-7a has since been implicated in angiogenesis(244, 245) and therefore, it was decided to further analyse the miRNA abundance per microvesicle. By doing this, another method of control was incorporated, yet it also reflected the fact that microvesicles from other cellular sources would have been present in the plasma, such as PMVs.

4.4.3. Increased Abundance of Key MiRNAs in SLE May Support Biomarker Development

The mode of analysis did not appear to make a difference in analysis of miR-126-3p abundance, as the same pattern was apparent across all methods; significantly increased levels in patients experiencing a disease flare. Consequently, it may be inferred that miR-126-3p abundance is linked to increased disease activity, which is supported by the understanding that this miRNA leads to increased autoreactivity through T cell activation(246). It cannot be known whether the increased inflammation upregulates miR-126-3p abundance or vice versa, but this is an area for further study; it is possible that they perpetuate each other. Indeed, miR-126-3p was associated with increased QRISK score and EMV release, as well as BLyS and IgM levels, and dyslipidaemia as measured by cholesterol ratios. Within patients, it was highest in those with renal disease and those undergoing

medical treatment, further indication of its relationship with active disease. A range of potential targets of miR-126-3p were identified; EGFR had the highest miTG score and is involved in vascular calcification through activation and migration of smooth muscle cells(247). Inhibition of EGFR in a murine model led to attenuated vascular inflammatory responses, smooth muscle cell proliferation and progression of atherosclerosis(248), which suggests the overabundance of this miRNA may be a protective mechanism in the context of SLE.

While miR-3148 abundance in patient plasma was elevated compared to controls, a similar trend was observed in abundance relative to let-7a and per microvesicle. The actual levels of this miRNA were extremely low, yet the difference in detectability between patients and controls demonstrates promise in its use as a biomarker i.e. if it is only detectable in people with SLE. Consequently, abundance correlated with relevant markers of inflammation and cardiovascular risk – QRISK3, EMVs, MCP-1 and ACR count. It also correlated negatively with glucose, implying another role in glucose homeostasis that is beyond the scope of this research. The increase in patients with serositis is interesting and may be significant; alternatively it may simply reflect the exacerbated disease and inflammation. It is also worth stressing that while serositis in SLE often refers to pleurisy, it conjointly encompasses pericarditis at a similar population rate(249); this may be part of the link between miR-3148 and cardiovascular dysfunction. As with miR-126-3p, the upregulation of miR-3148 may be a protective mechanism to counter the damaging inflammation, as inhibition of some of its key predicted targets may preserve vascular integrity and function; the pleotrophic effects of IGF1 are controversial but certain polymorphisms have been implicated in atherosclerosis(250, 251) whereas other studies suggest a beneficial role in angiogenesis(252, 253). Furthermore, inhibition of RUNX2 and MBL2 supports reduced vascular calcification and depressed thrombogenicity(254, 255).

Both of these miRNAs were associated with anticardiolipin antibodies, which have been previously linked to thrombosis and plaque progression, although the immunoglobulin isotype appears important in the potential function of these antibodies. It is interesting to consider why the two miRNAs with increased abundance in SLE demonstrate negative correlations with anticardiolipin antibodies(79, 94), while those that are decreased are also negatively associated. Thus the notion of a miRNA signature encompassing the complexity

of the disease and the contrasting effects of disease and homeostatic processes is supported.

4.4.4. The SLE Signature Contains Key MiRNAs at Reduced Levels

MiR-93-5p abundance was reduced in patients, albeit only when analysing relative to let-7a and per microvesicle. This highlights the difficulty in establishing a mode of analysis that takes into account the increased endothelial activation (and EMV release) in SLE and the necessity for consideration in future biomarker development. These data seem to suggest that while each vesicle (both endothelial and platelet-derived) may contain less miR-93-5p, the general plasma abundance is similar to that of controls due to the cumulative effect of increased microvesicle numbers. The associations with MCP-1, IgM and neutrophils insinuates a link to inflammation but whether this is coincidental or causative is difficult to tell – and if it is causative, is it protective or damaging? Predicted targets such as HIF-1α and MMP2 support the theory of miR-93-5p as atheroprotective(97, 256, 257); in this case, the downregulation of this miRNA in SLE may consequently result in increased inflammation and endothelial dysfunction. The highest ranking predicted target sortilin-1 is a known cardiovascular risk gene, promoting dyslipidaemia through lipoprotein uptake and transport(258). Thus, if miR-93-5p cannot bind and inhibit these targets, due to its own downregulation, patients may be at increased risk of atherogenesis.

Plasma abundance levels of both miR-30d-5p and miR-320a were variable and inconclusive, however miR-30d-5p demonstrated reduced levels in patients, relative to let-7a and per microvesicle, and miR-320a yielded the same per microvesicle only. It is therefore perhaps unsurprising that both were associated with microvesicle number (both EMV and PMV), although miR-30d-5p was also associated with a number of other factors. Negative correlations with cholesterol markers supported its implications in cardiovascular disease, while positive relationships with number of symptomatic years and haemoglobin, as well as negative correlations with white blood cells, affiliated it with disease activity; it is possibly lowest in those with acute or newly identified disease. Yet it appeared to be higher in patients experiencing photosensitivity, which is often one of the first symptoms reported

prior to diagnosis, especially in younger patients(259, 260). Therefore, further investigation is required, including other possible components that may be involved such as vitamin D status (due to sun avoidance/supplementation)(261).

MiR-320a was also implicated in inflammation, yielding a negative correlation with MCP-1. Furthermore, it was the only miRNA to be associated with fibromyalgia, a debilitating condition that will be discussed in chapter 6. Both miRNAs were predicted to target RUNX2 and as such, their downregulation may support the progression of vascular calcification. Consequently, it was hypothesised that their downregulation results in a lack of cardioprotection, which was strengthened by identification of further targets such as beclin-1(262) and BMP receptor 1α(263). The opposite may also be true – that downregulation is cardioprotective – based on the predicted binding of beneficial targets such as SOCS1(264, 265), angiomotin-like protein 2(266), and PRCP(267, 268). Hence, it is clear that improved understanding of these two miRNAs is needed to formulate a theory of action.

Indeed, for all of these miRNAs, the necessary next step is to probe functional effects in an *in vitro* cell model and confirm binding targets, in order to uncover their roles in SLE. It has become apparent that patients with SLE produce a distinct miRNA signature carried around their vasculature by EMVs. Within this signature, levels of individual miRNAs may be greater or smaller than in a healthy population and this holds huge promise for personalised medicine. For example, not only could an 'SLE signature' be used as a biomarker for improved diagnosis and monitoring, but novel therapeutics could also be designed to target the individual miRNAs.

4.5. Chapter Summary

Patients with SLE demonstrate differential expression of a number of vesicular miRNAs compared to healthy controls. This study considered a number of potential methods to measure miRNA abundance, and recognises that the identification of a housekeeping miRNA presents challenges for the future. MiR-126-3p and miR-3148 abundance is

increased in association with increased inflammation and cardiovascular risk, and may be a protective mechanism through binding of harmful targets. Inversely, miR-93-5p is reduced in SLE, concordant with reduced cardioprotection. Both miR-30d-5p and miR-320a appeared to be downregulated, which is possibly a protective mechanism but further investigation is needed. The effects of this miRNA signature on endothelial function will be tested in the following chapters.

Chapter 5

SLE-Specific MiRNA Interrogation of Endothelial Cell Viability and Angiogenic Capacity

5.1. Study Introduction

This chapter describes the evidence in support of the SLE-linked miRNAs, identified in the screen described in chapter 4, as being related to endothelial cell viability and angiogenic capacity. To do so, HUVECs were used as an *in vitro* endothelial cell model, and were transduced with a lentiviral-GFP vector containing the miRNA of interest, as described in methods section 2.6. In this way, the effects of precise overexpression of individual miRNAs on HUVEC function could be elucidated. Cell viability/cytotoxicity was tested and a tube formation assay was used to model the effects of these miRNAs on angiogenesis. By performing such functional testing, it is possible to identify key pathways targeted by individual miRNAs, thus allowing further elucidation of their molecular targets and the mechanisms by which they link to symptomatic disease. Accordingly, this part of the study aimed to characterise the effects of miRNA overexpression on basic endothelial cell function and the objectives were as follows:

- Generate individual lentiviral vectors that overexpress the five key miRNAs and use them to transduce HUVECs in order to test their function in cellular assays.
- Determine the effect of miRNA overexpression on cell viability and migration capability.
- Establish the effect of miRNA overexpression on endothelial tube formation ability.

5.2. Chapter Methodology

MiRNA overexpression constructs were generated as detailed in methods section 2.6; HUVECs were transduced with lentiviral vectors such that they overexpressed individual miRNAs, with successful integration confirmed by fluorescent microscopy and RT-qPCR (80% transduction efficiency). The effect of miRNA overexpression on HUVEC viability was then assessed using alamarBlue, on migration by scratch wound assay and on tube formation by Matrigel® assay, all of which are described in methods section 2.2. Effects of the miRNAs were further compared to control cells, which had been transduced with lentivirus generated with an empty pLL3.7 plasmid containing no miRNA construct.

5.3. Results

5.3.1. Overexpression of MiR-3148 and MiR-320a Increase Cell Viability

Overexpression of both miR-3148 (p=0.020) and miR-320a (p=0.034) appeared to increase cell viability, as assessed by alamarBlue assays, when compared to control cells transduced with the empty pLL3.7 lentivirus (figure 5.1). None of the other miRNAs demonstrated a significant effect (p>0.05; appendix).

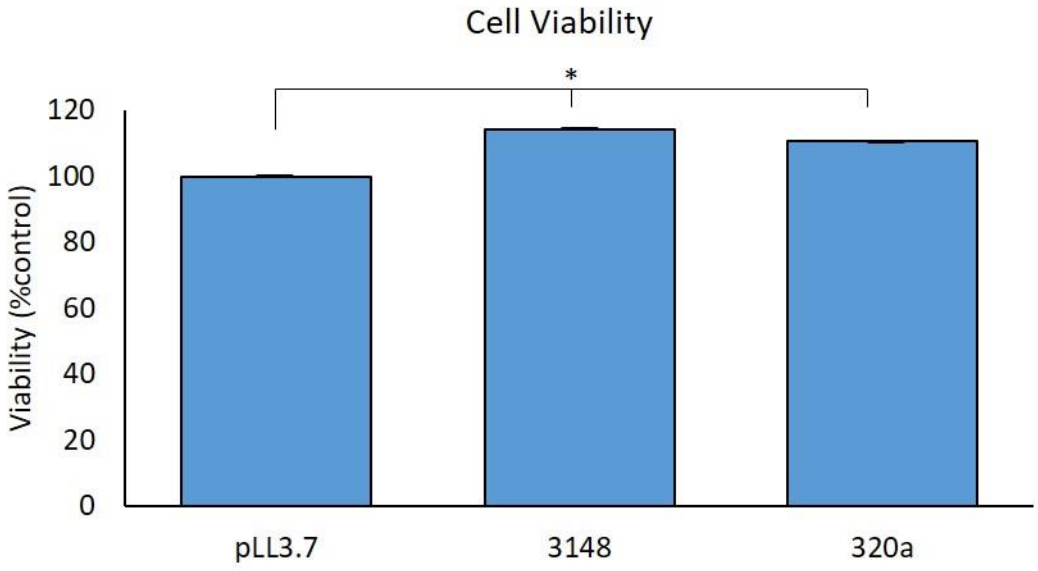

Figure 5.1: Cell viability of transduced HUVECs overexpressing miR-3148 or miR-320a. *HUVECs were transduced with lentiviral vectors containing either miRNA constructs or the empty pLL3.7 plasmid at passage 3 (80% transduction efficiency) and cell viability was tested at passages 4-6. Data shown represent absorbance at 570nm after 24 hours incubation with alamarBlue reagent. Analysis by independent samples t-test condensed into one graph. N=3 in triplicate. * denotes p≤0.05.*

5.3.2. MiRNA Overexpression Does Not Affect Scratch Migration

Cell migration was assessed by HUVECs ability to close a scratch 'wound' bisecting a confluent monolayer, at time points of 0, 5 and 24 hours (figure 5.2). All scratches were fully closed at 24 hours, therefore rate of closure was assessed from 0-5 hours. However, overexpression of all miRNAs tested exerted no significant effects on migratory ability in the scratch model compared to control cells transduced with the empty pLL3.7 lentiviral vector ($p>0.05$; figure 5.3).

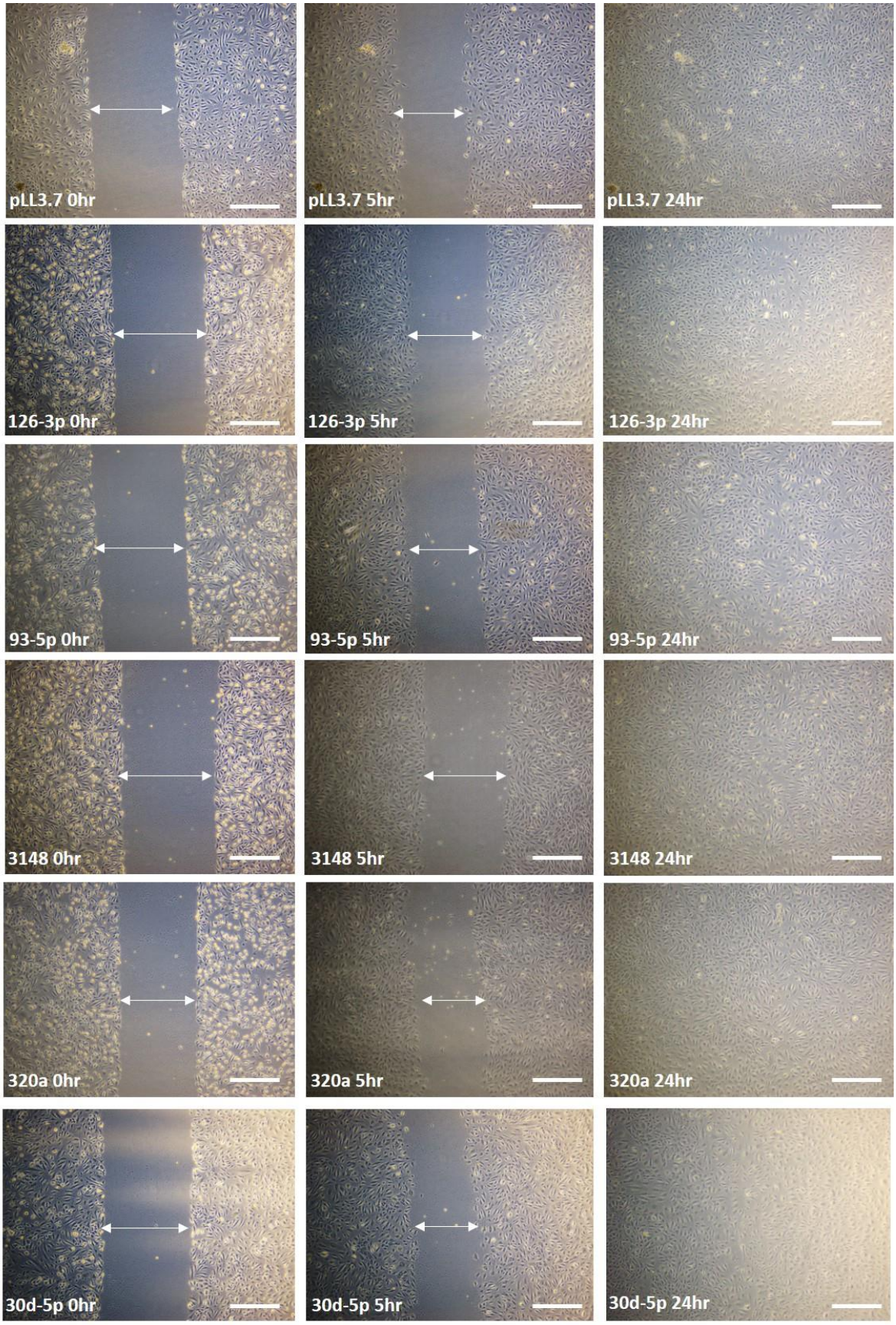
pLL3.7 0hr
pLL3.7 5hr
pLL3.7 24hr
126-3p 0hr
126-3p 5hr
126-3p 24hr
93-5p 0hr
93-5p 5hr
93-5p 24hr
3148 0hr
3148 5hr
3148 24hr
320a 0hr
320a 5hr
320a 24hr
30d-5p 0hr
30d-5p 5hr
30d-5p 24hr

Figure 5.2: Cell migration using a scratch assay. *A scratch wound was created by drawing a p200 pipette tip vertically down a confluent well of HUVECs (p4-5) and representative micrographs are shown at 0, 5 and 24 hours. Cells had previously been transduced with either lentiviral vectors overexpressing the miRNs or the empty pLL3.7 control at passage 3, with 80% transduction efficency. Scale bars represent 100µm. N=3 in triplicate.*

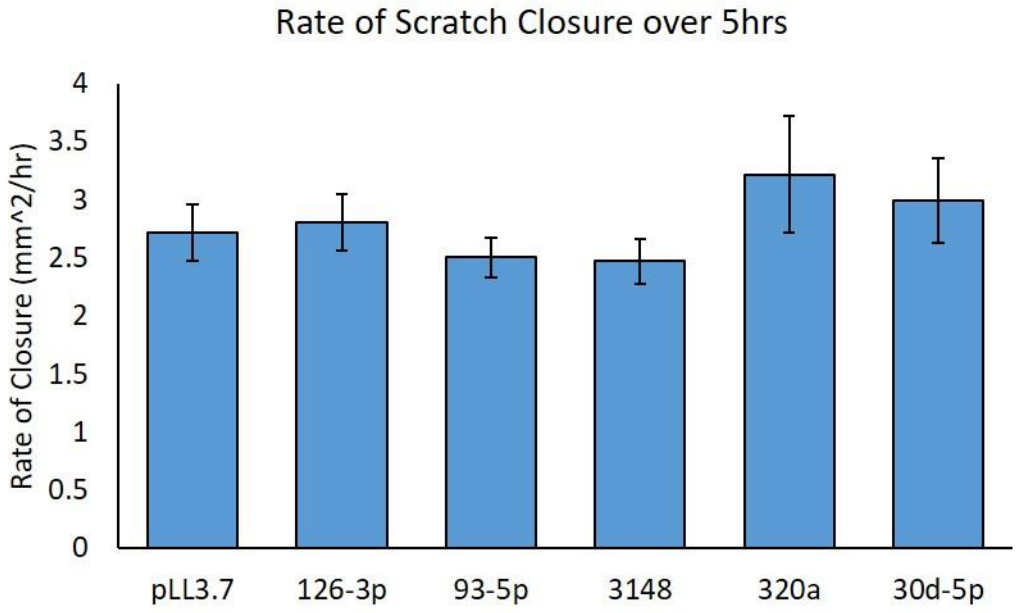

Figure 5.3: Rate of scratch closure over 5hrs. *Scratch closure was analysed in HUVECs (p4-5), which had been transduced with lentiviral vectors containing the five different miRNAs vs empty pLL3.7 vector at passage 3 (80% transduction efficiency). Analysis by one-way ANOVA and verified by independent samples t-test. N=3 in triplicate.*

5.3.3. Overexpression of MiR-93-5p, MiR-320a and MiR-30d-5p Affects Tube Formation in Endothelial Cells

A Matrigel®-based assay was utilised to model angiogenesis following miRNA overexpression by allowing measurement of angiogenic tube formation *in vitro*. A number of parameters were available to analyse, providing miRNA-specific data on angiogenic properties. Overexpression of both miR-93-5p and miR-320a significantly increased average tube length at 5 hours (p=0.038 and p=0.014 respectively), which was maintained at 24 hours (p=0.036 and p=0.035) compared to control cells transduced with empty pLL3.7 vector (figures 5.4 and 5.5).

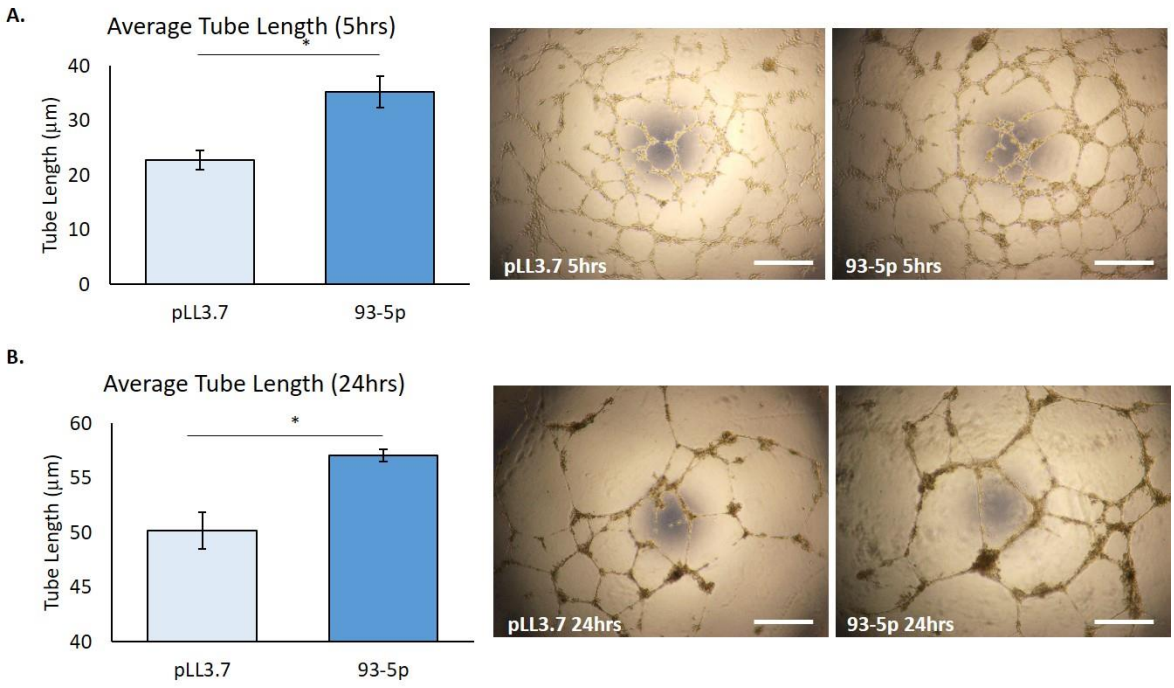

Figure 5.4: Overexpression of miR-93-5p increases angiogenic tube length. *Angiogenesis was tested using a Matrigel®-based tube formation assay, in HUVECs at p4-5, which had been transduced with either the control lentivirus (pLL3.7) or miR-93-5p lentivirus (80% transduction efficiency). Images were taken at 5 (A) and 24 hours (B) following plating. Tube length was measured using ImageJ software and statistical analysis using independent sample t-test. Scale bars represent 100µm. N=3 in triplicate. * denotes p≤0.05.*

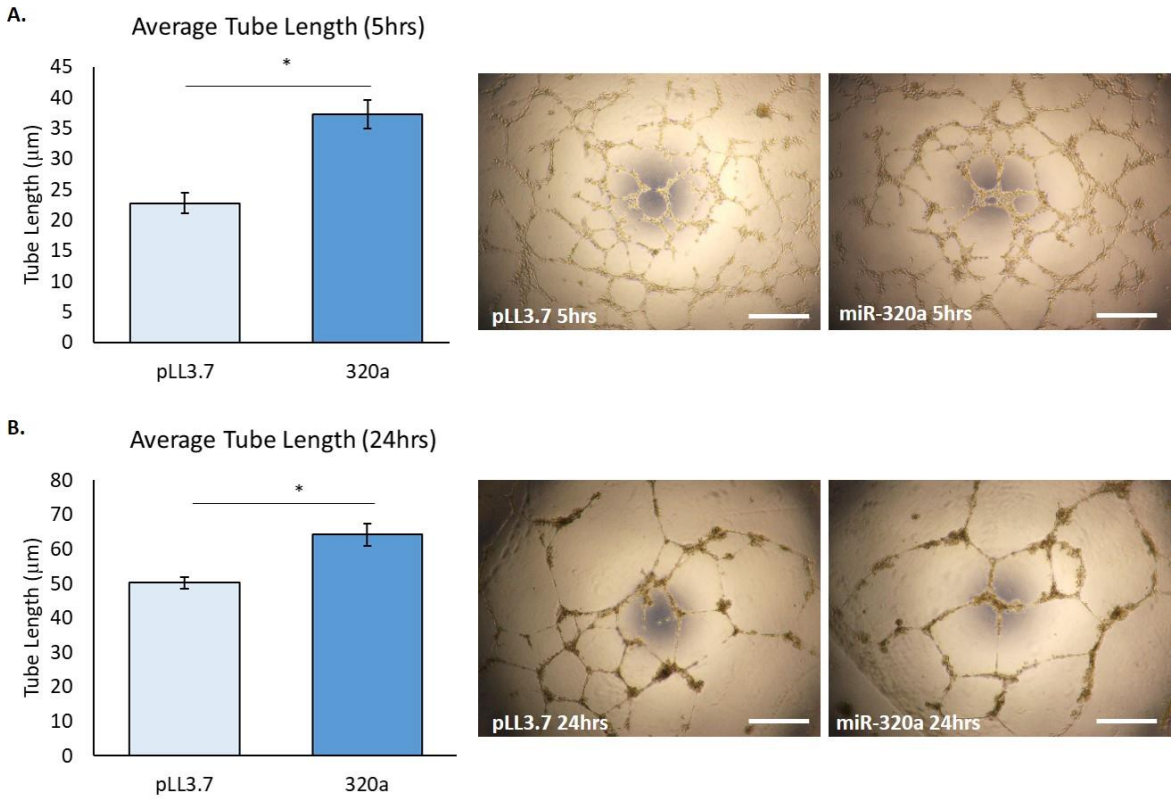

Figure 5.5: Overexpression of miR-320a increases angiogenic tube length. *Angiogenesis was tested using a Matrigel®-based tube formation assay, in HUVECs at p4-5, which had been transduced with either the control lentivirus (pLL3.7) or miR-320a lentivirus (80% transduction efficiency). Images were taken at 5 (A) and 24 hours (B) following plating. Tube length was measured using ImageJ software and statistical analysis using independent sample t-test. Scale bars represent 100µm. N=3 in triplicate. * denotes p≤0.05.*

Alternatively, while tube length was not affected, overexpression of miR-30d-5p yielded a significant decrease in numbers of angiogenic tubes at 5 hours (p=0.025; figure 5.6). However, this was not maintained at 24 hours (p=0.950, data not shown). Overexpression of neither miR-126-3p nor miR-3148 had any notable effect on tube formation (p>0.05; appendix).

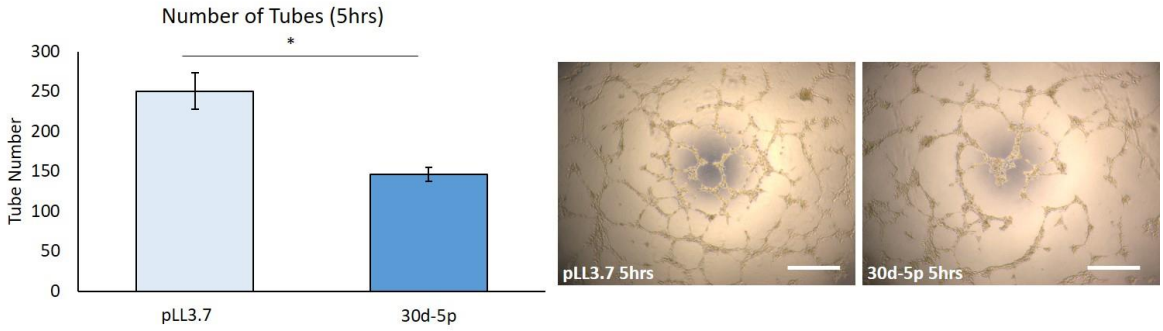

***Figure 5.6: Overexpression of miR-30d-5p decreases angiogenic tube number**. Angiogenesis was tested using a Matrigel®-based tube formation assay, in HUVECs at p4-5, which had been transduced with either the control lentivirus (pLL3.7) or miR-30d-5p lentivirus (80% transduction efficiency). Tubes counted via ImageJ software and statistical analysis made by independent sample t-test. Scale bars represent 100µm. N=3 in triplicate. * denotes p≤0.05.*

5.4. Chapter Discussion

5.4.1. The Effects of MiRNA Overexpression on Endothelial Cell Viability and Mobility

The use of *in vitro* functional testing provides key evidence to the pathways underlying miRNA function, indicating areas of focus for individual miRNAs. To enable this, miRNA overexpression constructs were generated and packaged into lentiviral vectors, which were used to transduce cells such that they overexpressed individual miRNAs. Transduction was successful, with 80% efficiency and GFP expression that was stable for three passages. In this way, an *in vitro* endothelial model of miRNA overexpression was established, supporting the interrogation of miRNA effects on cell function.

The first aspect of cell function to be tested was viability, primarily to ensure the miRNA overexpression constructs were not overtly damaging to the cells. This did not appear to be the case as none of the constructs resulted in a decrease in cell viability. Indeed, overexpression of both miR-3148 and miR-320a improved viability compared to controls, suggesting that overexpression of miR-3148 and miR-320a may increase cell proliferation or longevity, which may be validated in future studies.

Assessing cell migration using a scratch technique did not yield any differences across the miRNAs tested, however, the lack of migratory effects allows refinement of target pathways of interest. This highlights the importance of testing different functional parameters when faced with an extensive list of potential targets.

5.4.2. Assessing Angiogenesis in an Endothelial Model

Angiogenesis is notoriously difficult to model accurately *in vitro,* with critics preferring *in vivo* studies for more representative results. Nevertheless, Matrigel®- based assays are a popular method for *in vitro* assays as the tube formation witnessed in these experiments provides an accurate simulation for the processes observed *in vivo.* The most common method is that used here, in which endothelial cells are plated on a layer of Matrigel®, yet Matrigel® can also be used in 3D culture or to coat microbeads; it has been argued that

these techniques may be more representative of a body system but they face more challenges than the standard method in terms of experimental set up and image analysis(269).

Tube formation assays provide many parameters for analysis; in this study, it was decided to focus on tube number and length as images were analysed manually. Further parameters such as branch points can be analysed using image analysis software; this was attempted but was unsuccessful. It is interesting to note that in the two parameters assessed, miRNAs appear to stimulate different functional effects. Overexpression of miR-93-5p and miR-320a increased tube length at 5 hours and was maintained at 24 hours; this is not associated with increased tube number, which could reflect reduced network complexity and is typically detected in endothelial cells with advanced cellular age(270). However, intra-experimental cell passages were the same nor was cell viability reduced, indeed overexpression of miR-320a increased cell viability. One explanation of this is that miR-93-5p and miR-320a target pathways associated with angiogenic sprouting, meaning tubes may continue to form but are unable to maintain branches.

Network formation also appeared to be deleteriously affected with overexpression of miR-30d-5p, resulting in reduced numbers of tubes. Unlike tube length, tube number has often been used as a marker of angiogenic capacity, with reductions representing impaired angiogenesis(271). Equal numbers of cells were plated and, as before, viability was unaffected, implicating angiogenesis as an area of interest for miR-30d-5p target analysis.

This study has identified key distinct differences in endothelial cells overexpressing different miRNAs, which will be critical in highlighting key pathways affected and thereafter progressing to target identification.

5.5. Chapter Summary

Lentiviral vectors were successfully generated, supporting overexpression of target miRNAs in an endothelial cell model. Overexpression of miR-3148 and miR-320a increased cell viability of HUVECs, although none of the miRNA overexpression constructs affected cell

migration. Overexpression of miR-93-5p and miR-320a increased angiogenic tube length but not tube number, reducing network complexity, while overexpression of miR-30d-5p reduced tube number and thus implied reduced tube formation ability. Key targets affected by SLE-associated miRNAs may be implicated in angiogenesis although further investigation is needed to form a clear picture. The effects of miRNA overexpression on mitochondrial function and fatigue will next be discussed prior to later evaluation of the role of each miRNA in the pathology of SLE.

Chapter 6

Evaluation of SLE-Specific MiRNA Roles in Fatigue and Mitochondrial Dysfunction

6.1. Study Introduction

As discussed in chapter 1, fatigue is one of the most commonly reported symptoms of SLE, negatively affecting quality of life and presenting an unmet clinical need(52, 53). Improved understanding of the mechanisms underpinning fatigue in SLE would greatly contribute to better diagnosis and design of new therapies to improve this aspect of disease, which may also be applicable to other connective tissue disorders, such as fibromyalgia, promoting wellbeing in these patients. Following on from the cellular function tests described in chapter 5, SLE-specific miRNAs were analysed in relation to cellular respiration and associations with clinical fatigue data in an SLE population. It was hypothesised that SLE-specific miRNAs alter mitochondrial function and are associated with symptoms of fatigue, and the objectives were as follows:

- Establish the level of fatigue experienced by controls and patients with SLE.
- Correlate miRNA levels and patient data with clinical fatigue and quality of life scores.
- Determine miRNA associations with self-reported incidence of musculoskeletal symptoms.
- Ascertain the effects of overexpression of miRNAs of interest on HUVEC respiratory function.

6.2. Chapter Methodology

This study utilised the same patient cohort as that described in chapter 4 (14 controls and 25 patients with SLE). Motor and cognitive fatigue levels of the whole cohort were assessed using the FSMC questionnaire, and quality of life scores were recorded, all as detailed in 2.7.2. BILAG scores were also obtained during patient recruitment, although ACR criteria were favoured for analysis in previous chapters; musculoskeletal involvement was recorded during the BILAG assessment, the data of which were used in this study. As per BILAG guidelines, 'musculoskeletal involvement' includes myositis, arthritis, tendonitis, tenosynovitis, arthralgia and myalgia (272). Finally, HUVECs were transduced with lentiviral vectors to overexpress the specific miRNAs, as in chapter 5, to interrogate their effects on cellular respiration using Seahorse Cell Mito Stress assays and gene ontology; more details are found in sections 2.2.5, 2.4.4 and 2.6.2.

6.3. Results

6.3.1. Fatigue Scores are Elevated in SLE, and are Associated with Inflammation and MiRNA Abundance

When analysing fatigue across the cohort, the FSMC questionnaire was separated into motor and cognitive fatigue arms to provide the most specific data; higher scores indicated greater levels of fatigue. Nevertheless, patients with SLE demonstrated significantly greater fatigue scores across all arms compared to controls ($p<0.001$; figure 6.1), regardless of disease activity (stable and flare all $p<0.001$). There were no differences in patients with flared vs active disease (all $p=1.000$).

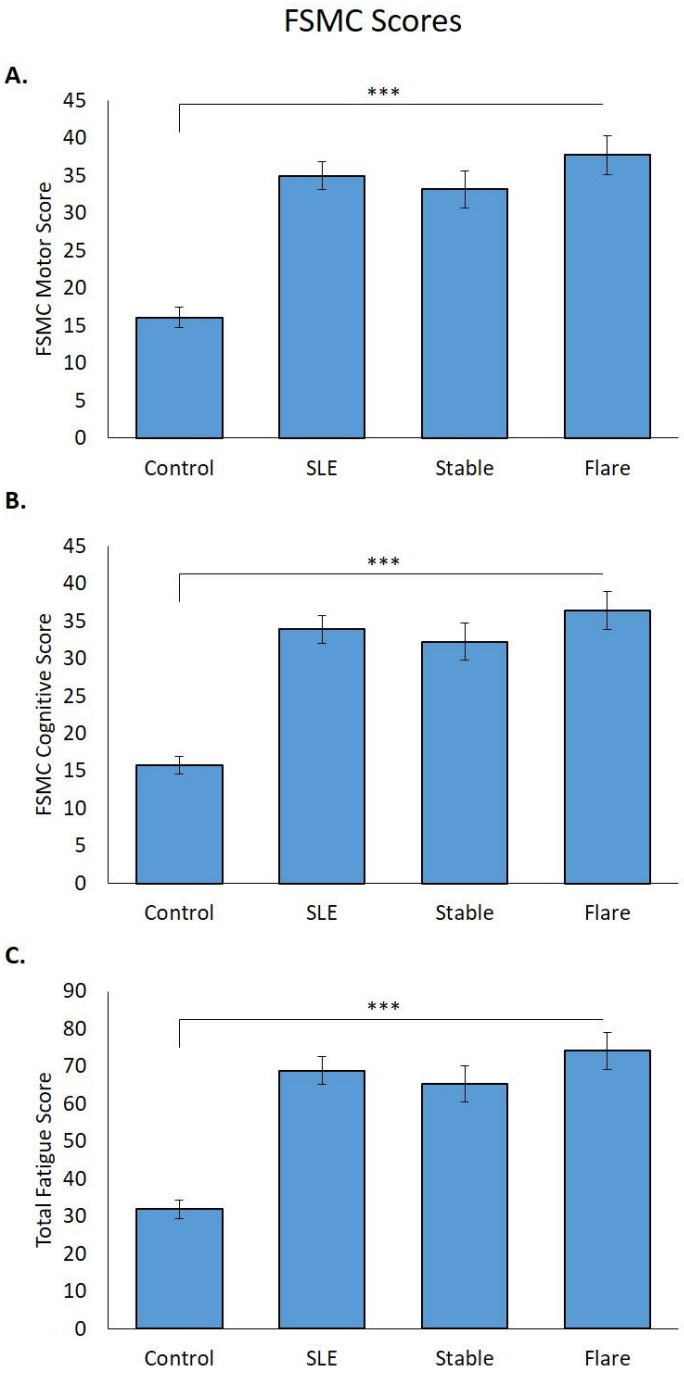

Figure 6.1: Fatigue scores in patients and controls. *Motor (A), cognitive (B) and total fatigue (C) scores were calculated using the FSMC questionnaire. Comparisons between controls and all patients were assessed by Mann-Whitney U test, and between controls and disease activity (stable and flare) by Kruskal-Wallis test. Error bars represent SEM. Control n=14, SLE n=25, stable n=15, flare n=11. *** denotes p≤0.001.*

Motor and cognitive fatigue scores correlated positively with EMV number ($p=0.001$) and QRISK scores ($p<0.02$), as well as IL-6 ($p<0.05$) and BLyS ($p<0.02$) across the whole cohort of participants (table 6.1). Singularly, motor fatigue scores correlated with MCP-1 ($p=0.041$) and PWV ($p=0.009$), whereas cognitive fatigue scores correlated with VEGF ($p=0.044$). Furthermore, motor fatigue scores were elevated in participants with fibromyalgia ($p=0.034$), while cognitive fatigue were highest in participants with a positive family history of hypertension ($p=0.024$). Finally, miR-3148 abundance was positively associated with fatigue scores ($p<0.05$) whereas miR-30d-5p and miR-320a abundance relative to let-7a was negatively associated with motor fatigue ($p<0.05$).

Variable		Motor	Cognition	Total FSMC Score
Age		0.424 **p=0.007**	0.301 p=0.062	0.361 **p=0.024**
QRISK2 Score		0.469 **p=0.003**	0.398 **p=0.012**	0.437 **p=0.005**
QRISK3 Score		0.536 **p<0.001**	0.460 **p=0.003**	0.503 **p=0.001**
$CD144^+$ MVs		0.530 **p=0.001**	0.491 **p=0.001**	0.505 **p=0.001**
VEGF		0.310 p=0.054	0.324 **p=0.044**	0.302 **p=0.062**
MCP-1		0.329 **p=0.041**	0.245 p=0.133	0.283 p=0.081
IL-6		0.379 **p=0.017**	0.330 **p=0.040**	0.365 **p=0.022**
BLyS		0.395 **p=0.013**	0.401 **p=0.011**	0.403 **p=0.011**
PWV		0.424 **p=0.009**	0.304 p=0.067	0.370 **p=0.024**
Diastolic BP		0.347 **p=0.035**	0.364 **p=0.027**	0.389 **p=0.017**
MiR-3148 Abundance		0.514 **p=0.001**	0.436 **p=0.006**	0.468 **p=0.003**
MiR-3148 Abundance per MV		0.328 **p=0.041**	0.244 p=0.134	0.272 p=0.095
MiR-30d-5p Abundance Relative to Let-7a		-0.319 **p=0.048**	-0.245 p=0.133	-0.286 p=0.078
MiR-320a Abundance Relative to Let-7a		-0.362 **p=0.024**	-0.279 p=0.085	-0.320 **p=0.047**
Fibromyalgia	Present (*n=4)* Absent	39.3 ± 10.8 25.9 ± 11.2 **p=0.034**	38.0 ± 11.5 25.3 ± 10.8 p=0.065	77.3 ± 22.3 51.2 ± 21.7 **p=0.039**
Family History of Hypertension	Present (*n=16*) Absent	32.5 ± 9.1 25.2 ± 13.1 p=0.069	31.9 ± 8.5 24.2 ± 12.5 **p=0.024**	64.4 ± 17.2 49.4 ± 25.5 **p=0.022**

Table 6.1: Correlations between FSMC scores, clinical data and miRNA abundance in total cohort. *Data shows the whole cohort (control n=14, SLE n=25), with separate comparisons according to FSMC motor, cognition and total scores. Upper section presents Spearman's rho correlation coefficients; lower section presents mean score (± standard deviation) with statistical analysis using Mann-Whitney U test.*

Within the patient cohort, both motor and cognitive fatigue correlated positively with VEGF levels ($p<0.015$; table 6.2). Motor fatigue alone correlated with total ACR score, lymphocyte number and C3 levels ($p<0.05$), however both fatigue arms correlated with miR-93-5p abundance per MV ($p<0.05$) and cognitive fatigue was further associated with miR-30d-5p abundance per MV ($p=0.048$). Additionally, fatigue scores were elevated in patients experiencing oral ulcers and those with a family history of high cholesterol levels ($p<0.03$) but were lowest in patients with reduced C4 and those with persistent migraines ($p<0.05$).

Variable		Motor	Cognition	Total FSMC Score
ACR Total		0.408 **p=0.043**	0.318 p=0.121	0.376 **p=0.064**
Lymphocytes		0.406 **p=0.044**	0.339 p=0.097	0.362 p=0.075
VEGF		0.540 **p=0.005**	0.483 **p=0.014**	0.479 **p=0.015**
C3		0.442 **p=0.027**	0.340 p=0.097	0.372 p=0.067
MiR-93-5p Abundance per MV		0.407 **p=0.043**	0.467 **p=0.018**	0.429 **p=0.032**
MiR-30d-5p Abundance per MV		0.357 p=0.079	0.399 **p=0.048**	0.374 p=0.066
ACR Criteria: Oral Ulcers	Present *(n=16)* Absent	39.2 ± 8.0 28.3 ± 6.8 **p=0.003**	37.1 ± 8.9 28.2 ± 6.6 **p=0.029**	76.3 ± 16.7 55.7 ± 12.9 **p=0.007**
Low C4	Present *(n=4)* Absent	23.8 ± 2.5 37.1 ± 8.7 **p=0.028**	22.0 ± 3.3 36.1 ± 8.2 **p=0.003**	45.8 ± 4.3 73.2 ± 16.6 **p=0.006**
Family History of Hypercholesterolaemia	Present *(n=13)* Absent	39.8 ± 5.8 29.8 ± 9.8 **p=0.019**	37.8 ± 6.8 29.6 ± 9.5 **p=0.019**	77.6 ± 12.4 60.5 ± 18.9 **p=0.011**
Migraines	Present *(n=4)* Absent	27.0 ± 8.7 36.5 ± 8.8 **p=0.113**	23.5 ± 6.2 35.9 ± 8.3 **p=0.019**	50.5 ± 14.8 72.3 ± 16.8 **p=0.047**

Table 6.2: Correlations between FSMC scores, clinical data and miRNA abundance in patient cohort. *Data are shown with separate comparisons according to FSMC motor, cognition and total scores. Upper section presents Spearman's rho correlation coefficients; lower section presents mean score (± standard deviation) with statistical analysis using Mann-Whitney U test. N=25.*

6.3.2. LQOL Scores are Associated with Markers of Disease as well as Prescribed Medications in SLE

Quality of life in patients with SLE was assessed using the LQOL score, which correlated negatively with both VEGF and C3 levels ($p<0.04$; table 6.3). Quality of life was also lowest in patients with oral ulcers, photosensitivity and those prescribed atypical immunosuppressives (in this case tacrolimus and/or rituximab; $p<0.04$). On the other hand, quality of life scores were highest in patients with low C4 and those prescribed acetylcholinesterase (ACE) inhibitors ($p<0.04$).

Variable		**LQOL Score**	
VEGF		-0.428 **p=0.033**	
C3		-0.496 **p=0.012**	
ACR Criteria: Oral Ulcers	Present (n=16) Absent	34.77 ± 26.32 75.69 ± 14.57	**p=0.002**
ACR Criteria: Photosensitivity	Present (n=20) Absent	42.19 ± 28.56 78.75 ± 14.03	**p=0.019**
Low C4	Present (n=12) Absent	59.38 ± 28.81 40.38 ± 28.34	**p=0.037**
ACE Inhibitors	Present (n=3) Absent	87.50 ± 8.84 44.32 ± 28.20	**p=0.010**
Atypical Immunosuppressives	Present (n=3) Absent	12.50 ± 13.50 54.55 ± 28.15	**p=0.033**

Table 6.3: Associations between LQOL and clinical data in patients with SLE. *Upper section represents data analysed by Spearman's Rank Correlation Coefficient and lower section uses Mann-Whitney U test to show data as mean score (± standard deviation). SLE population n=25.*

6.3.3. MiR-126-3p and MiR-93-5p are Increased in Patients with Musculoskeletal Symptoms

Two of the miRNAs analysed demonstrated associations with self-reported musculoskeletal symptoms in patients with SLE, namely miR-126-3p and miR-93-5p (figure 6.2). Both miRNAs were elevated in patients reporting musculoskeletal symptoms compared to those without (p=0.035 and p=0.008 respectively). Furthermore, abundance of miR-93-5p per microvesicle was also significantly higher in patients with musculoskeletal symptoms (p=0.009); abundance of miR-126-3p per microvesicle demonstrated a trend towards an elevation but was not significant (p=0.056). No other miRNAs tested demonstrated any significant differences between the groups (appendix).

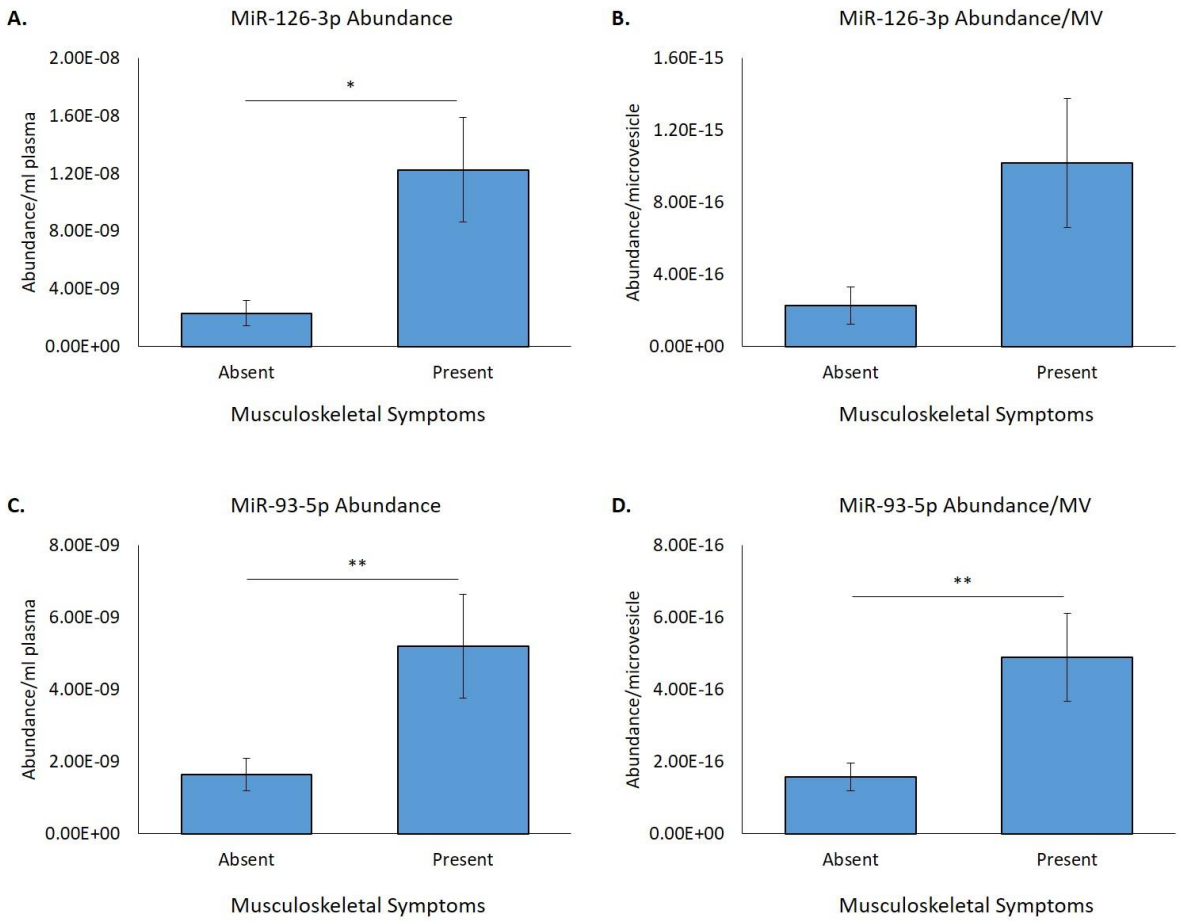

Figure 6.2: The presence of miRNAs alongside musculoskeletal involvement in SLE. *Abundance of miR-126-3p per ml of plasma (A) and per microvesicle (B) was quantified in patients with/without musculoskeletal symptoms, as was abundance of miR-93-5p per ml of plasma (C) and per microvesicle (D). Musculoskeletal symptoms were classed as a BILAG score of C or above (mild to severe symptoms at present time). Analysis was performed using Mann-Whitney U test and SEM. Musculoskeletal symptoms present in 9 patients, absent in 17. Asterisks used denote: * p≤0.05, and ** p≤0.01.*

6.3.4. Overexpression of MiR-126-3p and MiR-93-5p May Impact Cellular Respiration

Seahorse bioanalysis was performed to assess the effects of miRNA overexpression on cellular respiration. MiR-126-3p demonstrated a striking effect (figure 6.3), with increased basal ECAR ($p=0.028$) and trends towards increased maximal ECAR ($p=0.061$) and OCR ($p=0.372$) compared to cells transduced with the control lentivirus (pLL3.7). No difference in basal OCR was evident ($p=0.969$). Similar trends were observed with miR-93-5p, although an n=2 prevented complete statistical analysis. Thus, overexpression of both miRNAs yielded respiratory profiles that were more glycolytic than controls. No significant differences in respiratory effects were detected with the overexpression of the three other miRNAs (miR-3148, miR-320a or 30d-5p) compared to the pLL3.7 control (appendix).

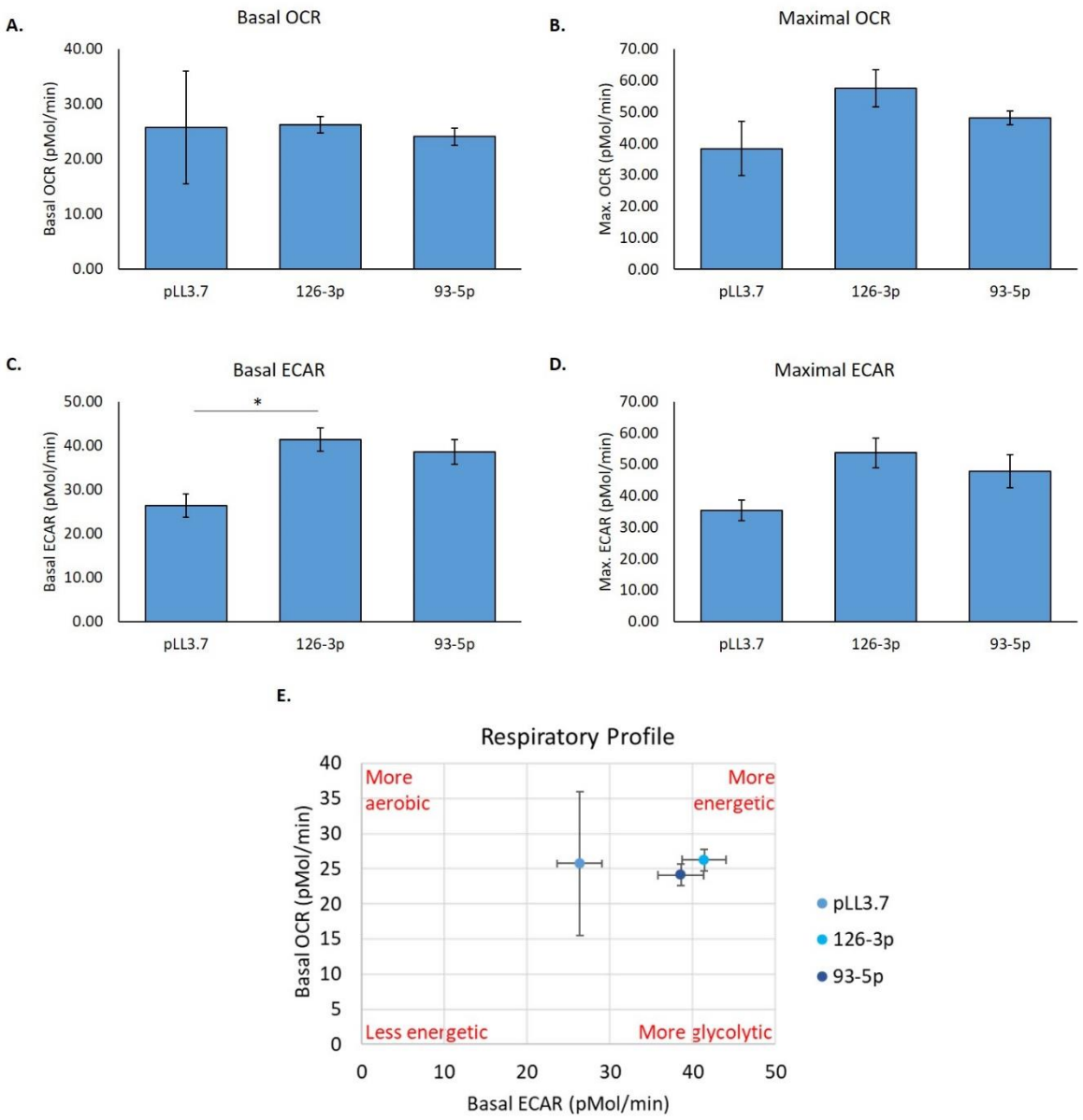

Figure 6.3: Seahorse bioanalysis of respiration in cells overexpressing miRNAs. *HUVECs at p3 were transduced with either lentiviral vectors containing either a miRNA overexpression construct or with a control empty pLL3.7 lentivirus at 80% transduction efficiency. Seahorse bioanalysis was performed using Seahorse Xfp Cell Mito Stress Test, with HUVECs plated at p5-7. Basal OCR (A), maximal OCR (B), basal ECAR (C) and maximal ECAR (D) were recorded, providing a profile of cellular respiration (E). Statistical analysis was performed using independent samples t-test. N=3 in duplicate, n=2 for miR-93-5p constructs. * denotes p≤0.05.*

To identify potential targets for future work, gene ontology was again performed for miR-126-3p, in this case using 'cellular respiration' as a search term. Targets that were also predicted for miRNAs producing no effect during Seahorse bioanalysis were removed, producing the shortlist below (table 6.4). Cytoscape rankings were unavailable for these data, nor is miR-93-5p data described due to the lack of understanding and predicted targets available for that miRNA.

Targets	DIANA miTG Score
NDUFS1	0.992
FXN	0.988
NDUFA9	0.885
NDUFV2	0.821
DLAT	0.764
COX5B	0.704

Table 6.4: Predicted miR-126 targets involved in cellular respiration.

6.4. Chapter Discussion

6.4.1. Fatigue and Quality of Life in SLE

Within the 2014 LUPUS UK study introduced in chapter 1, of 2299 patients with SLE, 91% reported fatigue/weakness(52). Another LUPUS UK study revealed that fatigue was a major contributing factor preventing patients with SLE from maintaining stable employment; of the 399 patients interviewed, 40.45% had left employment due to their disease(273). Cognitive function is also somewhat impaired in SLE, with patients unable to maintain sustained attention for as long a period of time as controls(274, 275). The pathological mechanisms underlying fatigue and cognition in SLE are not yet fully understood, although some structural differences have been noted in brain scans of patients with SLE such as larger perivascular spaces and alterations in the caudate(275).

Assessment of fatigue in SLE presents challenges due to the subjective nature of the data; questionnaires are arguably the most used method, and there are possibly more than 30

in use, with one of the most common being the Fatigue Severity Scale(274). The scales utilised in this study were the FSMC and the LQOL, assessing cognitive and motor fatigue, and patient quality of life. The FSMC tool is most often used in cases of multiple sclerosis, although it is also relevant to SLE(184, 275). In this case, the FSMC was applied rather than the more general Fatigue Severity Scale as it was found to be more comprehensive, providing feedback on both cognitive and motor aspects of fatigue. The lack of a consensus on measurements of fatigue, which are subjective in themselves, highlights a knowledge gap and the potential for consideration of biomarkers as an objective measure of fatigue levels across patients. Quality of life was also assessed to provide additional data on the extent to which SLE affects not only fatigue, but also critical inter- and intrapersonal measures.

When studying fatigue, patients with SLE were found to have higher FSMC scores than controls, supporting previously published data. Scores were also increased in patients with fibromyalgia compared to the rest of the population (controls and patients without fibromyalgia). Again, this is unsurprising as fibromyalgia is another condition characterised by excessive fatigue(276), although these data serve to demonstrate the unmet clinical need for improved recognition of fatigue in these poorly understood diseases.

FSMC scores were able to differentiate between patients and controls using a number of markers. Previous reports have concluded that fatigue does not correlate with disease activity in SLE(274), therefore it is interesting to note the associations with markers of inflammation in this study. The roles of MCP-1, IL-6 and BLyS in SLE have been discussed in previous chapters, and while it is true that they are not representative of disease activity *per se*, fatigue is a common symptom across inflammatory disease(277). Indeed, elevated IL-6 has already been linked to impaired cognitive function in SLE(278) and to fatigue measures in rheumatoid arthritis(277, 279). Cardiovascular factors also correlated with FSMC score; as discussed in chapters 1 and 3, inflammation and cardiovascular disease are interlinked in SLE and the connection between fatigue and cardiovascular measures could be reflective of this. Interestingly, $CD144^+$ EMVs showed a strong positive correlation with FSMC within the whole cohort; again, this could reflect the increased inflammation and endothelial dysfunction, but it also reintroduces the potential for EMVs to act as biomarkers of disease state, in this case fatigue.

Another potential biomarker identified in this study is miR-3148, which correlated positively with fatigue score across the cohort. Chapter 4 described an increase of miR-3148 in SLE yet so little is known about this miRNA that it is difficult to hypothesise whether miR-3148 directly affects fatigue symptoms or is solely a biomarker of underlying disease, a question that necessitates further study. Additionally, the associations between miR-320a and miR-30d-5p and motor fatigue were only present when analysing the miRNAs relative to let-7a, again supporting the use of more detailed miRNA housekeeper-based analysis.

The distinction between motor and cognitive branches of the FSMC allowed identification of separate pathways for future analysis, such as the link between a family history of hypertension and cognitive fatigue. It is interesting to note that the presence of hypertension was not significantly associated but the risk of its development was; a similar finding has been detected in young adults with sleep deprivation, and microvascular changes associated with endothelial dysfunction and hypertension have been known to result in cognitive impairment(280-282). The role of SLE vascular function in cognition will be further considered in the final chapter.

Within the patient only cohort, FSMC score correlated with ACR score, bringing into question the ability of fatigue scores to reflect disease activity, an area which evidently requires further refinement. It also correlated with lymphocyte number, VEGF and C3, reinforcing the association between markers of inflammation and fatigue symptoms. Furthermore, increased levels of VEGF could begin to explain the higher incidence of oral ulcers in patients with fatigue, as the VEGF pathway has been previously linked to mucosal ulceration in SLE(283). Oral ulceration is a factor in the ACR diagnostic criteria for SLE, thus its association with fatigue could be as a result of a disease flare; alternatively the presence of fatigue could have triggered or exacerbated ulceration(284). On the other hand, low levels of C4 was associated with reduced fatigue, which has already been noted in cases of chronic fatigue syndrome(285). Intriguingly, fatigue was increased in patients with a positive family history of hypercholesterolaemia but yielded no connection to patient lipid levels or statin use – the role of genetics in diseases characterised by high fatigue levels would be an interesting area for further study. As with hypertension, familial hypercholesterolaemia has been associated with cognitive impairment, most likely through microvascular dysfunction(286, 287). The incidence of migraine is relatively common in SLE

and may indicate structural differences in the brain that could contribute to fatigue(275, 288).

Regarding miRNAs as biomarkers, miR-93-5p correlated with measures of fatigue in patients with SLE, which may be related to its associations with musculoskeletal symptoms, as discussed below. MiR-30d-5p abundance was also associated with cognitive fatigue in SLE; the role of miRNAs in cognitive function is a fascinating area that will be considered in the proceeding future work section.

As with fatigue, reduced quality of life was associated with inflammation and disease activity (VEGF, C3, C4, oral ulcers and photosensitivity). Although the n numbers were small, quality of life appeared to be highest in patients taking ACE inhibitors and lowest in those taking non-standard immunosuppressives. This may reflect better disease management and symptomatic relief in patients taking typical medication as opposed to those needing stronger treatments.

6.4.2. The Role of MiRNAs in Musculoskeletal Symptoms in SLE

The next stage of this project utilised the BILAG data recorded at the time of patient recruitment, particularly the reporting of musculoskeletal symptoms. It became apparent that both miR-126-3p and miR-93-5p were increased in the circulation of patients reporting musculoskeletal involvement, which is striking as these miRNAs were also shown to perturb mitochondrial function *in vitro*. It appears obvious that if energy production is impaired, patients may experience fatigue, particularly motor fatigue or muscular weakness, as muscle tissue is mitochondria-dense(289). Impairments in mitophagy or mitochondrial function are present in myopathic diseases, including the autoimmune disease dermatomyositis, which shares with SLE a high involvement of type 1 IFNs and ROS(289, 290). However, it is clear that the two miRNAs must play different roles in fatigue in SLE as they follow opposite expression patterns and have different predicted targets. miR-126-3p is increased in SLE and thus any induced mitochondrial dysfunction may then contribute to the musculoskeletal symptoms. Alternatively, the overexpression of miR-126-3p could be an attempted salvage mechanism, although at this point it appears more likely that the

downregulation of miR-93-5p in SLE is protective. This is supported by the trend towards *in vitro* mitochondrial dysfunction combined with the increased musculoskeletal symptoms in patients with higher levels. Identification of the mitochondrial targets of miR-126-3p and miR-93-5p, as described earlier, would assist in identification of the pathological pathways underlying mitochondrial dysfunction and fatigue in SLE. Additional studies could focus on physiological testing of muscle function in patients to further differentiate symptoms, characterise cellular changes and relate this to miRNA function.

6.4.3. Do MiRNAs Protect or Damage Mitochondria in SLE?

Seahorse bioanalysis provides data on oxygen consumption and extracellular acidification rates, which respectively represent mitochondrial respiration and glycolysis, allowing detailed analysis of cellular energy metabolism. Unfortunately, OCR measurements were highly variable, particularly in control wells, and only an n=2 was available for miR-93-5p thus preventing statistical analysis. Nevertheless, this technique identified differences in energy profiles between HUVECs overexpressing miR-126-3p and controls, specifically an increase in ECAR when overexpressing the miRNA. Thus, when comparing respiratory profiles, cells overexpressing miR-126-3p appeared to favour more glycolytic pathways, potentially indicating a mitochondrial defect. In recent years, numerous groups have begun to consider cellular respiration in SLE, often focusing on leukocytes. The high incidence of inflammation and ROS accumulation, combined with disease-specific impairments in mitophagy and clearance of debris appears to reduce mitochondrial efficiency, which may warrant a switch towards glycolytic ATP production(291-293).

Gene ontology identified a number of potential miR-126-3p targets involved in cellular respiration, with unique targets being frataxin, dihydrolipoamide s-acetyltransferase and subunits of NADH:ubiquinone oxidoreductase and cytochrome c oxidase. Of these, all are found within the mitochondria (data from OMIM online catalogue of human genes) and have critical roles in respiration, which may lead to poor mitochondrial function when perturbed, for example reductions in frataxin or cytochrome c oxidase result in increased mitochondrial damage and a glycolytic shift respectively(294, 295). The mitochondrial

impairments could then result in fatigue symptoms; these links between miRNAs and fatigue symptoms have not yet been characterised, presenting fascinating new avenues for further study.

6.5. Chapter Summary

MiR-126-3p and miR-93-5p appear to increase glycolytic respiration *in vitro*, implying functional responses to mitochondrial dysfunction; they are also associated with musculoskeletal symptoms in patients with SLE, potentially presenting a link between cellular respiration and motor fatigue in this disease. Fatigue is indeed increased in patients with SLE, and is associated with markers of inflammation and cardiovascular disease. MiRNAs are also positively associated with fatigue levels, demonstrating potential as novel biomarkers of fatigue, a large unmet clinical need in autoimmune rheumatic diseases.

Chapter 7

Discussion and Conclusions

7.1. Discussion

7.1.1. AIM 1: Identification of Novel Biomarkers for Cardiovascular Risk in SLE

It is now clear that patients with SLE demonstrate increased levels of inflammatory and cardiovascular risk markers, which moves towards explaining the accelerated atherosclerosis, endothelial dysfunction and cardiovascular risk introduced in chapter 1. It is vital that this increased risk is recognised in order to prevent premature mortality and support patient wellbeing, however CVD risk algorithms differ in accuracy when compared to each other and also when used in different populations(114, 115). The discordance in risk score in SLE can be abrogated by inclusion of SLE factors(123, 296); indeed, this body of work identified a significant cohort of patients that had been missed by the current system. Missed patients were found to have higher levels of inflammation and cardiovascular factors, thus it can be construed that the QRISK3 algorithm is more representative of cardiovascular risk in SLE than its predecessors. It may be argued that this is obvious, as other algorithms do not include SLE as a factor, yet this only strengthens the argument of using QRISK3 to predict SLE cardiovascular risk. Nevertheless, the design of cardiovascular algorithms for risk prediction must also be questioned – can one algorithm reflect all intrapersonal differences and should one global algorithm be used? With the growing understanding of unique traits and epigenetics, it is difficult to conceive of a

universal calculation that applies to all, however the combination of prediction algorithms and biomarker panels shows great potential for personalised medicine.

In a recent publication, Felten *et al.* list the identification of relevant biomarkers for individualised treatment as one of the top 10 biggest challenges faced when managing SLE(297). Although biomarker panels consisting of circulating factors such as cytokines are under investigation by other groups(298), this research focused on EMVs as novel biomarkers for cardiovascular risk. Their use as such was supported by their associations with QRISK3 and other markers of cardiovascular and inflammatory disease. Furthermore, by being released directly from the endothelium, they more accurately reflect endothelial involvement than a panel of systemic cytokines would. Isolation and quantification of microvesicles is also relatively simple following protocol optimisation, and can be performed from a small volume of peripheral blood using only a centrifuge and a flow cytometer. Thus, EMVs provide promising alternatives to lengthy and complex biomarker panels for future characterisation of cardiovascular risk.

7.1.2. AIM 2: Determination of a Vesicular MiRNA Signature in Patient Plasma

Personalised medicine may be the key to management of heterogeneous diseases such as SLE and this was one reason why the contents of EMVs were probed in patients vs controls; another reason was that interrogation of functional effects may reveal mechanisms and novel targets for future therapies. MiRNAs were chosen over other contents due to their bioactivity and relative novelty, with their effects in SLE still uncharacterised.

Many studies have aimed to quantify miRNA abundance in CVDs and in SLE but a consensus panel is still lacking, with studies presenting conflicting results obtained from various different bodily fluids and cellular origins. This research study took a more measured approach, identifying key miRNAs through a bioinformatics workflow and analysing this core panel in the microvesicular fraction of plasma. The miRNAs were correlated with clinical measurements, in line with their potential use as biomarkers, before gene ontology and functional analysis, which will be discussed next. By doing this, a detailed picture began

to emerge, a snapshot of the complex interactions between vesicular miRNAs and the endothelium in SLE. Ideally, one miRNA would have been identified as a definitive biomarker and leading area of future research; however, the data proved to be more complex, indicating a number of potential molecular mechanisms and avenues for future study. This complexity reflects the numerous clinical symptoms observed in SLE and highlights the need for a more detailed understanding of their interaction, supporting a personalised medicine strategy to diagnose and treat SLE.

7.1.3. AIM 3: Elucidation of Functional Effects of SLE-Related MiRNAs in Endothelial Cells

Potential roles for each miRNA in the SLE panel were interrogated by combining the data produced in chapters 4-6. To do so, overexpression of each miRNA was modelled *in vitro* using lentiviral vectors in endothelial cells. These vectors are one of the most commonly used methods for investigating miRNA overexpression since they integrate into the genome of cells, thus maintaining higher and more prolonged levels of expression than more traditional methods such as miRNA mimics(299, 300). A number of *in vitro* tests followed, designed to assess endothelial cell function across a range of parameters to further characterise miRNA function, as discussed below.

7.1.3.1 The Role of MiR-126-3p in SLE

MiR-126-3p was elevated in patients experiencing a disease flare but this was not the case in stable patients, suggesting a possible link with disease activity, which was supported by correlations with the QRISK scores, EMV number, renal disorder and the use of immunosuppressives. A range of potential targets were identified, yet overexpression in endothelial cells produced an effect only when analysing cellular respiration where it induced a glycolytic shift. Thus, potential targets involved in mitochondrial function are of the most interest, such as frataxin and cytochrome c oxidase. Similar results have been noted in cancer cells(301), although the effect of miR-126-3p on mitochondria in CVD or

SLE is highly novel. If the overabundance of miR-126-3p in SLE flares did contribute to mitochondrial dysfunction, this may begin to explain the overabundance in patients with musculoskeletal symptoms such as myalgia, otherwise this finding may simply be utilised to further support the concept of miR-126-3p as an indicator of increased disease activity. Either way, its associations with SLE disease activity are striking and analysis of its mitochondrial targets and effects on other cell types will help to elucidate whether its effects are an attempt at protection or if they are damaging, with potential as a therapeutic target.

7.1.3.2 The Role of MiR-3148 in SLE

Very little was known regarding miR-3148 prior to this research, which found it to be increased in SLE and associated with cardiovascular risk. In lentiviral vector miR-3148 overexpression studies, although the levels of transduction efficiency were the same as for other miRNA containing lentiviral vectors, miR-3148 was not produced at the same high levels, suggesting that it is not expressed readily in endothelial cells or that levels were simply too low for accurate quantification. MiR-3148 correlated positively with FSMC levels, which may support its use as a biomarker for fatigue/disease activity, yet had no effect on HUVECs in terms of tube formation or mitochondrial function, but had a positive effect on viability, which necessitates further study. Many of its predicted targets were associated with vascular calcification, such as RUNX2. Indeed, unpublished work by our group has recently demonstrated that overexpression of miR-3148 resulted in decreased calcification of vascular smooth muscle cells *in vitro,* alongside reduced RUNX2 abundance, and is under further investigation. Thus, it may be that this miRNA plays a greater role in vascular smooth muscle cells, where it may offer vasculoprotection in SLE.

7.1.3.3 The Role of MiR-93-5p in SLE

Unlike miR-3148, miR-93-5p appeared to be more active in the studies presented, with overexpression in HUVECs resulting in impaired tube formation and a trend towards a glycolytic shift. The concurrent reduction in miR-93-5p abundance in patients with SLE thus suggests a protective mechanism, designed to prevent the destructive properties of this miRNA when it is overly abundant. It is interesting to consider the negative correlations with microvesicles, neutrophils and MCP-1, reinforcing the theory that this miRNA is purposefully downregulated in periods of inflammation. The increased abundance of miR-93-5p in patients with musculoskeletal symptoms and positive correlation with FSMC score supports the notion of this miRNA as damaging yet further study is needed to elucidate its potential role in fatigue.

7.1.3.4 The Role of MiR-320a in SLE

The abundance of miR-320a appeared to demonstrate a contrasting pattern in microvesicles generated *in vitro* compared to those isolated from patient plasma, emphasising the difference between cellular and human models. However, abundance in patients was only significantly lower than controls when expressed per microvesicle, therefore it is possible that more miR-320a is shuttled into microvesicles (as *in vitro*) but the increased number of vesicles masks this. Overexpression appeared to increase cell viability but also impaired tube formation. Furthermore, abundance was associated with incidence of fibromyalgia and FSMC score. Thus, the role of miR-320a appears complex and unclear; abundance per microvesicle may be reduced but if more microvesicles contain miR-320a and consequently interact with cells, this may lead to deleterious effects e.g. impaired angiogenesis and fatigue. Pathway and mechanistic analysis will enable further characterisation of the role of this miRNA, as discussed in 7.3.

7.1.3.5 The Role of MiR-30d-5p in SLE

The final miRNA to be studied was miR-30d-5p, which was reduced in SLE concurrent with disease activity, as indicated by negative correlations with EMV number, white blood cells and disease duration. A range of potential targets were identified and it is possible that this miRNA demonstrates pleiotrophic effects as overexpression reduced angiogenic tube number while plasma abundance was associated with fatigue. As with miR-93-5p, the reduction in SLE may be a protective mechanism, preventing angiogenic impairments. It is therefore interesting to note the positive correlation between reduced abundance per microvesicle and low cognitive fatigue score, and to determine in future work whether overabundance of miR-30d-5p is detrimental to pathways involved in cognition. Summary table 7.1. highlights the key findings generated by our laboratory regarding miRNA activity in SLE, which will be used to design future experiments.

MiRNA	Abundance in SLE	Key Effects of Overexpression *In Vitro*
MiR-126-3p	Increased in flares	Glycolytic shift in HUVECs
MiR-3148	Increased in SLE	Decreased calcification of VSMCs and reduced RUNX2 abundance
MiR-93-5p	Reduced in SLE	Reduced angiogenic tube length and trend towards glycolytic shift in HUVECs
MiR-320a	Reduced in SLE	Reduced angiogenic tube length and increased viability in HUVECs
MiR-30d-5p	Reduced in SLE	Reduced angiogenic tube number

Table 7.1. MiRNA summary table. *This table highlights key findings from our group regarding miRNA abundance in SLE and the effects of miRNA overexpression on in vitro cells models, which will be used to direct further study.*

7.2. Limitations and Considerations

While this research has been successful in achieving its aims, a review of its limitations and aspects for consideration provides useful insights for future work.

When studying the SLE and control cohorts, a larger population size would ensure greater representation and more accurate statistical analysis. In this instance, patient population size was limited due to availability – many patients treated at the Kellgren Centre for Rheumatology were already enrolled in other research studies such as drug trials, and were therefore unavailable. However, this was not deemed to limit interpretation of results as similar studies with smaller population sizes have previously been published(157, 158). Longitudinal studies would also be very interesting when considering the changes in EMV number, miRNA abundance and cardiovascular risk over time, but this was not feasible during the current project.

The research in question focused on EMVs yet microvesicles can be isolated from a number of cell types, therefore it would be interesting to consider circulating microvesicles of other origins, such as PMVs. These were discussed in chapter 4 but could also be probed for miRNAs in further work. Another factor to consider is the number and miRNA content of circulating exosomes, which were removed in this project, yet could enhance understanding of the SLE miRNA profile. Furthermore, although the methods for EMV isolation and quantification used in this work have been validated elsewhere, a consensus on EMV characterisation, as well as the preceeding considerations, must be determined before biomarker technology featuring EMVs can be developed. Such technology would ideally be quick, cheap and preferably automated to enable rapid patient stratification in a busy clinical environment; establishment of a further research project to address these issues is thus recommended prior to clinical use.

Difficulties arose when comparing miRNA abundance, firstly when optimising quantification from plasma samples and *in vitro*, which could be improved through development of a method to detect miRNAs at low abundance. A measured approach for selecting and quantifying miRNAs by qPCR was taken for this project, although it would also be possible to perform a larger scale screen followed by production of a shortlist based on the levels of miRNAs identified in the samples. It is worth noting that next generation sequencing was attempted early in the project but was unsuccessful due to the low abundance of RNA isolated from microvesicle samples as only 1ml of total plasma was available in this cohort for analysis. Furthermore, a defined method of analysing miRNA abundance would support improved comparisons across studies; while spiked controls

ensure accurate quantification, the identification of a 'housekeeper' miRNA would greatly enhance analysis based on human samples or between different conditions *in vitro*.

The final limitations pertain to functional analysis of miRNA activity *in vitro*. This research characterised the effects of miRNA overexpression on endothelial cells, however supplementing this with an underexpression model would further refine and support the conclusions drawn. Indeed, miRNA sponges were generated(302) but were discontinued due to a lack of efficacy. Other alternatives include antagomiRs(303) or gene knockouts, which will be considered in 7.3. Lastly, the functional tests employed in this project were selected to represent a range of cellular processes integral to endothelial function during basal conditions. Nevertheless, additional tests such as NO measurements or endothelial function in response to inflammatory treatment would provide further detail and act as an *in vitro* model of the endothelium in an inflammatory disease such as SLE. N numbers in future tests such as these could be increased to support statistical analysis and reduce variability.

7.3. Future Directions

This work offers many avenues for further study, starting with the development of miRNA silencing models to characterise the functional effects of miRNA underexpression *in vitro*. Following this, pathway and target analysis will be necessary for elucidation of the mechanisms identified during the functional testing. To do so, transcriptome analysis will be combined with pathway recognition software to identify key processes affected by the miRNAs. Individual targets can also be confirmed using, for example, luciferase reporter constructs, which allow identification of miRNA-target binding through luciferase

production(304); a luciferase reporter construct was attempted during the course of this project, but was unsuccessful.

An emerging area of particular interest is the role of EMVs and miRNAs in fatigue in SLE, as introduced in this project through correlations with fatigue scores and functional effects on cellular respiration. This could separate into two branches, studying motor fatigue through e.g. muscle testing, or cognitive function, which has been highlighted numerous times in this thesis as a major unmet need in SLE. When studying fatigue and cognitive function in SLE, the blood brain barrier (BBB) is a fascinating interface between the vascular endothelium and the nervous system, having already been associated with fatigue and impaired cognition in inflammatory diseases such as SLE(305-307). Therefore, full characterisation of the effects of the SLE environment on the BBB, including EMV trafficking and miRNA functions would shed light on an ongoing and underresearched area, providing novel avenues for therapeutic research.

The overarching aim of this project was to *establish whether EMVs can be added to the armament of risk factors used for identifying patients with SLE at elevated risk of future cardiovascular events.* By combining EMV levels with risk algorithms and miRNA abundance, the development of more a comprehensive stratification tool will support identification of future patients with high cardiovascular risk. One way to do this in future studies would be to utilise an artificial intelligence approach to provide personalised reports relevant to each patient and acknowledge the heterogeneous nature of SLE. In doing so, patients with SLE will be able to receive tailored treatment and monitoring plans, preventing premature mortality and improving quality of life.

7.4. Concluding Statements

Patients with SLE demonstrate increased levels of inflammation and cardiovascular risk, which is represented by the QRISK3 algorithm and by circulating numbers of EMVs. A distinct miRNA signature is present in the vesicular fraction of patient plasma, with individual miRNAs associated with measures of inflammation and cardiovascular risk. *In vitro* functional testing has characterised the effects of individual miRNA overexpression on endothelial cells, identifying key areas for future study such as fatigue and angiogenesis.

To conclude, EMVs demonstrate great potential for use as biomarkers of cardiovascular risk in SLE and provide novel avenues for further research through their miRNA content.

Chapter 8

References

1. BHF. Heart and Circulatory Diseases Statistics Factsheet 2018 2018 [Available from: https://www.bhf.org.uk/what-we-do/our-research/heart-statistics.

2. WHO. Cardiovascular Diseases (CVDs) Factsheet 2017 [Available from: http://www.who.int/mediacentre/factsheets/fs317/en/.
3. PHE. Public Health Profiles: Cardiovascular Disease 2019 [Available from: https://fingertips.phe.org.uk/profile/cardiovascular.
4. Lu D, Kassab GS. Role of shear stress and stretch in vascular mechanobiology. J R Soc Interface. 2011;8(63):1379-85.
5. Godo S, Shimokawa H. Endothelial Functions. Arterioscler Thromb Vasc Biol. 2017;37(9):e108-e14.
6. Liao JK. Linking endothelial dysfunction with endothelial cell activation. The Journal of Clinical Investigation. 2013;123(2):540-1.
7. Moroni L, Selmi C, Angelini C, Meroni PL. Evaluation of Endothelial Function by Flow-Mediated Dilation: a Comprehensive Review in Rheumatic Disease. Arch Immunol Ther Exp (Warsz). 2017;65(6):463-75.
8. Gimbrone MA, García-Cardeña G. Endothelial Cell Dysfunction and the Pathobiology of Atherosclerosis. Circulation research. 2016;118(4):620-36.
9. Wilck N, Ludwig A. Targeting the ubiquitin-proteasome system in atherosclerosis: status quo, challenges, and perspectives. Antioxid Redox Signal. 2014;21(17):2344-63.
10. De Caterina R, Libby P, Peng HB, Thannickal VJ, Rajavashisth TB, Gimbrone MA, Shin WS, Liao JK. Nitric oxide decreases cytokine-induced endothelial activation. Nitric oxide selectively reduces endothelial expression of adhesion molecules and proinflammatory cytokines. J Clin Invest. 1995;96(1):60-8.
11. Wang Y, Cui L, Xu H, Liu S, Zhu F, Yan F, Shen S, Zhu M. TRPV1 agonism inhibits endothelial cell inflammation via activation of eNOS/NO pathway. Atherosclerosis. 2017;260:13-9.
12. Zhou J, Li YS, Chien S. Shear stress-initiated signaling and its regulation of endothelial function. Arterioscler Thromb Vasc Biol. 2014;34(10):2191-8.
13. Lai B, Li Z, He M, Wang Y, Chen L, Zhang J, Yang Y, Shyy JY. Atheroprone flow enhances the endothelial-to-mesenchymal transition. Am J Physiol Heart Circ Physiol. 2018;1(315(5)):H1293-H303.
14. Harding IC, Mitra R, Mensah SA, Herman IM, Ebong EE. Pro-atherosclerotic disturbed flow disrupts caveolin-1 expression, localization, and function via glycocalyx degradation. J Transl Med. 2018;16(1):364.
15. Carallo C, Tripolino C, De Franceschi MS, Irace C, Xu XY, Gnasso A. Carotid endothelial shear stress reduction with aging is associated with plaque development in twelve years. Atherosclerosis. 2016;251:63-9.
16. Timmins LH, Molony DS, Eshtehardi P, McDaniel MC, Oshinski JN, Giddens DP, Samady H. Oscillatory wall shear stress is a dominant flow characteristic affecting lesion progression patterns and plaque vulnerability in patients with coronary artery disease. J R Soc Interface. 2017;14(127).
17. Luo Y, Duan H, Qian Y, Feng L, Wu Z, Wang F, Feng J, Yang D, Qin Z, Yan X. Macrophagic CD146 promotes foam cell formation and retention during atherosclerosis. Cell Res. 2017;27(3):352-72.
18. Wang R, Zhang Y, Xu L, Lin Y, Yang X, Bai L, Chen Y, Zhao S, Fan J, Cheng X, Liu E. Protein Inhibitor of Activated STAT3 Suppresses Oxidized LDL-induced Cell Responses during Atherosclerosis in Apolipoprotein E-deficient Mice. Sci Rep. 2016;6:36790.
19. Lara-Guzmán OJ, Gil-Izquierdo Á, Medina S, Osorio E, Álvarez-Quintero R, Zuluaga N, Oger C, Galano JM, Durand T, Muñoz-Durango K. Oxidized LDL triggers changes in

oxidative stress and inflammatory biomarkers in human macrophages. Redox Biol. 2018;15:1-11.
20. Barter P, Gotto AM, LaRosa JC, Maroni J, Szarek M, Grundy SM, Kastelein JJ, Bittner V, Fruchart JC. HDL cholesterol, very low levels of LDL cholesterol, and cardiovascular events. The New England journal of medicine. 2007;357(13):1301-10.
21. Rye K, Bursill C, Lambert G, Tabet F, Barter P. The metabolism and anti-atherogenic properties of HDL. J Lipid Res. 2009;50:S195-S200.
22. Feig JE, Feig JL, Dangas GD. The role of HDL in plaque stabilization and regression: basic mechanisms and clinical implications. Coron Artery Dis. 2016;27(7):592-603.
23. Ma A, Wang J, Yang L, An Y, Zhu H. AMPK activation enhances the anti-atherogenic effects of

high density lipoproteins in apoE-/- mice. J Lipid Res. 2017;58(8):1536-47.
24. Hao W, Friedman A. The LDL-HDL profile determines the risk of atherosclerosis: a mathematical model. PLoS One. 2014;9(3):e90497.
25. Nordestgaard BG. Triglyceride-Rich Lipoproteins and Atherosclerotic Cardiovascular Disease: New Insights From Epidemiology, Genetics, and Biology. Circ Res. 2016;118(4):547-63.
26. Dewey FE, Gusarova V, Dunbar RL, O'Dushlaine C, Schurmann C, Gottesman O, McCarthy S, Van Hout CV, Bruse S, Dansky HM, Leader JB, Murray MF, Ritchie MD, Kirchner HL, Habegger L, Lopez A, Penn J, Zhao A, Shao W, Stahl N, Murphy AJ, Hamon S, Bouzelmat A, Zhang R, Shumel B, Pordy R, Gipe D, Herman GA, Sheu WHH, Lee IT, Liang KW, Guo X, Rotter JI, Chen YI, Kraus WE, Shah SH, Damrauer S, Small A, Rader DJ, Wulff AB, Nordestgaard BG, Tybjaerg-Hansen A, van den Hoek AM, Princen HMG, Ledbetter DH, Carey DJ, Overton JD, Reid JG, Sasiela WJ, Banerjee P, Shuldiner AR, Borecki IB, Teslovich TM, Yancopoulos GD, Mellis SJ, Gromada J, Baras A. Genetic and Pharmacologic Inactivation of ANGPTL3 and Cardiovascular Disease. The New England journal of medicine. 2017;377(3):211-21.
27. Khera AV, Won HH, Peloso GM, O'Dushlaine C, Liu D, Stitziel NO, Natarajan P, Nomura A, Emdin CA, Gupta N, Borecki IB, Asselta R, Duga S, Merlini PA, Correa A, Kessler T, Wilson JG, Bown MJ, Hall AS, Braund PS, Carey DJ, Murray MF, Kirchner HL, Leader JB, Lavage DR, Manus JN, Hartzel DN, Samani NJ, Schunkert H, Marrugat J, Elosua R, McPherson R, Farrall M, Watkins H, Lander ES, Rader DJ, Danesh J, Ardissino D, Gabriel S, Willer C, Abecasis GR, Saleheen D, Dewey FE, Kathiresan S, Myocardial Infarction Genetics Consortium DsSG, C. A. R.DIoGRAM Exome Consortium, and Global Lipids Genetics Consortium. Association of Rare and Common Variation in the Lipoprotein Lipase Gene With Coronary Artery Disease. JAMA. 2017;317(9):937-46.
28. Rao Kondapally Seshasai S, Kaptoge S, Thompson A, Di Angelantonio E, Gao P, Sarwar N, Whincup PH, Mukamal KJ, Gillum RF, Holme I, Njølstad I, Fletcher A, Nilsson P, Lewington S, Collins R, Gudnason V, Thompson SG, Sattar N, Selvin E, Hu FB, Danesh J, Collaboration ERF. Diabetes mellitus, fasting glucose, and risk of cause-specific death. The New England journal of medicine. 2011;364(9):829-41.
29. Ren X, Ren L, Wei Q, Shao H, Chen L, Liu N. Advanced glycation end-products decreases expression of endothelial nitric oxide synthase through oxidative stress in human coronary artery endothelial cells. Cardiovasc Diabetol. 2017;16(1):52.
30. Shah MS, Brownlee M. Molecular and Cellular Mechanisms of Cardiovascular Disorders in Diabetes. Circ Res. 2016;118(11):1808-29.

31. Saremi A, Howell S, Schwenke DC, Bahn G, Beisswenger PJ, Reaven PD, Investigators V. Advanced Glycation End Products, Oxidation Products, and the Extent of Atherosclerosis During the VA Diabetes Trial and Follow-up Study. Diabetes Care. 2017;40(4):591-8.
32. Nakano M, Eguchi K, Sato T, Onoguchi A, Hoshide S, Kario K. Effect of Intensive Salt-Restriction Education on Clinic, Home, and Ambulatory Blood Pressure Levels in Treated Hypertensive Patients During a 3-Month Education Period. J Clin Hypertens (Greenwich). 2016;18(5):385-92.
33. Boegehold MA. The effect of high salt intake on endothelial function: reduced vascular nitric oxide in the absence of hypertension. J Vasc Res. 2013;50(6):458-67.
34. Cavka A, Cosic A, Jukic I, Jelakovic B, Lombard JH, Phillips SA, Seric V, Mihaljevic I, Drenjancevic I. The role of cyclo-oxygenase-1 in high-salt diet-induced microvascular dysfunction in humans. J Physiol. 2015;593(24):5313-24.
35. North BJ, Sinclair DA. The intersection between aging and cardiovascular disease. Circ Res. 2012;110(8):1097-108.
36. Wang JC, Bennett M. Aging and atherosclerosis: mechanisms, functional consequences, and potential therapeutics for cellular senescence. Circ Res. 2012;111(2):245-59.
37. Little R, Zi M, Hammad SK, Nguyen L, Njegic A, Kurusamy S, Prehar S, Armesilla AL, Neyses L, Austin C, Cartwright EJ. Reduced expression of PMCA1 is associated with increased blood pressure with age which is preceded by remodelling of resistance arteries. Aging Cell. 2017;16(5):1104-13.
38. Zhang L, Connelly JJ, Peppel K, Brian L, Shah SH, Nelson S, Crosslin DR, Wang T, Allen A, Kraus WE, Gregory SG, Hauser ER, Freedman NJ. Aging-related atherosclerosis is exacerbated by arterial expression of tumor necrosis factor receptor-1: evidence from mouse models and human association studies. Hum Mol Genet. 2010;19(14):2754-66.
39. Du W, Wong C, Song Y, Shen H, Mori D, Rotllan N, Price N, Dobrian AD, Meng H, Kleinstein SH, Fernandez-Hernando C, Goldstein DR. Age-associated vascular inflammation promotes monocytosis during atherogenesis. Aging Cell. 2016;15(4):766-77.
40. Steyers CM, Miller FJ. Endothelial dysfunction in chronic inflammatory diseases. Int J Mol Sci. 2014;15(7):11324-49.
41. Totoson P, Maguin-Gaté K, Nappey M, Wendling D, Demougeot C. Endothelial Dysfunction in Rheumatoid Arthritis: Mechanistic Insights and Correlation with Circulating Markers of Systemic Inflammation. PLoS One. 2016;11(1):e0146744.
42. Kojima Y, Volkmer JP, McKenna K, Civelek M, Lusis AJ, Miller CL, Direnzo D, Nanda V, Ye J, Connolly AJ, Schadt EE, Quertermous T, Betancur P, Maegdefessel L, Matic LP, Hedin U, Weissman IL, Leeper NJ. CD47-blocking antibodies restore phagocytosis and prevent atherosclerosis. Nature. 2016;536(7614):86-90.
43. Le Borgne M, Caligiuri G, Nicoletti A. Once Upon a Time: The Adaptive Immune Response in Atherosclerosis--a Fairy Tale No More. Mol Med. 2015;21 Suppl 1:S13-8.
44. Noack M, Miossec P. Th17 and regulatory T cell balance in autoimmune and inflammatory diseases. Autoimmun Rev. 2014;13(6):668-77.
45. Talaat RM, Mohamed SF, Bassyouni IH, Raouf AA. Th1/Th2/Th17/Treg cytokine imbalance in systemic lupus erythematosus (SLE) patients: Correlation with disease activity. Cytokine. 2015;72(2):146-53.

46. Zhu M, Mo H, Li D, Luo X, Zhang L. Th17/Treg imbalance induced by increased incidence of atherosclerosis in patients with systemic lupus erythematosus (SLE). Clin Rheumatol. 2013;32(7):1045-52.
47. Atehortúa L, Rojas M, Vásquez GM, Castaño D. Endothelial Alterations in Systemic Lupus Erythematosus and Rheumatoid Arthritis: Potential Effect of Monocyte Interaction. Mediators Inflamm. 2017;2017:9680729.
48. Mikołajczyk TP, Osmenda G, Batko B, Wilk G, Krezelok M, Skiba D, Sliwa T, Pryjma JR, Guzik TJ. Heterogeneity of peripheral blood monocytes, endothelial dysfunction and subclinical atherosclerosis in patients with systemic lupus erythematosus. Lupus. 2016;25(1):18-27.
49. Bian F, Yang X, Zhou F, Wu P, Xing S, Xu G, Li W, Chi J, Ouyang C, Zhang Y, Xiong B, Li Y, Zheng T, Wu D, Chen X, Jin S. C-reactive protein promotes atherosclerosis by increasing LDL transcytosis across endothelial cells. Br J Pharmacol. 2014;171(10):2671-84.
50. Rees F, Doherty M, Grainge M, Davenport G, Lanyon P, Zhang W. The incidence and prevalence of systemic lupus erythematosus in the UK, 1999-2012. Ann Rheum Dis. 2016;75(1):136-41.
51. Rees F, Doherty M, Grainge MJ, Lanyon P, Zhang W. The worldwide incidence and prevalence of systemic lupus erythematosus: a systematic review of epidemiological studies. Rheumatology (Oxford). 2017;56(11):1945-61.
52. Morgan C, Bland AR, Maker C, Dunnage J, Bruce IN. Individuals living with lupus: findings from the LUPUS UK Members Survey 2014. Lupus. 2018;27(4):681-7.
53. Nightingale AL, Davidson JE, Molta CT, Kan HJ, McHugh NJ. Presentation of SLE in UK primary care using the Clinical Practice Research Datalink. Lupus Sci Med. 2017;4(1):e000172.
54. Marks SD, Tullus K. Autoantibodies in systemic lupus erythematosus. Pediatric Nephrology. 2012;27(10):1855-68.
55. Fattal I, Shental N, Mevorach D, Anaya JM, Livneh A, Langevitz P, Zandman-Goddard G, Pauzner R, Lerner M, Blank M, Hincapie ME, Gafter U, Naparstek Y, Shoenfeld Y, Domany E, Cohen IR. An antibody profile of systemic lupus erythematosus detected by antigen microarray. Immunology. 2010;130(3):337-43.
56. Zhang H, Fu R, Guo C, Huang Y, Wang H, Wang S, Zhao J, Yang N. Anti-dsDNA antibodies bind to TLR4 and activate NLRP3 inflammasome in lupus monocytes/macrophages. J Transl Med. 2016;14(1):156.
57. Mayadas TN, Tsokos GC, Tsuboi N. Mechanisms of immune complex-mediated neutrophil recruitment and tissue injury. Circulation. 2009;120(20):2012-24.
58. Gronwall C, Hardt U, Gustafsson JT, Elvin K, Jensen-Urstad K, Kvarnstrom M, Grosso G, Ronnelid J, Padykov L, Gunnarsson I, Silverman GJ, Svenungsson E. Depressed serum IgM levels in SLE are restricted to defined subgroups. Clin Immunol. 2017;183:304-15.
59. Sun J, Lundstrom SL, Zhang B, Zubarev RA, Steuer J, Gillgren P, Rahman M, Ajeganova S, Liu A, Frostegard J. IgM antibodies against phosphorylcholine promote polarization of T regulatory cells from patients with atherosclerotic plaques, systemic lupus erythematosus and healthy donors. Atherosclerosis. 2018;268:36-48.
60. Gronwall C, Akhter E, Oh C, Burlingame RW, Petri M, Silverman GJ. IgM autoantibodies to distinct apoptosis-associated antigens correlate with protection from

cardiovascular events and renal disease in patients with SLE. Clin Immunol. 2012;142(3):390-8.
61. Su J, Hua X, Concha H, Svenungsson E, Cederholm A, Frostegard J. Natural antibodies against phosphorylcholine as potential protective factors in SLE. Rheumatology (Oxford). 2008;47(8):1144-50.
62. Macedo AC, Isaac L. Systemic Lupus Erythematosus and Deficiencies of Early Components of the Complement Classical Pathway. Front Immunol. 2016;7:55.
63. Sisirak V, Sally B, D'Agati V, Martinez-Ortiz W, Ozcakar ZB, David J, Rashidfarrokhi A, Yeste A, Panea C, Chida AS, Bogunovic M, Ivanov, II, Quintana FJ, Sanz I, Elkon KB, Tekin M, Yalcinkaya F, Cardozo TJ, Clancy RM, Buyon JP, Reizis B. Digestion of Chromatin in Apoptotic Cell Microparticles Prevents Autoimmunity. Cell. 2016;166(1):88-101.
64. Raymond W, Eilertsen G, Nossent J. Hypocomplementemia as a Risk Factor for Organ Damage Accrual in Patients with Systemic Lupus Erythematosus. J Immunol Res. 2018;2018:8051972.
65. Berthelot JM, Le Goff B, Neel A, Maugars Y, Hamidou M. NETosis: At the crossroads of rheumatoid arthritis, lupus, and vasculitis. Joint Bone Spine. 2017;84(3):255-62.
66. Khawaja AA, Pericleous C, Ripoll VM, Porter JC, Giles IP. Autoimmune rheumatic disease IgG has differential effects upon neutrophil integrin activation that is modulated by the endothelium. Sci Rep. 2019;9(1):1283.
67. Lood C, Arve S, Ledbetter J, Elkon KB. TLR7/8 activation in neutrophils impairs immune complex phagocytosis through shedding of FcgRIIA. The Journal of experimental medicine. 2017;214(7):2103-19.
68. Kaplan MJ. Neutrophils in the pathogenesis and manifestations of SLE. Nature reviews Rheumatology. 2011;7(12):691-9.
69. Caielli S, Athale S, Domic B, Murat E, Chandra M, Banchereau R, Baisch J, Phelps K, Clayton S, Gong M, Wright T, Punaro M, Palucka K, Guiducci C, Banchereau J, Pascual V. Oxidized mitochondrial nucleoids released by neutrophils drive type I interferon production in human lupus. The Journal of experimental medicine. 2016;213(5):697-713.
70. Chasset F, Arnaud L. Targeting interferons and their pathways in systemic lupus erythematosus. Autoimmun Rev. 2018;17(1):44-52.
71. Berggren O, Hagberg N, Alexsson A, Weber G, Ronnblom L, Eloranta ML. Plasmacytoid dendritic cells and RNA-containing immune complexes drive expansion of peripheral B cell subsets with an SLE-like phenotype. PLoS One. 2017;12(8):e0183946.
72. Menon M, Blair PA, Isenberg DA, Mauri C. A Regulatory Feedback between Plasmacytoid Dendritic Cells and Regulatory B Cells Is Aberrant in Systemic Lupus Erythematosus. Immunity. 2016;44(3):683-97.
73. Comte D, Karampetsou MP, Tsokos GC. T cells as a therapeutic target in SLE. Lupus. 2015;24(4-5):351-63.
74. Ohl K, Tenbrock K. Regulatory T cells in systemic lupus erythematosus. Eur J Immunol. 2015;45(2):344-55.
75. Rees F, Doherty M, Grainge MJ, Lanyon P, Davenport G, Zhang W. Mortality in systemic lupus erythematosus in the United Kingdom 1999-2012. Rheumatology (Oxford). 2016;55(5):854-60.
76. Bartels CM, Buhr KA, Goldberg JW, Bell CL, Visekruna M, Nekkanti S, Greenlee RT. Mortality and cardiovascular burden of systemic lupus erythematosus in a US population-based cohort. J Rheumatol. 2014;41(4):680-7.

77. Manzi S, Meilahn EN, Rairie JE, Conte CG, Medsger TA, Jr., Jansen-McWilliams L, D'Agostino RB, Kuller LH. Age-specific incidence rates of myocardial infarction and angina in women with systemic lupus erythematosus: comparison with the Framingham Study. Am J Epidemiol. 1997;145(5):408-15.
78. Hesselvig JH, Ahlehoff O, Dreyer L, Gislason G, Kofoed K. Cutaneous lupus erythematosus and systemic lupus erythematosus are associated with clinically significant cardiovascular risk: a Danish nationwide cohort study. Lupus. 2017;26(1):48-53.
79. Haque S, Skeoch S, Rakieh C, Edlin H, Ahmad Y, Ho P, Gorodkin R, Alexander MY, Bruce IN. Progression of subclinical and clinical cardiovascular disease in a UK SLE cohort: the role of classic and SLE-related factors. Lupus Sci Med. 2018;5(1):e000267.
80. Baragetti A, Ramirez GA, Magnoni M, Garlaschelli K, Grigore L, Berteotti M, Scotti I, Bozzolo E, Berti A, Camici PG, Catapano AL, Manfredi AA, Ammirati E, Norata GD. Disease trends over time and CD4(+)CCR5(+) T-cells expansion predict carotid atherosclerosis development in patients with systemic lupus erythematosus. Nutr Metab Cardiovasc Dis. 2018;28(1):53-63.
81. Mak A, Kow NY, Schwarz H, Gong L, Tay SH, Ling LH. Endothelial dysfunction in systemic lupus erythematosus - a case-control study and an updated meta-analysis and meta-regression. Sci Rep. 2017;7(1):7320.
82. Taraborelli M, Sciatti E, Bonadei I, Terlizzi V, Fredi M, Zani R, Cancarini G, Tincani A, Franceschini F, Vizzardi E, Cavazzana I. Endothelial Dysfunction in Early Systemic Lupus Erythematosus Patients and Controls Without Previous Cardiovascular Events. Arthritis Care Res (Hoboken). 2018;70(9):1277-83.
83. Thacker SG, Zhao W, Smith CK, Luo W, Wang H, Vivekanandan-Giri A, Rabquer BJ, Koch AE, Pennathur S, Davidson A, Eitzman DT, Kaplan MJ. Type I interferons modulate vascular function, repair, thrombosis, and plaque progression in murine models of lupus and atherosclerosis. Arthritis Rheum. 2012;64(9):2975-85.
84. Reynolds JA, Ray DW, Zeef LAH, O'Neill T, Bruce IN, Alexander MY. The Effect of Type 1 IFN on Human Aortic Endothelial Cell Function In Vitro: Relevance to Systemic Lupus Erythematosus. Journal of Interferon & Cytokine Research. 2014;34(5):404-12.
85. Buie JJ, Renaud LL, Muise-Helmericks R, Oates JC. IFN-alpha Negatively Regulates the Expression of Endothelial Nitric Oxide Synthase and Nitric Oxide Production: Implications for Systemic Lupus Erythematosus. J Immunol. 2017;199(6):1979-88.
86. Somers EC, Zhao W, Lewis EE, Wang L, Wing JJ, Sundaram B, Kazerooni EA, McCune WJ, Kaplan MJ. Type I Interferons Are Associated with Subclinical Markers of Cardiovascular Disease in a Cohort of Systemic Lupus Erythematosus Patients. PLoS ONE. 2012;7(5):e37000.
87. Li J, Fu Q, Cui H, Qu B, Pan W, Shen N, Bao C. Interferon-alpha priming promotes lipid uptake and macrophage-derived foam cell formation: a novel link between interferon-alpha and atherosclerosis in lupus. Arthritis Rheum. 2011;63(2):492-502.
88. Theodorou E, Nezos A, Antypa E, Ioakeimidis D, Koutsilieris M, Tektonidou M, Moutsopoulos HM, Mavragani CP. B-cell activating factor and related genetic variants in lupus related atherosclerosis. Journal of autoimmunity. 2018;92:87-92.
89. Svenungsson E, Cederholm A, Jensen-Urstad K, Fei GZ, de Faire U, Frostegard J. Endothelial function and markers of endothelial activation in relation to cardiovascular disease in systemic lupus erythematosus. Scandinavian journal of rheumatology. 2008;37(5):352-9.

90. Rho YH, Chung CP, Oeser A, Solus J, Raggi P, Gebretsadik T, Shintani A, Stein CM. Novel cardiovascular risk factors in premature coronary atherosclerosis associated with systemic lupus erythematosus. J Rheumatol. 2008;35(9):1789-94.
91. Eder L, Joshi AA, Dey AK, Cook R, Siegel EL, Gladman DD, Mehta NN. Association of Tumor Necrosis Factor Inhibitor Treatment With Reduced Indices of Subclinical Atherosclerosis in Patients With Psoriatic Disease. Arthritis Rheumatol. 2018;70(3):408-16.
92. McMahon M, Skaggs B. Autoimmunity: Do IgM antibodies protect against atherosclerosis in SLE? Nature reviews Rheumatology. 2016;12(8):442-4.
93. Rahman M, Sing S, Golabkesh Z, Fiskesund R, Gustafsson T, Jogestrand T, Frostegard AG, Hafstrom I, Liu A, Frostegard J. IgM antibodies against malondialdehyde and phosphorylcholine are together strong protection markers for atherosclerosis in systemic lupus erythematosus: Regulation and underlying mechanisms. Clin Immunol. 2016;166-167:27-37.
94. Domingues V, Magder L, Petri M. Assessment of the independent associations of IgG, IgM and IgA isotypes of anticardiolipin with thrombosis in SLE. Lupus Sci Med. 2016;3(1):e000107.
95. Lopez P, Rodriguez-Carrio J, Martinez-Zapico A, Perez-Alvarez AI, Lopez-Mejias R, Benavente L, Mozo L, Caminal-Montero L, Gonzalez-Gay MA, Suarez A. Serum Levels of Anti-PON1 and Anti-HDL Antibodies as Potential Biomarkers of Premature Atherosclerosis in Systemic Lupus Erythematosus. Thromb Haemost. 2017;117(11):2194-206.
96. Carlucci PM, Purmalek MM, Dey AK, Temesgen-Oyelakin Y, Sakhardande S, Joshi AA, Lerman JB, Fike A, Davis M, Chung JH, Playford MP, Naqi M, Mistry P, Gutierrez-Cruz G, Dell'Orso S, Naz F, Salahuddin T, Natarajan B, Manna Z, Tsai WL, Gupta S, Grayson P, Teague H, Chen MY, Sun HW, Hasni S, Mehta NN, Kaplan MJ. Neutrophil subsets and their gene signature associate with vascular inflammation and coronary atherosclerosis in lupus. JCI insight. 2018;3(8).
97. Carmona-Rivera C, Zhao W, Yalavarthi S, Kaplan MJ. Neutrophil extracellular traps induce endothelial dysfunction in systemic lupus erythematosus through the activation of matrix metalloproteinase-2. Ann Rheum Dis. 2015;74(7):1417-24.
98. Mikolajczyk TP, Osmenda G, Batko B, Wilk G, Krezelok M, Skiba D, Sliwa T, Pryjma JR, Guzik TJ. Heterogeneity of peripheral blood monocytes, endothelial dysfunction and subclinical atherosclerosis in patients with systemic lupus erythematosus. Lupus. 2016;25(1):18-27.
99. Korman BD, Huang CC, Skamra C, Wu P, Koessler R, Yao D, Huang QQ, Pearce W, Sutton-Tyrrell K, Kondos G, Edmundowicz D, Pope R, Ramsey-Goldman R. Inflammatory expression profiles in monocyte-to-macrophage differentiation in patients with systemic lupus erythematosus and relationship with atherosclerosis. Arthritis Res Ther. 2014;16(4):R147.
100. Skaggs BJ, Hahn BH, McMahon M. Accelerated atherosclerosis in patients with SLE--mechanisms and management. Nature reviews Rheumatology. 2012;8(4):214-23.
101. Reynolds JA, Rosenberg AZ, Smith CK, Sergeant JC, Rice GI, Briggs TA, Bruce IN, Kaplan MJ. Brief Report: Vitamin D Deficiency Is Associated With Endothelial Dysfunction and Increases Type I Interferon Gene Expression in a Murine Model of Systemic Lupus Erythematosus. Arthritis Rheumatol. 2016;68(12):2929-35.

102. Reynolds JA, Haque S, Williamson K, Ray DW, Alexander MY, Bruce IN. Vitamin D improves endothelial dysfunction and restores myeloid angiogenic cell function via reduced CXCL-10 expression in systemic lupus erythematosus. Sci Rep. 2016;6:22341.
103. Virdis A, Tani C, Duranti E, Vagnani S, Carli L, Kühl A, Solini A, Baldini C, Talarico R, Bombardieri S, Taddei S, Mosca M. Early treatment with hydroxychloroquine prevents the development of endothelial dysfunction in a murine model of systemic lupus erythematosus. Arthritis Res Ther. 2015;17:277.
104. Floris A, Piga M, Mangoni AA, Bortoluzzi A, Erre GL, Cauli A. Protective Effects of Hydroxychloroquine against Accelerated Atherosclerosis in Systemic Lupus Erythematosus. Mediators Inflamm. 2018;2018:3424136.
105. Tunnicliffe DJ, Singh-Grewal D, Kim S, Craig JC, Tong A. Diagnosis, Monitoring, and Treatment of Systemic Lupus Erythematosus: A Systematic Review of Clinical Practice Guidelines. Arthritis Care Res (Hoboken). 2015;67(10):1440-52.
106. Petri M, Orbai A-M, Alarcón GS, Gordon C, Merrill JT, Fortin PR, Bruce IN, Isenberg D, Wallace DJ, Nived O, Sturfelt G, Ramsey-Goldman R, Bae S-C, Hanly JG, Sanchez-Guerrero J, Clarke A, Aranow C, Manzi S, Urowitz M, Gladman D, Kalunian K, Costner M, Werth VP, Zoma A, Bernatsky S, Ruiz-Irastorza G, Khamashta MA, Jacobsen S, Buyon JP, Maddison P, Dooley MA, van Vollenhoven RF, Ginzler E, Stoll T, Peschken C, Jorizzo JL, Callen JP, Lim SS, Fessler BJ, Inanc M, Kamen DL, Rahman A, Steinsson K, Franks AG, Sigler L, Hameed S, Fang H, Pham N, Brey R, Weisman MH, McGwin G, Magder LS. Derivation and Validation of Systemic Lupus International Collaborating Clinics Classification Criteria for Systemic Lupus Erythematosus. Arthritis and rheumatism. 2012;64(8):2677-86.
107. Wichainun R, Kasitanon N, Wangkaew S, Hongsongkiat S, Sukitawut W, Louthrenoo W. Sensitivity and specificity of ANA and anti-dsDNA in the diagnosis of systemic lupus erythematosus: a comparison using control sera obtained from healthy individuals and patients with multiple medical problems. Asian Pac J Allergy Immunol. 2013;31(4):292-8.
108. Tedeschi SK, Johnson SR, Boumpas D, Daikh D, Dorner T, Jayne D, Kamen D, Lerstrom K, Mosca M, Ramsey-Goldman R, Sinnette C, Wofsy D, Smolen JS, Naden RP, Aringer M, Costenbader KH. Developing and Refining New Candidate Criteria for SLE Classification: An International Collaboration. Arthritis Care Res (Hoboken). 2017;70(4):571-81.
109. Hochberg MC. Updating the American College of Rheumatology revised criteria for the classification of systemic lupus erythematosus. Arthritis Rheum. 1997;40(9):1725.
110. Tan EM, Cohen AS, Fries JF, Masi AT, McShane DJ, Rothfield NF, Schaller JG, Talal N, Winchester RJ. The 1982 revised criteria for the classification of systemic lupus erythematosus. Arthritis Rheum. 1982;25(11):1271-7.
111. Gordon C, Sutcliffe N, Skan J, Stoll T, Isenberg DA. Definition and treatment of lupus flares measured by the BILAG index. Rheumatology (Oxford). 2003;42(11):1372-9.
112. Castrejon I, Tani C, Jolly M, Huang A, Mosca M. Indices to assess patients with systemic lupus erythematosus in clinical trials, long-term observational studies, and clinical care. Clin Exp Rheumatol. 2014;32(5 Suppl 85):S-85-95.
113. Murphy CL, Yee CS, Gordon C, Isenberg D. From BILAG to BILAG-based combined lupus assessment-30 years on. Rheumatology (Oxford). 2016;55(8):1357-63.
114. Simmonds MC, Wald NJ. Risk estimation versus screening performance: a comparison of six risk algorithms for cardiovascular disease. J Med Screen. 2012;19(4):201-5.

115. DeFilippis AP, Young R, Carrubba CJ, McEvoy JW, Budoff MJ, Blumenthal RS, Kronmal RA, McClelland RL, Nasir K, Blaha MJ. An analysis of calibration and discrimination among multiple cardiovascular risk scores in a modern multiethnic cohort. Ann Intern Med. 2015;162(4):266-75.
116. Bitton A, Gaziano T. The Framingham Heart Study's Impact on Global Risk Assessment. Progress in cardiovascular diseases. 2010;53(1):68-78.
117. Hippisley-Cox J, Coupland C, Vinogradova Y, Robson J, May M, Brindle P. Derivation and validation of QRISK, a new cardiovascular disease risk score for the United Kingdom: prospective open cohort study. BMJ. 2007;335(7611):136.
118. Hippisley-Cox J, Coupland C, Vinogradova Y, Robson J, Minhas R, Sheikh A, Brindle P. Predicting cardiovascular risk in England and Wales: prospective derivation and validation of QRISK2. BMJ. 2008;336(7659):1475-82.
119. Hippisley-Cox J, Coupland C, Brindle P. Development and validation of QRISK3 risk prediction algorithms to estimate future risk of cardiovascular disease: prospective cohort study. The BMJ. 2017;357:j2099.
120. Collins GS, Altman DG. An independent and external validation of QRISK2 cardiovascular disease risk score: a prospective open cohort study. BMJ. 2010;340:c2442.
121. NICE. Cardiovascular disease: risk assessment and reduction, including lipid modification (CG181). 2016 [cited 2017.
122. NICE. Lipid Modification: Cardiovascular Risk Assessment and the Modification of Blood Lipids for the Primary and Secondary Prevention of Cardiovascular Disease. London: National Clinical Guideline Centre, 2014.; 2014 Jul.
123. Boulos D, Koelmeyer RL, Morand EF, Hoi AY. Cardiovascular risk profiles in a lupus cohort: what do different calculators tell us? Lupus Sci Med. 2017;4(1):e000212.
124. Fava A, Petri M. Systemic lupus erythematosus: Diagnosis and clinical management. Journal of autoimmunity. 2019;96:1-13.
125. Schiro A, Wilkinson FL, Weston R, Smyth JV, Serracino-Inglott F, Alexander MY. Endothelial microparticles as conveyors of information in atherosclerotic disease. Atherosclerosis. 2014;234(2):295-302.
126. Yin M, Loyer X, Boulanger CM. Extracellular vesicles as new pharmacological targets to treat atherosclerosis. Eur J Pharmacol. 2015;763(Pt A):90-103.
127. Tetta C, Ghigo E, Silengo L, Deregibus MC, Camussi G. Extracellular vesicles as an emerging mechanism of cell-to-cell communication. Endocrine. 2013;44(1):11-9.
128. Wolf P. The Nature and Significance of Platelet Products in Human Plasma. British Journal of Haematology. 1967;13(3):269-88.
129. van der Pol E, Boing AN, Harrison P, Sturk A, Nieuwland R. Classification, functions, and clinical relevance of extracellular vesicles. Pharmacological reviews. 2012;64(3):676-705.
130. Todorova D, Simoncini S, Lacroix R, Sabatier F, Dignat-George F. Extracellular Vesicles in Angiogenesis. Circ Res. 2017;120(10):1658-73.
131. Mulcahy LA, Pink RC, Carter DR. Routes and mechanisms of extracellular vesicle uptake. J Extracell Vesicles. 2014;3.
132. Costa Verdera H, Gitz-Francois JJ, Schiffelers RM, Vader P. Cellular uptake of extracellular vesicles is mediated by clathrin-independent endocytosis and macropinocytosis. Journal of controlled release : official journal of the Controlled Release Society. 2017;266:100-8.

133. Jaiswal R, Sedger LM. Intercellular Vesicular Transfer by Exosomes, Microparticles and Oncosomes - Implications for Cancer Biology and Treatments. Frontiers in oncology. 2019;9:125.
134. Lai CP, Kim EY, Badr CE, Weissleder R, Mempel TR, Tannous BA, Breakefield XO. Visualization and tracking of tumour extracellular vesicle delivery and RNA translation using multiplexed reporters. Nat Commun. 2015;6:7029.
135. Scholz T, Temmler U, Krause S, Heptinstall S, Losche W. Transfer of tissue factor from platelets to monocytes: role of platelet-derived microvesicles and CD62P. Thromb Haemost. 2002;88(6):1033-8.
136. Valadi H, Ekstrom K, Bossios A, Sjostrand M, Lee JJ, Lotvall JO. Exosome-mediated transfer of mRNAs and microRNAs is a novel mechanism of genetic exchange between cells. Nat Cell Biol. 2007;9(6):654-9.
137. Yuan A, Farber EL, Rapoport AL, Tejada D, Deniskin R, Akhmedov NB, Farber DB. Transfer of microRNAs by embryonic stem cell microvesicles. PLoS One. 2009;4(3):e4722.
138. Moreno-Martinez D. An Investigation into The Role of Endothelial-derived Microparticles in an In vitro Model of Vascular Health and Disease: Manchester Metropolitan University; 2017.
139. de Gonzalo-Calvo D, Vea A, Bar C, Fiedler J, Couch LS, Brotons C, Llorente-Cortes V, Thum T. Circulating non-coding RNAs in biomarker-guided cardiovascular therapy: a novel tool for personalized medicine? Eur Heart J. 2019;40(20):1643-50.
140. Ha M, Kim VN. Regulation of microRNA biogenesis. Nature reviews Molecular cell biology. 2014;15(8):509-24.
141. Johnson JL. Elucidating the contributory role of microRNA to cardiovascular diseases (a review). Vascul Pharmacol. 2019;114:31-48.
142. Iwakawa HO, Tomari Y. The Functions of MicroRNAs: mRNA Decay and Translational Repression. Trends in cell biology. 2015;25(11):651-65.
143. Desvignes T, Batzel P, Berezikov E, Eilbeck K, Eppig JT, McAndrews MS, Singer A, Postlethwait JH. miRNA Nomenclature: A View Incorporating Genetic Origins, Biosynthetic Pathways, and Sequence Variants. Trends in genetics : TIG. 2015;31(11):613-26.
144. Barwari T, Joshi A, Mayr M. MicroRNAs in Cardiovascular Disease. J Am Coll Cardiol. 2016;68(23):2577-84.
145. Sala F, Aranda JF, Rotllan N, Ramirez CM, Aryal B, Elia L, Condorelli G, Catapano AL, Fernandez-Hernando C, Norata GD. MiR-143/145 deficiency attenuates the progression of atherosclerosis in Ldlr-/-mice. Thromb Haemost. 2014;112(4):796-802.
146. Zhang YN, Xie BD, Sun L, Chen W, Jiang SL, Liu W, Bian F, Tian H, Li RK. Phenotypic switching of vascular smooth muscle cells in the 'normal region' of aorta from atherosclerosis patients is regulated by miR-145. J Cell Mol Med. 2016;20(6):1049-61.
147. Cordes KR, Sheehy NT, White MP, Berry EC, Morton SU, Muth AN, Lee TH, Miano JM, Ivey KN, Srivastava D. miR-145 and miR-143 regulate smooth muscle cell fate and plasticity. Nature. 2009;460(7256):705-10.
148. Barwari T, Rienks M, Mayr M. MicroRNA-21 and the Vulnerability of Atherosclerotic Plaques. Mol Ther. 2018;26(4):938-40.
149. Yuan J, Chen H, Ge D, Xu Y, Xu H, Yang Y, Gu M, Zhou Y, Zhu J, Ge T, Chen Q, Gao Y, Wang Y, Li X, Zhao Y. Mir-21 Promotes Cardiac Fibrosis After Myocardial Infarction Via Targeting Smad7. Cell Physiol Biochem. 2017;42(6):2207-19.

150. Xue S, Liu D, Zhu W, Su Z, Zhang L, Zhou C, Li P. Circulating MiR-17-5p, MiR-126-5p and MiR-145-3p Are Novel Biomarkers for Diagnosis of Acute Myocardial Infarction. Front Physiol. 2019;10:123.
151. Ma Q, Li G, Tao Z, Wang J, Wang R, Liu P, Luo Y, Zhao H. Blood microRNA-93 as an indicator for diagnosis and prediction of functional recovery of acute stroke patients. Journal of clinical neuroscience : official journal of the Neurosurgical Society of Australasia. 2019;62:121-7.
152. JF OS, Neylon A, McGorrian C, Blake GJ. miRNA-93-5p and other miRNAs as predictors of coronary artery disease and STEMI. Int J Cardiol. 2016;224:310-6.
153. Cheng HL, Fu CY, Kuo WC, Chen YW, Chen YS, Lee YM, Li KH, Chen C, Ma HP, Huang PC, Wang YL, Lee GB. Detecting miRNA biomarkers from extracellular vesicles for cardiovascular disease with a microfluidic system. Lab on a chip. 2018;18(19):2917-25.
154. Schiro A, Wilkinson FL, Weston R, Smyth JV, Serracino-Inglott F, Alexander MY. Elevated levels of endothelial-derived microparticles, and serum CXCL9 and SCGF-beta are associated with unstable asymptomatic carotid plaques. Sci Rep. 2015;5:16658.
155. Werner N, Wassmann S, Ahlers P, Kosiol S, Nickenig G. Circulating CD31+/annexin V+ apoptotic microparticles correlate with coronary endothelial function in patients with coronary artery disease. Arterioscler Thromb Vasc Biol. 2006;26(1):112-6.
156. Sinning JM, Losch J, Walenta K, Böhm M, Nickenig G, Werner N. Circulating CD31+/Annexin V+ microparticles correlate with cardiovascular outcomes. Eur Heart J. 2011;32(16):2034-41.
157. McCarthy EM, Moreno-Martinez D, Wilkinson FL, McHugh NJ, Bruce IN, Pauling JD, Alexander MY, Parker B. Microparticle subpopulations are potential markers of disease progression and vascular dysfunction across a spectrum of connective tissue disease. BBA Clin. 2017;7:16-22.
158. Parker B, Al-Husain A, Pemberton P, Yates AP, Ho P, Gorodkin R, Teh LS, Alexander MY, Bruce IN. Suppression of inflammation reduces endothelial microparticles in active systemic lupus erythematosus. Annals of the Rheumatic Diseases. 2014;73(6):1144-50.
159. Edwards N, Langford-Smith AWW, Parker BJ, Bruce IN, Reynolds JA, Alexander MY, McCarthy EM, Wilkinson FL. QRISK3 improves detection of cardiovascular disease risk in patients with systemic lupus erythematosus. Lupus Sci Med. 2018;5(1):e000272.
160. Dieker J, Tel J, Pieterse E, Thielen A, Rother N, Bakker M, Fransen J, Dijkman HB, Berden JH, de Vries JM, Hilbrands LB, van der Vlag J. Circulating Apoptotic Microparticles in Systemic Lupus Erythematosus Patients Drive the Activation of Dendritic Cell Subsets and Prime Neutrophils for NETosis. Arthritis Rheumatol. 2016;68(2):462-72.
161. Burbano C, Villar-Vesga J, Orejuela J, Munoz C, Vanegas A, Vasquez G, Rojas M, Castano D. Potential Involvement of Platelet-Derived Microparticles and Microparticles Forming Immune Complexes during Monocyte Activation in Patients with Systemic Lupus Erythematosus. Front Immunol. 2018;9:322.
162. Winberg LK, Nielsen CH, Jacobsen S. Surface complement C3 fragments and cellular binding of microparticles in patients with SLE. Lupus Science & Medicine. 2017;4(1):e000193.
163. Winberg LK, Jacobsen S, Nielsen CH. Microparticles from patients with systemic lupus erythematosus induce production of reactive oxygen species and degranulation of polymorphonuclear leukocytes. Arthritis Res Ther. 2017;19(1):230.

164. Chen JQ, Papp G, Poliska S, Szabo K, Tarr T, Balint BL, Szodoray P, Zeher M. MicroRNA expression profiles identify disease-specific alterations in systemic lupus erythematosus and primary Sjogren's syndrome. PLoS One. 2017;12(3):e0174585.
165. Navarro-Quiroz E, Pacheco-Lugo L, Lorenzi H, Díaz-Olmos Y, Almendrales L, Rico E, Navarro R, España-Puccini P, Iglesias A, Egea E, Aroca G. High-Throughput Sequencing Reveals Circulating miRNAs as Potential Biomarkers of Kidney Damage in Patients with Systemic Lupus Erythematosus. PLoS ONE. 2016;11(11):e0166202.
166. Duroux-Richard I, Cuenca J, Ponsolles C, Pineiro AB, Gonzalez F, Roubert C, Areny R, Chea R, Pefaur J, Pers YM, Figueroa FE, Jorgensen C, Khoury M, Apparailly F. MicroRNA Profiling of B Cell Subsets from Systemic Lupus Erythematosus Patients Reveals Promising Novel Biomarkers. Int J Mol Sci. 2015;16(8):16953-65.
167. Honarpisheh M, Kohler P, von Rauchhaupt E, Lech M. The Involvement of MicroRNAs in Modulation of Innate and Adaptive Immunity in Systemic Lupus Erythematosus and Lupus Nephritis. J Immunol Res. 2018;2018:4126106.
168. Agilent TL. Agilent Seahorse XF Cell Mito Stress Test Kit User Guide. 2019.
169. Huang da W, Sherman BT, Lempicki RA. Systematic and integrative analysis of large gene lists using DAVID bioinformatics resources. Nature protocols. 2009;4(1):44-57.
170. Huang da W, Sherman BT, Lempicki RA. Bioinformatics enrichment tools: paths toward the comprehensive functional analysis of large gene lists. Nucleic acids research. 2009;37(1):1-13.
171. Agarwal V, Bell GW, Nam JW, Bartel DP. Predicting effective microRNA target sites in mammalian mRNAs. eLife. 2015;4.
172. Schwarzenbach H, da Silva AM, Calin G, Pantel K. Data Normalization Strategies for MicroRNA Quantification. Clinical chemistry. 2015;61(11):1333-42.
173. Peltier HJ, Latham GJ. Normalization of microRNA expression levels in quantitative RT-PCR assays: identification of suitable reference RNA targets in normal and cancerous human solid tissues. RNA (New York, NY). 2008;14(5):844-52.
174. Rice J, Roberts H, Rai SN, Galandiuk S. Housekeeping genes for studies of plasma microRNA: A need for more precise standardization. Surgery. 2015;158(5):1345-51.
175. Li Y, Xiang GM, Liu LL, Liu C, Liu F, Jiang DN, Pu XY. Assessment of endogenous reference gene suitability for serum exosomal microRNA expression analysis in liver carcinoma resection studies. Mol Med Rep. 2015;12(3):4683-91.
176. Kuosmanen SM, Kansanen E, Sihvola V, Levonen AL. MicroRNA Profiling Reveals Distinct Profiles for Tissue-Derived and Cultured Endothelial Cells. Sci Rep. 2017;7(1):10943.
177. Paraskevopoulou MD, Georgakilas G, Kostoulas N, Vlachos IS, Vergoulis T, Reczko M, Filippidis C, Dalamagas T, Hatzigeorgiou AG. DIANA-microT web server v5.0: service integration into miRNA functional analysis workflows. Nucleic acids research. 2013;41(Web Server issue):W169-73.
178. The Gene Ontology Resource: 20 years and still GOing strong. Nucleic acids research. 2019;47(D1):D330-d8.
179. Ashburner M, Ball CA, Blake JA, Botstein D, Butler H, Cherry JM, Davis AP, Dolinski K, Dwight SS, Eppig JT, Harris MA, Hill DP, Issel-Tarver L, Kasarskis A, Lewis S, Matese JC, Richardson JE, Ringwald M, Rubin GM, Sherlock G. Gene ontology: tool for the unification of biology. The Gene Ontology Consortium. Nature genetics. 2000;25(1):25-9.

180. Shannon P, Markiel A, Ozier O, Baliga NS, Wang JT, Ramage D, Amin N, Schwikowski B, Ideker T. Cytoscape: a software environment for integrated models of biomolecular interaction networks. Genome research. 2003;13(11):2498-504.
181. Katzen F. Gateway((R)) recombinational cloning: a biological operating system. Expert opinion on drug discovery. 2007;2(4):571-89.
182. Reece-Hoyes JS, Walhout AJM. Gateway Recombinational Cloning. Cold Spring Harbor protocols. 2018;2018(1).
183. Hartley JL, Temple GF, Brasch MA. DNA cloning using in vitro site-specific recombination. Genome research. 2000;10(11):1788-95.
184. Penner IK, Raselli C, Stocklin M, Opwis K, Kappos L, Calabrese P. The Fatigue Scale for Motor and Cognitive Functions (FSMC): validation of a new instrument to assess multiple sclerosis-related fatigue. Multiple sclerosis (Houndmills, Basingstoke, England). 2009;15(12):1509-17.
185. McElhone K, Abbott J, Shelmerdine J, Bruce IN, Ahmad Y, Gordon C, Peers K, Isenberg D, Ferenkeh-Koroma A, Griffiths B, Akil M, Maddison P, Teh LS. Development and validation of a disease-specific health-related quality of life measure, the LupusQol, for adults with systemic lupus erythematosus. Arthritis Rheum. 2007;57(6):972-9.
186. Cook N, Paynter N, Eaton C, Manson JE, Martin L, Robinson J, Rossouw J, Wassertheil-Smoller S, Ridker P. Comparison of the Framingham and Reynolds Risk Scores for Global Cardiovascular Risk Prediction in the Multiethnic Women's Health Initiative. Circulation. 2012;125(14):1748-56.
187. Wilson PW, D'Agostino RB, Levy D, Belanger AM, Silbershatz H, Kannel WB. Prediction of coronary heart disease using risk factor categories. Circulation. 1998;97(18):1837-47.
188. Magder LS, Petri M. Incidence of and Risk Factors for Adverse Cardiovascular Events Among Patients With Systemic Lupus Erythematosus. American Journal of Epidemiology. 2012;176(8):708-19.
189. McMahon M, Hahn BH, Skaggs BJ. Systemic lupus erythematosus and cardiovascular disease: prediction and potential for therapeutic intervention. Expert review of clinical immunology. 2011;7(2):227-41.
190. Bruce I. Cardiovascular disease in lupus patients: should all patients be treated with statins and aspirin? Best Pract Res Clin Rheumatol. 2005;19(5):823-38.
191. Kirton JP, Wilkinson FL, Canfield AE, Alexander MY. Dexamethasone downregulates calcification-inhibitor molecules and accelerates osteogenic differentiation of vascular pericytes: implications for vascular calcification. Circ Res. 2006;98(10):1264-72.
192. Karp I, Abrahamowicz M, Fortin P, Pilote L, Neville C, Pineau C, Esdaile J. Recent corticosteroid use and recent disease activity: independent determinants of coronary heart disease risk factors in systemic lupus erythematosus? Arthritis Rheum. 2008;59(2):169-75.
193. Svenungsson E, Gunnarsson I, Fei G, Lundberg I, Klareskog L, Frostegard J. Elevated triglycerides and low levels of high-density lipoprotein as markers of disease activity in association with up-regulation of the tumor necrosis factor alpha/tumor necrosis factor receptor system in systemic lupus erythematosus. Arthritis Rheum. 2003;48(9):2533-40.
194. Talayero B, Sacks F. The role of triglycerides in atherosclerosis. Curr Cardiol Rep. 2011;13(6):544-52.

195. Tydén H, Lood C, Gullstrand B, Tandrup-Nielsen C, Heegaard N, Kahn R, Jönsen A, Bengtsson A. Endothelial dysfunction is associated with activation of the type I interferon system and platelets in patients with systemic lupus erythematosus. RMD Open. 2017;3(2):e000508.
196. Gawaz M, Langer H, May A. Platelets in inflammation and atherogenesis. J Clin Invest. 2005;115(12):3378-84.
197. Shim C, Liu Y, Atkinson T, Xie A, Foster T, Davidson B, Treible M, Qi Y, López J, Munday A, Ruggeri Z, Lindner J. Molecular Imaging of Platelet-Endothelial Interactions and Endothelial von Willebrand Factor in Early and Mid-Stage Atherosclerosis. Circ Cardiovasc Imaging. 2015;8(7):e002765.
198. Lood C, Tydén H, Gullstrand B, Sturfelt G, Jönsen A, Truedsson L, Bengtsson A. Platelet Activation and Anti-Phospholipid Antibodies Collaborate in the Activation of the Complement System on Platelets in Systemic Lupus Erythematosus. PLoS ONE. 2014;9(6):e99386.
199. Peerschke E, Yin W, Alpert D, Roubey R, Salmon J, Ghebrehiwet B. Serum complement activation on heterologous platelets is associated with arterial thrombosis in patients with systemic lupus erythematosus and antiphospholipid antibodies. Lupus. 2009;18(6):530-8.
200. Soltesz P, Bereczki D, Szodoray P, Magyar MT, Der H, Csipo I, Hajas A, Paragh G, Szegedi G, Bodolay E. Endothelial cell markers reflecting endothelial cell dysfunction in patients with mixed connective tissue disease. Arthritis Res Ther. 2010;12(3):R78.
201. Eudy A, Vines A, Dooley M, Cooper G, Parks C. Elevated C-reactive protein and self-reported disease activity in systemic lupus erythematosus. Lupus. 2014;23(14):1460-7.
202. Stojan G, Fang H, Magder L, Petri M. Erythrocyte sedimentation rate is a predictor of renal and overall SLE disease activity. Lupus. 2013;22(8):827-34.
203. Schoenfeld S, Kasturi S, Costenbader KH. The epidemiology of atherosclerotic cardiovascular disease among patients with SLE: a systematic review. Semin Arthritis Rheum. 2013;43(1):77-95.
204. del Rincón I, Polak J, O'Leary D, Battafarano D, Erikson J, Restrepo J, Molina E, Escalante A. Systemic inflammation and cardiovascular risk factors predict rapid progression of atherosclerosis in rheumatoid arthritis. Ann Rheum Dis. 2015;74(6):1118-23.
205. Barbado J, Martin D, Vega L, Almansa R, Goncalves L, Nocito M, Jimeno A, Ortiz de Lejarazu R, Bermejo-Martin J. MCP-1 in urine as biomarker of disease activity in Systemic Lupus Erythematosus. Cytokine. 2012;60(2):583-6.
206. Abdel Galil S, Ezzeldin N, El-Boshy M. The role of serum IL-17 and IL-6 as biomarkers of disease activity and predictors of remission in patients with lupus nephritis. Cytokine. 2015;76(2):280-7.
207. Roth D, Thompson A, Tang Y, Hammer A, Molta C, Gordon D. Elevated BLyS levels in patients with systemic lupus erythematosus: Associated factors and responses to belimumab. Lupus. 2016;25(4):346-54.
208. Gustafsson J, Simard J, Gunnarsson I, Elvin K, Lundberg I, Hansson L, Larsson A, Svenungsson E. Risk factors for cardiovascular mortality in patients with systemic lupus erythematosus, a prospective cohort study. Arthritis Res Ther. 2012;14(2):R46.
209. Lisowska A, Siergiejko E, Tycińska A, Knapp M, Kemona H, Musial W, Dymicka-Piekarska V. sVCAM-1 concentration and carotid IMT values in patients with acute

myocardial infarction--Atherosclerotic markers of the presence, progress and prognosis. Adv Med Sci. 2015;60(1):101-6.
210. Kjaergaard A, Dige A, Krog J, Tønnesen E, Wogensen L. Soluble adhesion molecules correlate with surface expression in an in vitro model of endothelial activation. Basic Clin Pharmacol Toxicol. 2013;113(4):273-9.
211. Gómez-Martín D, Díaz-Zamudio M, Vanoye G, Crispín J, Alcocer-Varela J. Quantitative and functional profiles of CD4+ lymphocyte subsets in systemic lupus erythematosus patients with lymphopenia. Clin Exp Immunol. 2011;164(1):17-25.
212. Huang Y, Chung H, Chang C, Yeh K, Chen L, Huang J. Lymphopenia is a risk factor in the progression of carotid intima-media thickness in juvenile-onset systemic lupus erythematosus. Arthritis Rheum. 2009;60(12):3766-75.
213. Li C, Mu R, Lu X, He J, Jia R, Li Z. Antilymphocyte antibodies in systemic lupus erythematosus: association with disease activity and lymphopenia. J Immunol Res. 2014(2014):672126.
214. Voulgarelis M, Kokori S, Ioannidis J, Tzioufas A, Kyriaki D, Moutsopoulos H. Anaemia in systemic lupus erythematosus: aetiological profile and the role of erythropoietin. Ann Rheum Dis. 2000;59(3):217-22.
215. Hara A, Furuichi K, Higuchi M, Iwata Y, Sakai N, Kaneko S, Wada T. Autoantibodies to erythropoietin receptor in patients with immune-mediated diseases: relationship to anaemia with erythroid hypoplasia. Br J Haematol. 2013;160(2):244-50.
216. Jost SA, Tseng LC, Matthews LA, Vasquez R, Zhang S, Yancey KB, Chong BF. IgG, IgM, and IgA antinuclear antibodies in discoid and systemic lupus erythematosus patients. ScientificWorldJournal. 2014;2014:171028.
217. Grönwall C, Reynolds H, Kim J, Buyon J, Goldberg J, Clancy R, Silverman G. Relation of carotid plaque with natural IgM antibodies in patients with systemic lupus erythematosus. Clin Immunol. 2014;153(1):1-7.
218. Anania C, Gustafsson T, Hua X, Su J, Vikström M, de Faire U, Heimbürger M, Jogestrand T, Frostegard J. Increased prevalence of vulnerable atherosclerotic plaques and low levels of natural IgM antibodies against phosphorylcholine in patients with systemic lupus erythematosus. Arthritis Res Ther. 2010;12(6):R214.
219. Svenungsson E, Engelbertsen D, Wigren M, Gustafsson J, Gunnarsson I, Elvin K, Jensen-Urstad K, Fredrikson G, Nilsson J. Decreased levels of autoantibodies against apolipoprotein B-100 antigens are associated with cardiovascular disease in systemic lupus erythematosus. Clin Exp Immunol. 2015;181(3):417-26.
220. Gilbert E, Ryan M. Estrogen in cardiovascular disease during systemic lupus erythematosus. Clin Ther. 2014;36(12):1901-12.
221. Barbhaiya M, Costenbader K. Environmental Exposures and the Development of Systemic Lupus Erythematosus. Curr Opin Rheumatol. 2016;28(5):497-505.
222. Panchanathan R, Choubey D. Murine BAFF expression is up-regulated by estrogen and interferons: implications for sex bias in the development of autoimmunity. Mol Immunol. 2013;53(1-2):15-23.
223. Dai R, Phillips R, Zhang Y, Khan D, Crasta O, Ahmed S. Suppression of LPS-induced Interferon-γ and nitric oxide in splenic lymphocytes by select estrogen-regulated microRNAs: a novel mechanism of immune modulation. Blood. 2008;112(12):4591-7.
224. Heidarzadeh Z, Asadi B, Saadatnia M, Ghorbani A, Fatehi F. The effect of low-dose combined oral contraceptive pills on brachial artery endothelial function and common carotid artery intima-media thickness. J Stroke Cerebrovasc Dis. 2014;23(4):675-80.

225. Gómez-Guzmán M, Jiménez R, Romero M, Sánchez M, Zarzuelo M, Gómez-Morales M, O'Valle F, López-Farré A, Algieri F, Gálvez J, Pérez-Vizcaino F, Sabio J, Duarte J. Chronic hydroxychloroquine improves endothelial dysfunction and protects kidney in a mouse model of systemic lupus erythematosus. Hypertension. 2014;64(2):330-7.
226. Richez C, Richards R, Duffau P, Weitzner Z, Andry C, Rifkin I, Aprahamian T. The effect of mycophenolate mofetil on disease development in the gld.apoE (-/-) mouse model of accelerated atherosclerosis and systemic lupus erythematosus. PloS One. 2013;8(4):e61042.
227. van Leuven S, Mendez-Fernandez Y, Wilhelm A, Wade N, Gabriel C, Kastelein J, Stroes E, Tak P, Major A. Mycophenolate mofetil but not atorvastatin attenuates atherosclerosis in lupus-prone LDLr(-/-) mice. Ann Rheum Dis. 2012;71(3):408-14.
228. Wang H, Peng W, Ouyang X, Li W, Dai Y. Circulating microRNAs as candidate biomarkers in patients with systemic lupus erythematosus. Transl Res. 2012;160(3):198-206.
229. Casciaro M, Di Salvo E, Brizzi T, Rodolico C, Gangemi S. Involvement of miR-126 in autoimmune disorders. Clinical and molecular allergy : CMA. 2018;16:11.
230. Jansen F, Yang X, Proebsting S, Hoelscher M, Przybilla D, Baumann K, Schmitz T, Dolf A, Endl E, Franklin BS, Sinning JM, Vasa-Nicotera M, Nickenig G, Werner N. MicroRNA expression in circulating microvesicles predicts cardiovascular events in patients with coronary artery disease. J Am Heart Assoc. 2014;3(6):e001249.
231. Jansen F, Yang X, Hoelscher M, Cattelan A, Schmitz T, Proebsting S, Wenzel D, Vosen S, Franklin BS, Fleischmann BK, Nickenig G, Werner N. Endothelial microparticle-mediated transfer of MicroRNA-126 promotes vascular endothelial cell repair via SPRED1 and is abrogated in glucose-damaged endothelial microparticles. Circulation. 2013;128(18):2026-38.
232. Deng Y, Zhao J, Sakurai D, Kaufman KM, Edberg JC, Kimberly RP, Kamen DL, Gilkeson GS, Jacob CO, Scofield RH, Langefeld CD, Kelly JA, Ramsey-Goldman R, Petri MA, Reveille JD, Vila LM, Alarcon GS, Vyse TJ, Pons-Estel BA, Freedman BI, Gaffney PM, Sivils KM, James JA, Gregersen PK, Anaya JM, Niewold TB, Merrill JT, Criswell LA, Stevens AM, Boackle SA, Cantor RM, Chen W, Grossman JM, Hahn BH, Harley JB, Alarcomicronn-Riquelme ME, Brown EE, Tsao BP. MicroRNA-3148 modulates allelic expression of toll-like receptor 7 variant associated with systemic lupus erythematosus. PLoS Genet. 2013;9(2):e1003336.
233. Goettsch C, Hutcheson JD, Aikawa E. MicroRNA in cardiovascular calcification: focus on targets and extracellular vesicle delivery mechanisms. Circ Res. 2013;112(7):1073-84.
234. Melman YF, Shah R, Danielson K, Xiao J, Simonson B, Barth A, Chakir K, Lewis GD, Lavender Z, Truong QA, Kleber A, Das R, Rosenzweig A, Wang Y, Kass D, Singh JP, Das S. Circulating MicroRNA-30d Is Associated With Response to Cardiac Resynchronization Therapy in Heart Failure and Regulates Cardiomyocyte Apoptosis: A Translational Pilot Study. Circulation. 2015;131(25):2202-16.
235. Chen C, Wang Y, Yang S, Li H, Zhao G, Wang F, Yang L, Wang DW. MiR-320a contributes to atherogenesis by augmenting multiple risk factors and down-regulating SRF. J Cell Mol Med. 2015;19(5):970-85.
236. Nakaoka H, Hirono K, Yamamoto S, Takasaki I, Takahashi K, Kinoshita K, Takasaki A, Nishida N, Okabe M, Ce W, Miyao N, Saito K, Ibuki K, Ozawa S, Adachi Y, Ichida F. MicroRNA-145-5p and microRNA-320a encapsulated in endothelial microparticles

contribute to the progression of vasculitis in acute Kawasaki Disease. Sci Rep. 2018;8(1):1016.
237. Devaux Y, Mueller M, Haaf P, Goretti E, Twerenbold R, Zangrando J, Vausort M, Reichlin T, Wildi K, Moehring B, Wagner DR, Mueller C. Diagnostic and prognostic value of circulating microRNAs in patients with acute chest pain. J Intern Med. 2015;277(2):260-71.
238. van Boven N, Kardys I, van Vark LC, Akkerhuis KM, de Ronde MWJ, Khan MAF, Merkus D, Liu Z, Voors AA, Asselbergs FW, van den Bos EJ, Boersma E, Hillege H, Duncker DJ, Pinto YM, Postmus D. Serially measured circulating microRNAs and adverse clinical outcomes in patients with acute heart failure. Eur J Heart Fail. 2018;20(1):89-96.
239. Zhang H, Huang X, Ye L, Guo G, Li X, Chen C, Sun L, Li B, Chen N, Xue X. B Cell-Related Circulating MicroRNAs With the Potential Value of Biomarkers in the Differential Diagnosis, and Distinguishment Between the Disease Activity and Lupus Nephritis for Systemic Lupus Erythematosus. Front Immunol. 2018;9:1473.
240. Zhu LP, Zhou JP, Zhang JX, Wang JY, Wang ZY, Pan M, Li LF, Li CC, Wang KK, Bai YP, Zhang GG. MiR-15b-5p Regulates Collateral Artery Formation by Targeting AKT3 (Protein Kinase B-3). Arterioscler Thromb Vasc Biol. 2017;37(5):957-68.
241. Liu Z, Yang D, Xie P, Ren G, Sun G, Zeng X, Sun X. MiR-106b and MiR-15b modulate apoptosis and angiogenesis in myocardial infarction. Cell Physiol Biochem. 2012;29(5-6):851-62.
242. Dahdal S, Devetzis V, Chalikias G, Tziakas D, Chizzolini C, Ribi C, Trendelenburg M, Eisenberger U, Hauser T, Pasch A, Huynh-Do U, Arampatzis S. Serum calcification propensity is independently associated with disease activity in systemic lupus erythematosus. PLoS One. 2018;13(1):e0188695.
243. Chapman JR, Waldenstrom J. With Reference to Reference Genes: A Systematic Review of Endogenous Controls in Gene Expression Studies. PLoS One. 2015;10(11):e0141853.
244. Anene C, Graham AM, Boyne J, Roberts W. Platelet microparticle delivered microRNA-Let-7a promotes the angiogenic switch. Biochimica et biophysica acta Molecular basis of disease. 2018;1864(8):2633-43.
245. Wang S, Zhou H, Wu D, Ni H, Chen Z, Chen C, Xiang Y, Dai K, Chen X, Li X. MicroRNA let-7a regulates angiogenesis by targeting TGFBR3 mRNA. J Cell Mol Med. 2019;23(1):556-67.
246. Zhao S, Wang Y, Liang Y, Zhao M, Long H, Ding S, Yin H, Lu Q. MicroRNA-126 regulates DNA methylation in CD4+ T cells and contributes to systemic lupus erythematosus by targeting DNA methyltransferase 1. Arthritis Rheum. 2011;63(5):1376-86.
247. Yang X, Zhu MJ, Sreejayan N, Ren J, Du M. Angiotensin II promotes smooth muscle cell proliferation and migration through release of heparin-binding epidermal growth factor and activation of EGF-receptor pathway. Molecules and cells. 2005;20(2):263-70.
248. Wang L, Huang Z, Huang W, Chen X, Shan P, Zhong P, Khan Z, Wang J, Fang Q, Liang G, Wang Y. Inhibition of epidermal growth factor receptor attenuates atherosclerosis via decreasing inflammation and oxidative stress. Sci Rep. 2017;8:45917.
249. Ryu S, Fu W, Petri MA. Associates and predictors of pleurisy or pericarditis in SLE. Lupus Sci Med. 2017;4(1):e000221.
250. Higashi Y, Sukhanov S, Shai SY, Danchuk S, Tang R, Snarski P, Li Z, Lobelle-Rich P, Wang M, Wang D, Yu H, Korthuis R, Delafontaine P. Insulin-Like Growth Factor-1 Receptor

Deficiency in Macrophages Accelerates Atherosclerosis and Induces an Unstable Plaque Phenotype in Apolipoprotein E-Deficient Mice. Circulation. 2016;133(23):2263-78.
251. Sesti G, Mannino GC, Andreozzi F, Greco A, Perticone M, Sciacqua A, Marini MA, Perticone F. A polymorphism at IGF1 locus is associated with carotid intima media thickness and endothelium-dependent vasodilatation. Atherosclerosis. 2014;232(1):25-30.
252. Shigematsu S, Yamauchi K, Nakajima K, Iijima S, Aizawa T, Hashizume K. IGF-1 regulates migration and angiogenesis of human endothelial cells. Endocrine journal. 1999;46 Suppl:S59-62.
253. Ikeo S, Yamauchi K, Shigematsu S, Nakajima K, Aizawa T, Hashizume K. Differential effects of growth hormone and insulin-like growth factor I on human endothelial cell migration. Am J Physiol Cell Physiol. 2001;280(5):C1255-61.
254. Bartoli-Leonard F, Wilkinson FL, Schiro A, Inglott FS, Alexander MY, Weston R. Suppression of SIRT1 in Diabetic Conditions Induces Osteogenic Differentiation of Human Vascular Smooth Muscle Cells via RUNX2 Signalling. Sci Rep. 2019;9(1):878.
255. Pavlov VI, Tan YS, McClure EE, La Bonte LR, Zou C, Gorsuch WB, Stahl GL. Human mannose-binding lectin inhibitor prevents myocardial injury and arterial thrombogenesis in a novel animal model. Am J Pathol. 2015;185(2):347-55.
256. Aarup A, Pedersen TX, Junker N, Christoffersen C, Bartels ED, Madsen M, Nielsen CH, Nielsen LB. Hypoxia-Inducible Factor-1alpha Expression in Macrophages Promotes Development of Atherosclerosis. Arterioscler Thromb Vasc Biol. 2016;36(9):1782-90.
257. Tsai SH, Huang PH, Hsu YJ, Peng YJ, Lee CH, Wang JC, Chen JW, Lin SJ. Inhibition of hypoxia inducible factor-1alpha attenuates abdominal aortic aneurysm progression through the down-regulation of matrix metalloproteinases. Sci Rep. 2016;6:28612.
258. Goettsch C, Kjolby M, Aikawa E. Sortilin and Its Multiple Roles in Cardiovascular and Metabolic Diseases. Arterioscler Thromb Vasc Biol. 2018;38(1):19-25.
259. Leuchten N, Milke B, Winkler-Rohlfing B, Daikh D, Dorner T, Johnson SR, Aringer M. Early symptoms of systemic lupus erythematosus (SLE) recalled by 339 SLE patients. Lupus. 2018;27(9):1431-6.
260. Medlin JL, Hansen KE, Fitz SR, Bartels CM. A systematic review and meta-analysis of cutaneous manifestations in late- versus early-onset systemic lupus erythematosus. Semin Arthritis Rheum. 2016;45(6):691-7.
261. Ruiz-Irastorza G, Egurbide MV, Olivares N, Martinez-Berriotxoa A, Aguirre C. Vitamin D deficiency in systemic lupus erythematosus: prevalence, predictors and clinical consequences. Rheumatology (Oxford). 2008;47(6):920-3.
262. Bi R, Dai Y, Ma Z, Zhang S, Wang L, Lin Q. Endothelial cell autophagy in chronic intermittent hypoxia is impaired by miRNA-30a-mediated translational control of Beclin-1. J Cell Biochem. 2019;120(3):4214-24.
263. Gomez-Stallons MV, Wirrig-Schwendeman EE, Hassel KR, Conway SJ, Yutzey KE. Bone Morphogenetic Protein Signaling Is Required for Aortic Valve Calcification. Arterioscler Thromb Vasc Biol. 2016;36(7):1398-405.
264. Ye J, Guo R, Shi Y, Qi F, Guo C, Yang L. miR-155 Regulated Inflammation Response by the SOCS1-STAT3-PDCD4 Axis in Atherogenesis. Mediators Inflamm. 2016;2016:8060182.
265. Qin L, Huang Q, Zhang H, Liu R, Tellides G, Min W, Yu L. SOCS1 prevents graft arteriosclerosis by preserving endothelial cell function. J Am Coll Cardiol. 2014;63(1):21-9.

266. Wang Y, Li Z, Xu P, Huang L, Tong J, Huang H, Meng A. Angiomotin-like2 gene (amotl2) is required for migration and proliferation of endothelial cells during angiogenesis. J Biol Chem. 2011;286(47):41095-104.
267. Adams GN, LaRusch GA, Stavrou E, Zhou Y, Nieman MT, Jacobs GH, Cui Y, Lu Y, Jain MK, Mahdi F, Shariat-Madar Z, Okada Y, D'Alecy LG, Schmaier AH. Murine prolylcarboxypeptidase depletion induces vascular dysfunction with hypertension and faster arterial thrombosis. Blood. 2011;117(14):3929-37.
268. Adams GN, Stavrou EX, Fang C, Merkulova A, Alaiti MA, Nakajima K, Morooka T, Merkulov S, Larusch GA, Simon DI, Jain MK, Schmaier AH. Prolylcarboxypeptidase promotes angiogenesis and vascular repair. Blood. 2013;122(8):1522-31.
269. Staton CA, Reed MW, Brown NJ. A critical analysis of current in vitro and in vivo angiogenesis assays. International journal of experimental pathology. 2009;90(3):195-221.
270. Boisen L, Drasbek KR, Pedersen AS, Kristensen P. Evaluation of endothelial cell culture as a model system of vascular ageing. Experimental gerontology. 2010;45(10):779-87.
271. Langford-Smith AWW, Hasan A, Weston R, Edwards N, Jones AM, Boulton AJM, Bowling FL, Rashid ST, Wilkinson FL, Alexander MY. Diabetic endothelial colony forming cells have the potential for restoration with glycomimetics. Sci Rep. 2019;9(1):2309.
272. Yee CS, Cresswell L, Farewell V, Rahman A, Teh LS, Griffiths B, Bruce IN, Ahmad Y, Prabu A, Akil M, McHugh N, D'Cruz D, Khamashta MA, Isenberg DA, Gordon C. Numerical scoring for the BILAG-2004 index. Rheumatology (Oxford). 2010;49(9):1665-9.
273. Booth S, Price E, Walker E. Fluctuation, invisibility, fatigue - the barriers to maintaining employment with systemic lupus erythematosus: results of an online survey. Lupus. 2018;27(14):2284-91.
274. Ahn GE, Ramsey-Goldman R. Fatigue in systemic lupus erythematosus. International journal of clinical rheumatology. 2012;7(2):217-27.
275. Barraclough M, McKie S, Parker B, Jackson A, Pemberton P, Elliott R, Bruce IN. Altered cognitive function in systemic lupus erythematosus and associations with inflammation and functional and structural brain changes. Ann Rheum Dis. 2019;78(7):934-40.
276. Vincent A, Benzo RP, Whipple MO, McAllister SJ, Erwin PJ, Saligan LN. Beyond pain in fibromyalgia: insights into the symptom of fatigue. Arthritis Res Ther. 2013;15(6):221.
277. Louati K, Berenbaum F. Fatigue in chronic inflammation - a link to pain pathways. Arthritis Res Ther. 2015;17:254.
278. Wiseman SJ, Bastin ME, Hamilton IF, Hunt D, Ritchie SJ, Amft EN, Thomson S, Belch JF, Ralston SH, Wardlaw JM. Fatigue and cognitive function in systemic lupus erythematosus: associations with white matter microstructural damage. A diffusion tensor MRI study and meta-analysis. Lupus. 2017;26(6):588-97.
279. Choy EHS, Calabrese LH. Neuroendocrine and neurophysiological effects of interleukin 6 in rheumatoid arthritis. Rheumatology (Oxford). 2018;57(11):1885-95.
280. McCubbin JA, Peach H, Moore DD, Pilcher JJ. Decreased Cognitive/CNS Function in Young Adults at Risk for Hypertension: Effects of Sleep Deprivation. International journal of hypertension. 2012;2012:989345.
281. Meissner A. Hypertension and the Brain: A Risk Factor for More Than Heart Disease. Cerebrovascular diseases (Basel, Switzerland). 2016;42(3-4):255-62.

282. Czuriga-Kovacs KR, Czuriga D, Csiba L. Influence of Hypertension, Alone and in Combination with Other Vascular Risk Factors on Cognition. CNS & neurological disorders drug targets. 2016;15(6):690-8.
283. Aterido A, Julia A, Carreira P, Blanco R, Lopez-Longo JJ, Venegas JJP, Olive A, Andreu JL, Aguirre-Zamorano MA, Vela P, Nolla JM, Marenco-de la Fuente JL, Zea A, Pego JM, Freire M, Diez E, Lopez-Lasanta M, Lopez-Corbeto M, Palau N, Tortosa R, Gelpi JL, Absher D, Myers RM, Fernandez-Nebro A, Marsal S. Genome-wide pathway analysis identifies VEGF pathway association with oral ulceration in systemic lupus erythematosus. Arthritis Res Ther. 2017;19(1):138.
284. Howard P. April's Topic of the Month – Coping with Oral and Nasal Ulcers: LUPUS UK; 2017 [Available from: https://www.lupusuk.org.uk/coping-with-oral-and-nasal-ulcers/.
285. Nijs J, Van Oosterwijck J, Meeus M, Lambrecht L, Metzger K, Fremont M, Paul L. Unravelling the nature of postexertional malaise in myalgic encephalomyelitis/chronic fatigue syndrome: the role of elastase, complement C4a and interleukin-1beta. J Intern Med. 2010;267(4):418-35.
286. Zambon D, Quintana M, Mata P, Alonso R, Benavent J, Cruz-Sanchez F, Gich J, Pocovi M, Civeira F, Capurro S, Bachman D, Sambamurti K, Nicholas J, Pappolla MA. Higher incidence of mild cognitive impairment in familial hypercholesterolemia. Am J Med. 2010;123(3):267-74.
287. Suarez Bagnasco M. Psychological issues and cognitive impairment in adults with familial hypercholesterolemia. Family practice. 2017;34(5):520-4.
288. Tjensvoll AB, Lauvsnes MB, Hirohata S, Beyer MK, Greve OJ, Kvivik I, Kvaloy JT, Harboe E, Goransson LG, Omdal R. Migraine in patients with systemic lupus erythematosus is associated with reduced cerebral grey matter volume but not with measures of glial activation or anti-NR2 or anti-P antibodies. Eur J Neurol. 2016;23(4):780-6.
289. Russell AP, Foletta VC, Snow RJ, Wadley GD. Skeletal muscle mitochondria: a major player in exercise, health and disease. Biochim Biophys Acta. 2014;1840(4):1276-84.
290. Meyer A, Laverny G, Allenbach Y, Grelet E, Ueberschlag V, Echaniz-Laguna A, Lannes B, Alsaleh G, Charles AL, Singh F, Zoll J, Lonsdorfer E, Maurier F, Boyer O, Gottenberg JE, Nicot AS, Laporte J, Benveniste O, Metzger D, Sibilia J, Geny B. IFN-beta-induced reactive oxygen species and mitochondrial damage contribute to muscle impairment and inflammation maintenance in dermatomyositis. Acta neuropathologica. 2017;134(4):655-66.
291. Lee HT, Lin CS, Lee CS, Tsai CY, Wei YH. Increased 8-hydroxy-2'-deoxyguanosine in plasma and decreased mRNA expression of human 8-oxoguanine DNA glycosylase 1, anti-oxidant enzymes, mitochondrial biogenesis-related proteins and glycolytic enzymes in leucocytes in patients with systemic lupus erythematosus. Clin Exp Immunol. 2014;176(1):66-77.
292. Wu T, Xie C, Han J, Ye Y, Weiel J, Li Q, Blanco I, Ahn C, Olsen N, Putterman C, Saxena R, Mohan C. Metabolic disturbances associated with systemic lupus erythematosus. PLoS One. 2012;7(6):e37210.
293. Takeshima Y, Iwasaki Y, Fujio K, Yamamoto K. Metabolism as a key regulator in the pathogenesis of systemic lupus erythematosus. Semin Arthritis Rheum. 2019;48(6):1142-5.

294. Karthikeyan G, Santos JH, Graziewicz MA, Copeland WC, Isaya G, Van Houten B, Resnick MA. Reduction in frataxin causes progressive accumulation of mitochondrial damage. Hum Mol Genet. 2003;12(24):3331-42.
295. Dong DW, Srinivasan S, Guha M, Avadhani NG. Defects in cytochrome c oxidase expression induce a metabolic shift to glycolysis and carcinogenesis. Genomics data. 2015;6:99-107.
296. Jafri K, Ogdie A, Qasim A, Patterson SL, Gianfrancesco M, Izadi Z, Katz P, Yazdany J, Schmajuk G. Discordance of the Framingham cardiovascular risk score and the 2013 American College of Cardiology/American Heart Association risk score in systemic lupus erythematosus and rheumatoid arthritis. Clin Rheumatol. 2018;37(2):467-74.
297. Felten R, Sagez F, Gavand PE, Martin T, Korganow AS, Sordet C, Javier RM, Soulas-Sprauel P, Riviere M, Scher F, Poindron V, Guffroy A, Arnaud L. 10 most important contemporary challenges in the management of SLE. Lupus Sci Med. 2019;6(1):e000303.
298. McMahon M, Skaggs B, Grossman J, Wong WK, Sahakian L, Chen W, Hahn B. Comparison of PREDICTS atherosclerosis biomarker changes after initiation of new treatments in patients with SLE. Lupus Sci Med. 2019;6(1):e000321.
299. Wang Z. The guideline of the design and validation of MiRNA mimics. Methods Mol Biol. 2011;676:211-23.
300. Zollner H, Hahn SA, Maghnouj A. Lentiviral overexpression of miRNAs. Methods Mol Biol. 2014;1095:177-90.
301. Tomasetti M, Nocchi L, Staffolani S, Manzella N, Amati M, Goodwin J, Kluckova K, Nguyen M, Strafella E, Bajzikova M, Peterka M, Lettlova S, Truksa J, Lee W, Dong LF, Santarelli L, Neuzil J. MicroRNA-126 suppresses mesothelioma malignancy by targeting IRS1 and interfering with the mitochondrial function. Antioxid Redox Signal. 2014;21(15):2109-25.
302. Ebert MS, Sharp PA. MicroRNA sponges: progress and possibilities. RNA (New York, NY). 2010;16(11):2043-50.
303. Krutzfeldt J, Rajewsky N, Braich R, Rajeev KG, Tuschl T, Manoharan M, Stoffel M. Silencing of microRNAs in vivo with 'antagomirs'. Nature. 2005;438(7068):685-9.
304. Geiling B, Vandal G, Posner AR, de Bruyns A, Dutchak KL, Garnett S, Dankort D. A modular lentiviral and retroviral construction system to rapidly generate vectors for gene expression and gene knockdown in vitro and in vivo. PLoS One. 2013;8(10):e76279.
305. Stock AD, Gelb S, Pasternak O, Ben-Zvi A, Putterman C. The blood brain barrier and neuropsychiatric lupus: new perspectives in light of advances in understanding the neuroimmune interface. Autoimmun Rev. 2017;16(6):612-9.
306. Manjaly ZM, Harrison NA, Critchley HD, Do CT, Stefanics G, Wenderoth N, Lutterotti A, Muller A, Stephan KE. Pathophysiological and cognitive mechanisms of fatigue in multiple sclerosis. Journal of neurology, neurosurgery, and psychiatry. 2019;90(6):642-51.
307. Rochfort KD, Collins LE, Murphy RP, Cummins PM. Downregulation of blood-brain barrier phenotype by proinflammatory cytokines involves NADPH oxidase-dependent ROS generation: consequences for interendothelial adherens and tight junctions. PLoS One. 2014;9(7):e101815.

Chapter 9

Appendix

i. Effects of MiRNA Overexpression on Cell Viability

As described in chapter 5, only HUVECs transduced with miR-3148 and miR-320a lentiviral vectors demonstrated increased cell viability (app. figure i.; indicated by dashed line, significance only when analysed by t test as in chapter 5). No other miRNAs yielded significant differences when analysed by ANOVA or t-test (126-3p p=0.898; 93-5p p=0.735; 30d-5p p=0.424).

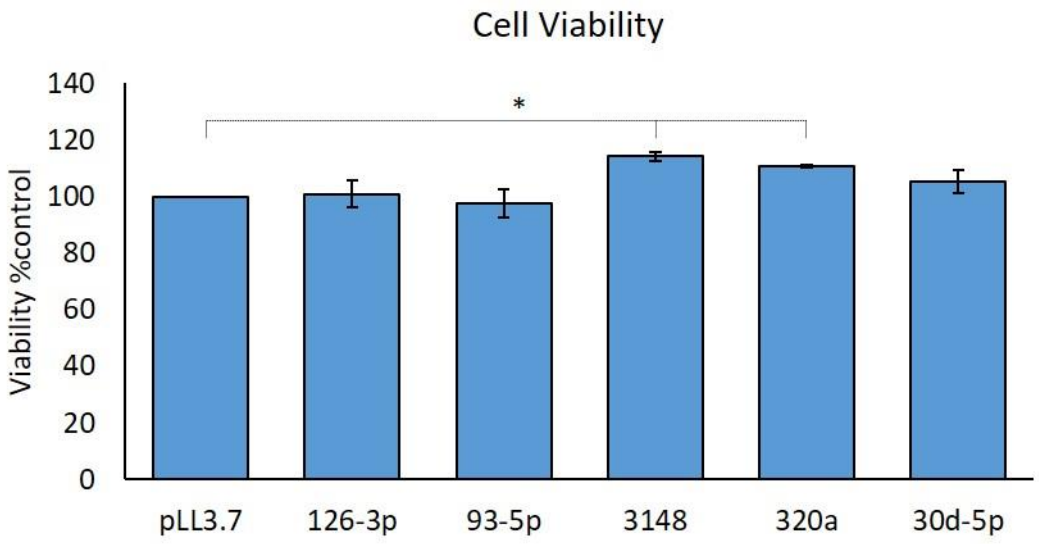

App. Figure i. Effects of miRNA overexpression on cell viability. *HUVECs were transduced with either miRNA lentiviral vectors or the control pLL3.7 lentivirus at passage 3 (80% transduction efficiency) and cell viability was tested at passages 4-6. Data shown represent absorbance at 570nm after 24 hours incubation with alamarBlue reagent. Analysis by one-way ANOVA and independent samples t-test. N=3 in triplicate. * denotes p≤0.05.*

ii. Effects of MiR-126-3p and MiR-3148 on Tube Formation

Chapter 5 highlighted the differences in tube length and number when HUVECs overexpressed miR-93-5p, miR-320a or miR-30d-5p, which have been highlighted with a dashed line in app. figure ii. Neither miR-93-5p nor miR-320a affected tube number at 5 hours (p=0.073 and p=0.104) or at 24 hours (p=0.607 and p=0.664). On the other hand, overexpression of miR-30d-5p had no effect on tube length at either 5 hours (p=0.085) or at 24 hours (p=0.268). Transduction with miR-126-3p lentivirus produced no significant effect on tube length (5hrs p=0.160, 24hrs p=0.120) or number (5hrs p=0.175; 24hrs p=0.707) compared to control and neither did miR-3148 (tube length 5hrs p=0.091; 24 hrs p=0.475; tube number 5hrs p= 0.549; 24hrs p=0.381). These statistics reflect independent t-test; no significance was apparent with one-way ANOVA.

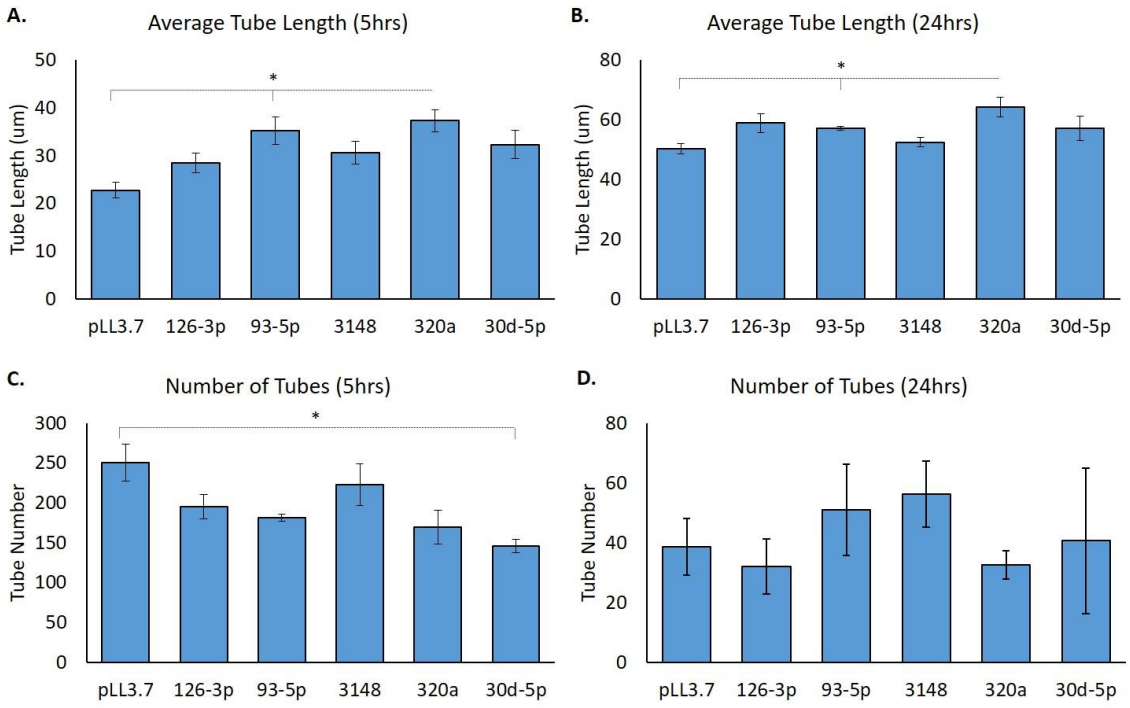

App. Figure ii. Tube formation in HUVECs overexpressing miRNAs. *Angiogenesis was tested using a Matrigel®-based tube formation assay, in HUVECs at p4-5, which had been transduced with either the control pLL3.7 lentivirus or miRNA lentivirus (80% transduction efficiency). Images were taken at 5 (A) and 24 hours (B) following plating. Tube formation was measured using ImageJ software and statistical analysis using one way ANOVA and independent samples t-test. N=3 in triplicate. * denotes p≤0.05.*

iii. MiRNA Abundance in Patients with Musculoskeletal Symptoms

As described in chapter 6, patients experiencing musculoskeletal symptoms were also found to have increased abundance of miR-126-3p and miR-93-5p. This was not the case with any of the other miRNAs tested (app. table i.).

MiR-126-3p	Abundance/ml plasma	Present Absent	$1.2x10^{8} \pm 1.1x10^{8}$ $2.3x10^{9} \pm 3.7x10^{9}$	**p=0.035**
	Abundance per MV	Present Absent	$1.2x10^{15} \pm 1.1x10^{15}$ $2.3x10^{16} \pm 4.3x10^{16}$	p=0.056
MiR-93-5p	Abundance/ml plasma	Present Absent	$5.2x10^{9} \pm 4.3x10^{9}$ $1.6x10^{9} \pm 1.8x10^{9}$	**p=0.008**

	Abundance per MV	Present Absent	$4.9x10^{16} \pm 3.7x10^{16}$ $1.6x10^{16} \pm 1.6x10^{16}$	**p=0.009**
MiR-3148	Abundance/ml plasma	Present Absent	$9.1x10^{12} \pm 9.7x10^{12}$ $5.3x10^{12} \pm 5.8x10^{12}$	p=0.798
	Abundance per MV	Present Absent	$8.3x10^{19} \pm 9.9x10^{19}$ $6.3x10^{19} \pm 7.8x10^{19}$	p=0.850
MiR-320a	Abundance/ml plasma	Present Absent	$4.7x10^{9} \pm 4.1x10^{0}$ $2.8x10^{9} \pm 2.1x10^{9}$	p=0.247
	Abundance per MV	Present Absent	$4.5x10^{16} \pm 4.3x10^{16}$ $3.1x10^{16} \pm 3.3x10^{16}$	p=0.138
MiR-30d-5p	Abundance/ml plasma	Present Absent	$2.6x10^{9} \pm 1.7x10^{9}$ $1.3x10^{9} \pm 7.8x10^{10}$	p=0.106
	Abundance per MV	Present Absent	$2.5x10^{16} \pm 1.7x10^{16}$ $1.5x10^{16} \pm 1.2x10^{16}$	p=0.080

App. Table i. MiRNA abundance in patients with musculoskeletal symptoms. *Musculoskeletal symptoms were classed as a BILAG score of C or above (mild to severe symptoms at present time). Data analysed by Mann-Whitney U test and displayed as mean abundance (± standard deviation). Symptoms present in 9 patients, absent in 17.*

iv. Effects of MiRNA Overexpression on Cellular Respiration

Chapter 6 also detailed a glycolytic shift in HUVECs overexpressing miR-126-3p and a similar trend in those overexpressing miR-93-5p, relating this to the musculoskeletal symptoms associated with these miRNAs. While other trends were apparent, overexpression of none of the other miRNAs yielded significant differences compared to controls (app. figure iii). Although miR-320a and miR-30d-5p appeared to increase basal OCR, this was not significant (p=0.315 and p=0.161) nor was it so at maximal OCR (p=0.316 and p=0.066). Overexpression of miR-3148 produced no discernible effect on OCR (basal p=0.662, maximal p=0.919). Moreover, none of these miRNAs affected basal (3148 p=0.147; 320a p=0.788; 30d-5p p=0.560) or maximal ECAR (3148 p=0.241; 320a p=0.480; 30d-5p p=0.793).

The statistics provided here were produced by independent samples t-test; no significance was apparent with one-way ANOVA.

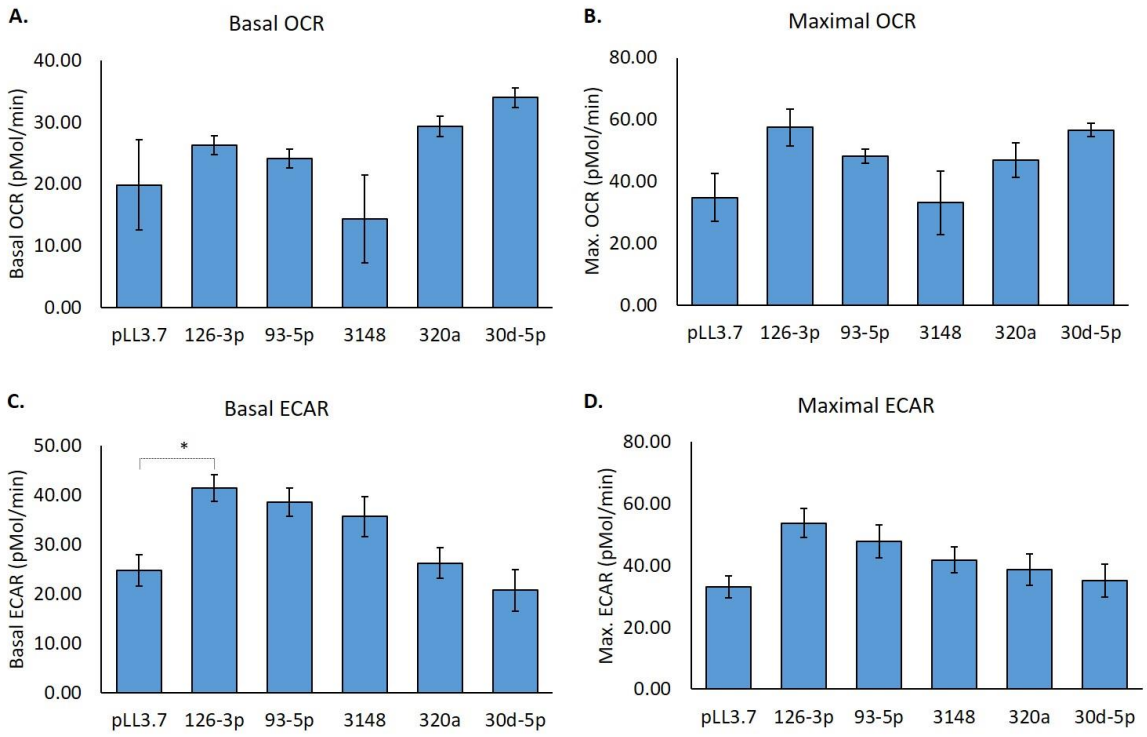

App. Figure iii. Seahorse bioanalysis of all miRNA overexpression constructs. *HUVECs at p3 were transduced with either miRNA lentivirus or control pLL3.7 lentivirus at 80% transduction efficiency. Seahorse bioanalysis was performed using Seahorse Xfp Cell Mito Stress Test, with HUVECs plated at p5-7. Basal OCR (A), maximal OCR (B), basal ECAR (C) and maximal ECAR (D) were recorded, providing a profile of cellular respiration (E). Statistical analysis was performed using one-way ANOVA and independent samples t-test. N=3 in duplicate, n=2 for miR-93-5p constructs. * denotes p≤0.05.*

v. Publications Arising From This Thesis

The attached publications were produced using data or techniques generated during the course of this project. Briefly, the first research article by Edwards *et al.* communicates much of the data from chapter 3 pertaining to QRISK3 scores and EMV abundance in SLE, while the second research article by Langford-Smith *et al.* utilises techniques such as Seahorse bioanalysis to interrogate the function of endothelial progenitor cells *in vitro*. The final article, a review article, provides more information on endothelial damage and repair in conditions associated with high cardiovascular risk.